Mediator-based electron transfer pathways in microorganisms

Dissertation

André Gemünde

Mediator-based electron transfer pathways in microorganisms

Dissertation

Zur

Erlangung des akademischen Grades des Doktors der Ingenieurwissenschaften (Dr.-Ing.)

Dem Promotionszentrum für Ingenieurwissenschaften am Forschungscampus Mittelhessen

vorgelegt von
André Gemünde
M.Sc

Aus Mainz

Bad Vilbel, den 30.09.2024

Begutachtung durch:
Prof. Dr.-Ing Dirk Holtmann und Prof. Dr. Jürgen Janek

Zusammenfassung

Herausforderungen in der industriellen Biotechnologie entstehen unter anderem, wenn gelöstes O_2 in wässrigen Fermentationsmedien als Elektronenakzeptor benötigt wird. Diese Herausforderungen bestehen hauptsächlich aus der geringen Löslichkeit des Gases bei den Kultivierungstemperaturen, erhöhter Schaumbildung und der Explosionsgefahr bei Kombination mit H_2 als Substrat. Elektroden könnten O_2 als Elektronenakzeptor ersetzen und so die Gasfermentation mit *Cupriavidus necator*, einem *β*-Proteobakterium zur Herstellung von Basischemikalien aus H_2/CO_2-Gemischen, ermöglichen. Obwohl der Elektronentransfer zwischen Mikroorganismen und Elektroden durch lösliche Mediatoren bereits gezeigt wurde, fehlt bisher das Wissen über deren genaue Interaktion, um O_2 vollständig zu ersetzen. Ziel dieser Dissertation war es, Screening- und Reaktorsysteme zu entwickeln und Schlüsselkomponenten im Stoffwechsel von *C. necator* zu identifizieren, die den extrazellulären Elektronentransfer beeinflussen.

Dazu wurde ein 300 mL bioelektrochemischer Reaktor konzipiert und zunächst mit *Vibrio natriegens* charakterisiert. Hier wurde der mediatorbasierte und direkte Elektronentransfer des Organismus gezeigt, der die Produkt- und Biomasseausbeute messbar beeinflusst. Als Maß für die Effizienz des artifiziellen mediatorvermittelten Transferprozesses wurde zusätzlich der prozentuale Anteil des durch anodischen Elektronentransfer ersetzten O_2 eingeführt.

Zudem wurde ein 3,5 mL Screening-System entwickelt, das eine Online-Messung der Zelldichte und des Redoxzustands der Mediatoren ermöglicht. *Pseudomonas putida* wurde zur Verifizierung genutzt, da dessen Kaliumhexacyanoferrat-vermittelter Elektronentransfer bereits in der Literatur beschrieben ist. Das Screening von 14 Mediatoren mit variablen Redoxpotentialen in Kombination mit *C. necator* in dem entwickelten System ergab ein Potentialfenster für die Mediator-Reduktion in Verbindung mit einer Stromproduktion von -365 bis 206 mV *vs*. Ag/AgCl, wobei Kaliumhexacyanoferrat mit insgesamt 8,4 Reduktions- und Oxidationszyklen (Turnover) am effizientesten war. Die etablierten 300 mL Reaktoren wurden dann für die elektrochemische Kultivierung von *C. necator* zur Aufklärung des Elektronentransfers eingesetzt. Cytochrom c-Reduktase, Cytochrom c-Oxidase und Nitrat/Nitrit-Reduktase wurden dabei als

Schlüsselkomplexe bei der Kaliumhexacyanoferrat-Reduktion durch RT-qPCR, spezifische Hemmung und Deletionsmutanten identifiziert.

Diese Arbeit legt die Basis für das Screening von Mediatoren mit Mikroorganismen, die in größeren Reaktoren validiert werden, und schafft zudem eine Grundlage für die Optimierung des Kaliumhexacyanoferrat-vermittelten Elektronentransfers in *C. necator* und weiteren Organismen.

Abstract

Challenges in industrial biotechnology arise, among other things, when dissolved O_2 is required as an electron acceptor in aqueous fermentation media. These challenges mainly consist of the low solubility of the gas at cultivation temperatures, increased foaming, and the risk of explosion when combined with H_2 as a substrate. Electrodes could replace O_2 as electron acceptors, thereby enabling gas fermentation with *Cupriavidus necator*, a β-proteobacterium used for the production of basic chemicals from H_2/CO_2 mixtures. Although electron transfer between microorganisms and electrodes has already been demonstrated using soluble mediators, knowledge of their precise interaction is still lacking to fully replace O_2. The aim of this dissertation was to develop screening and reactor systems and to identify key components in the metabolism of *C. necator* influencing the extracellular electron transfer.

To this end, a 300 mL bioelectrochemical reactor was designed and initially characterized with *Vibrio natriegens*. The mediator-based and direct electron transfer of the organism was demonstrated, showing a measurable impact on product and biomass yield. As a measure of the efficiency of the artificial mediated electron transfer process, the percentage of O_2 replaced by anodic electron transfer was introduced.

Furthermore, a 3.5 mL screening system was developed that enables online measurement of cell density and the redox state of the mediators. *Pseudomonas putida* was used for verification, as its ferricyanide-mediated electron transfer is already described in the literature. The screening of 14 mediators with variable redox potentials in combination with *C. necator* in the developed system revealed a potential window for mediator reduction, along with a current production of -365 to 206 mV *vs*. Ag/AgCl, with ferricyanide proving most efficient with a total of 8.4 reduction and oxidation cycles (turnovers). The established 300 mL reactors were then used for the electrochemical cultivation of *C. necator* to elucidate the electron transfer. Cytochrome c reductase, cytochrome c oxidase, and nitrate/nitrite reductase were identified as key complexes in ferricyanide reduction through RT-qPCR, specific inhibition, and deletion mutants.

This work lays the foundation for screening mediators with microorganisms that are validated in larger reactors and also provides a

basis for optimizing ferricyanide-mediated electron transfer in *C. necator* and other organisms.

Acknowledgements

I would like to express my deepest gratitude to all those who have supported and accompanied me throughout the creation of this dissertation.

My special thanks go to my advisor, Prof. Dr.-Ing Dirk Holtmann, who continuously stood by me with ideas, great trust, and support throughout my doctoral studies, even after his transition to the new institution in Karlsruhe. The open working atmosphere at his chair allowed me the freedom to explore the topics of this dissertation according to my own vision.

I am also deeply grateful to Prof. Dr. Jürgen Janek for his invaluable advice on all electrochemical issues and for providing access to his equipment. The regular exchanges and suggestions were crucial to the development of key parts of this work.

I extend my sincere thanks to the German Research Foundation for funding the priority program "eBiotech" under the leadership of Miriam Rosenbaum. The focus on collaboration and commitment to the education of doctoral candidates is a prime example of excellent project management.

A heartfelt thanks also goes to Markus Stöckl from the DECHEMA Research Institute in Frankfurt am Main for his expertise and our open discussions on bioelectrochemistry. Additionally, I would like to thank Hendrik Schewe for providing me equipment, which formed the basis for many of the results in this work.

I am especially grateful to all my colleagues and students in the research group. The celebrations, the straightforward interactions, and, of course, the scientific exchanges during lunch breaks helped me overcome the challenges of this dissertation. Special thanks to Jonas Gail and Nils-Lennart Ruppert, who accompanied my work over extended periods and collected extensive data in the laboratory.

Last but not least, I would like to thank my family. Their encouraging words and understanding meant a great deal to me.

Most importantly, I want to thank my fiancée, Anna. Her love, patience, and encouragement provided me with unwavering support during the most challenging moments. Her support has been an irreplaceable source of strength and motivation for me.

Thank you all!

Table of Contents

List of Symbols and Abbreviations

ANOVA	Analysis of variance
ATP	Adenosine triphosphate
BES	Bioelectrochemical system
CcO	Cytochrome c oxidase
CcR	Cytochrome c reductase
CDW	Cell dry weight
CE	Counter electrode
CTAB	Cetyltrimethylammonium bromide
CV	Cyclic voltammetry
DCIP	2,6-Dichloroindophenole
DET	Direct (extracellular) electron transfer
DHB	2,4-Dihydroxybenzaldehyde
DPV	Differential pulse voltammetry
EDTA	Ethylenediaminetetraacetic acid
EET	Extracellular electron transfer
EPS	Exopolysaccharides
FEC	Ferricyanide
HNQ	2-Hydroxy-1,4-naphtaquinone
HPLC	High performance liquid chromatography
IET	Indirect electron transfer
LB	Lysogeny broth
MBH	Membrane-bound hydrogenase
MET	Mediated (extracellular) electron transfer
MIS	Mediator interaction site
MR	Methyl red
NADH	Nicotinamide adenine dinucleotide
NPN	N-Phenyl-1-naphthylamine
OCP	Open circuit potential
OD	Optical density
PEI	Polyethylenimine
PHB	Polyhydroxybutyrate
PMS	Phenazine methosulfate
RE	Reference electrode
RM	Redox mediator
RT-qPCR	Real-time quantitative polymerase chain reaction

Abbreviations (continued)

SDH	Succinate dehydrogenase
SH	Soluble hydrogenase
STC	Soluble tetraheme cytochrome
TCA	Tricarboxylic acid (cycle)
TTN	Total turnover number
WE	Working electrode

Symbol		**Unit**
E^0	Standard redox potential	V
E_m	Midpoint potential	V
F	Faraday's constant	C mol^{-1}
F(x, y)	Statistical F-value with lower (x) and upper (y) border	
p	Statistical significance	
I	Current	A
N	Number of revolutions	min^{-1}
Q	Charge transfer	C
qO2	Oxygen consumption rate	$mM(O_2)\ gCDW^{-1}\ h^{-1}$
R	Resistance	Ω
U	Cell voltage	V
V	Volume	L
z	Electron stoichiometry	
λ_c	Characteristic wavelength	nm

Chapter 1

1 Introduction

1.1 Microbial extracellular electron transfer

Electron discharge from organic substrates through microbial decomposition processes has been known for more than 110 years now, with the first mention in a publication by M. C. Potter in 1911 [1]. But still, the underlying mechanisms and potential applications are a matter of current research. In general, every living organism necessitates a mechanism for electron exchange with its environment. Electrons generated from oxidative processes must be expelled from the cell to establish a proton gradient across the membrane, in turn driving ATP synthesis [2]. ATP then serves as the primary source of energy in the cell. This so-called "respiration" process can occur with different electron acceptors. Under aerobic conditions, the terminal electron acceptor of the respiration chain is O_2. The lack of, or intermittent availability of O_2 in some areas of the environment (like marsh areas with tidal changes) necessitated the use of different acceptors (e.g., insoluble oxide minerals) for survival [3]. Some organisms developed mechanisms for nitrate reduction [4], while others can utilize Fe(III) or Mn(IV) oxides to dispose of their electrons [5].

A specific form of Fe(III) oxide reduction was found within *Geobacter sulfurreducens*. The organism forms conductive nanowires over several microns to reach the solid electron acceptor [6]. A comparable utilization of conductive appendices was made in *Shewanella oneidensis* [7], where the trans-membrane electron transfer mechanism has been recognized with great detail. In short, the membrane-spanning extracellular electron transfer (EET) pathway consists of multiheme cytochromes, transferring electrons from the quinone pool in the inner membrane to the extracellular electron acceptor. First in the chain is CymA on the inner membrane, transferring electrons from the quinone pool towards the soluble tetraheme cytochrome (STC) in the periplasm. From STC, electrons are transferred to MtrA, which resides within the

barrel protein MtrB spanning the outer membrane, and finally transferred onto MtrC. This heme protein is then accessible from the phase surrounding the organism, allowing the EET onto an acceptor in direct contact (Figure 1) [8,9]. Hence, the mechanism was termed direct electron transfer (DET).

Organisms without the aforementioned EET pathway are not necessarily excluded from the benefits of using alternative electron acceptors. Via soluble electron shuttles, naturally produced within the cell or artificially added in biotechnological applications, electron transfer is possible over large distances. These shuttle molecules, or so-called redox mediators (RM), need to be redox active, enabling reversible electron transfer reactions over multiple turnovers to achieve mediated electron transfer (MET). *Pseudomonas aeruginosa* applies this technique by producing phenazines, mediating electrons to distant electron acceptors, like O_2 [10], or in a technical environment, an anode [11]. This mechanism can be transferred on the genomic level to other hosts lacking the expression of a natural mediator [12]. Alternatively, the metabolic burden of producing the mediators in the first place can be eliminated by adding artificial mediators, like ferricyanide (FEC) [13]. However, it has to be mentioned, that mediator choice is crucial and based on multiple factors. These aspects are examined in greater detail in the Chapter 1.2.

In specific cases, microbes can also be provided with artificially added electron sources or sinks via their natural electron transfer pathways. For example, when the water-splitting reaction at the electrodes delivers H_2 and O_2 (Figure 1). This bioelectrochemical cultivation mode is then referred to as indirect electron transfer (IET).

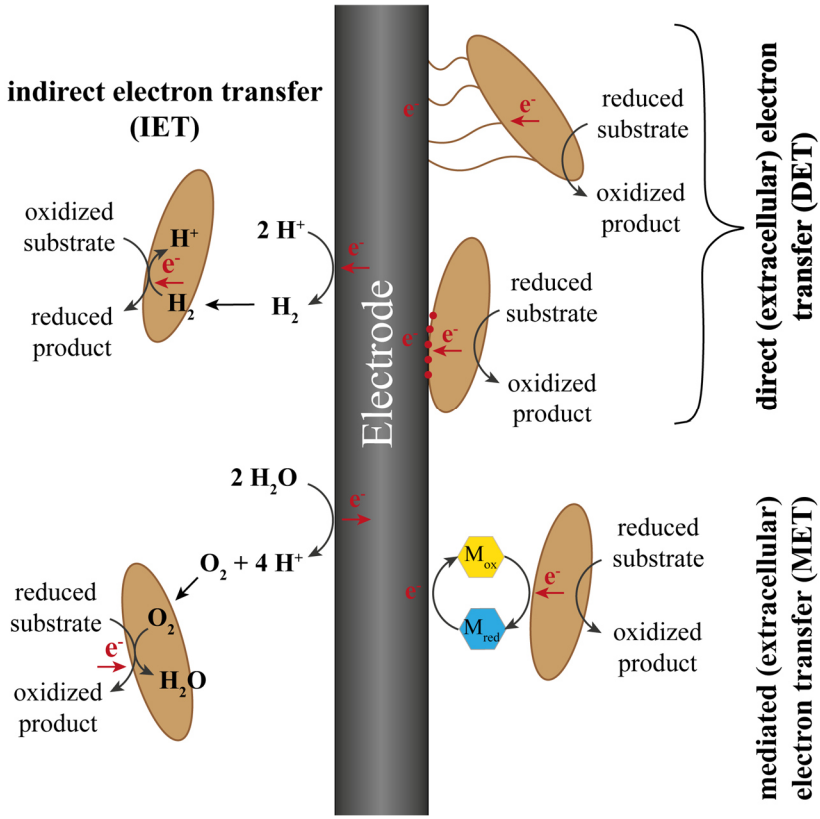

Figure 1: Known examples of mechanisms for electron transfer between microbes and an electrode. Adapted from [14].

1.2 Redox mediators

Redox mediators for bioelectrochemical applications are employed to couple electron transfer between microorganisms or enzymes and an electrode. They are based on many different molecular groups, like phenazines, thiazine and azo dyes, viologens, quinones, metal complexes, and flavins, to name a few. The diversity of these structures enables different physical properties, like multiple oxidation states, redox potentials, hydrophobicity, stability, solubility, cytotoxicity, and extinction characteristics. The extinction characteristics are especially valuable for process control. Some RMs present colorless leuco-forms upon reduction or oxidation, which enable the exact measurement of

the redox state. With all these characteristics and multiple compounds to choose from, several criteria for the shuttle molecules have already been raised in the literature [15,16]. These are:

- Defined electron stoichiometry
- Defined standard redox potential (E^0)
- Fast electron transfer
- Solubility in aqueous media at the relevant pH
- Stability in oxidized and reduced form
- No interference with optical monitoring of the microorganisms
- No interaction with the microorganism that alters the redox potential

Additionally, the molecular interaction site (MIS) for the RM can vary in different organisms. Therefore, it is preferable to know the MIS for the respective mediator in the process, to enable and potentially optimize electron transfer, e.g., by modifying membrane transfer if the MIS is located in the periplasm or cytosol. To elucidate more on durability, the long-term stability of a redox mediator throughout a batch process is critical for the sustained application of MET. Mediators within a bioreactor are subjected to various stresses, including physical factors (e.g., UV light), chemical factors (e.g., oxidative radicals), and biological factors (e.g., biodegradation), all of which can impact their long-term stability. Without enduring mediators, the electron transfer chain between the organism and the electrode weakens over time, ultimately leading to breakdown. Mediator loss over time is also conceivable through accumulation inside the cell, adsorption to cell membranes or electrodes, polymerization, or semi-reversible redox reactions at the electrodes. For future industrial applications, the reusability of the mediator is also desirable to reduce process costs. Of course, the mediator should also be biocompatible with the used microorganism and the environment, if downstream separation is not feasible.

To quantify the efficiency of any given mediator against another in a similar process, the total turnover number (often denoted as TTN, TN, or TON in the literature [17–19]) can be used. The TTN is a dimensionless parameter that quantifies the number of turnovers a catalyst can accomplish in a specific scenario. It has been widely

assessed and defined as the ratio of moles of product produced to moles of biocatalyst utilized [17]. The TTN for a respective mediator can be determined similarly, from the ratio of transferred electrons (measured as current) per total mediator molecules (either added or synthesized) under consideration of their stoichiometric electron transfer capability.

1.3 Bioelectrochemical systems

A microbial bioelectrochemical system (BES) is characterized by the combination of basic electrochemistry with a biotechnological cultivation system. In general, three electrodes are implemented for analytical purposes. A working electrode (WE) serves as an electron donor or acceptor for the respective microbes, while the counter electrode (CE) completes the electron circuit. A reference electrode (RE) is placed in direct vicinity to the WE, acting as the reference potential. Hence, the RE needs a constant potential with no current flowing through it during the experiment. A potentiostat is often used to apply a set potential to the WE while using the RE to control the potential. Keeping the WE and RE close together ensures minimal iR drop caused by the ohmic resistance of the electrolyte. The current is then measured between the WE and CE. Figure 2 illustrates the general setup of a BES with a potentiostat. In well-defined larger-scale production systems, the reference electrode can also be omitted. When the CE reaction leads to undesired side-products (like O_2 evolution), spatial separation of the two electrolyte chambers is imperative. This can be achieved via anion- or cation-exchange membranes, which separate higher molecular products and gases, but allow for charge balancing between both chambers.

In addition to the general capability of driving enzymatic or microbial reactions through electrochemical redox equivalents, BESs offer practical advantages. The foremost advantage is eliminating the need for O_2 transfer into the cultivation medium, a common challenge in scaling up aerobic stirred tank reactor processes [20]. This not only simplifies the operational aspects but also mitigates the risk of excessive foaming [12]. Established microbial electrochemical technologies, such as microbial electrosynthesis and microbial fuel cells, further expand the scope. Microbial electrosynthesis involves transferring electrons from the electrode through the metabolism of the microbe towards a desired reduced product, while microbial fuel cells

find applications in wastewater treatment, where electroactive bacteria degrade organic pollutants and transfer surplus electrons to the electrode, accompanied by electricity production [21,22].

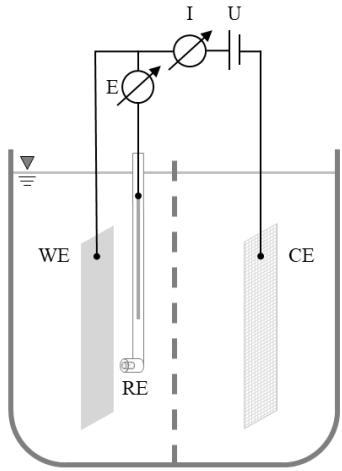

Figure 2: The principle three-electrode BES setup consists of two chambers, with the working electrode (WE) and counter electrode (CE) separated by a membrane (dashed line). The potentiostat controls the potential at the working electrode through the RE and measures the current flowing between WE and CE.

Defining the reactor geometry for a specific process requires knowledge of the underlying EET mechanism. With organisms relying on a DET, plate geometries with high surface-to-volume ratios become most viable, while MET processes need to be stirred and don't necessarily need large electrode surface areas, as long as recycling of the mediator is not limited by the electrode's surface [23]. The choice of electrode materials used depends on the application. Most often, carbon-based materials are chosen for their high biocompatibility, chemical stability, low cost, and high overpotential towards O_2 reduction [24,25]. The CE material can be adapted to the CE reaction, e.g., O_2 or water reduction. To prevent limitations, the CE surface area needs to be larger than the WE surface area. Therefore, mesh or tubular structures become useful, due to their high surface-to-volume ratio [26].

1.3.1 Stirred tank reactors

In stirred tank reactors, the entire reactor volume and the whole cell surface can interact with an electrode via RMs. Setups from recent literature offer high levels of process control with pH controlling and stirring options between magnetic stirring and Rushton turbines [13,27]. The scalability of these has been demonstrated on a laboratory level. The production of lysine on glucose with *Corynebacterium glutamicum* with anodic electron transfer via FEC has been successfully scaled up from 350 mL [28] to 2.4 L [29], achieving similar lysine production rates.

Though there are no large-scale processes for electrochemically supported productions yet, calculations have been performed to assess the competitiveness against established bioprocesses [30]. On the basis of an electroactive biofilm consisting of a model mixed culture of *Shewanella* and *Geobacter* strains, in theory, 2.5 g L^{-1} h^{-1} of acetoin could be produced assuming they deliver current densities of 600 µA cm^{-2} onto a graphite electrode [31]. At the same time, 1.34 L h^{-1} of hydrogen could be harnessed as an electrochemical by-product at the counter electrode. The calculation is also valid when changing the assumption of a biofilm to a mediated process. In turn, the same current would have to be delivered in a stirred tank reactor to surpass the typical industrial titers of >1 g L^{-1} h^{-1} [32].

It is further crucial to pre-screen various culture conditions, electrochemical potentials, and different electron shuttles, but the laboratory-scale reactors, which, despite their efficacy, require substantial effort for setup and maintenance. Furthermore, their sample size is usually on the lower end. These setups fall short of meeting the demand for rapid screening of different mediators and cultivation conditions. In traditional bioprocesses, a common approach to address this challenge involves downscaling and parallelizing established reactors while retaining the control capabilities of the system. This allows for more efficient and high-throughput screening of various factors in BES development [33].

1.3.2 Screening tools

Examples of automated and parallelized small-scale BESs for screening purposes have been developed over the past two decades. Via multiplexer potentiostats, even 96-well plates can be turned into a microbial fuel cell screening platform, as it has been demonstrated with *P. aeruginosa* in a two-electrode setup and a working volume of 5 µL [34] or a similar setup with unseparated chambers and a 1 mL working volume [35]. Both setups are capable of measuring the current density but prohibit a parallel photometric measurement for mediator characterization since it isn't recognized as a key performance parameter for microbial fuel cells. In the case of stirred tank BESs however, mediator characterization is crucial for an efficient process. A design published by Ley and co-workers for the investigation of a P450 monooxygenase library with the mediator cobalt sepulchrate as a substitute for NADPH could in theory be used for MET studies [36,37]. The device features 8 parallel channels in a 24-well plate with an unseparated three-electrode setup that can be used within a standard plate reader. However, the shaking has to be stopped for every measurement, and controlling the gas atmosphere requires an expensive plate-reader with the proper equipment or the use of a large anaerobic chamber. Therefore, the need for a rapid screening platform for MET-based systems is still not satisfied.

1.4 Electroactive microorganisms as production hosts

Besides the application of wastewater treatment or analytical uses, electroactive microorganisms are suitable for the production of bulk and fine chemicals. Hereby, the cellular redox metabolism can be affected by adding additional electron sinks or sources through electrochemical techniques. One example is the application of an unbalanced fermentation mode in *S. oneidensis.* Here, the limitation of a fermentative process leading to an identical average oxidation state of substrate and products [38] was overcome by adding an additional electron sink in the form of an anode. Thus, acetoin production on lactate was increased from 40 to 86% of the theoretical yield [39]. The same approach has been applied to *Escherichia coli* by Sturm-Richter and co-workers [40]. The *E. coli* strain was genetically engineered to express the *S. oneidensis* electron transfer chain cytochromes CymA, STC, and MtrA in combination with artificial methylene blue as RM.

With glycerol as substrate, the anode-supported fermentation mode led to an increased proportion of oxidized products in comparison to standard fermentation.

Turning the electron transfer pathway around to shift the redox balance towards reducing conditions can also be used to target specific products. In *Clostridium acetobutylicum*, the NAD^+ pool was regenerated by neutral red under cathodic conditions, in turn increasing butanol production significantly [41]. The possibilities have been further expanded by not only interfering with the redox balance but rather substituting the electron donor. This has been demonstrated with *Sporomusa ovata* growing on graphite cathodes, reducing CO_2 with the supplied electrons to acetate [42]. More examples of recent developments with anodic and cathodic production processes have been nicely summarized in a review by Kracke and co-workers [43].

1.4.1 *Vibrio natriegens*

Vibrio natriegens gained increasing attention in recent years owing to its remarkable capability to grow rapidly on various substrates. It is even recognized as the fastest-growing non-pathogenic microorganism on the planet, with a doubling time of under 10 minutes [44]. This attribute elevates expectations for *V. natriegens* as a promising host for broad-range production of low-molecular products, natural products (like beta-carotene), and protein expression [45,46]. The halophile bacterium depends on high salt concentrations in the environment, especially the availability of sodium ions [47]. In contrast to other organisms, *V. natriegens* exhibits adaptability in utilizing various electron acceptors, allowing it to thrive in fluctuating environments. It can donate electrons not only to O_2 but also to fumarate, nitrate, Fe(III) citrate, and fermentation products [3,48,49]. This raises the question, of whether *V. natriegens* is also able to transfer electrons to a solid electrode.

A recent study by Conley and co-workers proposed a hybrid EET mechanism, based on the pathways of *S. oneidensis* and *Aeromonas spp.* [3]. In their genomic analysis, a similarity of 77% for the cytoplasmic cytochrome CymA, and 68% for the periplasmic shuttle PdsA was observed between *V. natriegens* and the *Aeromonas spp.* analogue. The outer membrane electron transfer chain proteins MtrCAB exhibit the highest similarity to those found in *Aeromonas*

spp., with a 50% similarity to MtrC, 61-62% to MtrB, and 73-81% to MtrA [3]. With this hypothesized electron conduit in the membrane, an EET would be feasible for *V. natriegens*, but has yet not been demonstrated. The availability of an outer membrane cytochrome, in the form of a MtrC analogue, indicates the possibility of a DET. It has also been demonstrated, that *V. natriegens* can form biofilms on metallic surfaces [50,51], allowing for an effective DET. Alternatively, CymA, MtrA, and PdsA could be targets of mediators able to traverse the outer membrane. Therefore, the possibility of a MET is also given. In the case of *V. natriegens* transferring electrons onto an anode, it is expected that more oxidized products will be formed to keep the redox balance. This has already been demonstrated with *Propionibacterium freudenreichii* and *E. coli* before [52,53].

1.4.2 *Cupriavidus necator*

The Gram-negative and strictly respiratory β-proteobacterium *Cupriavidus necator* is among the most extensively researched industrially relevant "Knallgas" organisms. The bacterium underwent several name changes since its isolation in 1952 and is formerly known as *Hydrogenomonas facilis* [54], *Alcaligenes eutropha* [55], or *Ralstonia eutropha* [56], to name the most relevant. The bacterium promises to be a valuable production strain for multiple reasons. First, its ability to utilize a wide range of carbon sources such as fructose, organic acids, or glycerol in chemoorganotrophic cultivation facilitates process flexibility and reduces costs [57]. Furthermore, chemolithoautotrophic cultivation of *C. necator* utilizing "Knallgas", a gas mixture of H_2 and O_2, together with CO_2 as feedstock can be employed to produce valuable products such as α-humulene [58] or biopolymers like polyhydroxybutyrate (PHB) [59]. The product spectrum will most likely increase further over the upcoming decade since genetic accessibility and the necessary genetic tools are available [60,61].

In a bioelectrochemical context, isopropanol and α-humulene have been produced with a genetically engineered *C. necator* strain employing an IET mechanism [58,62]. Here, *C. necator* doesn't need to be electroactive in any form, since the applied potential supports water splitting into H_2 and O_2, while CO_2 is bubbled into the unseparated BES reactor to serve as carbon donor in the gas fermentation process. With a MET approach, *C. necator* exhibited effective extracellular electronic

interaction with different RMs. For instance, cultures of *C. necator* grown on 10 mM fructose demonstrated improved aerobic PHB production in the presence of the RM poly(2-methacryloyloxyethyl phosphorylcholine-co-vinylferrocene), which was recycled via an anode [63]. However, the attained current density of approximately 6.5 µA cm^{-2} was notably low, as O_2 was introduced as an additional electron acceptor into the working electrode chamber. In another approach, utilizing neutral red as RM and applying a constant current of 10 mA, the PHB yield was enhanced through cathodic supplementation of electrons [64]. This process was further improved in a recent study by Tu and colleagues [65]. In their work, the Mtr electron transfer pathway from *S. oneidensis* was implemented together with a *Gloeobacter* rhodopsin. The rhodopsin facilitated the generation of a proton motive force, while the Mtr pathway provided electrons for NAD^+ reduction to drive CO_2 fixation into biomass. Additionally, flavins were artificially introduced to enhance electron transfer from the cathode towards the Mtr pathway. Nevertheless, an anode working as the only terminal electron acceptor together with a suitable RM to substitute O_2 in "Knallgas" fermentation has not been demonstrated yet.

1.5 Aims and Objectives

The present thesis aims to resolve the MET mechanism of *C. necator* for the substitution of O_2 to enable CO_2 conversion with H_2 as an electron donor, eliminating the risk of explosive gas mixtures in bioreactors. In addition, a novel screening tool that imitates a stirred tank reactor is to be developed and applied for parallel rapid screening of diverse redox mediators with *C. necator*. The mentioned research questions and gaps are addressed in this thesis as pictured in Figure 3. The two phases of this thesis consist of a first phase including a literature overview of mediators and their proposed interaction sites as well as two technical tasks. These include the setup of stirred tank BES reactors and the development and verification of the screening tool. The second phase is then dedicated to reveal the underlying mechanism of mediated electron transfer of *C. necator* in a BES.

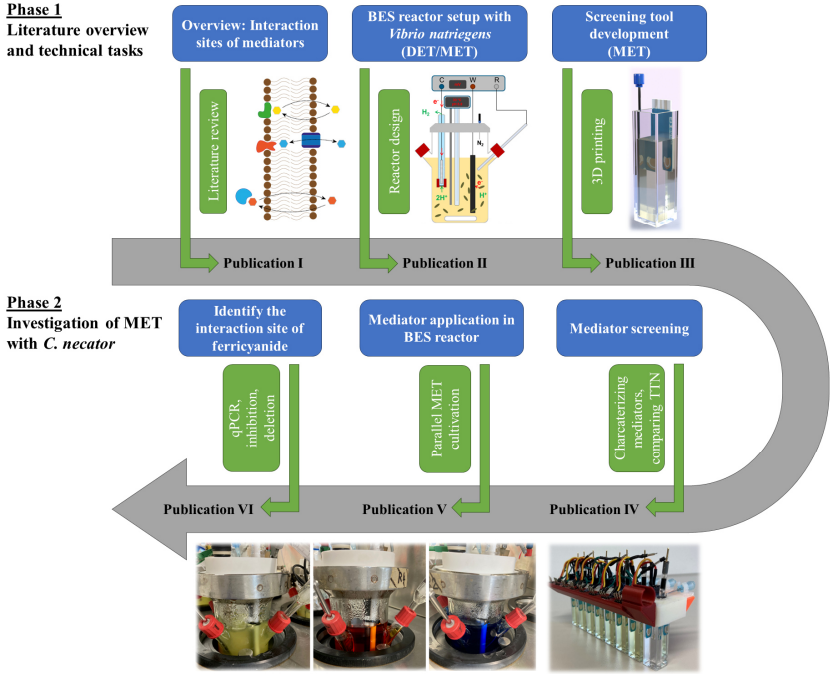

Figure 3: Graphical outline of the present thesis.

In Phase 1, a broad literature overview of the so far known or hypothesized MIS in different microorganisms is conducted. The resulting list of RMs with their respective potentials linked to MIS shall aid in RM selection and understanding of the EET mechanism in *C. necator*. The work was published in Publication I [14], attached in Appendix A.1:

> "Gemünde, A., Lai, B., Pause, L., Krömer, J. & Holtmann, D. Redox mediators in microbial electrochemical systems. *ChemElectroChem,* DOI: 10.1002/celc.202200216 (2022)"

At the same time, a lab-scale electrochemical reactor system is necessary for anodic cultivation in a controlled environment. To verify the setup, the fast-growing and potentially electroactive bacterium *V. natriegens* is proposed since it can most likely make use of a DET and MET mechanism. The detailed description of DET and MET with *V. natriegens* can be found in Publication II [66], attached in Appendix A.2:

> "Gemünde, A., Gail, J. & Holtmann, D. Anodic Respiration of *Vibrio natriegens* in a Bioelectrochemical System. *Chemsuschem,* DOI: 10.1002/cssc.202300181 (2023)"

To fill the gap of a parallel and automated screening device for MET applications, a cuvette-based system is to be developed and verified with literature known *P. putida* with ferricyanide as RM. The system shall be able to mimic the conditions in a stirred tank bioelectrochemical reactor as accurately as possible. The details of the device are described in Publication III [67], attached in Appendix A.3:

> "Gemünde, A., Gail, J., Janek, J. & Holtmann, D. e-Cuvettes parallelize electrochemical and photometric measurements in cuvettes and facilitate applications in bio-electrochemistry. *Biosens. Bioelectron. X,* DOI: 10.1016/j.biosx.2023.100378 (2023)"

In Phase 2, the developed screening device (e-Cuvettes) is used on a library of RMs combined with *C. necator*. For each mediator, the specific extinction wavelength (λ_c) is determined by spectroelectrochemical analysis. This enables online analysis of the RMs in 8 parallel channels. Abiotic controls and biotic triplicates of two RMs can be obtained at the same time in one batch. The work is published in Publication IV [68], attached in Appendix A.4:

> "Gemünde, A., Gail, J. & Holtmann, D. Redox mediator interaction with *Cupriavidus necator* – spectroelectrochemical online analysis. *Electrochem. commun*. DOI: 10.1016/j.elecom.2024.107705 (2024)"

The results gained via RM screening in e-Cuvettes are then verified in lab-scale reactors with four exemplary mediators. To assess the stability of the selected mediators, additional voltametric methods are employed. The details are published in Publication V [69], attached in Appendix A.5:

> "Gemünde, A., Rossini, E., Lenz, O., Frielingsdorf, S. & Holtmann, D. Chemoorganotrophic electrofermentation by *Cupriavidus necator* using redox mediators.

> *Bioelectrochemistry* DOI: 10.1016/j.bioelechem.2024.108694 (2024)"

For a more detailed understanding of the MET mechanism, the exact MIS of the most efficient RM, ferricyanide, is then investigated via RT-qPCR, a deletion mutant strain, and site-specific inhibition. Detailed knowledge about the MIS enables then further optimization of the process. As an example, the outer cell membrane of *C. necator* is perforated with a chemical permeabilization agent to effectively increase RM membrane transfer. A detailed description of the work is published in Publication VI [70], and is attached in Appendix A.6:

> "Gemünde, A., Ruppert, N.-L. & Holtmann, D. Unraveling the Electron Transfer in *Cupriavidus necator* – Insights Into Mediator Reduction Mechanics. *ChemElectroChem*, DOI: 10.1002/celc.202400273 (2024)"

Chapter 2

2 Materials and Methods

The scientific methodology used in this thesis draws from 5 published research articles, including a wide range of techniques. This section presents an overview of the methodologies, with more detailed descriptions available within the Publications included in Appendix A.

2.1 Chemicals

All chemicals used for this work were supplied by Merck KGaA (Germany), VWR Chemicals (USA), Carl Roth GmbH & Co. KG (Germany), Alfa Aesar (USA), or Sigma Aldrich (USA).

2.2 Strains and cultivation conditions

The strains used and their origin and cultivation conditions are listed in Table 1. Every strain was cultivated at 30 °C. Aeration was chosen depending on the process. The detailed media compositions can be taken from the associated Publications attached in Appendix A. Cryo stocks of each strain were prepared by adding 25% glycerol to an aerobic exponential culture and subsequent freezing at -80 °C.

Table 1: Cultivation media, origin, and associated publications of the strains used in this work.

Strain	Medium	Origin	Associated Publication
V. natriegens DSM 759	BHIN M1 M2	German Collection of Microorganisms and Cell Cultures GmbH (DSMZ)	II
P. putida KT2440	LB DM9	Helmholtz Centre for Environmental Research – UFZ (Leipzig, Germany)	III
C. necator PHB$^-$4	LB MMasy	German Collection of Microorganisms and Cell Cultures GmbH (DSMZ)	IV, V, VI
C. necator HF210	LB MMasy	Institute of Chemistry, Biophysical Chemistry, Technische Universität Berlin (Berlin, Germany)	VI

2.3 Bioelectrochemical reactor setup

This section provides a summary of two distinct bioelectrochemical setups. The first setup is used for pH-controlled cultivation within a parallel cultivation system. The second setup is specifically designed to replicate the aforementioned system, featuring 8 downscaled parallel cultivation chambers. Notably, this setup incorporates automated measurement capabilities for cell density, current density, and the redox state of the mediator.

2.3.1 Parallel stirred tank reactors

Four stirred tank BES reactors with a working volume of 300 mL, (SR0400SS, Eppendorf DASGIP, Germany) served as the cultivation chambers. To keep the media anoxic, 99.999% nitrogen was purged through the reactor headspace at 45 mL min^{-1} throughout the experiment (Figure 4a, b). When CO_2 was supplemented to the medium, 45 mL min^{-1} of 20% CO_2 in N_2 was added through micro spargers. A

polished graphite rod measuring 80 mm in length and 7 mm in diameter (Graphite 24, Germany), secured in position by a PTFE rod, served as the working electrode (Figure 4d). It was paired with a stainless-steel mesh counter electrode (1.4404, mesh size 0.1 mm, wire diameter 0.065 mm, Jaera GmbH + Co.KG, Germany), resulting in a geometrical surface area of 20 cm² (Figure 4c).

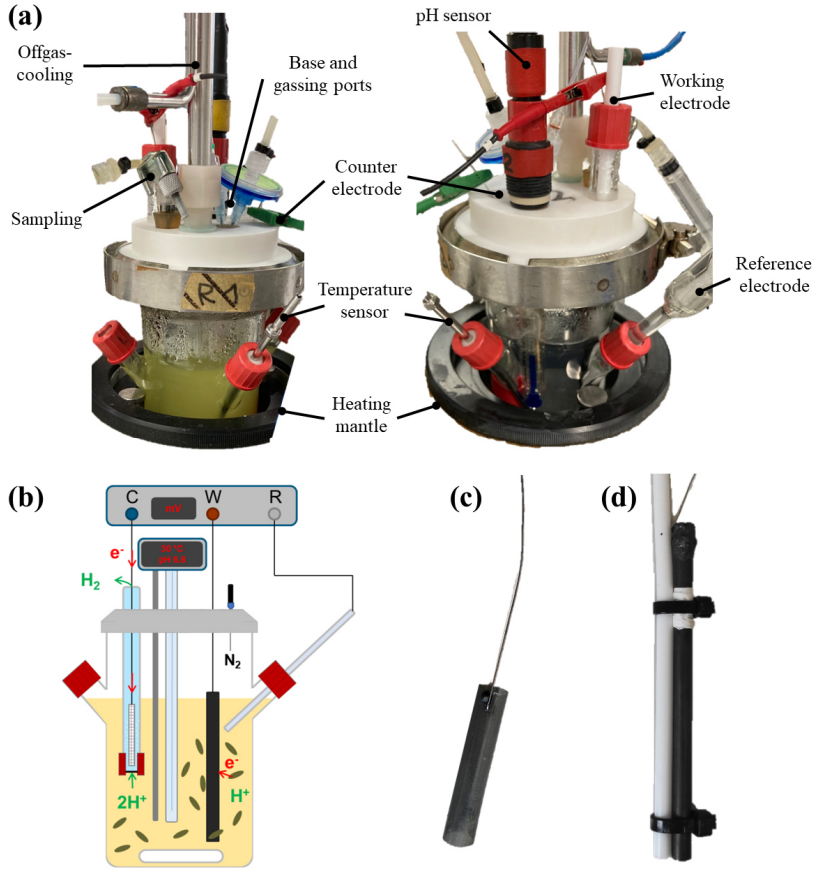

Figure 4: DASGIP bioelectrochemical reactor setup with peripherals (a). Scheme of the reactor with electron and proton flows (b). Stainless steel mesh cathode (c) and graphite anode with PTFE stabilization rod (d).

The anodic and cathodic compartments were spatially isolated from each other using a cation exchange membrane (Nafion117, QuinTech, Germany). The cathodic compartment consisted of a glass tube with threading on one end located in the anodic chamber and an open end at

the top, containing 10 mL of cathode buffer. As cathodic electrolytes, the buffers of the associated media (Table 1) were used. The exact composition can be found in the methods section of each paper attached in Appendix A.

The applied potential was controlled via a multi-channel potentiostat (MultiEmStat3+, PalmSens, Netherlands) and an Ag/AgCl (satd. KCl) reference electrode (Xylem Analytics, Germany). The device can't compensate for the ohmic drop originating from the resistance between the working and reference electrode. However, the estimated resistance values, ranging from 8 to 24 Ω in each reactor as determined by double potential step amperometry, were insignificantly small when compared to the applied overpotentials for mediator oxidation.

In general, an anodic overpotential of around 200 mV above the oxidation potential of the corresponding RM was applied to ensure a sufficient driving force for mediator oxidation. In case of the mediators being sensitive to light, the reactors were covered in aluminum foil to exclude light-induced decomposition. If the solubility in aqueous buffer allowed, the mediators were added from concentrated stock solutions into the anodic chamber 24 h after polarization of the electrodes started. The pH in the anodic chamber was regulated using pH sensors (Easyferm plus K8, 120 mm, Hamilton, Germany) in conjunction with Eppendorf DASGIP pH and pump modules. 2.5 M NaOH for MMasy medium and 5 M KOH for M1 or M2 medium was used to control the pH. This maintained a pH of 6.8 for MMasy and 7.5 for M1/M2 medium in the anodic compartment, while the cathodic chamber remained uncontrolled.

2.3.2 e-Cuvettes

The e-Cuvette system comprises 8 parallel 4 mL capacity polystyrene macro cuvettes (Th. Geyer GmbH & Co. KG, Germany) enclosed by a 3D-printed lid out of Rigur (RGD450) resin using a stereolithographic printer (Stratasys, USA). Peripheral attachments for cable and gas line management were printed from polylactic acid filament sourced from Prusa Research a. s. (Czech Republic).

The medium was filled to a maximum of 3.5 mL in each vessel to prevent overflowing. Sterile cannulas with a diameter of 0.6 mm (B. Braun, Germany) were inserted through holes in the lid for sparging and

mixing of the medium with sterile filtered 99.999% N_2 gas. Gas flow was individually regulated for all channels using needle valves (Wagner GmbH, Germany). Additionally, a wash bottle was incorporated to humidify the gas and reduce evaporation losses. The flow rates were set between 1.2 and 5±0.1 mL min^{-1} prior to each experiment, with each rate determined by water displacement in triplicates.

The three electrodes were introduced into each cuvette by submerging screen-printed electrodes (SPE, C220 AT, Deutsche Metrohm GmbH & Co. KG, Germany) into the medium. Each SPE comprised a working and counter electrode, both made from gold with a working electrode area of 0.125 cm^2, along with a silver pseudo-reference electrode printed on a ceramic backplate. All electrodes are connected to the top connector via paths of silver ink covered by a layer of insulating material (Figure 5e). The contacts are designed to fit into a circuit board plug on the 3D-printed lid, which is sealed with silicone against the surrounding atmosphere.

In total, two designs were developed. Both use the working and counter electrode on one chip. The difference lies in the use of the reference electrode. One design uses the pseudo Ag reference electrodes on the SPE (Figure 5a,b), while the other was modified to fit Ag/AgCl (3 M KCl) reference electrodes (Pine Research Instrumentation Inc., USA) through fittings in the lid (Figure 5c,d). The SPEs reference electrodes and lid underwent sterilization by immersion in 80% isopropanol for 5 min before being combined with the pre-filled sterile cuvettes and transferred into the automatic sampler of the photometer (Evolution 201, Thermo Scientific GmbH, Germany). The cultivation temperature was regulated using a thermostat (Julabo GmbH, Germany), which circulated water at 30 °C through the autosampler unit.

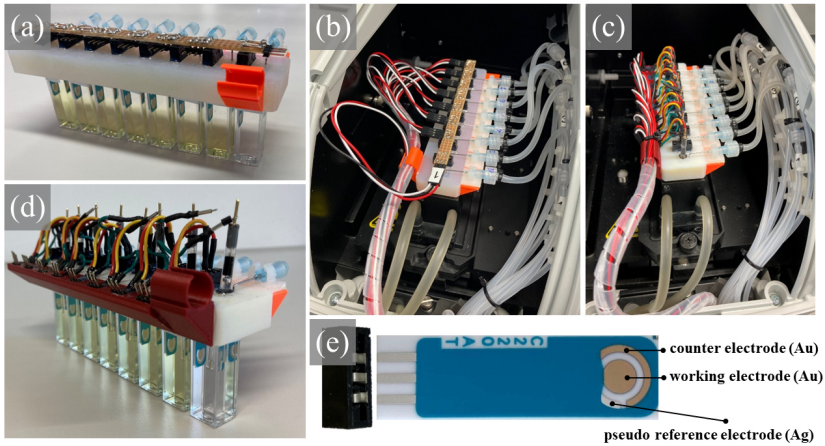

Figure 5: e-Cuvette setups from Publication III. Setup with pseudo Ag reference electrodes in use outside (a) and inside the photometer (b). Identical setup with the addition of Ag/AgCl reference electrodes (c, d). Screen printed electrode with the respective three-pin circuit board plug (e). Adapted from [67].

The extinction measurement is based on the spectroelectrochemical pre-screening of the respective redox mediator. Details on the process can be found in Chapter 2.4.2 and in Publication IV.

2.4 Analytics

2.4.1 Substrate and product quantification

Substrate and product quantification was achieved by HPLC analysis. Therefore, culture broth samples were first centrifuged at 16,900 x g at 4 °C for 5 min. The resulting supernatant was filtered through a 0.2 µm PTFE filter. HPLC analysis was conducted using an Agilent 1200 high-performance liquid chromatography system equipped with an Aminex HPX-87H column (Bio-Rad Laboratories GmbH, Germany). Concentrations of the substrates fructose and glucose were determined using a refractive index detector at 32 °C. The column temperature was maintained at 50 °C, and 5 mM H_2SO_4 at a flow rate of 0.6 mL min^{-1} was used for isocratic elution of the analytes. Fructose analysis in MMasy medium was conducted at a flow rate of 0.5 mL min^{-1}. Substrate and product standards were measured in 7 concentration steps within the relevant concentration ranges in every analysis. The corresponding areas were fitted using linear regression. The calibration

graphs have been published within the supplementary information of each Publication.

2.4.2 Spectroelectrochemical mediator characterization

Extinction characteristics of various mediators were determined via spectroelectrochemical analysis, combining spectroscopic measurements with cyclic voltammetry (CV). Here, a spectroelectrochemical cell kit in a quartz cuvette (AKSTCKIT3, Pine Research Instrumentation Inc., USA) was utilized. The electrode setup consisted of a gold working electrode with micro holes and a gold counter electrode on a ceramic substrate. A micro Ag/AgCl (3 M KCl) reference electrode (RRPEAGCL2, Pine Research Instrumentation Inc., USA) was submerged into the solution separately. The cell was maintained at 30 °C via a Peltier element and rendered oxygen-free by purging the headspace with N_2 (99.999%). To mitigate any pH fluctuations affecting the CV, measurements were conducted in 100 mM phosphate buffer (8.23 g L^{-1} Na_2HPO_4, 5.04 g L^{-1} NaH_2PO_4) at pH 7. Data acquisition was performed using a Gamry Interface 1010B potentiostat (Gamry Instruments Inc., USA) at scan rates of 50 and 10 mV s^{-1}.

2.4.3 Cell dry weight and optical density

The optical density (OD_{600}) was measured by assessing the absorption of the culture broth at 600 nm using a UV-vis spectrophotometer (Evolution 201, Thermo Scientific GmbH, Germany). To obtain the cell dry weight (CDW), samples of at least 10 to 20 mL of culture broth were collected and centrifuged for 15 min at 4 °C at 3214 x g (Centrifuge 5810 R, Eppendorf, Germany). The supernatant was then discarded, and the pellet washed in pure water to wash out inorganic media components. Subsequently, the cell suspension in water was dried and weighed simultaneously using a scale equipped with a heating element (Kern, Germany) until no further water loss could be measured.

2.4.4 Real-time quantitative PCR

Expression rates of genes encoding possible mediator interaction sites were determined via real-time quantitative PCR (RT-qPCR). Similar to qPCR reactions performed with *C. necator* mRNA in the literature, the housekeeping gene gyrB served as a positive control [71]. The cell's mRNA was prepared immediately after sampling from the cultures. Since all experiments were conducted in triplicates, mRNA extraction

was performed for each triplicate using the Monarch Total RNA Miniprep Kit (T2010, New England Biolabs - NEB, USA), following the protocol for tough-to-lyse samples from NEB (available online). An enzymatic lysis with 1 g L^{-1} lysozyme in 10 mM TRIS buffer (pH 8.4) at 25 °C for 5 min was carried out before adding Monarch RNA lysis buffer. During the extraction, an on-column DNAse I treatment (included in the Monarch Kit) was conducted to remove any DNA residues. Transcription into cDNA was performed using the Luna® Universal One-Step RT-qPCR Kit (E3005, NEB, USA) with a total RNA concentration of <0.05 g L^{-1}. The reaction setup was conducted as described in the associated manual. Primers were synthesized by Sigma-Aldrich and the sequences for the specific genes of interest are provided in the supplementary file (Table S1) of Publication VI. The transcription and qPCR reactions were conducted using an Agilent AriaMX qPCR system with the SYBR® scan mode. Relative gene expression rates were determined against aerobic control cultivations as the calibrator using the $2^{-\Delta\Delta Ct}$ method [72].

2.4.5 Electrochemical analysis

CV and differential pulse voltammetry (DPV) analysis were employed in a three-electrode setup to investigate interactions between redox-active species and the electrode. These species may include the microorganism, the mediator, as well as fermentation products or compounds from the cultivation medium. Each experiment was conducted with the gas and mixers turned off to maintain static conditions within the liquid phase. In CV experiments, the potential was then swept in the relevant potential range vs. Ag/AgCl (satd. KCl) for at least 5 cycles to ensure reproducibility. Detailed descriptions of these methods can be found in the method sections of the corresponding Publications.

2.4.6 Cell membrane permeability assay

Cell membrane permeability was assessed using the N-Phenyl-1-naphthylamine (NPN) uptake assay, following the methodology outlined by Helander and colleagues [73]. Each microbial culture sample was diluted in 5 mM HEPES buffer to achieve an OD_{600} of 1. A stock solution of the fluorescent probe NPN was prepared by dissolving in 5 mM HEPES to a final concentration of 40 µM. In a black, flat-bottom 96-well plate, 150 µL of each sample was combined with 50 µL of the NPN stock solution to achieve a final NPN concentration of

10 µM for the assay. Fluorescence measurements of the samples were conducted using a Synergy HT microplate reader (BioTek-Instruments, USA) at 30 °C, with excitation at 380 nm and emission at 405 nm, following an initial shaking step for 6 s.

2.5 Calculations

2.5.1 Midpoint potential and total turnover number

The midpoint potential (E_m) of redox-active substances was determined as the average of the anodic and cathodic peak potentials from CV measurements and calculated using the equation:

$$E_m = \frac{E_{ox} + E_{red}}{2}$$

The total turnover number (TTN) for a single mediator system was calculated as follows:

$$TTN = \frac{Q_{anode}}{F * M_{mediator} * z_{mediator}}$$

Were $M_{mediator}$ is the absolute amount of mediator in the system in [mol], $z_{mediator}$ represents the electron stoichiometry, meaning the number of electrons that can be transferred by the mediator in one turnover, and F is Faraday's constant (96485.3365 C mol^{-1}). Q_{anode} represents the charge transferred to the anode in [C] in the process. It is calculated by integrating the current curve from the inoculation onwards.

2.5.2 Carbon/electron recovery and coulombic efficiency

The carbon recovery was determined as the total carbon content in the products and biomass relative to the carbon content provided by the substrate. Electron recovery rates were determined similarly, by calculating the percentage of substrate-derived electrons present in the products and transferred to the anode. Further details on both equations are provided in the supplementary file of Publication II.

The coulombic efficiency (CE) was calculated following established methods in the literature [11,74]:

$$CE\ [\%] = \frac{Q_{anode}}{Q_{substrate} - Q_{products}} * 100$$

$Q_{substrate}$/$Q_{products}$ represent the charge present in the available substrate and the microbial products.

2.5.3 Relative anodic electron uptake

The O_2 demand for growing cells of the respective organism was taken from literature. The corresponding measure for anodic conditions is the electron uptake by the anode, expressed as mol(e^-) g_{CDW}^{-1} h^{-1}, where mol(e^-) is denoted as q and is calculated from the integration of the current curve. For O_2, this value can be converted to the unit of mol(e^-) g_{CDW}^{-1} h^{-1} using the equivalent electrons for the O_2 molecule (-2 per O atom). For anodic electron transfer, q can be calculated with respect to the CDW and cultivation time, and then compared to the value obtained with O_2 from the literature. This allows the determination of the percentage of respiratory anodic electron uptake relative to aerobic respiration. The concept was first introduced in Publication II and is described in more detail in the corresponding supplementary file.

2.5.4 Analysis of variance

The e-Cuvette screening tool was statistically assessed using a one-way analysis of variance (ANOVA) with the OriginPro® 2022 Software. Levenes's test [75] was applied to test the equality of variance between the experimental groups. These two groups contained two reference experiments each and were performed before and after the screening of different redox mediators. The Tukey test [76] was further applied to compare both experimental groups regarding the differences in TTN.

Chapter 3

3 Summaries of Publications

The following Chapter contains short summaries of the Publications which serve as the basis for this cumulative dissertation.

3.1 Redox Mediators in Microbial Electrochemical Systems

André Gemünde, Bin Lai, Laura Pause, Jens Krömer, and Dirk Holtmann

3.1.1 Summary of the Publication

Redox mediators (RM) enable electron transfer between otherwise non-electroactive microorganisms and electrodes in both ways. Despite their common use in microbial and enzymatic electrochemical systems, knowledge about the mechanism behind the electron transfer pathway remains scarce. In microorganisms, the molecular interaction site (MIS) of a RM significantly impacts the electron transfer efficiency in different ways. E.g., the location of the MIS within the cytosol, periplasm, or on the outer membrane determines the transfer kinetics. Therefore, in the present review, the membrane transfer of multiple RMs is discussed as a critical parameter for mediator selection. Furthermore, the so far known or hypothesized MIS for different mediators are summarized and connected with the standard redox potential (E^0) of the respective RM. The dataset is further expanded by summarizing the latest key characteristics for an ideal redox mediator, combining them with previous parameters reviewed in 1982 by Fultz and Durst [15].

Besides the mechanism of the MET, the overall process efficiency for a mediator-based BES needs to be considered. To quantify the effectiveness of a RM in a process, the TTN is suggested as a metric. This parameter enables comparison among RMs irrespective of their

concentration, while also considering their stability. Moreover, the downstream removal or recycling of the RM has to be considered as well, since some mediators are toxic to the environment and/or expensive in their acquisition. To date, research in this field is rather scarce. The so far suggested techniques, like ion exchange chromatography, membrane filtration, or photodegradation are reviewed and summarized.

The created database is meant to give researchers a tool for designing an efficient MET-based process, with the key parameters for mediator selection at their hand. Additionally, the summarized MIS can be used to hypothesize possible interaction sites of a given mediator for a detailed study of the MET mechanism.

3.1.2 Individual contributions of the author

The present review article [14] was published in the international peer-reviewed journal *ChemElectroChem* in 2022. My contribution to the Publication was the initial conceptualization and selection of the key parameters of a MET process to review from current literature. Additionally, I created all figures and tables and wrote the Chapters 1 to 4 of the manuscript.

3.2 Anodic Respiration of *Vibrio natriegens* in a Bioelectrochemical System

André Gemünde, Jonas Gail, and Dirk Holtmann

3.2.1 Summary of the Publication

The discovery of the extremely fast growth rate of Gram-negative *V. natriegens* led to high expectations as a production host for biotechnological applications. Besides the attribute as the fastest-growing bacterium known, *V. natriegens* also surpasses the substrate uptake of the biotechnological model production host, *E. coli*, by a factor of 2 in aerobic and anaerobic cultivation conditions [77]. The high ribosome count per cell may also benefit cell-free protein synthesis [78], while already available genetic tools increase the production spectrum significantly [45]. A recently proposed EET mechanism [3], resembling a combination of *Shewanella* and *Aeromonas spp.*, suggests a DET and MET mechanism should be possible with *V. natriegens*.

Hence, the present Publication explores the applicability of *V. natriegens* in a stirred tank BES via a MET and DET mechanism and the influence of bioelectrochemical cultivation on the product spectrum. Therefore, a commercial parallel fermentation system was equipped with a three-electrode setup to make use of the pH control system. MET to a carbon electrode was shown to be possible via ferricyanide as mediator and glucose as electron and carbon donor. The addition of CO_2 into the medium together with a regulated pH at 7.5 resulted in stable currents around 196 µA cm^{-2} and the production of typical fermentation products, mainly acetate, formate, and ethanol (Figure 6a,b). Without a mediator in place and with no potential applied, the anaerobic metabolism of *V. natriegens* led to reducing conditions in the cultivation chamber and similar products (Figure 6c,d). However, the additional electron sink in the form of an anode shifted the product spectrum towards lower formate and succinate yields and simultaneously higher acetate yields.

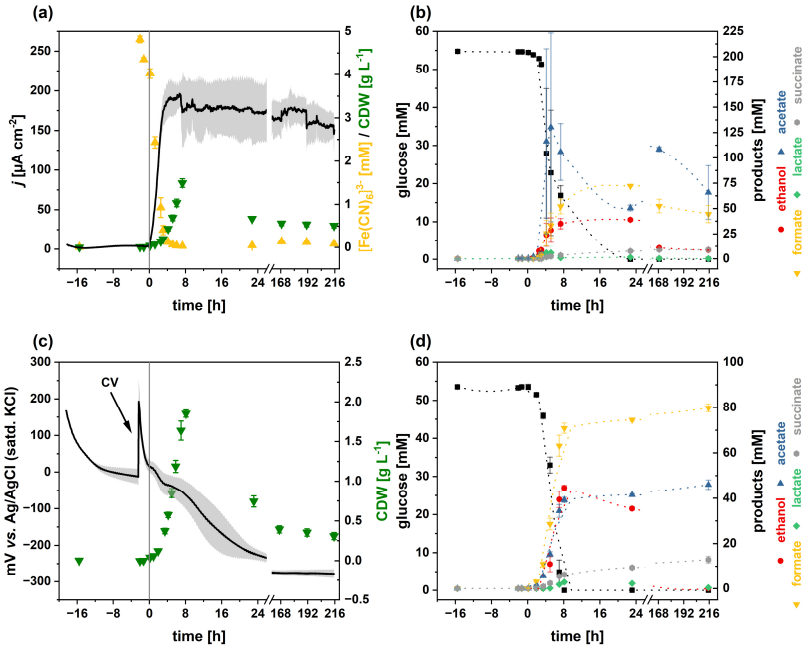

Figure 6: BES cultivation with applied potential *vs.* open circuit potential (OCP) cultivation of *V. natriegens* in M2 medium with supplementary CO_2. Current density (black line) at 500 mV *vs*. Ag/AgCl (satd. KCl), concentration of oxidized mediator (yellow) starting at 5 mM, and cell density measured by OD_{600} (green) (a). Poducts during BES/OCP cultivation (b,d). Glucose (black squares), ethanol (red dots), acetate (blue triangles), formate (yellow triangles), lactate (green diamonds), and succinate (grey circles). Identical experiment setup with no potential applied (OCP) and no mediator added (c).

Moreover, the experiments revealed the feasibility of a DET to an anode, but with a distinct reduction in current density to a maximum of 6.6 µA cm^{-2}. This can most likely be attributed to the low surface-to-volume ratio of the anode and provided the first experimental validation for the EET model as suggested by Conley and co-workers [3].

3.2.2 Individual contributions of the author

The present manuscript [66] was published in the international peer-reviewed journal *ChemSusChem* in 2023. My contribution to the work was the reactor design and setup, the process conceptualization, and the supervision of the experimental work performed by Jonas Gail. Furthermore, I wrote the entire original manuscript.

3.3 e-Cuvettes parallelize electrochemical and photometric measurements in cuvettes and facilitate applications in bio-electrochemistry

André Gemünde, Jonas Gail, Jürgen Janek, and Dirk Holtmann

3.3.1 Summary of the Publication

BES face similar challenges to traditional bioprocesses, necessitating extensive experimentation expenses to reduce the time to market. However, parallelization is hindered by the laborious setup of reactors and manual sampling. Establishing a BES further requires extensive pre-screening of electroactive organisms, culture conditions, electrochemical potentials, and electron shuttles. Current laboratory-scale BES typically utilize small double-chambered electrochemical cells, like the H-cell-type or even larger reactors [13,63,79], which demand for significant setup and maintenance efforts. Consequently, the rapid screening of mediators and cultivation conditions remains laborious and time consuming. Traditional bioprocesses often address this challenge by downscaling and parallelizing established reactors while maintaining the control capabilities [33]. The same approach led to the development of the novel e-Cuvette system described in the present Publication.

Here, commercial 4 mL macro cuvettes are converted into a BES by implementing screen-printed electrodes (SPE) and stirring through a continuous gas flow. This enables the use of soluble mediators in 8 parallel channels (see also Figure 5 in Chapter 2.3.2). The setup within a photometer enables parallel measurement of the redox state of the ferricyanide mediator and the cell density via online OD measurement. The design was evaluated using the well-known *Pseudomonas putida* KT2440 strain with ferricyanide as a redox mediator. Optimization of the gas flow rate was required for sufficient mixing, dissolved O_2 removal, and minimal evaporation loss over time. This led to stable currents over cultivation times up to 120 h with 4.5 mL min^{-1} N_2 sparged through each cuvette. The parallel extinction measurement

further enabled monitoring of ferricyanide reduction during the rising current phase, while microbial growth was not observed (Figure 7).

In addition to parallelization, a key advantage of the system is its working volume of 3.5 mL, enabling liquid sample taking during the process. Moreover, the system is capable of long-term experiments due to low evaporation rates, thus, complementing existing platforms for rapid process development. Nevertheless, the cell densities are limited to the lower range due to the photometric measurement.

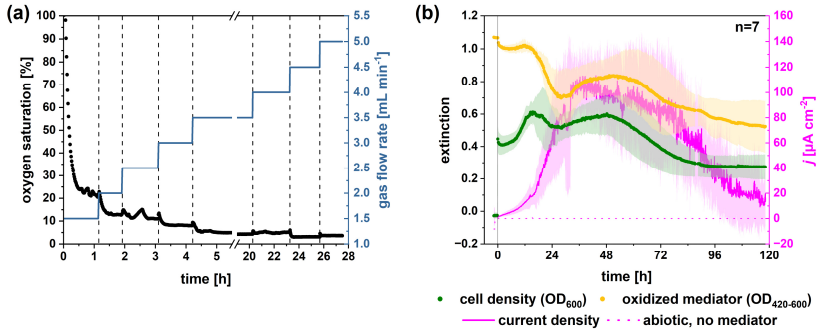

Figure 7: Oxygen saturation (black dots) at different gas flow rates (blue) in a single e-Cuvette (a). BES cultivation with the adapted N_2 flow rate of 4.5 mL min^{-1} at 500 mV *vs*. Ag/AgCl in 8 e-Cuvettes (b). Obtained current density (magenta), extinction of the oxidized mediator (yellow) and cell density at 600 nm (green) during 118 h of cultivation. Dotted line: abiotic control without mediator.

3.3.2 Individual contributions of the author

The work was published in the international and peer-reviewed journal *Biosensors and Bioelectronics: X* in 2023 [67]. My contribution to this work was the development and testing of the e-Cuvette apparatus, the development of all methods mentioned in the Publication, and the execution of the experiments. The original draft and all figures were also created by myself.

3.4 Redox mediator interaction with *Cupriavidus necator* – spectroelectrochemical online analysis

André Gemünde, Jonas Gail, and Dirk Holtmann

3.4.1 Summary of the Publication

Bioelectrochemical systems using *C. necator* as production organism offer a promising solution for utilizing H_2/CO_2 mixtures as substrates. By employing a mediated electron transfer to an inexhaustible electron acceptor in the form of an anode, O_2 can in theory be replaced to eliminate explosion risks, bypass gas transfer limitations into the cultivation medium, and avoid excessive foaming. So far, this process has not been demonstrated and lacks a model for extracellular electron transfer.

Based on the previously established e-Cuvette screening tool (Publication III) and the literature-based dataset (Publication I), a comprehensive mediator screening of 14 different redox mediators was tested with *C. necator* to gain insights about potential interaction sites for MET. All mediators were spectroelectrochemically characterized before the screening in triplicates to collect their E_m values and characteristic wavelengths (λ_c) for reduction rate kinetics.

Figure 8 depicts an overview for all 14 mediators in combination with *C. necator* in an anodic BES for 118 h. Here, different concentrations of the mediators have to be applied to achieve solubility and avoid oversaturation of the extinction measurement. This is compensated by calculating the concentration independent TTN and comparing the values for each mediator. In the end, both phenazines demonstrated high efficiency, with maximum reduction rates of 2.49 mM h^{-1} and 0.25 mM h^{-1} for PMS/PES, alongside a TTN of 5.16 and 6.15, respectively. However, their limited stability constrains their long-term applications.

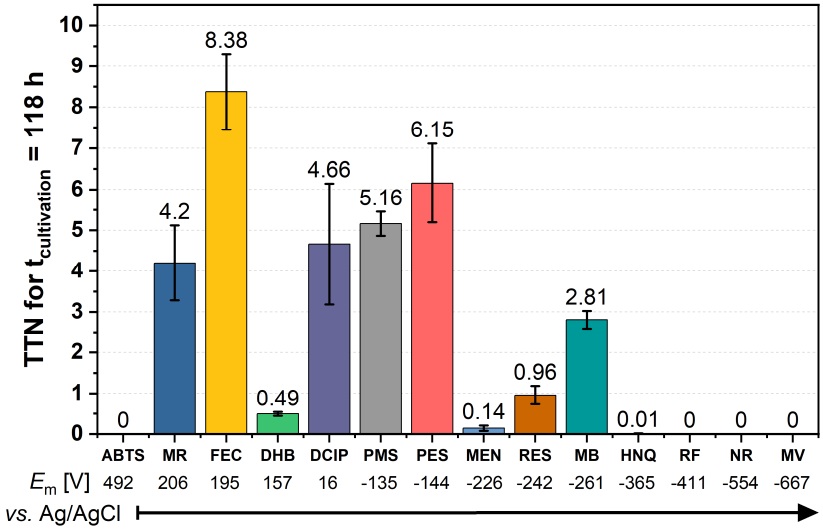

Figure 8: TTN for 14 redox mediators in biotic electrochemical cultivations over 118 h with their respective midpoint potential *vs.* Ag/AgCl (3 M KCl). Error bars depict the standard deviation for n=3.

FEC exhibited 8.38 turnovers while being reduced at a rate of only 49.43 µM h^{-1}. The selection of mediators demonstrated a cutoff E_m for anodic electron transfer below -365 mV *vs.* Ag/AgCl. Furthermore, the affinity of the mediators towards organic solvents was termed a secondary characteristic, as both hydrophobic and hydrophilic mediators yielded similar TTNs. Yet, optimal mediated electron transfer might require a combination of both types for an efficient process.

3.4.2 Individual contributions of the author

The work was published in the international peer-reviewed journal *Electrochemistry Communications* in 2024 [68]. My contribution to this work was the spectroelectrochemical screening of the mediators, the development of all methods mentioned in the Publication, and the data analysis of the experiments. Furthermore, I supervised the experimental work performed by Jonas Gail. The original draft and all figures were also created by myself.

3.5 Chemoorganotrophic electrofermentation by *Cupriavidus necator* using redox mediators

André Gemünde*, Elena Rossini*, Oliver Lenz, Stefan Frielingsdorf, and Dirk Holtmann

*Both authors contributed equally to this work

3.5.1 Summary of the Publication

Next to the electrochemical and spectroscopical characterization of redox mediators, the biocompatibility with the production strain has to be considered. The present Publication first explores the limits of biocompatibility of 11 out of the 14 mediators characterized and tested in Publication IV, before comparing 4 of the mediators in the larger scale BES reactors established in Publication II.

Growth rate analysis under non-electrochemical conditions with ascending mediator concentrations revealed high biocompatibility for ferricyanide (FEC), resazurin, and riboflavin. 2,6-dichloroindophenole (DCIP), phenazine metho- and ethosulfate, and methyl viologen on the other hand, exerted high stress on the cells and led to impaired growth rates at lower concentrations. With fructose as electron and carbon source in replacement for H_2/CO_2, anodic electron transfer was achieved between stationary *C. necator* cells and an anode in stirred tank BES reactors with FEC, DCIP, phenazine methosulfate (PMS), and 2-hydroxy-1,4-naphtaquinone (HNQ). Among these, FEC demonstrated 10-fold higher current densities than the other tested mediators with up to 260 µA cm^{-2}.

As already hypothesized for *P. putida*, the $[Fe(CN)_6]^{3-}$ molecule's high charge and hydrophilic nature likely hinder it from penetrating the hydrophobic cytoplasmic membrane [13,80]. Consequently, interaction with periplasmic electron-transferring proteins is most plausible. Outer membrane transfer is speculated to be achieved through natural outer membrane porins with sufficient pore size, such as OmpF in *P. putida* [13].

In contrast, membrane traversing of PMS and DCIP is very likely due to their lipophilic characteristics [81,82]. This alone, however, is not enough for a more efficient electron transfer process, resulting in low but stable current densities between 12 and 22 µA cm^{-2}. Furthermore, with the minor currents, substrate consumption was minimal which in turn means low production capabilities.

Differential pulse voltammetry (DPV) was further used to evaluate the stability of the mediator compounds over 195 h of anodic cultivation. The results indicate a side reaction occurring with artificially added PMS and decreasing peak currents for DCIP, which renders these mediators impractical for long-term cultivation.

3.5.2 Individual contributions of the author

The work was published in the international and peer-reviewed journal *Bioelectrochemistry* in 2024 [69]. My involvement in this study included the application of mediators in BES reactors and the electrochemical analysis detailed in Chapters 3.2 and 3.3 of the Publication. I also undertook conceptualization and initial drafting. This concept extends from Elena Rossini's mediator pre-screening for biocompatibility (Chapter 3.1), thereby, both of us are credited equally as authors of this Publication.

3.6 Unraveling the Electron Transfer in *Cupriavidus necator* - Insights into Mediator Reduction Mechanics

André Gemünde, Nils-Lennart Ruppert, and Dirk Holtmann

3.6.1 Summary of the Publication

The Publication is based on the previous Publications I, IV, and V, opening up the question of where exactly the so far most efficient redox mediator ferricyanide is reduced within the cell. With a solid model for MET in *C. necator*, optimization studies could be carried out to achieve O_2 substitution within a BES.

Therefore, in the present Publication, a method set was applied to narrow down possible interaction sites for ferricyanide in *C. necator*. First, targets for RT-qPCR were selected based on already available literature and mediator screening results. These qPCR targets were then compared regarding their expression rate between three conditions: chemolithoautotrophic cultivation with CO_2 as carbon source, H_2 as electron source, and O_2 as electron acceptor; heterotrophic conditions with fructose as carbon and electron donor and O_2 as electron acceptor; and anodic conditions with fructose and the anode as electron acceptor (Scheme 1). Previous work by Nishio and co-workers [63] revealed higher expression levels of three nitrate reductases (NapD, NarK, NasD) when a polymeric ferrocene mediator transferred surplus electrons to an anode during aerobic cultivation. In this work, nitrite reductase NirS proposedly plays a role, as evidenced by its 3.9±1.1-fold higher expression under anodic conditions. Additionally, the 2.9±0.6-fold increase in the expression of the natural porin OmpA under anodic conditions suggests its potential involvement in FEC uptake through the outer membrane.

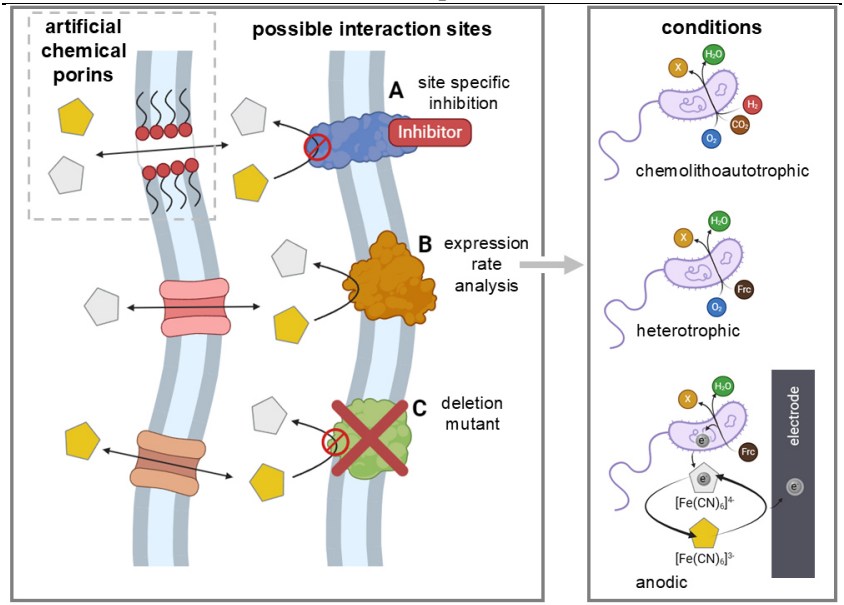

Scheme 1: Illustration of the aims of the study. Possible interaction sites of ferricyanide (pentagons, yellow: oxidized, grey: reduced) within *C. necator* are narrowed down via specific inhibition, applying a deletion mutant, and expression rate analysis comparing chemolithoautotrophic, heterotrophic, and anodic cultivation conditions. Furthermore, the influence of creating artificial porins with chemical permeabilizers on anodic electron transfer is studied.

In addition to qPCR, individual sites were specifically inhibited during BES cultivation, and a pHG1 megaplasmid deficient strain was used to elucidate the interaction sites encoded on the plasmid. Here, all sites on the pHG1 megaplasmid could be ruled out, since the pHG1 deficient strain delivered identical current densities compared to the non-deficient strain. Inhibition with 5 mM azide suggested cytochrome c oxidase as a reduction site, as evidenced by a decrease to 14% of the original current density post-inhibition, consistent with the findings of Ertl and Unterladstaetter [83] in *E. coli*. However, the specific inhibition with azide targeting the O_2 reduction site, which is not accessible for ferricyanide, results in an unclear mechanism for ferricyanide reduction.

Moreover, chemically permeabilizing cell membranes with cetyltrimethylammonium bromide doubled FEC reduction rates without an anode present, providing insights for optimizing redox mediation in *C. necator*-based BES.

3.6.2 Individual contributions of the author

The present manuscript [70] was published in the international peer-reviewed journal *ChemElectroChem* in 2024. My contribution to the work was the experiment design and setup, the conceptualization, and the supervision of the experimental work performed by Nils-Lennart Ruppert, who carried out the NPN assays. Furthermore, I wrote the original manuscript.

Chapter 4

4 Discussion and outlook

The present thesis describes extracellular electron transfer models in two Organisms, *V. natriegens*, and *C. necator*, mainly via redox mediators, and showcases a tool for parallel screening of these shuttle molecules. With the aid of a stirred tank reactor system, the screening results are verified on a larger scale, and mechanics of MET are explored. The following discussion sets the results of each Publication in context and evaluates the accomplished objectives. Additionally, future aspects obtained from the results are addressed.

4.1 *Vibrio natriegens* – a novel bioelectrochemical workhorse?

A detailed EET pathway of *V. natriegens* was proposed by Conley and co-workers [3] in 2020 via genetic comparison to *Shewanella* and *Aeromonas* EET genes. Together with the fast growth, it promises to be a novel bioelectrochemical workhorse. The EET pathway hypothesis comprises of the MtrCAB outer membrane conduit analogous to *S. oneidensis*, a soluble cytochrome for periplasmic transfer derived from *Aeromonas* spp. (PdsA), and a CymA alike tetraheme cytochrome on the cytoplasmic membrane (see also Figure 1 in Publication II). The pathway should enable a DET through the MtrC outer membrane cytochrome, which can be proven via BES cultivation.

By demonstrating an anodic DET with pure *V. natriegens* cultures leading to current densities of up to 6.6 µA cm^{-2}, the presence of outer membrane cytochromes could be proven (Figure 4 in Publication II). A functional MET demonstrated with FEC further supports the availability of an outer membrane cytochrome. It has to be considered though, that FEC is most likely able to enter the periplasm through natural porins [13], which opens up the possible interaction sites to periplasmic MtrA, PdsA, and CymA analogues of *V. natriegens*. If the

CymA analogue is used for anodic respiration in parallel to fermentation, it has to be verified if this analogue can contribute to the proton motive force to drive ATP synthesis. In *S. oneidensis* CymA itself doesn't act as a proton translocating respiratory enzyme, but contributes to the proton motive force by oxidizing the quinone pool, in turn transferring protons into the periplasm [84].

In the MET process, the addition of 1 mM FEC leads to a maximum of 157 µA cm^{-2}. Now, the significantly higher current density compared to a DET can be explained by the number of cells available for anodic electron transfer. *V. natriegens* didn't form dense biofilms on the polished graphite electrode, which reduces the cell count performing anodic electron transfer drastically. By adding FEC, every cell in the bulk medium is now able to direct electrons towards the anode. The efficiency of DET *vs.* MET in *V. natriegens* can therefore not be evaluated. For this, the same number of cells would have to be employed with both mechanisms, to compare electron transfer kinetics.

A cultivation study by Hoffart and co-workers [77] together with the work published by Thoma and colleagues [85] suggested the addition of CO_2 into the medium to facilitate the reductive tricarboxylic acid (TCA) cycle through the anaplerotic reaction of pyruvate to oxaloacetate or malonate, which requires CO_2. This, together with a constant pH at 7.5 and an increased FEC concentration of 5 mM resulted in stable currents around 196 µA cm^{-2} and total FEC reduction in the bulk medium. The total reduction of the mediator suggests that even the higher FEC concentration of 5 mM still limits the electron transfer efficiency. Now, the electron conduit proposed by Conley and colleagues can't be exactly verified via the demonstration of anodic electron transfer alone, since the interaction site of FEC is unknown. However, the current EET model fits the experimental observations.

With the EET capabilities demonstrated, the question arises, whether the additional electron sink in the form of the anode influences the metabolism of *V. natriegens*, like it was observed for unbalanced fermentation mode in other organisms (see Chapter 1.4). From the observed yields with the CO_2 supplemented BES, it can be deduced that with an anode as only electron sink, less formate (0.209 g g^{-1}) and succinate (0.109 g g^{-1}) are produced than under open circuit (OCP) conditions (0.381 g g^{-1} formate and 0.159 g g^{-1} succinate), where

fermentation is the only respiration mode available. In contrast, anodic conditions lead to more acetate (and therefore CO_2) with 0.403 g g^{-1} in anodic *vs.* 0.286 g g^{-1} in OCP conditions and more biomass (0.048 *vs.* 0.018 g g^{-1}). This result is unexpected, as the presence of an extracellular electron acceptor (e.g., O_2) typically results in reduced acetate accumulation, as observed in studies comparing metabolites under aerobic and anaerobic (or micro-aerobic) conditions [44,77,86]. For instance, aerobic cultivation on glucose yielded 0.193 g g^{-1} acetate, whereas anaerobic conditions produced 0.177 g g^{-1} acetate [77]. Overall, the alteration of the metabolism in *V. natriegens* observed in the results of Publication II is marginal when comparing anaerobic fermentation to unbalanced fermentation with an additional electron sink, despite the high current densities recorded. To get a better view of the dimensions of the current density, the concept of relative anodic electron uptake *vs.* respiration on O_2 was introduced. In brief, the method calculates the ratio of electrons that are taken up by the anode instead of being transferred to O_2 from growing *V. natriegens* cells (see also Chapter 2.5.3). The value obtained stays below 1.4% during the whole cultivation period, demonstrating that anodic electron transfer only has a small impact on the overall respiration, which is again represented in the product spectrum discussed before.

In general, the oxidation state of substrates and products should remain equal on average. However, oxidized products outweigh the identified reduced product (ethanol) by far. Additionally, in both OCP and anodic conditions, ethanol is taken up again from the fermentation broth. By comparing the electron and carbon recovery (Figure 9), a gap in the carbon and electron recovery is clearly visible. To close the carbon and electron gap in the experiments, another yet unidentified reduced product has to be produced, since the anode only makes up for up to 6% of the electrons, and no further products were identified. Hoffart and co-workers [77] identified the amino acid alanine in non-growing *V. natriegens* cultures in high amounts of up to 0.31 g L^{-1} (3.5 mM). The reduced amino acid could compensate for the redox balance but was not detected via HPLC with an evaporative light scattering detector. To close the minimum of 20.6% in carbon recovery for anodic conditions and supplemented CO_2, 26.7 mM of alanine would have to be produced. This, however, is unreasonable comparing the literature value. Additionally, HPLC analysis would reveal such high concentrations in cultivation supernatants.

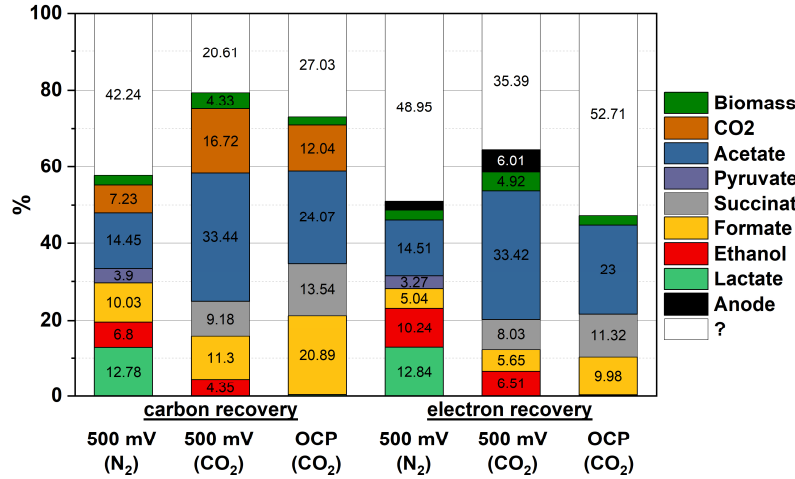

Figure 9: Carbon and electron recovery in BES reactors after 216 h of cultivation from the substrate glucose in %. Additional carbon due to CO_2 addition could not be quantified and is therefore left out. The respective conditions are mentioned below each bar. Data points represent the mean values of triplicates. Error bars have been omitted for clarity.

Therefore, the gap in the balance has to be attributed to more reduced products. An additional electron sink in the medium is of course the 5 mM of ferricyanide itself being reduced entirely. Nevertheless, this makes up for only 0.3% of the total electrons available through glucose and can be disregarded.

Since the release of Publication II, new insights about the production of exopolysaccharides (EPS) in *V. natriegens* were gained. A study by Schulze and colleagues in 2024 [87] reported an EPS formation of up to 0.157±0.020 g L^{-1} with the wild-type strain. These carbohydrate polymers are excreted from the cell and facilitate biofilm formation alongside with protection of the cell from environmental stress factors [88]. The analysis of the carbohydrates in the EPS of *V. natriegens* revealed a content of 53±6% glucose, alongside 14±4% galactose, and 12±4% rhamnose, to name the most dominant parts. Still, the marginal amount of EPS formed cannot compensate for the huge gaps in the balance.

This gap has also been reported in the literature with 12% of the carbon atoms missing from glucose as substrate and has since been closed by intracellular flux distribution analysis [85]. Here, the CO_2 release in the oxidative TCA cycle accounts for an additional 10% of the missing carbon atoms derived from glucose. In Publication II, the amount of CO_2 released was calculated based on the amount of acetate produced in a 1:1 ratio, and the oxidative TCA cycle was found not to be active under BES conditions since no succinate was produced without the addition of CO_2. This, and the fact that CO_2 release cannot make up for the gap in the electron balance, results in a still unidentified by-product.

To summarize, *V. natriegens* is a promising new strain for microbial electrochemical applications for multiple reasons:

- Its flexibility to use a DET and MET pathway with a well-defined and experimentally confirmed model of complexes involved
- The observed high current densities with FEC
- The stable current over long cultivation periods, even when glucose is metabolized
- The availability of genetic tools for further applications

Still, the metabolism is not significantly altered with the unbalanced fermentation pathway. Nevertheless, higher mediator concentrations might enable even higher current densities, in turn diverting more electrons towards the anode leading to a more significant shift in the product spectrum.

4.2 Parallel redox mediator screening

A wide variety of different redox mediators are available for bioelectrochemical applications with little information about their exact interaction site or membrane transfer characteristics (see Publication I). Additionally, the number of tools available to identify suitable redox mediators for a given task in a reasonable time is scarce. With the e-Cuvette system presented in Publications III and IV, the screening times can be reduced significantly, and screen-printed electrodes (SPE) allow for easy changes of electrode materials and the use of different coatings.

Nevertheless, the use of SPEs comes with two major drawbacks. Firstly, the physical stability of the pseudo reference electrode was termed insufficient for cultivation periods up to 120 h, as the material visibly deteriorated (see also supplementary file of Publication III). Secondly, the anode and cathode are not spatially separated. This allows for side reactions of electrochemically active compounds (like the mediator or metal oxides) at both electrodes. Using FEC as an example, at the start of an experiment, 100% oxidized $[Fe(CN)_6]^{3-}$ is present. With a potential difference of 500 mV between the electrodes, $[Fe(CN)_6]^{3-}$ is reduced to $[Fe(CN)_6]^{4-}$ at the cathode (Figure 10a). This reaction was observed experimentally in abiotic control cuvettes. Figure 10b depicts the extinction values of $[Fe(CN)_6]^{3-}$ in yellow in an abiotic cuvette over 120 h at 500 mV. The concentration of $[Fe(CN)_6]^{3-}$ declines linearly while the current increases equally linear (magenta line). A reducing reaction from a contaminant microbe was ruled out since OD_{600} measurements showed no increase over time. The spatial separation of the electrodes, e.g., through a membrane, is therefore highly desirable for further iterations of the e-Cuvette system.

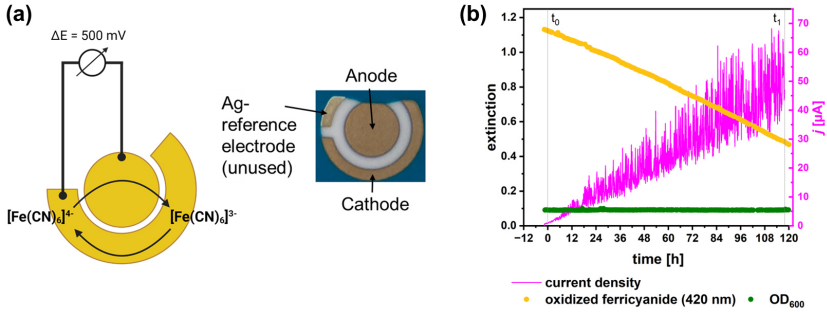

Figure 10: Possible side reaction of FEC at the cathode and the SPE arrangement (a). Observed current (magenta line) and extinction values for FEC (yellow) and cell density (OD_{600}, green) in an abiotic control cuvette with 1 mM FEC polarized at 500 mV.

When screening methods or devices are designed, the robustness of the system is key. The robustness of the e-Cuvette system has not been evaluated within Publications III and IV yet. The precision (as a measure of the spread of the measured TTN values) and stability (as a measure of repeatability with the same conditions applied) can be evaluated with reference experiments conducted before and after the screening of the different redox mediators. Accuracy, as a value of deviance from the true value, can't be assessed though, since the "true value" of the TTN of FEC with *C. necator* during BES cultivation is unknown.

Now, a one-way ANOVA was conducted to evaluate the difference in TTN with FEC before and after the screening of the different redox mediators. In both stages, before and after the screening, two experiments were conducted (pre- and post-validation). The hypothesis was defined as equal mean TTNs across all groups. Levenes's test revealed a significance of $p = 0.181$, which is determined non-significant. Hence, equal variances within the groups were assumed. Between the two experimental groups, the difference in TTN is statistically significant, with $F(3, 13) = 22.8$, $p < 0.001$, leading to the alternative hypothesis, that the mean TTN differs between the two groups. The Tukey test [76] was further used to compare each experiment within both groups for their mean TTN. It revealed that within pre-validation experiments and post-validation experiments that were conducted in a short time period the mean TTN doesn't differ significantly (1.68 to 1.03 mean difference, Figure 11). However, the

mean TTN between both groups diverges significantly, with the mean difference TTN values ranging from 3.34 to 6.05. Here, the up-scaled reactor can be used as reference, reaching a comparable TTN of 4.18 with a graphite electrode (see Publication V).

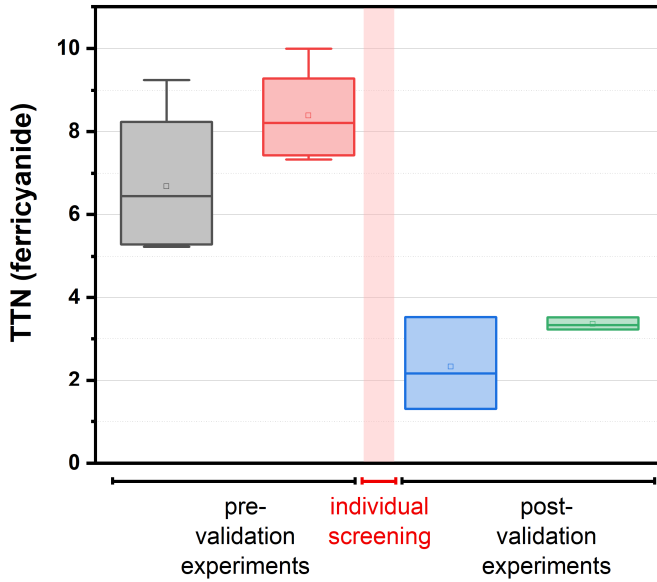

Figure 11: Mean TTN values of reference experiments with FEC as box-plots before and after the screening of different mediators.

To summarize, the precision of the screening tool can be evaluated as very high with low standard deviations within a single experiment. The stability can be termed as sufficient over short time periods. Long-term experiments with multiple setups of the screening system therefore need statistical verification with a reference cultivation in between. The error can most likely be attributed to minimal changes in gas flow rate due to the manual operation affecting the mass transfer kinetics within the cuvettes.

With this, the screening results of *C. necator* published in Publication IV can be evaluated. First of all, the general interaction of each mediator with *C. necator* is not prone to any error caused by the setup. The mediator can only interact or not interact. To summarize these interaction results, a potential window between -365 and 206 mV *vs.* Ag/AgCl (Figure 8) was observed, where mediator reduction can take

place at the respective interaction site. Comparing the interacting mediators with the literature data collected in Publication I, hypothetical interaction sites can be deduced and further analyzed.

FEC is hereby one of the most studied mediators, with hypothesized interactions involving cytochrome c reductase (CcR), soluble cytochrome c, and cytochrome c oxidase (CcO) [28,80,83]. For methyl red (MR) and 2,4-dihydroxybenzaldehyde (DHB), little is known so far for their interaction with whole cells. MR can most likely penetrate the membrane and interact with intracellular NADH, as postulated for yeast cells [89]. The resulting TTN with the use of DHB (0.49) suggests an inefficient electron transfer, hence the mechanism was not further looked into.

The E^0 of DCIP (217 mV *vs.* SHE) fits that of cytochrome c1 in the CcR complex (220 mV *vs.* SHE) [90], adding further to the hypothesis that CcR plays a major role in MET of *C. necator*. Both phenazines possess lower redox potentials than CcR and it has been reported that phenazine methosulphate oxidizes a periplasmic hydrogenase from *Dehalococcoides ethenogenes* [91], leading to the assumption that hydrogenases from *C. necator* could also take part in MET. The reduction rates of the phenazine sulphates that were determined in Publication IV, surpass those of other mediators by far. Given the lipophilic character of these molecules and their known affinity towards the intracellular electron transfer chain [11,81], the interaction with NAD(P)H is also feasible. Interaction of menadione was previously linked to acting as a replacement for ubiquinone, due to the similar base structure and redox potential. This would enable menadione to oxidize succinate dehydrogenase (SDH) in the respiration chain [90]. However, the TTN was very low and the growth rate massively reduced from 0.011 h^{-1} to 0.003 h^{-1} (see Publication IV, Table 2). These undesired effects exclude menadione from further investigations. Both resazurin and methylene blue have been shown to oxidize *Shewanella*-specific membrane-spanning cytochromes (CymA, MtrA, MtrC, STC, OmcA) [92,93], which are not present in *C. necator*. HNQ on the other hand, is most likely able to interact with the quinone pool directly via various quinone reductases [94]. However, the resulting TTN from screening suggests the interaction is too small to play a significant role in MET. While these screening results together with literature data can build a

solid hypothesis for MET mechanisms, a definite experimental proof is still necessary.

As a final proof of concept, results from the e-Cuvette screening system were reproduced qualitatively in larger-scale stirred tank reactors that have been established with *V. natriegens* in Publication II. Comparing the 4 RMs, FEC, phenazine methosulfate (PMS), DCIP, and HNQ should yield roughly identical current density curves between the reactor and e-Cuvettes, assuming equal mixing and electrode interaction. However, the more inefficient mass transfer within the cuvettes due to the mixing via gas sparging is already known. Additionally, e-Cuvettes use gold electrodes compared to graphite in the reactor and concentration ranges for RMs are lower in e-Cuvettes, to prevent saturation of the extinction measurement. Figure 12 depicts current density curves measured in e-Cuvettes and a stirred tank BES from Publication V in the same scale with the different concentrations added to each curve. For PMS and DCIP, the e-Cuvette system mimics the current density curves with the expected lower currents values.

FEC, on the other hand, performs differently in e-Cuvettes. The current rises slowly, opposite to the immediate rise in the stirred tank vessel. Later on, the current drops in a stirred tank, while it continues to rise within the cuvettes. While it was generally believed that gold electrodes are inert, recent interaction studies between gold electrodes and ferricyanide revealed a competing reduction of the gold electrode forming $Au(CN)_2^-$ and consequently dissolving the electrode [95]. Whether this affects the e-Cuvette performance needs to be further investigated. Nevertheless, the highest current densities can be reached with FEC, making it the best available RM so far discovered. Within the comparison, only HNQ delivers exceptionally low currents, not comparable to a BES reactor cultivation.

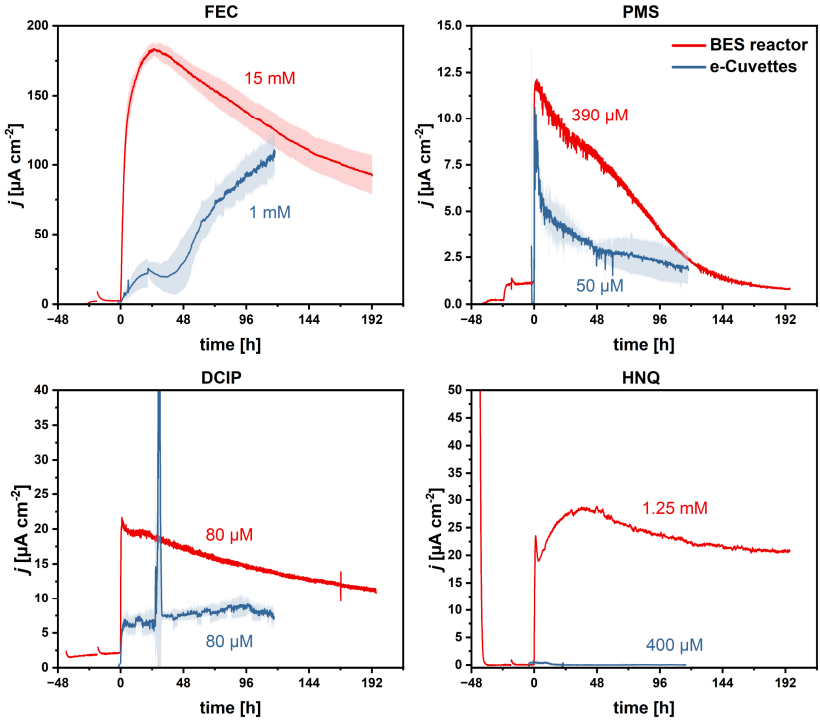

Figure 12: Comparison of current densities between stirred tank BES (red lines) and e-Cuvettes (blue lines) for 4 mediators with their respective concentrations (FEC: top left, PMS: top right, DCIP: bottom left, HNQ: bottom right). Data combined from Publication IV and V. Conditions: MMasy medium with 4 g L^{-1} fructose, anodic polarization. BES reactor: V=300 mL, N=400 rpm, n=1; e-Cuvettes: V=3.5 mL, 3.5 mL min^{-1} N_2, n=3.

These results underline the capability of the e-Cuvette system. It is primarily usable to pre-screen and compare the interaction of different RMs with high precision, and has secondary use for the sufficient scale-down of the 300 mL batch reactor system, which requires a lot of time and resources to set up.

4.3 Anodes as alternative electron acceptors for *C. necator*

C. necator reached high current densities of up to 183±5 µA cm^{-2} within triplicate BES cultures with 5 mM FEC and a graphite anode poised at 500 mV *vs.* Ag/AgCl (satd. KCl). This is comparable to the value reached with *V. natriegens* (196 µA cm^{-2}) and even higher than literature values of *P. putida* F1 producing 2-ketogluconate with FEC as mediator reaching a maximum current density of 66 µA cm^{-2} [74]. The CE is calculated with 63.1±5.7%, without any products detectable in HPLC analysis. Therefore, around 37% of the available electrons from consumed fructose are not (yet) transferred to the anode and are presumably used within the metabolism.

To assess if the target of substituting O_2 in BES cultivation was achieved with the reached current density, the relative anodic electron uptake *vs.* O_2 was calculated as described in Publication II. Therefore, the specific O_2 consumption rate (qO2) was taken from literature. Under chemolithoautotrophic conditions with O_2 concentrations below toxic limits for *C. necator*, 1.4 mM(O_2) g_{CDW}^{-1} h^{-1} was proposed [96,97]. Using this value for the calculation of relative anodic electron uptake within the BES cultivation, stable values between 10 to 12% *vs.* O_2 in comparison to the literature value were achieved (Figure 13). This gives an idea of how many more electrons need to be transferred to achieve equal cultivation conditions in a BES without supplying O_2. However, since MET is apparently not limited by mediator concentration for *C. necator* (see Figure 1 in Publication VI), it remains unclear how the electron transfer capabilities can be increased by a factor of 8-10 to achieve 100% relative anodic electron uptake. One option could be to increase the concentration of available mediator molecules at the interaction site through enhancing membrane transfer, which is further discussed in Chapter 4.5.

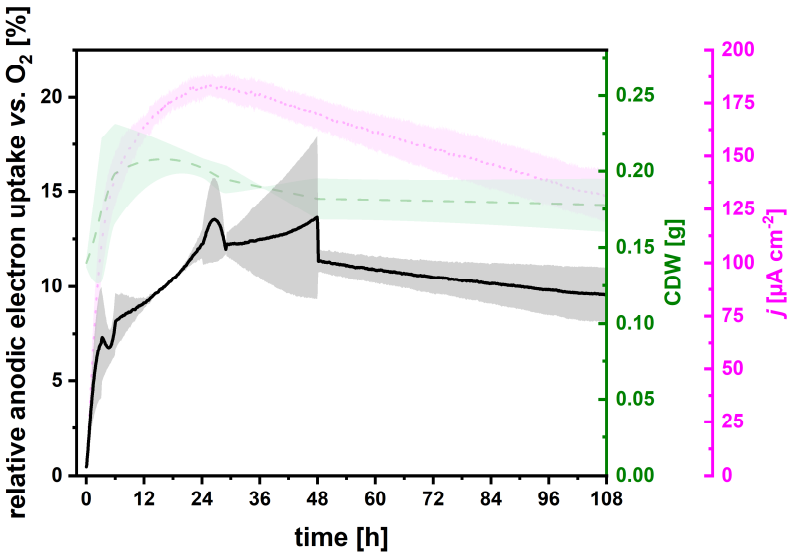

Figure 13: Relative electron uptake of the anode in relation to cultivation on O_2 (black line) over the cultivation time for three anaerobic BES reactors with 5 mM FEC and 500 mV *vs*. Ag/AgCl (satd. KCl) applied potential in MMasy medium. CDW (green) was interpolated over offline data points. The current density is plotted in magenta for comparison.

4.4 Mediated electron transfer mechanism in *C. necator*

Based on the demonstrated MET with multiple different redox mediators, the question of the exact mechanism arises. From the already discussed screening experiments, it is clear that mediator interaction can occur at different levels of microbial metabolism. In Publication VI, a method set combining RT-qPCR, specific inhibitors, and deletion strains for identifying mediator interaction sites was applied to shed light on the mechanism of the so far most efficient mediator FEC.

From the literature overview on interaction sites in different microorganisms with FEC in Publication I and the mediator screening results described in Chapter 4.2, several sites for FEC reduction can be summarized in groups. The first includes respiration chain complexes, as they have been part of intensive studies regarding FEC interaction in the past [28,80,83]. The suspected interaction with hydrogenases based on the previously discussed interaction with PMS leads to a second

group, which comprises the soluble and membrane-bound hydrogenase of *C. necator*. Furthermore, the nitrate respiration system was examined, since FEC could also take up electrons from these complexes based on the redox potential, and especially from the nitrate reductase which has been shown to interact with FEC in *E. coli* [98]. At last, FEC needs a transfer pathway to cross the outer membrane. The kinetics of this mechanism will ultimately affect the anodic electron transfer and could be a target for optimization. A selection of porins and the transporters of the nitrate respiration chain were summarized in a separate group. The groups with the respective sites and their genetic locations are summarized in Table 2. These sites were then further studied by RT-qPCR to assess their expression rates under "normal" aerobic and chemolithoautotrophic (here short: autotrophic) conditions, compared against BES cultivation with FEC. Additionally, a pHG1 megaplasmid deficient mutant strain (*C. necator* ΔpHG1) was used to study the effects of eliminating all sites encoded on the megaplasmid.

Within the respiration chain, qualitative RT-qPCR revealed no significant expression rate differences of CcR, SDH, and the ATPase in BES conditions (Figure 14a) However, the cbb3 subunit of CcO was found to be over-expressed by a factor of 1.9±0.3 *vs.* aerobic conditions. Regarding FEC membrane transfer, only OmpA stood out with a significant over-expression in BES (2.9±0.6) and autotrophic (3.8±1.9) conditions. As expected, both hydrogenases were expressed in autotrophic environments with hydrogen present, while being absent within the ΔpHG1 mutant strain which is genetically unable to express them. In the BES with FEC, the SH was expressed 2.6±0.5-fold, and the MBH 1.8±0.1-fold higher than under aerobic conditions (Figure 14b). This is remarkable since BES conditions lack hydrogen as an inducer for the expression. However, since *C. necator* ΔpHG1 could deliver equal current densities within the stirred tank BES (see Publication VI), these hydrogenases are apparently not necessary for MET. The same applies to all other sites located on the pHG1 megaplasmid.

Table 2: hypothesized interaction sites with their respective genetic location.

Group	Site	Abbreviation	Gene location
Respiratory chain complexes	Cytochrome c oxidase	CcO	Chromosome 1
	Cytochrome c reductase	CcR	
	Succinate dehydrogenase	SDH	
	ATPase	ATPase	
Hydrogenases	Soluble hydrogenase	SH	pHG1 megaplasmid
	Membrane-bound hydrogenase	MBH	
Nitrate respiration	Respiratory nitrate reductase	NarG	pHG1/ Chromosome 1
	Periplasmic nitrate reductase	NapA	pHG1
	Nitric oxide reductase	NorB	pHG1
	Nitrous oxide reductase	NosZ	pHG1
	Nitrite reductase	NirS	Chromosome 2
Transporters and porins	Nitrate/H^+ symporter	NarKI	pHG1
	Nitrate/Nitrite antiporter	NarKII	pHG1
	Outer membrane porin	OmpA	Chromosome 1
	Type VI secretion protein	ImpK	Chromosome 2
	Outer membrane porin (heavy metal efflux system)	CzcC2	Chromosome 2

Nevertheless, nitrate reductase (NarG) has a genetic duplicate on the chromosome and nitrite reductase (NirS) is located there as well. Hence, their involvement in MET is still possible. RT-qPCR reveals that NarG is not significantly over-expressed within the BES (1.5±0.2-fold *vs.* aerobic), while NirS is expressed 3.9±1.1-times more than in aerobic conditions (Figure 14c). Comparing this to autotrophic conditions (2.2±0.1-fold *vs.* aerobic) confirms that the absence of O_2 enables NarG and NirS expression [99] but to a lesser extent. From a thermodynamical point of view, electron transfer from both reductases is only possible with a suitable E^0. NarG catalyzes the first reduction of nitrate to nitrite at E^0=420 mV *vs.* SHE before NirS converts nitrite into the intermediate nitric oxide at E^0=375 mV *vs.* SHE [99]. Therefore, both enzymes could in theory enable electron transfer towards FEC with E^0=416 mV *vs.* SHE.

For a decisive determination of the now further narrowed down interaction sites, specific inhibition was used. Of special interest were both CcR and CcO from the respiratory chain as well as NarG and NirS from the nitrate reduction pathway. CcR can be inhibited with Antimycin A, while the CcO O_2 binding site is inhibited by sodium azide. As a side effect of azide, both nitrate reductases (NapA and NarG) are also inhibited via an unknown mechanism. BES cultures treated with these inhibitors separately, exhibit a direct current response. Antimycin A treated cultures (Figure 15b) show a continuously declining current output over 72 h following the inhibition, while $[Fe(CN)_6]^{4-}$ is not re-oxidized back to $[Fe(CN)_6]^{3-}$ by the anode. This makes the interpretation of the inhibition more difficult since the effect of Antimycin A can be attributed to the CcR being deactivated, or a side reaction with either FEC or the anode. The same observation was made for *P. putida* F1 cultures in a study by Lai and co-workers [80] with a similar BES and FEC as mediator. An influence of Antimycin A on the photometric FEC quantification as well as passivation of the graphite electrode could be ruled out in their study. The cause of this observation is therefore still unknown.

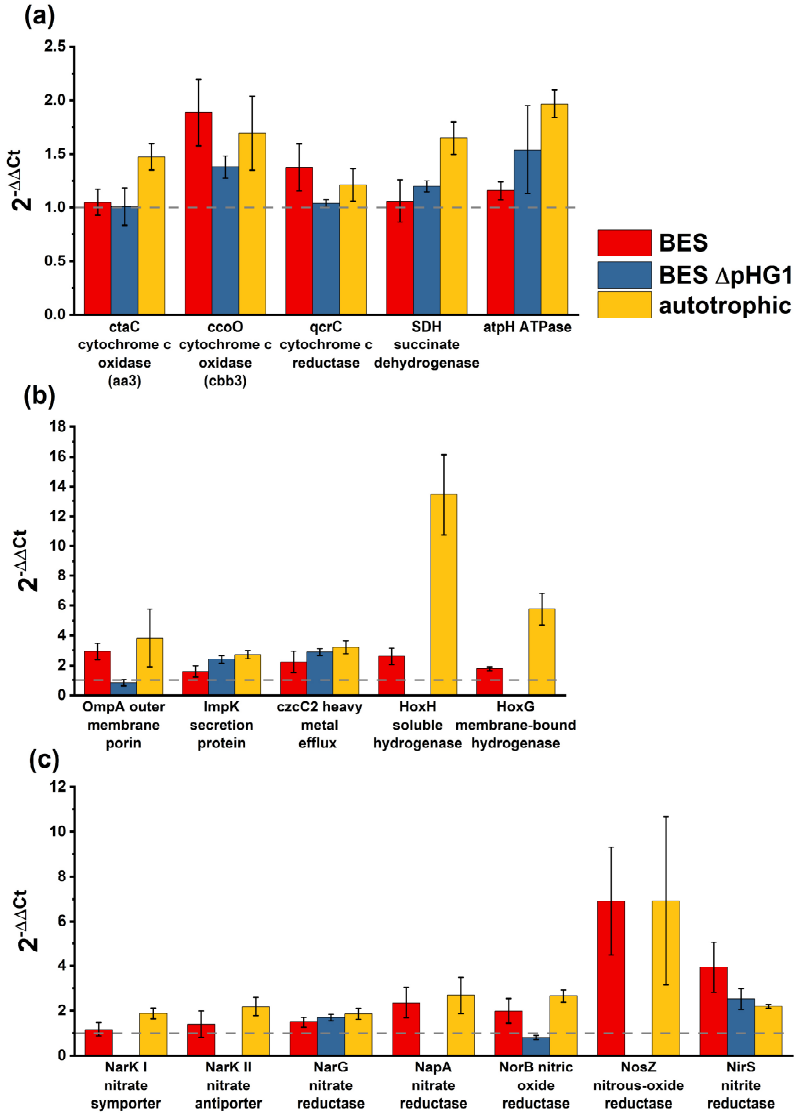

Figure 14: Relative gene expression levels in BES and autotrophic cultures of hypothesized proteins involved in the MET process vs. stationary aerobic culture as calibrator. BES samples were taken from the reactor 24 h after inoculation. Autotrophic samples were cultivated until stationary (54 h). Error bars depict the standard deviation.

With azide-treated cultures, the results can be interpreted clearly at first glance. After azide addition, the current declines immediately while $[Fe(CN)_6]^{4-}$ is re-oxidized to $[Fe(CN)_6]^{3-}$ by the anode (Figure 15a). The reduction power by the cells is therefore clearly affected and the specific inhibition of CcO suggests that the oxidase is a major interaction site for FEC. However, looking deeper into the mechanism of CcO catalysis reveals that azide binds specifically to the heme a_3/Cu_b binuclear O_2 reduction site deep within the complex [100]. O_2 and azide both enter the active site through a channel opening towards the intermembrane space of the cytoplasmic membrane [101]. This space, however, is most likely unreachable for the charged FEC molecule. The interaction site for FEC therefore needs to be facing the cytoplasm, e.g., the soluble cytochrome c oxidation site. Why the electron transfer mechanism to FEC would then still be interrupted by azide binding deep within the complex, remains unsolved. Since azide will also inhibit the respiratory nitrate reductase NarG at the same time, the involvement of this enzyme is also feasible. NarG can further provide proton translocation through the cytoplasmic membrane, aiding in ATP synthesis [102]. However, the enzyme is oriented towards the cytoplasm on the inner membrane, where FEC cannot enter. Hence, the interaction would have to take place at the membrane integral NarI subunit, which contains two b-type cytochromes that oxidize menaquinol for nitrate reduction [102]. A further possibility is supported by the observation that 14% of the current before inhibition remains 120 h past inhibition. This current could be attributed to nitrite reductase NirS, which remains active in the presence of azide. The enzyme was also identified as a potential interaction site via RT-qPCR and is located in the periplasm, where it is accessible to FEC [103].

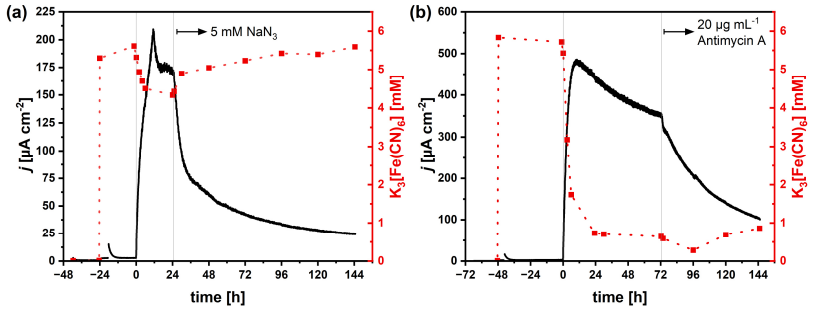

Figure 15: Inhibition of CcO with 5 mM azide (a) and CcR with 20 µg mL^{-1} Antimycin A (b) in *C. necator* BES cultures. Online current density is plotted in black, offline measured $[Fe(CN)_6]^{3-}$ concentration values are plotted in red.

To conclude, via qPCR, inhibition, and the BES cultivation of a pHG1 deficient *C. necator* strain, the interaction sites could be narrowed down to cytochrome c reductase, cytochrome c oxidase, and nitrate/nitrite reductases. While pinpointing the exact mechanisms via the aforementioned methods is not possible, a deeper understanding of the FEC reduction mechanism was gained and further optimization of MET can be based on these findings.

4.5 Optimization approaches

To enhance the MET capabilities of *C. necator*, several approaches can be considered. One option is to increase the number of interaction sites for the mediator to boost reduction rates, although this is challenging due to the difficulty of increasing the number of available respiratory chain complexes. Alternatively, given that the mediator interaction site is likely accessible from the periplasm, a second strategy is to increase the availability of oxidized mediator molecules at the interaction site by improving outer-membrane transfer. The concept was briefly mentioned in Publication VI and will be discussed in more detail here. To increase mediator uptake into the periplasm, the outer membrane must become more permeable to the mediator. FEC was chosen as the exemplary mediator due to its superior performance within a BES. Two strategies were tested to enhance FEC membrane transfer. First, heterologous porins were expressed in *C. necator* under the control of a rhamnose promoter to artificially increase the number of channels in the outer membrane. Second, artificial pores were created using chemical permeabilization agents to allow more mediator molecules to traverse the outer membrane.

The heterologous expression of various porins, including *E. coli* FhuA and its FhuA Δ1-160 derivative missing the "cork" domain, as well as *P. aeruginosa* OprF, in *C. necator* did not enhance mediated electron transfer and resulted in reduced current densities (Figure 16a), most likely due to the metabolic burden of producing the additional proteins and keeping up the plasmids with the antibiotic resistance genes. From this, two hypotheses arise. First, the increase of available mediator molecules to the interaction site doesn't increase overall EET, hence, the mediator membrane transfer kinetics are not the limiting factor. Second, the heterologous porins are not secreted or folded correctly. Regarding the second hypothesis, the effect of increased membrane transfer could be demonstrated via the NPN uptake assay in all porin-producing mutants. Here, these mutants could take up more NPN in the same amount of time, leading to an increased fluorescence of the probe (Figure 16b). This observation leaves the hypothesis of membrane transfer being not limiting for EET.

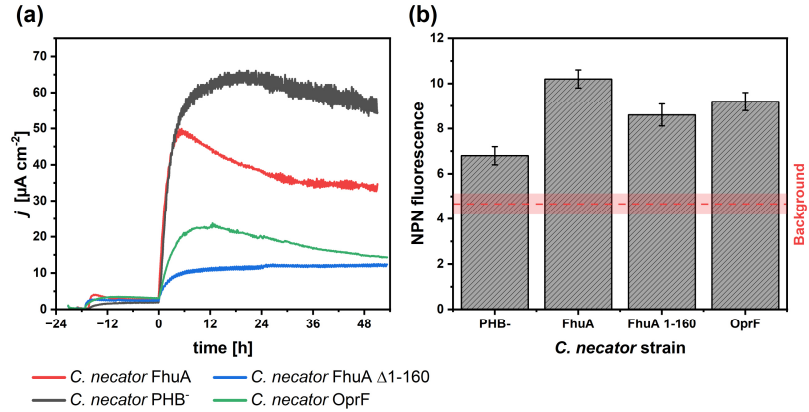

Figure 16: BES cultivation of porin-producing *C. necator*. Porin expression (FhuA, red line; FhuA Δ1-160, blue line; OprF, green line) leads to significantly decreased current densities in comparison to PHB$^-$ strain (black line). Expression of the porins was already started in the pre-culture (a). NPN uptake assay with porin-producing strains. The fluorescence signal is increased with expressed porins, indicating an increased membrane permeation of the fluorescent probe NPN (b). Conditions: MMasy minimal medium, 30 °C, 400 rpm, pH 6.8, n=1, 500 mV *vs*. Ag/AgCl (satd. KCl). Error bars depict the standard deviation of the NPN assay.

A further test to this hypothesis is to rule out misfolded porins and instead apply chemical permeabilization agents. Pre-screening via NPN uptake assays of cetyltrimethylammonium bromide (CTAB), benzalkonium chloride, ethylenediaminetetraacetic acid (EDTA), Triton X 100, polyethylenimine (PEI), Tween 20, and succimer (dimercaptosuccinic acid) with *C. necator* revealed increased membrane permeability for succimer, PEI, benzalkonium chloride, and CTAB (see supplementary information of Publication VI). However, side reactions with the mediator and the cultivation medium, such as clumping, precipitation, increased turbidity, and reduction of FEC, prevented the use of succimer, PEI, and benzalkonium chloride for BES cultivation. 20 µM CTAB on the other hand proved to be applicable with the medium and FEC. Serum flask experiments with FEC and *C. necator* treated with 20 µM CTAB showed doubled mediator reduction rates. However, BES reactor cultures treated with CTAB did not exhibit increased mediator reduction rates or higher current densities (see Figures 5 and 6 in Publication VI).

To conclude, expressed porins and artificial chemical pores could both increase the membrane permeability for the fluorescent probe NPN, but neither permeabilization method led to a benefit for MET efficiency in a BES reactor with FEC as mediator. This leads to the assumption, that membrane permeation is not the limiting step in anodic electron transfer via FEC in *C. necator*. Nevertheless, the expression of OmpA as a natural *C. necator* porin should be explored in the future to verify this hypothesis.

4.6 Summary and Outlook

The direct and mediator-based electron transfer mechanisms of *V. natriegens* have been experimentally validated. As a result of the application of different gas supplies in the medium, CO_2 or N_2, the product spectrum was shifted. With anodic cultivation conditions, a slight change in the product spectrum from formate and succinate to more acetate and ethanol was noticeable. The currents generated were high in comparison to *P. putida* and could potentially be increased further if mediator limitations are overcome. *V. natriegens* could therefore be used as an electroactive production strain and potentially be fed with additional electrons through the Mtr pathway or via mediators to produce more reduced products, such as succinate.

For *C. necator*, current densities were comparable to *V. natriegens* in the stirred tank BES with FEC, but with no apparent limitation caused by mediator shortage. This suggests that maximum currents are already reached. However, the percentage of replaced O_2 by the anode needs to increase by a factor of 8-10 for an effective bioprocess comparable to chemolithoautotrophic conditions. Additionally, fructose consumption under BES conditions needs to increase drastically to allow for the production of valuable compounds. Still, a high coulombic efficiency with 63.1% for *C. necator* has been achieved for the amount of fructose consumed. The underlying limitations should be explored, as the mediator was not the limiting factor. As a control, OmpA, which is *C. necator*'s own porin, should be expressed under the control of a promoter to ensure that mediator membrane transfer is also not limiting.

The e-Cuvette screening tool was proven to be a valuable asset in mediator screening and the first ever system to enable online analysis of cell density and redox state of the mediator. Nevertheless, a significant improvement of the setup could be achieved by separating the working and counter electrodes to eliminate electrochemical side reactions. Furthermore, more data for statistical validation should be gathered to enable balancing calculations within the small-scale system.

A major achievement was the circumscription of possible interaction sites of FEC in *C. necator* to four complexes from the O_2 and nitrate respiration chain. The determined complexes were cytochrome c reductase and oxidase, as well as nitrate/nitrite reductases.

Nevertheless, further clarification of the role of these four complexes is needed. A proteome analysis (as referenced in source [80]) for the three conditions should further be considered to broaden the view of interaction sites, as some may be overlooked due to the manual selection.

To achieve the overall goal of eliminating explosion risks with O_2/H_2 gas mixtures, another way could be to reverse the EET to cathodic conditions. Hereby, electrons are supplied through the electrode and a suitable mediator instead of H_2. Then, O_2 can act as the preferred electron acceptor.

References

1. Potter, M. C. Electrical effects accompanying the decomposition of organic compounds. *Proc. R. Soc. Lond. B.* **84,** 260–276 (1911).
2. Melin, F. & Hellwig, P. Redox Properties of the Membrane Proteins from the Respiratory Chain. *Chem. Rev.* **120,** 10244–10297 (2020).
3. Conley, B. E., Weinstock, M. T., Bond, D. R. & Gralnick, J. A. A Hybrid Extracellular Electron Transfer Pathway Enhances the Survival of *Vibrio natriegens*. *Appl. Environ. Microbiol.* **86** (2020).
4. Pfitzner, J. & Schlegel, H. G. Denitrifikation bei *Hydrogenomonas eutropha* Stamm H16. *Arch. Microbiol.* **90,** 199–211 (1973).
5. Lovley, D. R., Holmes, D. E. & Nevin, K. P. Dissimilatory Fe(III) and Mn(IV) reduction. *Adv. Microb. Physiol.* **49,** 219–286 (2004).
6. Reguera, G. *et al.* Extracellular electron transfer via microbial nanowires. *Nature* **435,** 1098–1101 (2005).
7. Gorby, Y. A. *et al.* Electrically conductive bacterial nanowires produced by *Shewanella oneidensis* strain MR-1 and other microorganisms. *Proc. Natl. Acad. Sci. USA* **103,** 11358–11363 (2006).
8. Beliaev, A. S., Saffarini, D. A., McLaughlin, J. L. & Hunnicutt, D. MtrC, an outer membrane decahaem c cytochrome required for metal reduction in *Shewanella putrefaciens* MR-1. *Mol. Microbiol.* **39,** 722–730 (2001).
9. Myers, C. R. & Myers, J. M. Cloning and sequence of cymA, a gene encoding a tetraheme cytochrome c required for reduction of iron(III), fumarate, and nitrate by *Shewanella putrefaciens* MR-1. *J. Bacteriol.* **179,** 1143–1152 (1997).
10. Wang, Y., Kern, S. E. & Newman, D. K. Endogenous phenazine antibiotics promote anaerobic survival of *Pseudomonas aeruginosa* via extracellular electron transfer. *J. Bacteriol.* **192,** 365–369 (2010).
11. Chukwubuikem, A., Berger, C., Mady, A. & Rosenbaum, M. A. Role of phenazine-enzyme physiology for current generation in a bioelectrochemical system. *Microb. biotechnol.* (2021).

12. Schmitz, S., Nies, S., Wierckx, N., Blank, L. M. & Rosenbaum, M. A. Engineering mediator-based electroactivity in the obligate aerobic bacterium *Pseudomonas putida* KT2440. *Front. Microbiol.* **6,** 284 (2015).
13. Hintermayer, S., Yu, S., Krömer, J. O. & Weuster-Botz, D. Anodic respiration of *Pseudomonas putida* KT2440 in a stirred-tank bioreactor. *Biochem. Eng. J.* **115,** 1–13 (2016).
14. Gemünde, A., Lai, B., Pause, L., Krömer, J. & Holtmann, D. Redox mediators in microbial electrochemical systems. *ChemElectroChem* **9** (2022).
15. Fultz, M. L. & Durst, R. A. Mediator compounds for the electrochemical study of biological redox systems: a compilation. *Anal. Chim. Acta* **140,** 1–18 (1982).
16. Szentrimay, R., Yeh, P. & Kuwana, T. in *Electrochemical Studies of biological systems,* edited by D. T. Sawyer (American Chem. Soc, 1977), pp. 143–169.
17. Kozuch, S. & Martin, J. M. L. "Turning Over" Definitions in Catalytic Cycles. *ACS Catal.* **2,** 2787–2794 (2012).
18. Manjón, A., Obón, J. M., Casanova, P., Fernández, V. M. & Ilborra, J. L. Increased activity of glucose dehydrogenase co-immobilized with a redox mediator in a bioreactor with electrochemical NAD+ regeneration. *Biotechnol. lett.* **24,** 1227–1232 (2002).
19. Kochius, S., Magnusson, A. O., Hollmann, F., Schrader, J. & Holtmann, D. Immobilized redox mediators for electrochemical NAD(P)+ regeneration. *Appl. Microbiol. Biotechnol.* **93,** 2251–2264 (2012).
20. Garcia-Ochoa, F. & Gomez, E. Bioreactor scale-up and oxygen transfer rate in microbial processes: an overview. *Biotechnol. Adv.* **27,** 153–176 (2009).
21. Logan, B. E. Scaling up microbial fuel cells and other bioelectrochemical systems. *Appl. Microbiol. Biotechnol.* **85,** 1665–1671 (2010).
22. Sydow, A., Krieg, T., Mayer, F., Schrader, J. & Holtmann, D. Electroactive bacteria - molecular mechanisms and genetic tools. *Appl. Microbiol. Biotechnol.* **98,** 8481–8495 (2014).

23. Bin Lai & Jens Krömer. Steering Redox Metabolism in *Pseudomonas putida* with Microbial Electrochemical Technologies. In: *Microbial Electrochemical Technologies* (CRC Press, 2020), pp. 59–75.
24. Logan, B. E. *et al.* Microbial fuel cells: methodology and technology. *Environ. Sci. Technol.* **40,** 5181–5192 (2006).
25. Wei, J., Liang, P. & Huang, X. Recent progress in electrodes for microbial fuel cells. *Bioresour. Technol.* **102,** 9335–9344 (2011).
26. Deng, Q., Li, X., Zuo, J., Ling, A. & Logan, B. E. Power generation using an activated carbon fiber felt cathode in an upflow microbial fuel cell. *J. Power Sources* **195,** 1130–1135 (2010).
27. Lai, B., Nguyen, A. V. & Krömer, J. O. Characterizing the Anoxic Phenotype of *Pseudomonas putida* Using a Bioelectrochemical System. *Methods protoc. 2* **2** (2019).
28. Vassilev, I. *et al.* Anodic electro-fermentation: Anaerobic production of L-Lysine by recombinant *Corynebacterium glutamicum*. *Biotechnol. Bioeng.* **115,** 1499–1508 (2018).
29. Krieg, T. *et al.* Characterization of a membrane-separated and a membrane-less electrobioreactor for bioelectrochemical syntheses. *Biotechnol. Bioeng.* **115,** 1705–1716 (2018).
30. Delgado, V. P., Gescher, J. & Sturm, G. Electrode-Assisted Fermentations: Their Limitations and Future Research Directions. In: *Microbial Electrochemical Technologies* (CRC Press, 2020), pp. 85–96.
31. Prokhorova, A., Sturm-Richter, K., Doetsch, A. & Gescher, J. Resilience, Dynamics, and Interactions within a Model Multispecies Exoelectrogenic-Biofilm Community. *Appl. Environ. Microbiol.* **83** (2017).
32. Yang, O., Qadan, M. & Ierapetritou, M. Economic Analysis of Batch and Continuous Biopharmaceutical Antibody Production: A Review. *J. Pharm. Innov.* **14,** 1–19 (2019).
33. Kostov, Y., Harms, P., Randers-Eichhorn, L. & Rao, G. Low-cost microbioreactor for high-throughput bioprocessing. *Biotechnol. Bioeng.* **72,** 346–352 (2001).
34. Tahernia, M. *et al.* A 96-well high-throughput, rapid-screening platform of extracellular electron transfer in microbial fuel cells. *Biosens. Bioelectron.* **162,** 112259 (2020).

35. Szydlowski, L., Ehlich, J., Goryanin, I. & Pasternak, G. High-throughput 96-well bioelectrochemical platform for screening of electroactive microbial consortia. *Chem. Eng. J.* **427,** 131692 (2022).
36. Ley, C. *et al.* An electrochemical microtiter plate for parallel spectroelectrochemical measurements. *Electrochim. Acta* **89,** 98–105 (2013).
37. Ley, C. *et al.* Coupling of electrochemical and optical measurements in a microtiter plate for the fast development of electro enzymatic processes with P450s. *J. Mol. Catal. B: Enzym.* **92,** 71–78 (2013).
38. Johnson, M. J., Peterson, W. H. & Fred, E. B. Oxidation and Reduction Relations between Substrate and Products in the Acetone-butyl Alcohol Fermentation. *J. Biol. Chem.* **91,** 569–591 (1931).
39. Bursac, T., Gralnick, J. A. & Gescher, J. Acetoin production via unbalanced fermentation in *Shewanella oneidensis*. *Biotechnol. Bioeng.* **114,** 1283–1289 (2017).
40. Sturm-Richter, K. *et al.* Unbalanced fermentation of glycerol in *Escherichia coli* via heterologous production of an electron transport chain and electrode interaction in microbial electrochemical cells. *Bioresour. Technol.* **186,** 89–96 (2015).
41. Guerrero, K. *et al.* Butanol production by *Clostridium acetobutylicum* ATCC 824 using electro-fermentation in culture medium supplemented with butyrate and neutral red. *J. Chem. Technol. Biotechnol.* **97,** 1526–1535 (2022).
42. Nevin, K. P., Woodard, T. L., Franks, A. E., Summers, Z. M. & Lovley, D. R. Microbial electrosynthesis: feeding microbes electricity to convert carbon dioxide and water to multicarbon extracellular organic compounds. *mBio* **1** (2010).
43. Kracke, F., Lai, B., Yu, S. & Krömer, J. O. Balancing cellular redox metabolism in microbial electrosynthesis and electro fermentation - A chance for metabolic engineering. *Metab. Eng.* **45,** 109–120 (2018).
44. Eagon, R. G. *Pseudomonas natriegens*, a marine bacterium with a generation time of less than 10 minutes. *J. Bacteriol.* **83,** 736–737 (1962).
45. Ellis, G. A. *et al.* Exploiting the Feedstock Flexibility of the Emergent Synthetic Biology Chassis *Vibrio natriegens* for Engineered Natural Product Production. *Mar. Drugs* **17** (2019).

46. Xu, J. *et al. Vibrio natriegens* as a pET-Compatible Expression Host Complementary to Escherichia coli. *Front. Microbiol.* **12,** 627181 (2021).
47. Payne, W. J. Effects of sodium and potassium ions on growth and substrate penetration of a marine *pseudomonad*. *J. Bacteriol.* **80,** 696–700 (1960).
48. Macfarlane, G. T. & Herbert, R. A. Nitrate Dissimilation by *Vibrio* spp. Isolated From Estuarine Sediments. *Microbiol.* **128,** 2463–2468 (1982).
49. Proctor, L. M. & Gunsalus, R. P. Anaerobic respiratory growth of *Vibrio harveyi*, *Vibrio fischeri* and *Photobacterium leiognathi* with trimethylamine N-oxide, nitrate and fumarate: ecological implications. *Environ. Microbiol.* **2,** 399–406 (2000).
50. Dong, Y. H., Guo, N., Liu, T., Dong, L. H. & Yin, Y. S. Effect of extracellular polymeric substances isolated from *Vibrio natriegens* on corrosion of carbon steel in seawater. *Corros. Eng., Sci.* **51,** 455–462 (2016).
51. Cheng, S. *et al.* Microscopical Observation of the Marine Bacterium *Vibrio Natriegeus* Growth on Metallic Corrosion. *Mater. Manuf. Process.* **25,** 293–297 (2010).
52. Emde, R. & Schink, B. Oxidation of glycerol, lactate, and propionate by *Propionibacterium freudenreichii* in a poised-potential amperometric culture system. *Arch. Microbiol.* **153,** 506–512 (1990).
53. Emde, R., Swain, A. & Schink, B. Anaerobic oxidation of glycerol by *Escherichia* coli in an amperometric poised-potential culture system. *Appl. Microbiol. Biotechnol.* **32,** 170–175 (1989).
54. Albert Schatz & Carlton Bovell. Growth and hydrogenase activity of a new bacterium, *Hydrogenomonas Facilis*. *J. Bacteriol.* **63,** 87–98 (1952).
55. Davis, D. H., Dourdoroff, M., Stanier, R. Y. & Mandel, M. Proposal to reject the genus *Hydrogenomonas*: Taxonomic implications. *Int. J. Syst. Bacteriol.* **19,** 375–390 (1969).
56. Eiko Yabuuchi, Yoshimasa Kosako, Ikuya Yano, Hisako Hotta & Yukiko Nishiuchi. Transfer of Two Burkholderia and An *Alcaligenes* Species to *Ralstonia* Gen. Nov.: Proposal of *Ralstonia pickettii* (Ralston, Palleroni and Doudoroff 1973) Comb. Nov., *Ralstonia solanacearum* (Smith 1896) Comb. Nov. and *Ralstonia eutropha* (Davis 1969) Comb. Nov. *Microbiol. Immunol.* **39,** 897–904 (1995).

57. Friedrich, C. G., Friedrich, B. & Bowien, B. Formation of Enzymes of Autotrophic Metabolism During Heterotrophic Growth of *Alcaligenes eutrophus*. *J. Gen. Microbiol.* **122,** 69–78 (1981).
58. Krieg, T., Sydow, A., Faust, S., Huth, I. & Holtmann, D. CO_2 to Terpenes: Autotrophic and Electroautotrophic α-Humulene Production with *Cupriavidus necator*. *Angew. Chem. Int. Ed. Engl.* **57,** 1879–1882 (2018).
59. Dalsasso, R. R., Pavan, F. A., Bordignon, S. E., Aragão, G. M. F. de & Poletto, P. Polyhydroxybutyrate (PHB) production by *Cupriavidus necator* from sugarcane vinasse and molasses as mixed substrate. *Process Biochem.* **85,** 12–18 (2019).
60. Panich, J., Fong, B. & Singer, S. W. Metabolic Engineering of *Cupriavidus necator* H16 for Sustainable Biofuels from CO_2. *Trends Biotechnol.* **39,** 412–424 (2021).
61. Lenz, O., Lauterbach, L. & Frielingsdorf, S. Chapter Five - O_2-tolerant [NiFe]-hydrogenases of *Ralstonia eutropha* H16: Physiology, molecular biology, purification, and biochemical analysis. In: *Methods in Enzymology: Enzymes of Energy Technology,* edited by F. Armstrong (Academic Press, 2018), pp. 117–151.
62. Torella, J. P. *et al.* Efficient solar-to-fuels production from a hybrid microbial-water-splitting catalyst system. *PNAS* **112,** 2337–2342 (2015).
63. Nishio, K. *et al.* Extracellular Electron Transfer Enhances Polyhydroxybutyrate Productivity in *Ralstonia eutropha*. *Environ. Sci. Technol. Lett.* **1,** 40–43 (2014).
64. Lai, Y. H. & Lan, J. C.-W. Enhanced polyhydroxybutyrate production through incorporation of a hydrogen fuel cell and electro-fermentation system. *Int. J. Hydrogen Energy* **46,** 16787–16800 (2021).
65. Tu, W., Xu, J., Thompson, I. P. & Huang, W. E. Engineering artificial photosynthesis based on rhodopsin for CO_2 fixation. *Nat. Commun.* **14,** 8012 (2023).
66. Gemünde, A., Gail, J. & Holtmann, D. Anodic Respiration of *Vibrio natriegens* in a Bioelectrochemical System. *Chemsuschem* **16,** e202300181 (2023).

67. Gemünde, A., Gail, J., Janek, J. & Holtmann, D. e-Cuvettes parallelize electrochemical and photometric measurements in cuvettes and facilitate applications in bio-electrochemistry. *Biosens. Bioelectron. X* **14,** 100378 (2023).
68. Gemünde, A., Gail, J. & Holtmann, D. Redox mediator interaction with *Cupriavidus necator* – spectroelectrochemical online analysis. *Electrochem. commun.* **162,** 107705 (2024).
69. Gemünde, A., Rossini, E., Lenz, O., Frielingsdorf, S. & Holtmann, D. Chemoorganotrophic electrofermentation by *Cupriavidus necator* using redox mediators. *Bioelectrochemistry* **158,** 108694 (2024).
70. Gemünde, A., Ruppert, N.-L. & Holtmann, D. Unraveling the Electron Transfer in *Cupriavidus necator* – Insights Into Mediator Reduction Mechanics. *ChemElectroChem* **11,** e202400273 (2024).
71. Windhorst, C. & Gescher, J. Efficient biochemical production of acetoin from carbon dioxide using *Cupriavidus necator* H16. *Biotechnol. biofuels* **12,** 163 (2019).
72. Livak, K. J. & Schmittgen, T. D. Analysis of relative gene expression data using real-time quantitative PCR and the 2(-Delta Delta C(T)) Method. *Methods* **25,** 402–408 (2001).
73. Helander, I. M. & Mattila-Sandholm, T. Permeability barrier of the Gram-negative bacterial outer membrane with special reference to nisin. *Int. J. Food Microbiol.* **60,** 153–161 (2000).
74. Lai, B. *et al.* Anoxic metabolism and biochemical production in *Pseudomonas putida* F1 driven by a bioelectrochemical system. *Biotechnol. biofuels* **9,** 39 (2016).
75. Levene, H. Robust testes for equality of variances. *Contributions to Probability and Statistics,* 278–292 (1960).
76. Tukey, J. W. A Quick Compact Two Sample Test To Duckworth's Specifications. *Technometrics* **1,** 31–48 (1959).
77. Hoffart, E. *et al.* High Substrate Uptake Rates Empower *Vibrio natriegens* as Production Host for Industrial Biotechnology. *Appl. Environ. Microbiol.* **83** (2017).
78. Failmezger, J., Scholz, S., Blombach, B. & Siemann-Herzberg, M. Cell-Free Protein Synthesis From Fast-Growing *Vibrio natriegens*. *Front. Microbiol.* **9,** 1146 (2018).
79. Langsdorf, A., Schütz, J. P., Ulber, R., Stöckl, M. & Holtmann, D. Production of polyhydroxybutyrate from industrial flue gas by microbial electrosynthesis. *J. CO2 Util.* **83,** 102800 (2024).

80. Lai, B., Bernhardt, P. V. & Krömer, J. O. Cytochrome c Reductase is a Key Enzyme Involved in the Extracellular Electron Transfer Pathway towards Transition Metal Complexes in *Pseudomonas Putida*. *Chemsuschem* **13,** 5308–5317 (2020).
81. Rawson, F. J., Downard, A. J. & Baronian, K. H. Electrochemical detection of intracellular and cell membrane redox systems in *Saccharomyces cerevisiae*. *Sci. Rep.* **4,** 5216 (2014).
82. Hassan, R. Y. A. & Wollenberger, U. Mediated bioelectrochemical system for biosensing the cell viability of *Staphylococcus aureus*. *Anal. Bioanal. Chem.* **408,** 579–587 (2016).
83. Ertl, P., Unterladstaetter, B., Bayer, K. & Mikkelsen, S. R. Ferricyanide reduction by *Escherichia coli*: kinetics, mechanism, and application to the optimization of recombinant fermentations. *Anal. Chem.* **72,** 4949–4956 (2000).
84. Marritt, S. J. *et al.* A functional description of CymA, an electron-transfer hub supporting anaerobic respiratory flexibility in *Shewanella*. *Biochem. J.* **444,** 465–474 (2012).
85. Thoma, F. *et al.* Metabolic engineering of *Vibrio natriegens* for anaerobic succinate production. *Microb. biotechnol.* **15,** 1671–1684 (2022).
86. Linton, J. D., Harrison, D. E. & Bull, A. T. Molar growth yields, respiration and cytochrome patterns of *Beneckea natriegens* when grown at different medium dissolved-oxygen tensions. *J. Gen. Microbiol.* **90,** 237–246 (1975).
87. Schulze, C. *et al.* Investigation of exopolysaccharide formation and its impact on anaerobic succinate production with *Vibrio natriegens*. *Microb. biotechnol.* **17,** e14277 (2024).
88. Moradali, M. F. & Rehm, B. H. A. Bacterial biopolymers: from pathogenesis to advanced materials. *Nat. Rev. Microbiol.* **18,** 195–210 (2020).
89. Christwardana, M., Frattini, D., Accardo, G., Yoon, S. P. & Kwon, Y. Effects of methylene blue and methyl red mediators on performance of yeast based microbial fuel cells adopting polyethylenimine coated carbon felt as anode. *J. Power Sources* **396,** 1–11 (2018).
90. Zhao, J., Wang, Z., Fu, C., Wang, M. & He, Q. The Mediated Electrochemical Method for Rapid Fermentation Ability Assessment. *Electroanalysis* **20,** 1587–1592 (2008).

91. Nijenhuis, I. & Zinder, S. H. Characterization of hydrogenase and reductive dehalogenase activities of *Dehalococcoides ethenogenes* strain 195. *Appl. Environ. Microbiol.* **71,** 1664–1667 (2005).
92. Wu, Y., Liu, T., Li, X. & Li, F. Exogenous electron shuttle-mediated extracellular electron transfer of *Shewanella putrefaciens* 200: electrochemical parameters and thermodynamics. *Environ. Sci. Technol.* **48,** 9306–9314 (2014).
93. Förster, A. H., Beblawy, S., Golitsch, F. & Gescher, J. Electrode-assisted acetoin production in a metabolically engineered *Escherichia coli* strain. *Biotechnol. biofuels* **10,** 65 (2017).
94. Kim, C. *et al.* Anodic electro-fermentation of 3-hydroxypropionic acid from glycerol by recombinant *Klebsiella pneumoniae* L17 in a bioelectrochemical system. *Biotechnol. biofuels* **10,** 199 (2017).
95. Hua, X., Xia, H.-L. & Long, Y.-T. Revisiting a classical redox process on a gold electrode by operando ToF-SIMS: where does the gold go? *Chem. Sci.* **10,** 6215–6219 (2019).
96. Lambauer, V. & Kratzer, R. Lab-Scale Cultivation of *Cupriavidus necator* on Explosive Gas Mixtures: Carbon Dioxide Fixation into Polyhydroxybutyrate. *Bioeng.* **9,** 204 (2022).
97. Yu, J. & Lu, Y. Carbon dioxide fixation by a hydrogen-oxidizing bacterium: Biomass yield, reversal respiratory quotient, stoichiometric equations and bioenergetics. *Biochem. Eng. J.* **152,** 107369 (2019).
98. Boonstra, J., Sips, H. J. & Konings, W. N. Active transport by membrane vesicles from anaerobically grown *Escherichia coli* energized by electron transfer to ferricyanide and chlorate. *Eur. J. Biochem.* **69,** 35–44 (1976).
99. Berks, B. C., Ferguson, S. J., Moir, J. W. & Richardson, D. J. Enzymes and associated electron transport systems that catalyse the respiratory reduction of nitrogen oxides and oxyanions. *Biochim. Biophys. Acta* **1232,** 97–173 (1995).
100. Fei, M. J. *et al.* X-ray structure of azide-bound fully oxidized cytochrome c oxidase from bovine heart at 2.9 A resolution. *Acta Cryst. D* **56,** 529–535 (2000).
101. Al-Abdul-Wahid, M. S., Evanics, F. & Prosser, R. S. Dioxygen transmembrane distributions and partitioning thermodynamics in lipid bilayers and micelles. *Biochem.* **50,** 3975–3983 (2011).
102. Hille, R., Hall, J. & Basu, P. The mononuclear molybdenum enzymes. *Chem. Rev.* **114,** 3963–4038 (2014).

103. Sam, K. A., Strampraad, M. J. F., Vries, S. de & Ferguson, S. J. Very early reaction intermediates detected by microsecond time scale kinetics of cytochrome cd1-catalyzed reduction of nitrite. *J. Biol. Chem.* **283,** 27403–27409 (2008).

Appendix A: Original Journal Publications

This appendix contains all relevant Publications for this work, published in peer-reviewed journals.

A.1 Publication I

André Gemünde, Bin Lai, Laura Pause, Jens Krömer, and Dirk Holtmann

Redox mediators in microbial electrochemical systems

In C*hemElectroChem*, Volume 9, Issue 13, 2022,
DOI: https://doi.org/10.1002/celc.202200216

Contribution: My contribution to the Publication was the initial conceptualization and selection of the key parameters of a MET process to review from current literature. Additionally, I created all figures and tables and wrote the Chapters 1 to 4 of the manuscript.

Check for updates

ChemElectroChem

Review
doi.org/10.1002/celc.202200216

Chemistry Europe
European Chemical Societies Publishing

www.chemelectrochem.org

Redox Mediators in Microbial Electrochemical Systems

André Gemünde,*[a] Bin Lai,[b] Laura Pause,[b] Jens Krömer,[b] and Dirk Holtmann*[a]

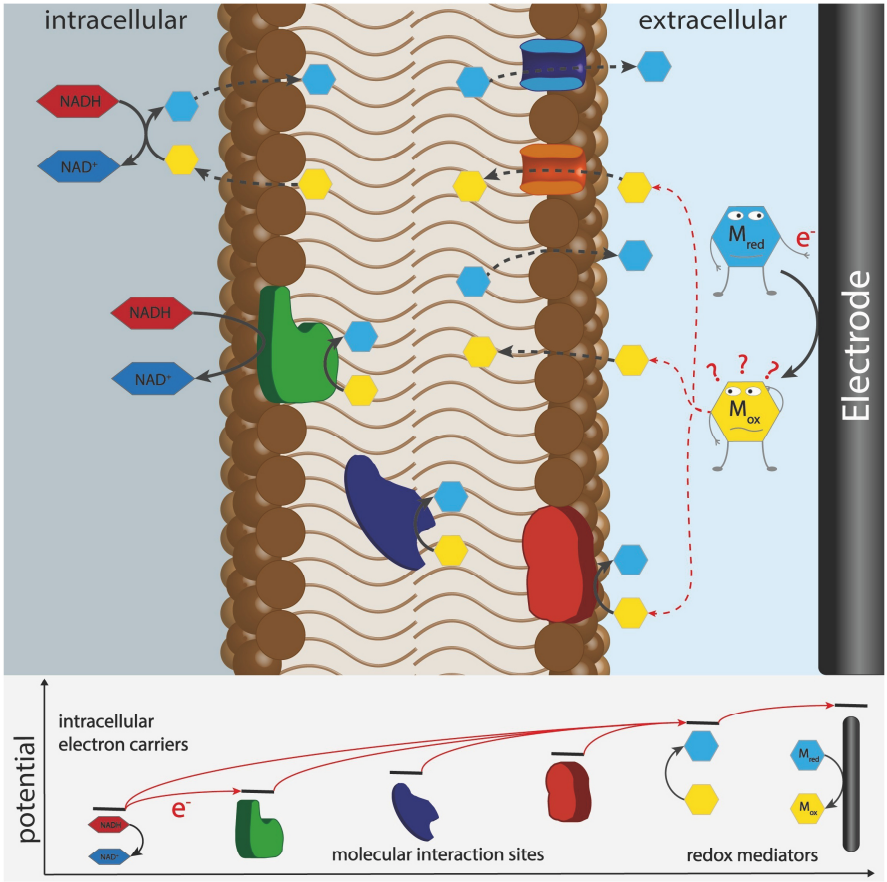

Redox mediators are commonly used in microbial electrochemical systems to enable or enhance the electron transfer between microorganisms and electrodes. In recent studies, new insights into the mechanism of mediated extracellular electron transfer were gained, but some questions remain unanswered. In this review, some of the most outstanding research questions regarding the use of redox mediators in microbial electrochemical systems were discussed. These included the recycling of artificial and natural redox mediators, limitations in electron transfer rates by mediator turnover, metabolic burden, membrane permeability, and the putative interaction sites between commonly used redox mediators and the proteins of the electron transport chain of diverse electroactive microorganisms. To simplify the planning of mediator-based bioelectrochemical systems, these molecular interaction sites were defined by their redox potential and are assigned to redox mediators, known or hypothesized to be able to transfer electrons from or to the specific interaction site. Furthermore, we addressed the kinetics of mediator transfer through the membrane and the potential rate-limiting step in mediator-based processes.

1. Introduction

Besides the general possibility to drive enzymatic and microbial reactions by electrochemical redox equivalents, there are also some further practical advantages to the use of bioelectrochemical systems (BES). The first and, at the same time, greatest advantage is making the oxygen transfer into the cultivation medium obsolete, which is often a major obstacle for scaling up aerobic stirred tank reactor processes.[1] In addition, the risk of excessive foaming is also decreased by removing the need for sparging the culture, especially when biodetergents like rhamnolipids are the desired product.[2,3] The term anodic electro-fermentation (AEF) was shaped by Vassilev et al.[4,5] for such processes, where an anode acts as an inexhaustible electron acceptor in replacement of oxygen. Additionally, established microbial electrochemical technologies are microbial electrosynthesis (MES), where the electrons are transferred from the electrode to a desired reduced product, and microbial fuel cells (MFC). MFCs are typically used in wastewater treatment, where electroactive bacteria break down organic pollutants and transfer the surplus electrons to the electrode, which is accompanied by electricity production.[6,7] It has to be noted that in the following, the term "BES" is exclusively used for microbial electrochemical reactions. For the sake of simplicity, we will not introduce a new abbreviation.

Recently, Fruehauf et al.[8] briefly described three main obstacles for microbial electrosynthesis, whereby two directly refer to mediator-based BESs. The first one being the removal of mediators from the fermentation broth; the second one states that artificially added mediators are oftentimes limited in turnover number. The third unsettled question mentioned by the authors is the mostly unknown interaction site between microorganism and electrode, regardless of the determining electron transfer mechanism. Therefore, this review aims to look further into those obstacles and unsettled questions and shed some light on solutions, which are already in existence for mediator-based BESs. After looking further into those research gaps and possible obstacles, we further want to extend the list of properties an ideal redox mediator has to offer based on the publications by Yang et al.[9] and Fultz and Durst.[10]

1.1. Mechanisms of extracellular electron transfer

Any living organism requires a mechanism to exchange electrons with its environment. For the most part, electrons emerging from oxidative processes need to be discarded from the cell to create a proton gradient from the negative outside of the membrane to the more positive counterpart on the inside, which in turn drives ATP synthesis as the cell's main source of energy. This process is then called "respiration".[11] For numerous microorganisms, many of them electroactive, oxygen is by far not the only terminal electron acceptor the cells can make use of. Those include, among others, iron-, manganese-, copper- or chromium oxides.[12] These organisms developed different extracellular electron transfer (EET) mechanisms to exchange electrons through the non-conductive cell membrane by mainly three methods, shown in Figure 1. The first one being a direct electron transfer (DET) between the surface of the microbial membrane and, in this case, an electrode. Therefore, the organisms have to express proteins, which reside in the membranes and can bridge the isolating gap to transfer electrons to an external acceptor. Inside such a redox-active protein, electron transfer usually takes place through heme-, iron-sulfur, or copper groups. The direction of electron flow is thereby determined by the formal potential of the reaction partners involved. In general, electrons are transferred from a lower potential donor to an acceptor with a higher redox potential.[13] A more specialized form of DET can be used by organisms like *Shewanella oneidensis* or *Geobacter sulfurreducens*, which form conductive nanowires, spanning several microns between electron acceptor and cell surface.[14,15]

Suppose the organism doesn't exhibit redox-active proteins on the cell surface or forms nanowires, which can utilize the

[a] A. Gemünde, Prof. Dr. D. Holtmann
Institute of Bioprocess Engineering and Pharmaceutical Technology and Competence Centre for Sustainable Engineering and Environmental Systems
Technische Hochschule Mittelhessen
35390 Gießen, Germany
E-mail: andre.gemuende@lse.thm.de
dirk.holtmann@lse.thm.de
[b] Dr. B. Lai, L. Pause, Dr. J. Krömer
Systems Biotechnology group, Department of Solar Materials
Helmholtz Centre for Environmental Research – UFZ
04318 Leipzig, Germany

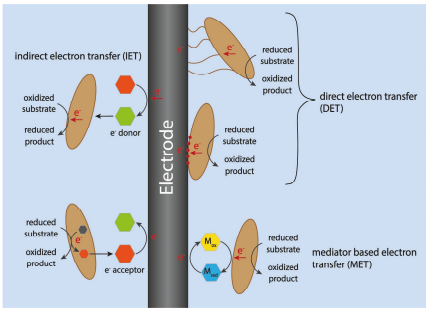

Figure 1. General electron transfer mechanisms between electrode and electroactive microorganisms.

DET pathway. In that case, it might still be able to move electrons through the cell membrane by taking advantage of a mediator-based electron transfer (MET). The mediator hereby acts as an electron shuttle between electrode and microorganism. For the process to work, the molecular interaction site (MIS) has to be reachable for the shuttle molecule. So, in many cases, when the MIS lies beneath or on the cytoplasmic membrane, the mediator must be able to cross the outer membrane by transportation or diffusion. In contrast to DET, one major advantage of MET is the utilization of the whole reactor volume for biocatalytic conversions.[16] To clarify, a mediator can make use of the entire microbial surface area, while the DET pathway can only cover a proportion of it, which leads to unsatisfactory efficiency in standard stirred tank vessels. Additionally, mediators could be used to target specific known MIS, which in reverse could be used to study electron transfer pathways in electroactive microorganisms.[17]

The third pathway is referred to as indirect electron transfer (IET) and shares similarities to MET regarding the use of the whole reactor volume. The important difference lies in the irreversible redox reaction of the shuttle compound. Those compounds can be synthesized at the electrode and transfer electrons to the organism, using up the shuttle molecule in the process like it is depicted in Figure 1. In reverse, reduced metabolic substances can be secreted by the microorganism and transfer electrons in a one-way process to the electrode.[6]

1.2. The obstacles and unsettled research questions

The first obstacle described by Fruehauf et al.[8] mentions the costly downstream removal of mediators from the fermentation broth. Some artificial redox mediators are expensive chemicals

André Gemünde received his MSc degree in Biochemical and Chemical Engineering from the Technical University of Kaiserslautern in 2021. He is a PhD student at the THM (Gießen, Germany) and part of the group "Intensification of Bioprocesses". His current research is focused on mediator-based electron transfer mechanisms in bioelectrochemical systems.

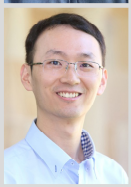

Bin Lai received his PhD degree from the University of Queensland, Australia in 2017, and then moved to UFZ, Leipzig for his postdoc research. He is interested in the fundamental and quantitative understanding of extracellular electron transfer pathways and the microbial phenotype steered by the electrode for rational optimization of microbial electrochemical process for targeted bioproduction. Since 2020, he leads the research team Biophotovoltaics at UFZ, Leipzig, focusing on white hydrogen production from photoautotrophs in a bioelectrochemical system.

Laura Pause completed her MSc degree in biochemistry at the University of Leipzig in 2020. She is in the first year of her promotion at SOMA department at the UFZ in Leipzig. Her PhD studies are focusing on the development of a tunable electrofermentation process using metabolically engineered Pseudomonas putida.

Jens Krömer holds a Diploma in Biology and a PhD in Systems Biotechnology from the Saarland University (Germany). He has focused on systems biology platforms for microbes and metabolic engineering with a special interest in steering redox metabolism with electrodes. He was a faculty member of the University of Queensland, Australia, and directing the Centre for Microbial Electrochemical Systems. Since 2017, he is at UFZ in Leipzig, Germany, and applies his systems biotechnology tools also to tapping into photosynthetic electron fluxes of Cyanobacteria.

Dirk Holtmann has completed his diploma in chemical engineering/biotechnology in 1999. He obtained his PhD at the Otto von Guericke University of Magdeburg on the electrochemical measurement of the microbial activities. He is head of the group "Intensification of Bioprocesses" at the THM (Gießen, Germany). His current research activities concentrate on biocatalysis and bioelectrochemical synthesis.

and are putatively toxic to the environment, so downstream removal techniques or biodegradable electron shuttles are highly desirable.[16] If such a shuttle component is fully recoverable, the second question arises, if there is a limit on how often they can be recycled and, even if they are intended for a single batch use, how long they are stable in the BES. This, in turn, means that the stability and total turnover have to be considered for each mediator beforehand. This is especially the case for "natural" redox mediators like riboflavin (RF) or phenazines, which some organisms can secrete for themselves since these substances are susceptible to degradation in BESs.

A particular obstacle comes up if we extend the view of interaction sites from nanowires and outer membrane cytochromes to the specific interaction sites of redox mediators and electron transport chains of different organisms. For the most part, they are unknown or can only be hypothesized. Only for a few well-studied BES model organisms, like *S. oneidensis*, profound information was acquired on which enzymes are involved and what range their respective electrochemical windows span. This knowledge gap hinders further optimization of electron transfer rates in many electroactive bacteria.[16,18] Also, since most known MIS can be found on the cytoplasmic membrane, the mediator must eventually cross the membrane barrier to reach the intended site. This, in turn, means that transmembrane electron transfer might be a rate-limiting step for MET pathways.

2. Downstream Removal and Recycling of Redox Mediators

The toxicity of redox mediators to the environment is one major concern when the MET-based bioelectrochemical process comes to industrial application. Many of the electron shuttles, like menadione or methyl viologen (MV), exhibit high toxicity on living organisms, even in low concentrations.[19,20] The mediators would thus need to be either recycled or removed before discharging them into nature, meaning purification and/or degradation have to be implemented into the downstream process. This adds costs to the process and requires a balancing of the entire bioprocess, which means the value of the product has to be considered when mediators are introduced. So far, the research regarding the recycling or removal of mediators in BESs is rather scarce but can benefit readily from the research efforts in other relevant fields. For instance, the reuse of culture medium has been a long-term desire in biotechnology (especially for large scale cultivation) to reduce the operation cost.[21–23] Membrane or chromatography-based approaches are used mostly to separate and recycle usable nutrients. These might also be applicable in BESs for mediator recycling, while the economic feasibility might be a key limitation.

Since many redox-active dyes have been used as mediators in BESs, removal or degradation technologies developed for the waste streams of the textile industry could also be transferred to BESs. Table 1 summarizes methods for downstream removal from an aqueous solution of some dyes or substances that have been employed as redox mediators in BESs. As an example, Çoruh and Gürkan[24] could adsorb up to 98 % of neutral red (NR) from an aqueous solution onto waste foundry sand. But still, to achieve full reusability of the mediators after their removal by adsorption, a suitable desorption method has to be developed as well. With a desorption method added to the process, an adsorber/desorber unit could be used on an industrial scale to achieve sufficient regeneration. The same applies to membrane filtration, since continuous downstream recycling would be possible.[25] In contrast, degradation processes like photodegradation are only viable when a toxic mediator has to be removed, since recycling is not an option in those cases.

In reverse, new MFC or MES applications involving mediators could also be used for wastewater treatment in the textile

Table 1. Downstream removal techniques for common redox mediators used in BESs.

Technique	Mediator	System specifics	Removal efficiency	Reference
Ion exchange chromatography	Methylene blue	Adsorption with Amberlite XAD-16 Desorption with Methanol	>99% within 30 min	Lunn et al.[41,42]
	Neutral red	Adsorption with Amberlite XAD-16	>99% within 10 min	Lunn et al.[41,42]
	Safranine O	Adsorption with Amberlite XAD-16	>99% within 60 min	Lunn et al.[41,42]
Adsorption	Neutral red	Adsorption from aqueous solution onto waste foundry sand	Up to 98 % within 120 min	Çoruh and Gürkan[24]
	Methylene blue	Adsorption from aqueous solution onto dried urban sewage sludge	Not determined	Otero et al.[43]
Membrane filtration	Humic acid (analogues are e.g.: AQS, AQDS)	Membrane filtration with carbon polymer composite	80% within 120 min	Hwang et al.[25]
Extraction	DCIP	Extraction from aqueous solution into chloroform as organic phase. Porous PTFE capillary for separation	>99% at a flow rate of 30 µL/min	Phillips et al.[44]
	Methylene blue Neutral red Methyl red	Phase-transfer liquid phase microextraction	Up to 100% within 10 min Up to 99.97 % within 10 min Up to 85 % within 10 min	Chen et al.[45]
Coagulation-flocculation	Methyl red	Coagulants: bentonite clay and polyaluminium chloride	>97 % within 15–20 min mixing and 60 min settling	Fosso-Kankeu et al.[46]
Photodegradation	Methyl red Methylene blue	Simulated solar irradiation catalysed by nanocomposites of Zn, Cd, S	95 % within 60 min	Pouretedal and Sabzevari[47]
Mechanical	Riboflavin	Immobilization on magnetic beads	Up to 90% (no time interval stated)	Arinda et al.[31]

industry since the dye pollutants are often times redox-active mediators.[26]

One approach to bypass the necessity of downstream processing of mediators is the use of biodegradable redox chemicals. For example, some humic substances, already endogenous in waste sludge, can be harvested and used as an electron shuttle in a BES.[27] Also, flavins are occurring naturally in the environment and can therefore potentially be discarded safely in low concentrations. Another possible way can be to immobilize the redox-active compound on the electrode, as it was shown multiple times in literature.[28–31] However, this comes with a severe disadvantage for scale-up because it negates the advantage of soluble redox mediators to use the whole reactor volume for the biotransformation process. Therefore, a downstream removal technique or possibly biodegradable redox mediators are still desirable for the broad mass of organisms used in BESs.

3. Turnover Number in Mediated Electron Transfer

The turnover number (often referred to as TN or TON in the literature[32,33]) is a dimensionless number, which describes the number of turnovers a catalyst can achieve in a given case. In the context of enzymatic catalysis, the total turnover number (TTN) has been widely accessed and defined as the quotient of mol product per mol of biocatalyst used.[32,34] The concept of TTN was only rarely touched in the field of microbial electrochemical technologies but is especially critical while a MET is involved.[35,36] The proper calculation of the TTN plays an important role when determining the electrochemical behaviour of mediators in a BES, which will be further discussed in section 3.2. Prior to that, the stability of the redox compounds against physical, chemical, and biological stresses in a BES system should be evaluated, which consequently affects the precise estimation and calculation of TTN.

3.1. Defining the TTN

The definition of TTN has been used in the field of mediated enzymatic processes by, e.g., Kochius et al.[36] to calculate the TTN for a mediated NAD(P)$^+$ regeneration system. It is defined by the quotient of mol product in the system at the end of the enzymatic reaction per mol of added mediator. For the enzymatic process, the transformation reaction is rather simple in terms of the profiles of substrate(s) and product(s), and thus the electron donor(s) and sink(s) can be defined and determined relatively easy. When the definition of TTN comes to the MET using whole cells as the catalysts, it is much more challenging to precisely determine all the involved electron donors and sinks, which is one key issue that needs to be considered. Apart from the fed-in substrate and desired product(s), possible substrate(s) coming from the medium or inoculum and the by-products have to be screened and quantified. Moreover, biomass accumulation should also be considered, where in this case, the chemical formula of the biomass can be measured[37] (especially for pure culture systems or defined consortium), or a general formula can be assumed[38] (particular for undefined systems). An electron balance analysis, based on the degree of reduction, can even be conducted prior to the TTN calculation.[38,39] This can examine the coverage of all possible electron donors and sinks in the system in the calculations and subsequently affect the accuracy of TTN calculation.

The TTN for the mediator (TTN_{RM}) can be calculated from the measured current and the total mediator concentration (added or synthesized amount). We propose an equation similar to the one used by Kaneko et al.,[40] which calculates the TTN_{RM} by dividing the total amount of electrons q in [mol] transferred to or from the electrode by the total amount of mediator used (n_{RM}) in [mol], also taking in mind its electron transfer capabilities, indicated by the number of electrons that can be transferred per molecule of redox mediator in one turnover (z_{RM}):

$$TTN_{RM} = \frac{q}{n_{RM} * z_{RM}} \tag{1}$$

The amount of electrons q can hereby be determined by the measured current I in [A] over the reaction time t in [s] divided by Faraday's constant C in [A*s/mol]:

$$q = \frac{\int |I| \, dt}{C} \tag{2}$$

Still, it is not possible to distinguish the electron flux coming from DET or MET using the approach described above if they are both present in the system. These have to be selectively activated or deactivated on a genetic level. In addition, redox-active compounds other than the mediator can also cause under- or over-estimation of the charge transfer via the mediator, meaning, possible side reactions at the electrode surface will lead to a falsely higher TTN. Therefore, abiotic tests of the working conditions should always be carried out to exclude such effects while attempting the TTN calculation of the mediator.

3.2. Stability of mediators in bioelectrochemical environments

The stability of redox mediators over one batch process is essential for the long-term application of BESs. The mediator in a BES is exposed to physical (e.g., UV light), chemical (e.g., oxidative radicals), and biological (e.g., biodegradation) stresses, while all of them can affect its long-term stability. Without long-lasting mediators, the electron transfer chain between organism and electrode is weakened over time and ultimately breaks down, which is reflected in the TTN. Conceivable reasons for mediator loss in a BES would be: accumulation inside the cell, permanent adsorption to cell membranes or electrodes, mem-

brane permeability restrictions for one of the redox states, instability, unwanted polymerisation, and semi-reversible redox reactions at the working electrode. Numerous artificial redox mediators are sufficiently stable and can withstand the influence of UV-light in the typical time period of a BES cultivation. For example, ferricyanide, 2-hydroxy-1,4-naphtaquinone (HNQ), and MV are very stable under neutral pH and oxygen-free conditions.[48–50] In contrast, the metachromatic dye thionine is unstable and can adsorb onto the electrode surface, weakening the long-term BES efficiency.[49] Furthermore, NR can be adsorbed to the cell membranes of gram-negative bacteria, like *A. succinogenes*, as shown by Park and Zeikus.[51] This, however, facilitated the EET of the bacteria, which was likely due to the reduction of NR by membrane-bound redox proteins.

Choi et al.[52] observed the current gradually increased in the cyclic voltammetry cycles for a L-α-phosphatidylcholine coated electrode, while the phenazine-derivative mediator safranine O was present in the electrolyte. This indicated an accumulation of mediator on the electrode surface, which was due to the changes in permeability crossing the fatty acid membrane: the oxidized safranine O can diffuse through the membrane but not the reduced form. This accumulates the redox chemical on the electrode surface, resulting in increased current response along the CV scans. Similar phenomena were also found for the bipyridines MV and benzyl viologen (BV). These mediators cannot pass the bacterial membrane barrier in their oxidized MV^{2+}/BV^{2+} states. BV^{+}, however, is able to cross the membrane.[53]

Continuous feeding of artificial redox mediators might be needed to sustain the BES system performance while using these dwindling or unstable mediators in BES. This will increase the operating cost of the process and can lead to toxicity effects of the chemicals on microbes after reaching a certain concentration. Another approach to compensate for the declining efficiency could be microbial self-secreted mediators, e.g., phenazines, flavins, or pyrroloquinoline quinone (PQQ).[54] This, however, also comes with an additional metabolic burden to the microbial host, which could further impact the EET efficiency and system performance. Pyocyanine (PYO), for example, is a natural redox mediator secreted by *Pseudomonas aeruginosa*, and it was also found to be an effective mediator for many other strains interacting with NADPH:pyocyanin oxidoreductase.[55] However, the stability of PYO is quite low. Its half-life was only one day, determined by Chukwubuikem et al.[56] in a PYO supplemented BES of *Pseudomonas putida* KT2440. Similar results were obtained by Clifford et al.,[57] as no electrochemical activity for PYO could be measured after 15 hours of redox cycling in a biophotovoltaic system. In addition to the poor stability, the redox activity of PYO was also found to be semi-reversible under BES conditions[58] and toxic for bacteria like *Escherichia coli*, even in concentrations below 3 μg/mL.[59] All these render PYO ineffective as an external redox mediator in organisms other than *P. aeruginosa*. Stability issues were also found for phenazine methosulfate, a derivative of PYO synthesized chemically. The current signal halved after 500 cycles of cyclic voltammetry.[36] Instead, the PYO precursor phenazine-1-carboxylic acid (PCA) could be a more promising candidate as a recombinant redox mediator. Its half-life in a BES spans more than 10 days, and the compound can be reversibly oxidized and reduced.[56,58] Still, phenazine redox mediators might also adsorb to electrodes or even further chemically react at the surface, which would limit their long-term usability in BESs.[60]

3.3. Metabolic burden of recombinant mediator production

For MET experiments, redox mediators can be supplied to the system in two different ways. Either a chemically synthesized mediator can be added externally, or the cells can be metabolically engineered to secrete self-synthesized mediators if they don't already have a way to produce them.[61] The usage of an artificial redox mediator comes with the clear advantage that timing, amount, and redox potential can be adjusted to fit the individual purpose of the experiment. On the downside, this approach generates additional costs and an increased ecological footprint. Conducting electromicrobial experiments with the aid of self-secreted mediators might be the cheaper option, but one has to rely on naturally occurring compounds and their synthetic pathways. Furthermore, this approach might require the use of genetically modified strains, timing, and the amount of redox mediator produced is far less controllable. Anyways, in both approaches, downstream processing might be needed to recover the mediators as large amounts of these chemical compounds cannot be discharged easily, as they might be toxic to the environment. Therefore, the question of which approach is the favourable choice for MET experiments is not easy to answer. In this section, we attempt to estimate the impact of producing a natural mediator in a recombinant strain on the process yields. For this purpose, we assume that PCA is produced in a recombinant *P. putida* strain from the hexose glucose. Such a production has been published recently by Schmitz and Rosenbaum.[62]

We used our existing elementary flux mode analysis model for *P. putida* and included the reactions necessary to produce PCA from *P. aeruginosa*.[62] Using the computation tool *efmtool*,[63] we predicted the amount of glucose that would be needed per mol of PCA synthesized in the metabolic network with glucose as carbon and ammonia as nitrogen source. The resulting theoretical carbon yield is 0.71 c-mol·c-mol^{-1}, which translates to a mass yield of 0.4 $g_{PCA} \cdot g_{glucose}^{-1}$, or 2.46 $g_{glucose} \cdot g_{PCA}^{-1}$ (1.99 $mol_{glucose} \cdot mol_{PCA}^{-1}$). Looking at the degree of reduction of glucose, one would invest 1.99*24 mol electrons into the mediator. Hence, the mediator will need to complete 24 two electron cycles until the equivalent amount of electrons invested into the mediator are transferred to the anode. This might be highly relevant if the mediator is not stable enough and cannot be fully degraded by the cell to recover the invested electrons. This would be even more problematic when the carbon sources are less reduced than sugars. In terms of the metabolic burden, based on the theoretical yields and the observed glucose uptake rate, one can estimate how much substrate would be invested into the mediator. According to the calculations, 13.4% of the observed

glucose uptake will end up in PCA in *P. putida* (estimated from Figure 2A Schmitz & Rosenbaum, 2020[62]) in the first 5 hours of cultivation. It has to be stated that this calculation does not account for the metabolic costs of producing the recombinant enzymes for the pathway or plasmid maintenance, if applicable. Therefore, the actual metabolic burden for the cell will be even higher. At the same time, this scenario only provided mediator concentrations around 200 µM, which might be, depending on the TTN of the chosen mediator, insufficient for a high current output (fast process).

To conclude, when choosing a mediator, one has to keep in mind that not every redox-active compound is an ideal redox mediator. Especially the stability of the compound is a crucial factor. The TTN can help estimate the compound's stability and classify between redox mediators and one-way shuttle compounds. Basically, a TTN above 1, hence the ability of a chemical to be reduced and also re-oxidized more than once, accounts for a redox mediator. Therefore, self-secreted phenazines can be termed redox mediators. For a long-term stable process, one should aim for a redox mediator with TTN that leads to significantly more electrons shuttled to the electrode than invested in making the mediator. From this perspective, PYO, with its short half-life, might not be an optimal redox mediator. PCA, instead, has a significantly longer half-life in BES coupled with a higher TTN (e.g., over 100 estimated for the wild type during stationary phase) and seems to be a better choice for

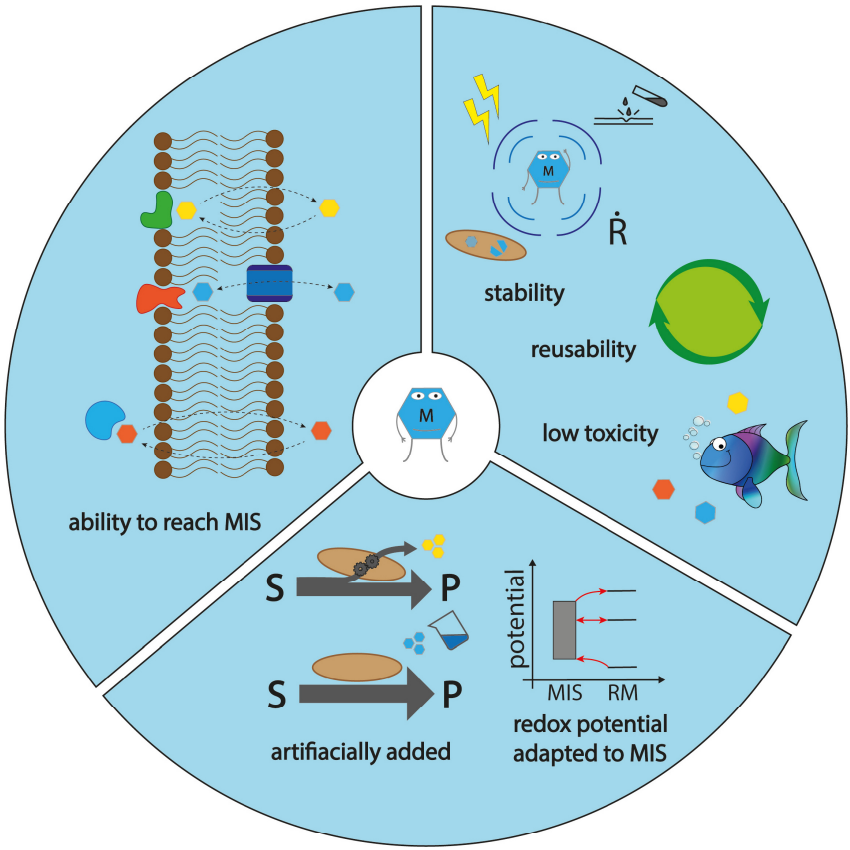

Figure 2. Extended criteria for an ideal redox mediator in a BES.

the usage in a mediated BES system. Anyways, the production of phenazines comes with a high metabolic burden for the cell and drains a high share of carbon to the mediator production. Keeping in mind that also self-secreted mediators have to be removed in downstream processing. The usage of an artificial mediator, which is separately added to the BES, seems to be more promising. Such a mediator would not pose a metabolic burden for synthesis of the substance. Good candidates for such mediators are transition metal complexes. Their redox potential, molecular charge, and polarity can be customized by coupling different metal ions and ligands.[64] Therefore, depending on the target product, the chemical to be used can be rationally tuned and allow relatively easy separation and recycling in the downstream process using, e.g., charge separation approaches. Cobalt-organic complexes, for instance, have been successfully applied in some BES studies.[65,66]

4. Interaction Between Redox Mediators and Electroactive Microorganisms

In recent years, numerous electroactive organisms and their associated EET pathways have been examined. Zhao et al.[67] recently summarized how the different microorganisms use their respective native redox proteins to perform EET and proposed potential engineering solutions to improve them. However, this review focuses on the interaction between redox mediators and cellular components (e.g., redox proteins) involved in the MET pathway. Understanding how the redox mediator withdraws electrons from the cellular electron carrier is crucial for effective MES processes or to improve the power density of a MFC based on MET. The complexity of the MET process could be well underestimated. The electron flux mediated by the redox chemicals can either be inward from the cathode or outward to the anode with respect to the cells. In addition, the cellular energy metabolism can be significantly impacted by the MET pathway. This is dependent on the MIS between mediator and microorganism, e.g., whether the membrane protein containing the transmembrane proton pump is involved or not. Consequently, this would impact the electrode-steered bioprocess, e.g., the yield of the target product.[13,68] Further, the potential difference between MIS and mediator has to be considered. Already in 1982, Fultz and Durst[10] published their review on formal potentials of redox mediators and proposed an ideal range of ± 118 mV in redox potential between a "biocomponent" and a mediator, based on the Nernst equation.

Table 2 and 3 summarize the so far known MIS for different artificial and natural redox mediators for different microorganisms, ascendingly sorted by their standard redox potential vs. the standard hydrogen electrode (SHE) and preferably those already used in BESs. In cases where redox potentials of the MIS are marked with a (b), the potential was estimated based on the different mediators tested in the publication. For instance Liang et al.[69] could only see influences on electron transfer with mediators which possess lower redox potentials than thionine. So, in turn, the potential of the MIS has to be lower than the 60 mV vs. SHE for thionine, or alternatively, the mediator is for other reasons, such as membrane restrictions or stability issues not interacting with the organism.

It must also be noted that the redox potentials of mediators and interaction sites are not always fixed. The E^0 values of mediators can be affected by the prevailing pH, and the redox potentials of the MIS are sometimes stated as a potential range. This has multiple reasons. Firstly, the standard redox potential E^0 of membrane proteins depends on pH, ionic strength, and the presence of surrounding lipids.[11] Secondly, many MIS are heme, iron-sulfur, or copper groups, which reside inside the protein and are partly restricted for mediators due to accessibility reasons. This, in turn, results in a broad range of potentials for many MIS, instead of one fixed redox potential, like it can be stated for most redox mediators at defined pH. As an example, Marritt et al.[70] could identify the redox potentials of the four hemes in purified CymA from *S. oneidensis* MR-1 by spectropotentiometric titration. Their determined redox potentials range from -265 mV (heme IV) to -110 mV (heme II). The electron transfer chain can hereby act unexpectedly by allowing thermodynamically unfavourable ("uphill") reactions from higher to lower potentials between nearby redox centres, typically within the range of 14 Ångstrom, through electron tunnelling.[11,71,72]

Firer-Sherwood et al.[73] used protein film voltammetry on the Mtr-Proteins from *S. oneidensis* to determine their respective E^0 values. Among other cytochromes, these values and their respective electrochemical windows can be taken from Table 4. The potential ranges of the electron transfer proteins in the Mtr-chain overlap significantly, allowing for the thermodynamically favoured transport along the chain to the outer membrane. Only the entry point redox potential of the electrons from the menaquinone couple lies higher in potential than the E^0 value for the first electron acceptor in the electron transfer chain, CymA. The authors presume that the binding of the quinone cofactor alters the redox potential of the complex to allow for the electron transfer to CymA and afterwards further down the chain.[73] This is also the case for the binding of flavins like riboflavin or flavin mononucleotide (FMN) to outer membrane cytochromes like MtrC. The formed complex alters the redox properties of both components, which enables thermodynamically favoured electron transfer. Okamoto et al.[74] could provide data on this process by using differential pulse voltammetry on whole cells with flavins as redox shuttling compound. The complex of FMN and MtrC showed a midpoint potential of -145 mV vs. SHE in comparison to -219 mV for free FMN. For RF and OmcA, respectively, a positive shift of 69 mV was recorded for the complex.[74]

Still, the number of known interaction sites in whole-cell electrobiocatalysis is scarce, and further research in this field would benefit the understanding, as well as the optimization of MET in diverse organisms.

Table 2. Artificial redox mediators with their respective redox potentials (E^0_{RM}) and MIS (E^0_{MIS}). The electroactive organism used, as well as the working electrode potential of the BES (E_{WE}) from the associated reference, are also given. The E^0 values below are reported against the conditions: 25 °C, 1 atm, pH 7.

Mediator	E^0_{RM} vs. SHE [mV]	Molecular interaction site	E^0_{MIS} vs. SHE [mV]	Organism	E_{WE} vs. SHE [mV]	Ref.
$[Co(trans\text{-}diammac)]^{3+}$	−555	Hypothesis: Rnf complex (ferredoxin dependent transhydrogenase)	$-500 \le x \le -400$	*Clostridium autoethanogenum*	−603	[65]
Methyl viologen ($MV^{2+}/MV^{\bullet+}$)	−440	Periplasmatic hydrogenase	−414[c]	*Dehalococcoides ethenogenes*	No BES	[82]
		Periplasmatic hydrogenase	−442	*Dehalococcoides* spp.	−500	[83]
		Periplasmatic Fe-hydrogenase (pH 7.5)	−351	*Desulfovibrio vulgaris*	No BES	[84]
		Periplasmatic hydrogenase	−412[c]	*Desulfovibrio vulgaris*	MFC	[85]
		Recombinant nitrogenase from *Paenibacillus* sp. WLY78.7	275[c] [86]	*Synechococcus elongatus* PCC 7942	−606	[87]
Benzyl viologen (BV)	−360	Periplasmatic hydrogenase	−414[c]	*Dehalococcoides ethenogenes*	No BES	[82]
Neutral red (NR)	−325	Cytochrome c: CcdA, a cytochrome c synthesis gene, was upregulated	$-180 \le x < 60$[b]	*Methanosarcina barkeri*	−651	[69]
		Menaquinone	−72	*Escherichia coli*	−451	[88]
		Fumarate reductase	−55	*Actinobacillis succinogens*	−2000	[51, 89]
		NAD^+	−320	*Actinobacillis succinogens*	−2000	[51]
		Hypothesis: NAD^+	−325	*Methylobacterium extorquens*	−551	[90]
Safranine O	−300	Bound as cofactor to: OmcA, MtrC	−450	*Shewanella oneidensis* MR-1	−450	[91]
pMBVi (poly (2-methacryloyloxyethyl phosphorylcholine-co-butyl methacrylate-co-viologen))	−280	Hypothesis: ubiquinone and/or FAD, which further donate electrons to nitrate reductase	90/−220	*Escherichia coli*	−400	[40]
9,10-anthraquinone-2-carboxylic acid (AQC)	−247	Outer membrane cytochrome c (OmcA, OmcB, OmcS, MtrC,…)	$-400 \le x \le 0$	*Shewanella putrefaciens* 200	−186	[92]
		Cytochrome c: CcdA, a cytochrome c synthesis gene, was upregulated	$-180 \le x < 60$[b]	*Methanosarcina barkeri*	−651	[69]
9,10-anthraquinone-2-sulfonic acid (AQS)	−225	Outer membrane cytochrome c (OmcA, OmcB, OmcS, MtrC,…)	$-400 \le x \le 0$	*Shewanella putrefaciens* 200	−198	[92]
		Bound specifically as cofactor to OmcA	−550	*Shewanella oneidensis* MR-1	−450	[91]
		Cytochrome c: CcdA, a cytochrome c synthesis gene, was upregulated	$-180 \le x < 60$[b]	*Methanosarcina barkeri*	−651	[69]
		Periplasmatic hydrogenase	−412[c]	*Desulfovibrio vulgaris*	MFC	[85]
9,10-anthraquinone-2,6-disulfonic acid (AQDS)	−184	Outer membrane cytochrome c (OmcA, OmcB, OmcS, MtrC,…)	$-400 \le x \le 0$	*Shewanella putrefaciens* 200	−178	[92]
		AQDS replaces menaquinone and shuttles electrons between NADH and Complex I of the respiratory chain	$-320 \le x \le -73$[93]	*Paracoccus versutus*	No BES	[94]
		Periplasmatic hydrogenase	−414[c]	*Dehalococcoides ethenogenes*	No BES	[82]
		Cytochrome c: CcdA, a cytochrome c synthesis gene, was upregulated	$-180 \le x < 60$[b]	*Methanosarcina barkeri*	−651	[69]
		OcwA from *Thermincola potens* JR	$-450 \le x \le 100$	Purified protein	CV analysis	[95]
2-hydroxy-1,4-naphthoquinone (HNQ)	−137	Putative quinone hydrogenase(s)	$-73 \le x \le 90$[93] (Menaquinone, Ubiquinone)	*Klebsiella pneumoniae*	699	[96]
		Outer membrane cytochrome c (OmcA, OmcB, OmcS, MtrC,…)	$-400 \le x \le 0$	*Shewanella putrefaciens* 200	−93	[92]
Resazurin	−51	Outer membrane cytochrome c (OmcA, OmcB, OmcS, MtrC,…)	$-400 \le x \le 0$	*Shewanella putrefaciens* 200	61	[92]
Methylene blue (MB)	11	CymA, MtrA, STC	[a]	Recombinant *Escherichia coli*	200	[97]
		FMN cofactor / Fe–S clusters of pyruvate dehydrogenase and several dehydrogenases from the TCA cycle	< -150[98]	*Saccharomyces cerevisiae*	MFC	[99]
Menadione (+ $[Fe(CN)_6]^{3-/4-}$)	30	Succinate dehydrogenase	30	*Saccharomyces cerevisiae*	500	[100]
Dichloroindophenol (DCIP/DCPIP)	217	Cytochrome c1 subunit of complex III	220	*Saccharomyces cerevisiae*	500	[100]

Table 2. continued

Mediator	E^0_{RM} vs. SHE [mV]	Molecular interaction site	E^0_{MIS} vs. SHE [mV]	Organism	E_{WE} vs. SHE [mV]	Ref.
DCIP + $[Fe(CN)_6]^{3-/4-}$		NADH-ubiquinone oxireductase I (Complex I)	$-320 \leq x \leq 90$	*Staphylococcus aureus*	405	[101]
$[Co(bpy)_3]^{3+/2+}$	310	Cytochrome c reductase (Complex III)	$78 \leq x \leq 208$[b]	*Pseudomonas putida* F1	699	[16]
		Soluble cytochrome c	[a]			
		Periplasmatic subunits of cytochrome c oxidase (Cu_A, ccoO, ccoP)	270			
$[Fe(CN)_6]^{3-/4-}$	416	Cytochrome c reductase (Complex III)	$78 \leq x \leq 208$[b]	*Pseudomonas putida* F1	699	[16]
		Soluble cytochrome c	[a]			
		Periplasmatic subunits of cytochrome c oxidase (Cu_A, ccoO, ccoP)	270			
		Cytochrome o/bd I/bdII oxidase	[a]	Recombinant *Escherichia coli*	No BES	[102]
		Hypothesis: complex IV, cytochrome supercomplex (aa3, bc1c)	[a]	*Corynebacterium glutamicum*	697	[4]
		Cytochrome bd oxidase (unlikely, due to a resulting lack of proton motive force)	[a]			
		Succinate dehydrogenase (unlikely, due to a resulting lack of proton motive force)	30			
		Menaquinone (unlikely, due to a resulting lack of proton motive force)	−73			
PMF [poly(2-methacryloyloxyethyl phosphorylcholine-co-vinylferrocene)]	500	Nitrate reductases. Upregulated genes encoding for: narK1, nasD	420[c]	*Ralstonia eutropha* (aka. *Cupriavidus necator*)	600	[103]
MB combined with NR:						
MB	11	FAD cofactor from succinate dehydrogenase	30	*Saccharomyces cerevisiae*	MFC	[99]
NR	−325	NADH is oxidized by NR in the cytoplasm to NAD^+	−320[c]	*Saccharomyces cerevisiae*	MFC	[99]

[a] See list of cytochromes. [b] Interpretation based on the mediators tested. [c] Potential for the catalysed reaction.

5. Cross-Membrane Transportation as a Key Process for Redox Mediator Selection

Most of the known or hypothesized MISs for redox mediators are located on the cytoplasmic membrane (Table 2 and 3). Thus, the transportation of redox mediators across the cellular membrane (especially the outer membrane) becomes a critical parameter determining the MET efficiency. That particularly matters for the cases using hydrophilic mediators to bridge the electron flux between suspended cells and the electrode. Kinetically, it has been shown that the intramolecular electron transfer rate constant between the microbial membrane protein hemes can reach 10^5–10^9 s^{-1},[75–77] and the intermolecular electron transfer rate constant between the heme and external electron acceptor is also on the level of 10^8 $M^{-1}s^{-1}$.[78] All these considerations above raise critical concerns of the transmembrane electron transfer (via artificial or self-secreted electron carriers) as the potential rate-limiting step for the MET pathways.

5.1. The potential challenges

Understanding the transportation pathway of mediators is critical to rationally improve the MET efficiency. Although the MET pathway has been found and used in the field of microbial electrochemical technologies for decades,[79–81] revealing the fundamental mechanism is still facing many challenges and needs more investigations.

Firstly, differential transporters might be required for the uptake and secretion of a redox mediator, respectively. Riboflavin, for instance, is an effective mediator widely present in different microorganisms, including *Shewanella*, *Geobacter*, and many other microorganisms.[110–112] An outer membrane cytochrome was reported to be interacting with riboflavin for *Geobacter*, and thus a membrane transporter might not be absolutely essential.[113] But for many other strains, including *Shewanella*, specialized membrane transporters for its secretion and uptake are needed. The pathway was nicely reviewed by García-Angulo[114] in 2017, where outer membrane transporters Bfe from *Shewanella* and YeeO from *E. coli* were proposed for RF secretion, and diverse receptors were reported as the likely transporters for its uptake.

In addition, different transporters might also be required for the mediator's varied redox status. This was briefly discussed in section 3 above, as it might significantly affect its precise TTN calculation. Still, this phenomenon could also raise critical concerns and difficulties to screen, identify and optimize the respective transporters. Balancing the transportation kinetics for

Table 3. Natural redox mediators with their respective redox potentials (E^0_{RM}) and MIS (E^0_{MIS}). The electroactive organism used, as well as the working electrode potential of the BES (E_{WE}) from the associated reference, are also given. The E^0 values below are reported against the conditions: 25 °C, 1 atm, pH 7.

Mediator	E^0_{RM} vs. SHE [mV]	Molecular interaction site	E^0_{MIS} vs. SHE [mV]	Organism	E_{WE} vs. SHE [mV]	Ref.
Ferredoxin	−432	Periplasmatic hydrogenase	−414[c]	*Dehalococcoides ethenogenes*	No BES	[82]
FMN/FAD	−219	MtrF (MtrC homologous)	$-400 \leq x \leq 100$	*Shewanella oneidensis* MR-1	No BES	[104]
FMN	−219	MtrC	50	*Shewanella oneidensis* MR-1	399	[74]
		Outer membrane cytochrome c (OmcA, OmcB, OmcS, MtrC,…)	$-400 \leq x \leq 0$	*Shewanella putrefaciens* 200	−178	[92]
		OcwA from *Thermincola potens* JR	$-450 \leq x \leq 100$	Purified protein	CV analysis	[95]
FMN (bound)[b]	−145	MtrC	−145	*Shewanella oneidensis* MR-1	399	[74]
Riboflavin (RF)	−208	Outer membrane cytochrome c (OmcA, OmcB, OmcS, MtrC,…)	$-400 \leq x \leq 0$	*Shewanella putrefaciens* 200	−184	[92]
		OcwA from *Thermincola potens* JR	$-450 \leq x \leq 100$	Purified protein	CV analysis	[95]
RF (bound)[b]	−139	Bound to OmcA	−139	*Shewanella oneidensis* MR-1	399	[74]
	−110	FMN(ox) > FMNH(Sq) bound to OmcA	−110	*Shewanella oneidensis* MR-1	−450	[105,106]
	−400	FMNH(Sq) > FMNH-(Hq) bound to OmcA	−400	*Shewanella oneidensis* MR-1	−450	[105,106]
Phenazine−1-carboxamide (PCN)	−140[107]	Terminal heme-copper oxidases: aa_3, bo_3, $cbb_3(1)$, $cbb_3(2)$	[a]	*Pseudomonas aeruginosa* PA14	No BES	[108]
		Terminal quinol oxidase: cyanide insensitive oxidase (Cio)	Unknown			
Phenazine−1-carboxylic acid (PCA)	−116[107]	Glucose dehydrogenase (PQQ dependent)	40 / 344[109]	*Pseudomonas aeruginosa* *Pseudomonas putida*	399	[56]
		Terminal heme-copper oxidases: aa_3, bo_3, $cbb_3(1)$, $cbb_3(2)$	[a]	*Pseudomonas aeruginosa* PA14	No BES	[108]
		Terminal quinol oxidase: cyanide insensitive oxidase (Cio)	Unknown			
recombinant PCA from *P. aeruginosa*		Menaquinone	−73[93]	Recombinant *Escherichia coli*	−401	[54]
Pyocyanine (PYO)	−40[107]	Glucose dehydrogenase	40 / 344[109]	*Pseudomonas aeruginosa* *Pseudomonas putida*	399	[56]
		Periplasmatic hydrogenase	−414[c]	*Dehalococcoides ethenogenes*	No BES	[82]
		Terminal heme-copper oxidases: aa_3, bo_3, $cbb_3(1)$, $cbb_3(2)$	[a]	*Pseudomonas aeruginosa* PA14	No BES	[108]
		Terminal quinol oxidase: cyanide insensitive oxidase (Cio)	Unknown			
Phenazine methosulfate	80	Periplasmatic hydrogenase	−414[c]	*Dehalococcoides ethenogenes*	No BES	[82]
		OcwA from *Thermincola potens* JR	$-450 \leq x \leq 100$	Purified protein	CV analysis	[95]

[a] See list of cytochromes. [b] Complex of mediator and MIS. The E^0 values of MIS and redox mediator are therefore equal. [c] Potential for the catalysed reaction. Sq: Semiquinone. Hq: Hydroquinone.

the mediator in different redox statuses can be very challenging.

Last but not least, the transportation pathways are largely unclear for many of the mediators used in the MET field. The efflux pump MexGHI-OpmD in *P. aeruginosa* was found to act on the secretion of phenazines,[115] but such efflux pump was not widely found in other strains where phenazines can also act as an effective mediator, e.g., *E. coli*, *Enterococcus faecium*, etc.[61] Although the uptake of PCA into the cytosol of *P. putida* was recently proven by Chukwubuikem et al.,[56] more studies will still be needed to elucidate its detailed pathway and the presence of a similar uptake mechanism in other strains. For the artificial redox mediators, compounds like NR and AQDS have been studied intensively in biochemical studies for decades, and their interactions with the microbial membrane are well-known. For instance, NR can readily penetrate into the cell membrane via non-ionic diffusion, and it has been used as a common assay for cell viability tests.[122] On the other hand, the transportation pathways for other inorganic or metal-organic compounds need more investigation. In vitro studies have shown interactions between redox compounds (e.g., ferricyanide, cobalt organic complex, etc.) with the cytoplasmic redox proteins[123–125] or periplasmic electron carriers.[126–128] The outer membrane is very likely permeable for these charged hydro-

Table 4. List of cytochromes and their redox-active subunits with the respective standard redox potential (E^0). The E^0 values below are reported against the conditions: 25 °C, 1 atm, pH 7.

Cytochrome	Redox-active subunit	E^0 vs. SHE [mV]	Electron donor/ acceptor	E^0 vs. SHE [mV]	Organism	Reference
Cytochrome aa_3	aa_3(1)	143			*C. glutamicum*	Kao et al., 2016[93]
	aa_3(2)	317				
	CuA	150	cc di-heme (bcc)	100		
Cytochrome bcc	Heme b (low)	−291			*C. glutamicum*	Kao et al., 2016[93]
	Heme b (high)	−163				
	cc di-heme	100				
	Rieske iron sulfur cluster	160	Menaquinone	−73		
Cytochrome bo_3	Heme b (low)	220–250	Ubiquinone	90	*E. coli*	Salerno et al., 1989[116] Ingledew et al., 1995[117] Salerno et al., 1989[116]
	Heme o (high)	160				
Cytochrome cbb_3	Heme c	260	Soluble cytochrome c	260	*P. stutzeri*	Melin et al., 2016[118]
	Heme b	372				
	Heme b_3	−54	O_2	820		
	CcoP	269			*P. stutzeri*	Melin et al., 2016[118]
Cytochrome bd	Heme d	260			*E. coli*	Pudek and Bragg, 1976[119]
	Heme b_{558}	165				
	Heme b_{556}	35				
Soluble cytochrome c	Heme c	260				Melin and Hellwig, 2020[11]
CymA	Heme I	−240			*S. oneidensis* MR−1	Marritt et al., 2012[70]
	Heme II	−110				
	Heme III	−190				
	Heme IV	−265				
	Whole enzyme	−200 ± 125	Donor: Menaquinone Acceptor: STC (among others)	−73 −160 ± 125	*S. oneidensis*	Firer-Sherwood et al., 2008[73], pH 6 McMillan et al., 2012[120]
Small tetraheme cytochrome (STC)		$-138 < x < -248$			*S. oneidensis*	Harada et al., 2002[121], pH 9,1
		−160 ± 125	MtrA	−100 ± 150	*S. oneidensis*	Firer-Sherwood et al., 2008[73], pH 6
MtrA		−100 ± 150	MtrC	−138 ± 137.5	*S. oneidensis*	Firer-Sherwood et al., 2008[73], pH 6
MtrC		−138 ± 137.5			*S. oneidensis*	Firer-Sherwood et al., 2008[73], pH 6

philic molecules, but not the cytoplasmic membrane.[125,129] An outer-membrane-crossing pathway will thus be a key for this type of mediator.

5.2. The proposed solutions

The high diversity of transportation mechanisms for different mediators and different strains poses significant challenges for rationally improving the MET efficiency. To overcome this problem, we propose two potential solutions from the aspects of biology and technology, respectively.

Strain engineering. Identifying the respective membrane transporter and optimizing its efficiency is an ultimate solution to rationally improve the MET rates. Systems and synthetic biology, which have gained increased interest in the field of microbial electrochemical technologies, provide efficient approaches to achieve it. Omics, especially proteomics and transcriptomics, can be used to identify potential candidates by comparative analysis. They have been applied to fundamental studies of EET pathways,[16,130] and similar approaches could be adapted for transporter identifications. Afterwards, the (over-) expression of the target transporter using synthetic biology or the improvement of the transporting kinetics by protein engineering can be applied. This will be challenging, especially for those microorganisms that are less well-studied. Sound and fundamental understandings of the host organisms are prerequisites for efficient protein engineering. Finally, other approaches can also be effective. For instance, metabolic modelling can be used to simulate the optimized scenario to balance the MET and metabolic turnover rates under certain physiology conditions if the transporter kinetic is known and structural understanding of the interaction between the transporter and mediator can provide a molecular basis for efficient, rational engineering.

System configurations. The strain engineering solutions can be applied to model microorganisms where the genetic tools are available and microbial physiology is well-understood. But for many other non-model microorganisms, improving the MET efficiency by tuning the system configuration might be more practical. In that case, a dual mediator system or amphiphilic mediator can probably be used. The hydrophobic mediator (or hydrophobic head of the amphiphilic compound) integrates with and thus electrify the cellular membrane by extracting the metabolic electrons to the cell surface, and then the second hydrophilic mediator (or the hydrophilic head of the amphi-

philic mediator) bridges the electron flux from the cell membrane to the electrode. Rawson et al.[131] examined the dual mediator system in yeast by combining ferricyanide and different hydrophobic compounds. The MIS of the hydrophobic mediator was found to be a determining factor for the MET efficiency, while the bulk phase was well-mixed. On the other hand, the amphiphilic mediator could overcome the diffusion issue in the bulk phase, and a redox-active polymer layer can be built with this mediator with the microbial cells. This concept was nicely reviewed by Kaneko et al.[132] in 2020, and thus will not be discussed in detail here.

6. Summary and Outlook

MET-based EET has been overlooked in the community in the past two decades (at least partially) due to the concerns of toxicity effect and add-up operation cost. When working with mediator-based BESs, the focus often lies on, e.g., maximizing space-time product yields, coulombic efficiency, mediator turnover, etc. The reusability of the mediators is, at least until now, far away from being sufficiently studied. However, mediator-based electron transfer brings a variety of possibilities to bioelectrochemical applications, especially for the integration with industrial biotechnology for bioproduction purposes. Extensive research has to be focused on understanding the interactions between mediators and electroactive microorganisms to realize those possibilities. In this review, we summarized those so far known or hypothesized MIS for different mediators, which have been used in whole-cell electrobiocatalysis. More research in this field is urgently needed and would benefit the rational optimization of future MET applications, e.g., the fundamental understandings of the EET pathways using omics techniques.

To conclude the findings of this review, we want to extend the criteria of an ideal redox mediator by Yang et al.[6] and Fultz and Durst[10] as depicted in Figure 2: First, long-term stability regarding the definition stated above and therefore reusability, as well as low toxicity to the environment in case a sufficient separation is not achievable, has to be reached. Second, the ideal mediator most likely has to be added artificially since the transportation through the membrane exerts a lower metabolic burden on the organism than the natural production. As well as that, a redox potential that fits the targeted MIS is crucial. Third and final, the ability to reach the MIS by penetrating the microbial membrane has to be one of the key features of an ideal redox mediator. As we discussed, the mechanism of membrane transfer is most likely rate-limiting and therefore has to be investigated in further detail.

Acknowledgements

This work was created as part of the project "Bioelectrochemical and engineering fundamentals to establish electro-biotechnology for biosynthesis – Power to value-added products (eBiotech)", which is funded by the Deutsche Forschungsgemeinschaft (DFG, German Research Foundation) – Project number 422694804. Open Access funding enabled and organized by Projekt DEAL.

Conflict of Interest

The authors declare no conflict of interest.

Keywords: cross membrane mediator transport · electromicrobiology · mediated extracellular electron transfer · redox mediators · total turnover number

[1] F. Garcia-Ochoa, E. Gomez, *Biotechnol. Adv.* **2009**, *27*, 153.
[2] S. Schmitz, S. Nies, N. Wierckx, L. M. Blank, M. A. Rosenbaum, *Front. Microbiol.* **2015**, *6*, 284.
[3] B. Küpper, A. Mause, L. Halka, A. Imhoff, C. Nowacki, R. Wichmann, *Chem. Ing. Tech.* **2013**, *85*, 834.
[4] I. Vassilev, G. Gießelmann, S. K. Schwechheimer, C. Wittmann, B. Virdis, J. O. Krömer, *Biotechnol. Bioeng.* **2018**, *115*, 1499.
[5] I. Vassilev, N. J. H. Averesch, P. Ledezma, M. Kokko, *Biotechnol. Adv.* **2021**, 107728.
[6] A. Sydow, T. Krieg, F. Mayer, J. Schrader, D. Holtmann, *Appl. Microbiol. Biotechnol.* **2014**, *98*, 8481.
[7] B. E. Logan, *Appl. Microbiol. Biotechnol.* **2010**, *85*, 1665.
[8] H. M. Fruehauf, F. Enzmann, F. Harnisch, R. Ulber, D. Holtmann, *Biotechnol. J.* **2020**, *15*, e2000066.
[9] Y. Yang, M. Xu, J. Guo, G. Sun, *Process Biochem.* **2012**, *47*, 1707.
[10] M. L. Fultz, R. A. Durst, *Anal. Chim. Acta* **1982**, *140*, 1.
[11] F. Melin, P. Hellwig, *Chem. Rev.* **2020**, *120*, 10244.
[12] J. Esther, L. B. Sukla, N. Pradhan, S. Panda, *Korean J. Chem. Eng.* **2015**, *32*, 1.
[13] F. Kracke, I. Vassilev, J. O. Krömer, *Front. Microbiol.* **2015**, *6*, 575.
[14] K. M. Leung, G. Wanger, M. Y. El-Naggar, Y. Gorby, G. Southam, W. M. Lau, J. Yang, *Nano Lett.* **2013**, *13*, 2407.
[15] N. S. Malvankar, M. Vargas, K. P. Nevin, A. E. Franks, C. Leang, B.-C. Kim, K. Inoue, T. Mester, S. F. Covalla, J. P. Johnson, V. M. Rotello, M. T. Tuominen, D. R. Lovley, *Nat. Nanotechnol.* **2011**, *6*, 573.
[16] B. Lai, P. V. Bernhardt, J. O. Krömer, *ChemSusChem* **2020**, *13*, 5308.
[17] J. Tschörtner, B. Lai, J. O. Krömer, *Front. Microbiol.* **2019**, *10*, 866.
[18] Y. Yi, T. Zhao, Y. Zang, B. Xie, H. Liu, *Electrochem. Commun.* **2021**, *124*, 106966.
[19] S. Yonei, A. Noda, A. Tachibana, S. Akasaka, *Mutat. Res., Fundam. Mol. Mech. Mutagen.* **1986**, *163*, 15.
[20] F. A. V. Castro, D. Mariani, A. D. Panek, E. C. A. Eleutherio, M. D. Pereira, *PLoS One* **2008**, *3*, e3999.
[21] M. Wu, M. Du, G. Wu, F. Lu, J. Li, A. Lei, H. Zhu, Z. Hu, J. Wang, *Biotechnol. Biofuels* **2021**, *14*, 132.
[22] O. Depraetere, G. Pierre, W. Noppe, D. Vandamme, I. Foubert, P. Michaud, K. Muylaert, *Algal Res.* **2015**, *10*, 48.
[23] U. Riese, D. Lütkemeyer, R. Heidemann, H. Büntemeyer, J. Lehmann, *J. Biotechnol.* **1994**, *34*, 247.
[24] S. Çoruh, E. H. Gürkan, *Environ. Prog. Sustainable Energy* **2013**.
[25] L.-L. Hwang, J.-C. Chen, M.-Y. Wey, *Desalination* **2013**, *313*, 166.
[26] R. Marcílio, S. A. Neto, B. M. Ruvieri, F. D. Andreote, A. R. de Andrade, V. Reginatto, *Braz. J. Chem. Eng.* **2021**, 471.
[27] X. Xin, H. Pang, Y. She, J. Hong, *Bioresour. Technol.* **2020**, *311*, 123469.
[28] W. Huang, J. Chen, Y. Hu, J. Chen, J. Sun, L. Zhang, *Int. J. Hydrogen Energy* **2017**, *42*, 2349.
[29] S. Kochius, A. O. Magnusson, F. Hollmann, J. Schrader, D. Holtmann, *Appl. Microbiol. Biotechnol.* **2012**, *93*, 2251.
[30] H.-Y. Yang, Y.-X. Wang, C.-S. He, Y. Qin, W.-Q. Li, W.-H. Li, Y. Mu, *Appl. Energy* **2020**, *274*, 115292.
[31] T. Arinda, L.-A. Philipp, D. Rehnlund, M. Edel, J. Chodorski, M. Stöckl, D. Holtmann, R. Ulber, J. Gescher, K. Sturm-Richter, *Front. Microbiol.* **2019**, *10*, 126.
[32] S. Kozuch, J. M. L. Martin, *ACS Catal.* **2012**, *2*, 2787.
[33] A. Manjón, J. M. Obón, P. Casanova, V. M. Fernández, J. L. Ilborra, *Biotechnol. Lett.* **2002**, *24*, 1227.
[34] T. A. Rogers, A. S. Bommarius, *Chem. Eng. Sci.* **2010**, *65*, 2118.

[35] L. Tetianec, A. Chaleckaja, J. Kulys, R. Janciene, L. Marcinkeviciene, R. Meskiene, J. Stankeviciute, R. Meskys, *Process Biochem.* **2017**, *54*, 41.
[36] S. Kochius, J. B. Park, C. Ley, P. Könst, F. Hollmann, J. Schrader, D. Holtmann, *J. Mol. Catal. B* **2014**, *103*, 94.
[37] L. K. Nielsen, L. M. Blank, J. O. Krömer (Eds.) *SpringerLink Books, Vol. 1191*, Humana Press, New York, NY, **2014**.
[38] G. N. Stephanopoulos, A. A. Aristidou, J. H. Nielsen, *Metabolic engineering. Principles and methodologies*, Academic Press, San Diego, California, **1998**.
[39] S. Hintermayer, S. Yu, J. O. Krömer, D. Weuster-Botz, *Biochem. Eng. J.* **2016**, *115*, 1.
[40] M. Kaneko, M. Ishikawa, J. Song, S. Kato, K. Hashimoto, S. Nakanishi, *Electrochem. Commun.* **2017**, *75*, 17.
[41] G. Lunn, P. J. Klausmeyer, E. B. Sansone, *Biotech. Histochem.* **1994**, *69*, 45.
[42] G. Lunn, E. B. Sansone, *Biotech. Histochem.* **1991**, *66*, 307.
[43] M. Otero, F. Rozada, L. Calvo, A. García, A. Morán, *Biochem. Eng. J.* **2003**, *15*, 59.
[44] T. W. Phillips, J. H. Bannock, J. C. deMello, *Lab Chip* **2015**, *15*, 2960.
[45] H.-L. Chen, S.-K. Chang, C.-Y. Lee, L.-L. Chuang, G.-T. Wei, *Anal. Chim. Acta* **2012**, *742*, 54.
[46] E. Fosso-Kankeu, A. Webster, I. O. Ntwampe, F. B. Waanders, *Arabian J. Sci. Eng.* **2017**, *42*, 1389.
[47] H. R. Pouretedal, S. Sabzevari, *Desalin. Water Treat.* **2011**, *28*, 247.
[48] J. Luo, A. Sam, B. Hu, C. DeBruler, X. Wei, W. Wang, T. L. Liu, *Nano Energy* **2017**, *42*, 215.
[49] R. M. Allen, H. P. Bennetto, *Appl. Biochem. Biotechnol.* **1993**, *39–40*, 27.
[50] C. Kong, L. Qin, J. Liu, X. Zhong, L. Zhu, Y.-T. Long, *Anal. Methods* **2010**, *2*, 1056.
[51] D. H. Park, J. G. Zeikus, *J. Bacteriol.* **1999**, *181*, 2403.
[52] Y. Choi, N. Kim, S. Kim, S. Jung, *Bull. Korean Chem. Soc.* **2003**, *24*, 437.
[53] R. W. Jones, T. A. Gray, P. B. Garland, *Biochem. Soc. Trans.* **1976**, *4*, 671.
[54] J. Feng, Q. Lu, K. Li, S. Xu, X. Wang, K. Chen, P. Ouyang, *Front. Bioeng. Biotechnol.* **2020**, *8*, 590667.
[55] D. J. Hassett, L. Charniga, K. Bean, D. E. Ohman, M. S. Cohen, *Infect. Immun.* **1992**, *60*, 328.
[56] A. Chukwubuikem, C. Berger, A. Mady, M. A. Rosenbaum, *Microb. Biotechnol.* **2021**.
[57] E. R. Clifford, R. W. Bradley, L. T. Wey, J. M. Lawrence, X. Chen, C. J. Howe, J. Z. Zhang, *Chem. Sci.* **2021**, *12*, 3328.
[58] E. M. Bosire, L. M. Blank, M. A. Rosenbaum, *Appl. Environ. Microbiol.* **2016**, *82*, 5026.
[59] A. J. Da Silva, J. d. S. Cunha, T. Hreha, K. C. Micocci, H. S. Selistre-de-Araujo, B. Barquera, M. A. G. Koffas, *Metab. Eng.* **2021**, *64*, 15.
[60] Z. Rhodes, O. Simoska, A. Dantanarayana, K. J. Stevenson, S. D. Minteer, *iScience* **2021**, 103033.
[61] K. Rabaey, N. Boon, M. Höfte, W. Verstraete, *Environ. Sci. Technol.* **2005**, *39*, 3401.
[62] S. Schmitz, M. A. Rosenbaum, *ACS Chem. Biol.* **2020**, *15*, 3244.
[63] M. Terzer, J. Stelling, *Bioinformatics* **2008**, *24*, 2229.
[64] K. Y. Chen, P. A. Schauer, B. O. Patrick, C. P. Berlinguette, *Dalton Trans.* **2018**, *47*, 11942.
[65] F. Kracke, B. Virdis, P. V. Bernhardt, K. Rabaey, J. O. Krömer, *Biotechnol. Biofuels* **2016**, *9*, 249.
[66] B. Lai, S. Yu, P. V. Bernhardt, K. Rabaey, B. Virdis, J. O. Krömer, *Biotechnol. Biofuels* **2016**, *9*, 39.
[67] J. Zhao, F. Li, Y. Cao, X. Zhang, T. Chen, H. Song, Z. Wang, *Biotechnol. Adv.* **2020**, 107682.
[68] F. Kracke, J. O. Krömer, *BMC Bioinf.* **2014**, *15*, 410.
[69] T.-T. Liang, L. Zhou, M. Irfan, Y. Bai, X.-Z. Liu, J.-L. Zhang, Z.-Y. Wu, W.-Z. Wang, J.-F. Liu, L. Cheng, S.-Z. Yang, R.-Q. Ye, J.-D. Gu, B.-Z. Mu, *ChemElectroChem* **2020**, *7*, 3783.
[70] S. J. Marritt, T. G. Lowe, J. Bye, D. G. G. McMillan, L. Shi, J. Fredrickson, J. Zachara, D. J. Richardson, M. R. Cheesman, L. J. C. Jeuken, J. N. Butt, *Biochem. J.* **2012**, *444*, 465.
[71] C. C. Page, C. C. Moser, X. Chen, P. L. Dutton, *Nature* **1999**, *402*, 47.
[72] V. Fülöp, C. J. Ridout, C. Greenwood, J. Hajdu, *Structure* **1995**, *3*, 1225.
[73] M. Firer-Sherwood, G. S. Pulcu, S. J. Elliott, *JBIC J. Biol. Inorg. Chem.* **2008**, *13*, 849.
[74] A. Okamoto, K. Hashimoto, K. H. Nealson, R. Nakamura, *Proc. Natl. Acad. Sci. USA* **2013**, *110*, 7856.
[75] H. Santos, J. J. Moura, I. Moura, J. LeGall, A. V. Xavier, *Eur. J. Biochem.* **1984**, *141*, 283.
[76] M. Y. El-Naggar, G. Wanger, K. M. Leung, T. D. Yuzvinsky, G. Southam, J. Yang, W. M. Lau, K. H. Nealson, Y. A. Gorby, *Proc. Natl. Acad. Sci. USA* **2010**, *107*, 18127.
[77] J. H. van Wonderen, K. Adamczyk, X. Wu, X. Jiang, S. E. H. Piper, C. R. Hall, M. J. Edwards, T. A. Clarke, H. Zhang, L. J. C. Jeuken, I. V. Sazanovich, M. Towrie, J. Blumberger, S. R. Meech, J. N. Butt, *Proc. Natl. Acad. Sci. USA* **2021**, *118*.
[78] W. van Leeuwen, C. van Dijk, H. J. Grande, C. Veeger, *Eur. J. Biochem.* **1982**, *127*, 631.
[79] B. Schuppert, B. Schink, W. Trsch, *Appl. Microbiol. Biotechnol.* **1992**, *37*, 549.
[80] S. D. Roller, H. P. Bennetto, G. M. Delaney, J. R. Mason, J. L. Stirling, C. F. Thurston, *J. Chem. Technol. Biotechnol.* **1984**, *34*, 3.
[81] D. H. Park, J. G. Zeikus, *Appl. Environ. Microbiol.* **2000**, *66*, 1292.
[82] I. Nijenhuis, S. H. Zinder, *Appl. Environ. Microbiol.* **2005**, *71*, 1664.
[83] F. Aulenta, A. Catervi, M. Majone, S. Panero, P. Reale, S. Rossetti, *Environ. Sci. Technol.* **2007**, *41*, 2554.
[84] H. Tatsumi, K. Takagi, M. Fujita, K. Kano, T. Ikeda, *Anal. Chem.* **1999**, *71*, 1753.
[85] S. Tsujimura, M. Fujita, H. Tatsumi, K. Kano, T. Ikeda, *Phys. Chem. Chem. Phys.* **2001**, *3*, 1331.
[86] B. M. Lindley, A. M. Appel, K. Krogh-Jespersen, J. M. Mayer, A. J. M. Miller, *ACS Energy Lett.* **2016**, *1*, 698.
[87] F. Dong, Y. S. Lee, E. M. Gaffney, M. Grattieri, H. Haddadin, S. D. Minteer, H. Chen, *Cell Rep. Phys. Sci.* **2021**, 100444.
[88] T. D. Harrington, V. N. Tran, A. Mohamed, R. Renslow, S. Biria, L. Orfe, D. R. Call, H. Beyenal, *Bioresour. Technol.* **2015**, *192*, 689.
[89] D. H. Park, M. Laivenieks, M. V. Guettler, M. K. Jain, J. G. Zeikus, *Appl. Environ. Microbiol.* **1999**, *65*, 2912.
[90] H. Seelajaroen, M. Haberbauer, C. Hemmelmair, A. Aljabour, L. M. Dumitru, A. W. Hassel, N. S. Sariciftci, *ChemBioChem* **2019**, *20*, 1196.
[91] Y. Tokunou, K. Hashimoto, A. Okamoto, *J. Phys. Chem. C* **2016**, *120*, 16168.
[92] Y. Wu, T. Liu, X. Li, F. Li, *Environ. Sci. Technol.* **2014**, *48*, 9306.
[93] W.-C. Kao, T. Kleinschroth, W. Nitschke, F. Baymann, Y. Neehaul, P. Hellwig, S. Richers, J. Vonck, M. Bott, C. Hunte, *Biochim. Biophys. Acta* **2016**, *1857*, 1705.
[94] Z. Xi, J. Guo, J. Lian, H. Li, L. Zhao, X. Liu, C. Zhang, J. Yang, *Bioresour. Technol.* **2013**, *140*, 22.
[95] N. L. Costa, B. Hermann, V. Fourmond, M. M. Faustino, M. Teixeira, O. Einsle, C. M. Paquete, R. O. Louro, *mBio* **2019**, *10*.
[96] C. Kim, M. Y. Kim, I. Michie, B.-H. Jeon, G. C. Premier, S. Park, J. R. Kim, *Biotechnol. Biofuels* **2017**, *10*, 199.
[97] A. H. Förster, S. Beblawy, F. Golitsch, J. Gescher, *Biotechnol. Biofuels* **2017**, *10*, 65.
[98] E. N. Brown, R. Friemann, A. Karlsson, J. V. Parales, M. M.-J. Couture, L. D. Eltis, S. Ramaswamy, *JBIC J. Biol. Inorg. Chem.* **2008**, *13*, 1301.
[99] S. Wilkinson, J. Klar, S. Applegarth, *Electroanalysis* **2006**, *18*, 2001.
[100] J. Zhao, Z. Wang, C. Fu, M. Wang, Q. He, *Electroanalysis* **2008**, *20*, 1587.
[101] R. Y. A. Hassan, U. Wollenberger, *Anal. Bioanal. Chem.* **2016**, *408*, 579.
[102] P. Ertl, B. Unterladstaetter, K. Bayer, S. R. Mikkelsen, *Anal. Chem.* **2000**, *72*, 4949.
[103] K. Nishio, Y. Kimoto, J. Song, T. Konno, K. Ishihara, S. Kato, K. Hashimoto, S. Nakanishi, *Environ. Sci. Technol. Lett.* **2014**, *1*, 40.
[104] T. A. Clarke, M. J. Edwards, A. J. Gates, A. Hall, G. F. White, J. Bradley, C. L. Reardon, L. Shi, A. S. Beliaev, M. J. Marshall, Z. Wang, N. J. Watmough, J. K. Fredrickson, J. M. Zachara, J. N. Butt, D. J. Richardson, *Proc. Natl. Acad. Sci. USA* **2011**, *108*, 9384.
[105] A. Okamoto, K. Hashimoto, K. H. Nealson, *Angew. Chem. Int. Ed.* **2014**, *53*, 10988.
[106] A. Okamoto, R. Nakamura, K. H. Nealson, K. Hashimoto, *ChemElectroChem* **2014**, *1*, 1808.
[107] Y. Wang, D. K. Newman, *Environ. Sci. Technol.* **2008**, *42*, 2380.
[108] J. Jo, A. Price-Whelan, W. C. Cornell, L. E. P. Dietrich, *J. Bacteriol.* **2020**, *202*.
[109] V. Flexer, F. Durand, S. Tsujimura, N. Mano, *Anal. Chem.* **2011**, *83*, 5721.
[110] E. Marsili, D. B. Baron, I. D. Shikhare, D. Coursolle, J. A. Gralnick, D. R. Bond, *Proc. Natl. Acad. Sci. USA* **2008**, *105*, 3968.
[111] L. Huang, X. Liu, Y. Ye, M. Chen, S. Zhou, *Environ. Microbiol.* **2020**, *22*, 243.
[112] S. H. Light, L. Su, R. Rivera-Lugo, J. A. Cornejo, A. Louie, A. T. Iavarone, C. M. Ajo-Franklin, D. A. Portnoy, *Nature* **2018**, *562*, 140.
[113] A. Okamoto, K. Saito, K. Inoue, K. H. Nealson, K. Hashimoto, R. Nakamura, *Energy Environ. Sci.* **2014**, *7*, 1357.
[114] V. A. García-Angulo, *Crit. Rev. Microbiol.* **2017**, *43*, 196.

[115] H. Sakhtah, L. Koyama, Y. Zhang, D. K. Morales, B. L. Fields, A. Price-Whelan, D. A. Hogan, K. Shepard, L. E. P. Dietrich, *Proc. Natl. Acad. Sci. USA* **2016**, *113*, E3538–47.
[116] J. C. Salerno, B. Bolgiano, W. Ingledew, *FEBS Lett.* **1989**, *247*, 101.
[117] W. J. Ingledew, T. Ohnishi, J. C. Salerno, *Eur. J. Biochem.* **1995**, *227*, 903.
[118] F. Melin, H. Xie, T. Meyer, Y. O. Ahn, R. B. Gennis, H. Michel, P. Hellwig, *Biochim. Biophys. Acta* **2016**, *1857*, 1892.
[119] M. R. Pudek, P. D. Bragg, *Arch. Biochem. Biophys.* **1976**, *174*, 546.
[120] D. G. McMillan, S. J. Marritt, J. N. Butt, L. J. Jeuken, *J. Biol. Chem.* **2012**, *287*, 14215.
[121] E. Harada, J. Kumagai, K. Ozawa, S. Imabayashi, A. S. Tsapin, K. H. Nealson, T. E. Meyer, M. A. Cusanovich, H. Akutsu, *FEBS Lett.* **2002**, *532*, 333.
[122] G. Repetto, A. Del Peso, J. L. Zurita, *Nat. Protoc.* **2008**, *3*, 1125.
[123] K. Matsushita, Y. Ohno, E. Shinagawa, O. Adachi, M. Ameyama, *Agric. Biol. Chem.* **1980**, *44*, 1505.
[124] N. Ohno, M. A. Cusanovich, *Biophys. J.* **1981**, *36*, 589.
[125] R. W. Jones, P. B. Garland, *Biochem. J.* **1977**, *164*, 199.
[126] J. A. Mccray, T. Kihara, *Biochim. Biophys. Acta* **1979**, *548*, 417.
[127] C. G. Eley, E. Ragg, G. R. Moore, *J. Inorg. Biochem.* **1984**, *21*, 295.
[128] M. Meier, R. van Eldik, *Chem. Eur. J.* **1997**, *3*, 39.
[129] C. Cai, B. Liu, M. V. Mirkin, H. A. Frank, J. F. Rusling, *Anal. Chem.* **2002**, *74*, 114.
[130] S. Ishii, S. Suzuki, T. M. Norden-Krichmar, A. Tenney, P. S. G. Chain, M. B. Scholz, K. H. Nealson, O. Bretschger, *Nat. Commun.* **2013**, *4*, 1601.
[131] F. J. Rawson, A. J. Downard, K. H. Baronian, *Sci. Rep.* **2014**, *4*, 5216.
[132] M. Kaneko, K. Ishihara, S. Nakanishi, *Small* **2020**, *16*, e2001849.

Manuscript received: February 26, 2022
Revised manuscript received: May 10, 2022
Accepted manuscript online: May 12, 2022

A.2 Publication II

André Gemünde, Jonas Gail, and Dirk Holtmann

Anodic Respiration of *Vibrio natriegens* in a Bioelectrochemical System

In *ChemSusChem*, Volume 16, Issue 16, 2023,
DOI: https://doi.org/10.1002/cssc.202300181

Contribution: My contribution to the work was the reactor design and setup, the process conceptualization, and the supervision of the experimental work performed by Jonas Gail. Furthermore, I wrote the entire original manuscript.

Check for updates

ChemSusChem

Research Article
doi.org/10.1002/cssc.202300181

Chemistry Europe
European Chemical Societies Publishing

www.chemsuschem.org

VIP *Very Important Paper*

Anodic Respiration of *Vibrio natriegens* in a Bioelectrochemical System

André Gemünde,[a] Jonas Gail,[a] and Dirk Holtmann*[a]

Vibrio natriegens promises to be a new standard biotechnological working organism since it grows extraordinarily fast, its productivity surpasses *E. coli* by far, and genomic tools are getting readily available. Recent studies provided insights into its extracellular electron transfer pathway, revealing it to be similar to other well-known electroactive organisms. Therefore, we aimed to show for the first time that *V. natriegens* donates electrons from its metabolism to an electrode by direct contact as well as via an artificial redox mediator. Our results demonstrate current densities up to 196 $\mu A\,cm^{-2}$ using an artificial mediator. Via direct electron transfer, 6.6 $\mu A\,cm^{-2}$ were achieved within the first 24 h of cultivation. In the mediated system, mainly formate, acetate, and succinate were produced from glucose. These findings favor *V. natriegens* over established electroactive organisms due to its superior electron-transfer capabilities combined with an outstanding metabolism.

Introduction

V. natriegens receives more and more attention in biochemical engineering due to its ability to grow very fast on different substrates. It is referred to as the fastest-growing non-pathogenic microorganism on the planet.[1] This attribute raises high expectations for the microorganism as a promising broad-range production host.[2,3] Essential for growth of the gram-negative, rod-shaped marine bacterium is the availability of sodium ions.[4] Another advantage for surviving in changing environments compared to other organisms is the flexibility in using different electron acceptors. *V. natriegens* can donate electrons to oxygen as well as fumarate, nitrate, nitrite, Fe^{III} citrate and fermentation products.[5,6] Nevertheless, the fast growth also demands for high oxygen uptake, which calls for reactors enabling high oxygen transfer rates. However, this can theoretically also be addressed by using bioelectrochemical methods.

Bioelectrochemical systems (BES) offer electrodes as electron donors or acceptors. For electrodes polarized as anodes, meaning the electrode acts as an acceptor, organisms can respire through this electrode in a process therefore termed "anodic respiration". Compared to conventional processes, this offers the advantage that no oxygen has to be introduced into the medium. In theory, scale-up limitations originating from oxygen transfer can therefore be eliminated. However, for this to happen, the organisms need to be electroactive, meaning that mechanisms are required to enable electron transfer through the isolating cell membrane.[7] Detailed knowledge about those mechanisms still remains unknown. In case of the model organisms *Shewanella oneidensis* and *Geobacter sulfurreducens* detailed models existed for several years.[8] For *V. natriegens*, Conley et al. recently proposed a mechanism describing the extracellular electron transfer (EET) pathway as a hybrid of *S. oneidensis* and *Aeromonas spp.*[5] Genomic analysis revealed 77% similarity between CymA, an inner membrane tetraheme cytochrome transporting electrons from the quinone pool to the periplasm (Figure 1), of *V. natriegens* to the *Aeromonas schubertii* analogue. Further, the periplasmatic shuttle molecule

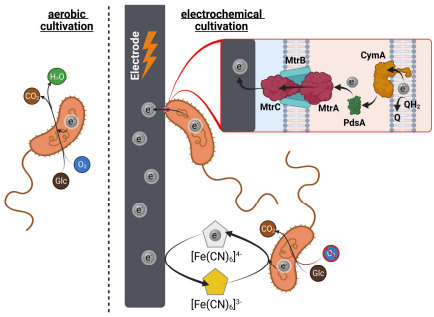

Figure 1. Electron transfer pathways in aerobic vs. anaerobic BES cultivation for *V. natriegens*. Under aerobic conditions, oxygen acts as a terminal electron acceptor. With an electrode as a terminal electron acceptor, *V. natriegens* can transfer electrons from the quinone pool to the anode via direct transfer. This is enabled by an electron transfer chain made up from multiple c-type cytochromes. Additionally, planktonic cells can "respire" through the anode by using $[Fe(CN)_6]^{3-/4-}$ as soluble electron shuttle. Created with BioRender.com.

[a] *A. Gemünde, J. Gail, Prof. Dr.-Ing. D. Holtmann*
Institute of Bioprocess Engineering and Pharmaceutical Technology and Competence Centre for Sustainable Engineering and Environmental Systems
University of Applied Sciences Mittelhessen
35390 Gießen (Germany)
E-mail: andre.gemuende@lse.thm.de
dirk.holtmann@lse.thm.de

Supporting information for this article is available on the WWW under https://doi.org/10.1002/cssc.202300181

PdsA from *Aeromonas hydrophila* and *A. schubertii* is 68% similar to the respective *V. natriegens* periplasmatic electron shuttle. The outer membrane electron transfer chain proteins MtrCAB share the most similarity to *Aeromonas spp.* with 50% to MtrC, 61–62% for MtrB, and 73–81% for MtrA.[5] In theory, those cytochromes should enable a direct electron transfer (DET) between *V. natriegens* and electrodes or mediators.

To the best of our knowledge, only the experimental studies by Lam et al. provide evidence of an EET with an unspecified *Vibrio* strain isolated from a BES.[9] In their study, mixed cultures were investigated and it was shown that a *Vibrio sp.* isolate was able to transfer electrons to anodes as well as cathodes. However, it has not yet been shown whether pure cultures of *V. natriegens* are electroactive or able to produce industrial-relevant chemicals in a BES.

A further way to enable EET is the mediated electron transfer (MET). Hereby, redox-active shuttle molecules, so-called mediators are able to transfer electrons between electrodes and microorganisms. Some of those shuttles are capable of traversing the (outer) membrane which grants them access to periplasmic or cytoplasmic interaction sites.[10] The mediators can be distinguished into two main groups, artificial or self-synthesized natural molecules.[11]

This study aimed to investigate the mediated and direct electron transfer of *V. natriegens*. Hence, special attention is devoted to characterizing growth and product formation under the artificial electrochemical cultivation conditions.

Results and Discussion

In a first step, batch cultivations of *V. natriegens* were conducted in 300 mL BES reactors containing 1 mM of $K_3[Fe(CN)_6]$ as an artificial mediator in mineral medium. Immediately after inoculation, a current production could be observed and a maximum current density of $157 \pm 28.55\ \mu A\,cm^{-2}$ was obtained after 19.5 h (Figure 2a). The concentration of oxidized mediator mirrored the current density in the opposite direction, although the desired concentration of 1 mM was not reached in the beginning. This could be due to errors during the addition by syringes or by decomposition reactions since the mediator is added 24 h prior to inoculation. When the maximum current density was reached, the concentration of the oxidized species ($[Fe(CN_6)]^{3-}$) dropped to a minimum of 0.13 mM.

Therefore, around 16.3% of the initially added mediator was still in its oxidized state. It is therefore likely that the electrode reaction was not limiting the maximum current density at this point. Though it is still conceivable, a higher amount of available $[Fe(CN_6)]^{3-}$ could enhance the electron transfer from the microorganism to the electrode. Similar results were shown for *Pseudomonas putida* KT2440 in a stirred tank electrochemical bioreactor and *Lactococcus lactis* cultivated with $[Fe(CN_6)]^{3-}$, where increasing the concentration of the redox shuttle $[Fe(CN_6)]^{3-}$ led to higher growth rates.[12] After the current density decreased, the electrode was again able to re-oxidize the mediator to 100%. The mediator's total turnover number (TTN) was calculated as 18.84 ± 2.15. This demonstrates the reversibility of the mediator's redox reaction over the entire batch cultivation. As under strictly anaerobic conditions, *V. natriegens* was able to grow under BES conditions from a

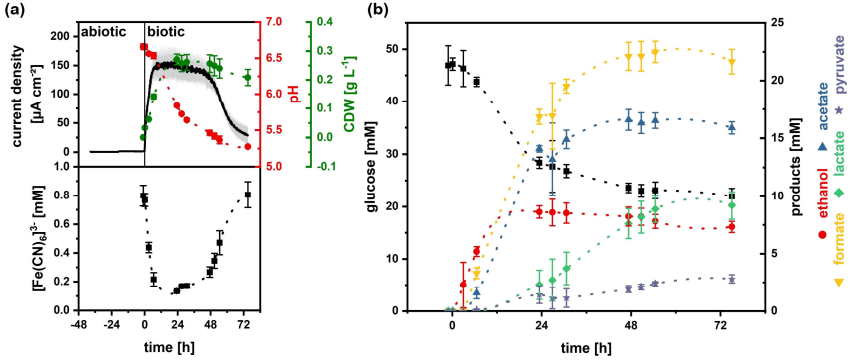

Figure 2. (**a**) Anaerobic batch cultivation of *V. natriegens* at 30 °C in 300 mL stirred-tank bioreactors at 400 rpm and applied potential 500 mV vs. Ag/AgCl (satd. KCl) with 1 mM added $[Fe(CN)_6]^{3-}$ as redox mediator to the M1 medium. The headspace of each reactor was flushed with 45 mL min^{-1} N_2. Black line: current density, red dots: pH value, green dots: cell density measured at 600 nm, black squares: $[Fe(CN)_6]^{3-}$ concentration in mM. (**b**) Substrate and product concentrations over the course of the batch process. Concentrations of glucose (black squares), ethanol (red dots), acetate (blue triangles), formate (yellow triangles), lactate (green diamonds), and pyruvate (purple stars). Dotted lines: interpolation of the data points. Error bars depict the standard deviation from triplicates.

starting cell dry weight (CDW) of 0.04 g L^{-1} to a maximum of 0.26 g L^{-1} with a growth rate of 0.228 h^{-1} (Figure S4b and S4c in the Supporting Information). During growth, the acidic products formate, acetate, and lactate were excreted and subsequently, the pH dropped. Then, at a pH below 5.5, the glucose metabolization stopped, no further products were synthesized and the current began to drop (Figure 2b). When the pH was manually corrected in the range of 6–6.5, the current generation was extended, but the metabolic activity declined over time (Figure S6). Overall, the pH plays a significant role within the system. The metabolism stops at a pH below 5.5 in the M1 medium. With a low pH in the anodic chamber, the pH drop between the anodic and cathodic chamber increases, leading to a potential loss of around 0.06 V per pH unit according to the Nernst equation.[13] Furthermore, the formal redox potential of the mediator ferricyanide is affected by pH changes. Due to protonation of the ligands in aqueous environments, the formal potential changes to more positive values in acidic conditions.[14] However, stability is not affected until very high pH values are reached.[15]

In order to understand the electron flow within the metabolism of *V. natriegens*, the electron balance was calculated. In total, from the amount of electrons that were available through glucose consumption, 2.3 ± 0.29 % were found to be transferred to the anode resulting in a current flow (Figure 2a, Figure S10). In contrast, 45.91 ± 1.21 % could be attributed to all products, and 2.84 ± 0.93 % were calculated for generated biomass, which leaves 48.95 % undetected. Therefore, a coulombic efficiency (CE) of 4.25 ± 0.42 % was reached. The missing electrons could be attributed to the biomass accumulating as biofilm on the reactor internals or the formation of extracellular polymeric substances since no oxygen or other known electron sinks were present in the system (Figure S9). We compared the anodic respiration to the common aerobic respiration on oxygen via the oxygen uptake rate known from the literature (Supporting Information, Section 2.5.6).[16] This resulted in only 1.44 % of the electron uptake needed for growing cells on oxygen being available through anodic respiration. In contrast, 29.08 % were reached via fermentation products. Since the electron balance is not closed so far, other electron sinks might influence the respiratory electron flow. In addition, the carbon balance could only show 55.2 ± 1.38 % of the added carbon in the products and 2.56 ± 0.36 % in the biomass, leaving until now 42.24 % undetected. From the literature, the amino acid alanine is known to be produced with high titers by non-growing *V. natriegens* cells in anaerobic cultivations.[17] However, in our study, alanine could not be detected via the chosen HPLC method in supernatants at the end of BES cultivations with both media.

In the anaerobic batch culture supernatants of *V. natriegens*, no succinate could be detected. This might be due to the fact, that only nitrogen and no additional carbonate was fed into the medium. Therefore, there was not enough CO_2 available to enable the carboxylation of phosphoenolpyruvate or pyruvate through the reductive TCA cycle (Figure S2).[18] This may also explain the accumulation of pyruvate in our experiments.

To circumvent this metabolic "obstacle", we added CO_2 and HCO_3^- to the medium according to Thoma et al. for anaerobic succinate production. In the anodic cultivation chamber, the pH was controlled at 7.5.[18]

Hereby, a maximum current density of 196.27 ± 16.95 μA cm^{-2} was obtained and held nearly constant throughout the 216 h of cultivation time (Figure 3a). Furthermore, the CDW reached a maximum of 1.49 g L^{-1} with a growth rate of 0.493 h^{-1}, which is about half the rate compared to aerobic conditions (0.965 h^{-1}, Figure S4a and S4e). $[Fe(CN)_6]^{3-}$ was reduced entirely to $[Fe(CN)_6]^{4-}$ after 5 h, indicating the total mediator concentration or the anode re-oxidation was limiting the maximum current. Another possible limitation might be that the buffer in the (abiotic) cathodic compartment becomes too basic due to the excessive H^+ consumption, resulting in a potential loss in the system (Figure S7).

With a gaseous phase containing 20 % (v/v) CO_2 and 10 g L^{-1} HCO_3^- added to the medium, glucose was quickly consumed and typical anaerobic products like acetate, ethanol, formate, and lactate were formed. This time, pyruvate accumulated during the exponential growth between 3 and 23 h and was taken up again (Figure S8), as it was already demonstrated under aerobic conditions (Figure S3b) and reported in the literature.[19] More importantly, succinate was produced to an amount of 9.06 ± 0.68 mM (Figure 3b). Interestingly, after the primary substrate was depleted, the current density stayed at a high level, unlike it is the case with *P. putida* F1, where the current drops immediately after glucose is taken up.[20] The electrons in our case might derive from a metabolic shift from glucose to the excreted fermentation products. In fact, it can be seen from Figure 3b that acetate is accumulated in high concentrations during exponential growth. When the stationary phase is reached, the acetate concentration starts to decrease. Ethanol, formate, and to a lesser extent lactate, are also accumulated during the exponential phase and re-assimilated in the stationary phase. However, gas striping can also explain the decrease in ethanol concentration.

With the continuous CO_2 supply, coulombic efficiencies (CE) up to 13.67 ± 2.55 % can be reached. This represents a comparatively high value. A Wild-type *S. oneidensis* MR-1 reaches only CE values of around 8.6 % on lactate.[21] The determined electron uptake of the anode relative to the oxygen demand during the cultivation never exceeds 1.4 % (Figure S12), meaning that fermentation is still the predominant way to dispose of electrons.

The experiment was repeated without applying a potential or adding a redox mediator to the reactors. Instead of current, the system's open circuit potential (OCP) was measured. In the first abiotic 16 h, the OCP dropped steadily from 167 mV vs. Ag/AgCl (satd. KCl) to −12 mV (Figure 3c). A control cyclic voltammetry (CV) scan caused the OCP to spike to 193 mV and consequently drop to 14 mV right before the inoculation took place. The addition of the cells then led to a fast decrease in the OCP, eventually reaching a constant level of around −280 mV.

V. natriegens was also able to grow with an OCP in the reactor as long as glucose was available. On glucose, the CDW reached a maximum of 1.85 g L^{-1} with a growth rate of

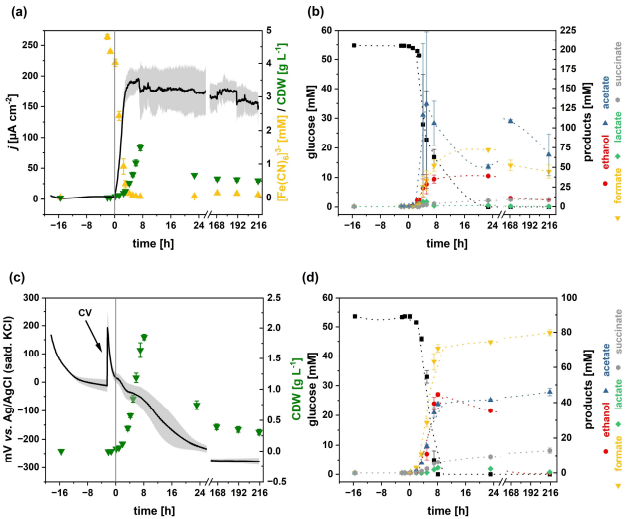

Figure 3. 500 mV BES vs. open-circuit potential (OCP) cultivation of *V. natriegens* in M2 medium with supplementary CO_2. (**a**) Current density (black line) at 500 mV vs. Ag/AgCl (satd. KCl), concentration of oxidized mediator (yellow) starting at 5 mM, and cell density measured by OD_{600} (green). (**b**) Respective products during BES cultivation. Glucose (black squares), ethanol (red dots), acetate (blue triangles), formate (yellow triangles), lactate (green diamonds), and succinate (grey circles). (**c**) Identical experiment setup with no potential applied and no mediator added: OCP and cell density at OD_{600}. (**d**) Respective products during OCP cultivation. Dotted lines: interpolation of the data points. Error bars depict the standard deviation from triplicates. Conditions: 300 mL M2 medium, 30 °C, 400 rpm.

0.647 h^{-1} (Figure S4f). 8 h after inoculation, the glucose was already depleted (Figure 3d). Subsequently, the product formation was negligible. The changes can be mostly attributed to evaporation losses leading to higher concentrations. E.g., with the prevailing evaporation rate of 0.103 mL h^{-1}, the concentration of formate would increase by 0.026 mM h^{-1} without any product synthesis. However, it is obvious that the concentrations of ethanol and lactate are decreasing again, although it is still conceivable that ethanol is being stripped from the liquid phase.

Observed product yields from BES and OCP cultivations lead to the assumption, that BES conditions do not have a particularly strong effect on the metabolism of *V. natriegens* when CO_2 is available (Table 1). In both experiments, neither lactate nor pyruvate was accumulated. Instead, more formate, acetate, and biomass were produced. Interestingly, the succi-

Table 1. Observed product yields from glucose as substrate. Comparison of anaerobic reactor cultivations from Hoffart et al.[17] to anaerobic serum flask and BES reactor cultivations in M1 medium on pure N_2 and in M2 medium with supplementary CO_2 with and without polarization at 500 mV vs. Ag/AgCl (satd. KCl). Standard deviations are calculated from triplicates.

Product	Observed yield $Y'_{P/S}$ [g g^{-1}] Anaerobic (HCO_3^-)[17]	Anaerobic serum flask (N_2)	BES (N_2)	BES (CO_2)	OCP (CO_2)
lactate	0.17 ⊥ 0.01	0.138 ⊥ 0.001	0.207 ⊥ 0.018	0.001 ⊥ 0.001	0.004 ⊥ 0.003
ethanol	0.141 ± 0.06	0.153 ± 0.002	0.062 ± 0.004	0.04 ± 0.001	0
formate	0.301 ± 0.22	0.178 ± 0.003	0.231 ± 0.014	0.209 ± 0.03	0.381 ± 0.01
succinate	0.066 ± 0.05	0	0	0.109 ± 0.007	0.159 ± 0.019
pyruvate	n.d.	0.101 ± 0.002	0.059 ± 0.009	0	0
acetate	0.193 ± 0.15	0.096	0.234 ± 0.029	0.403 ± 0.132	0.286 ± 0.014
alanine	0.31 ± 0.01	n.d.	n.d.	n.d.	n.d.
biomass	0.12 ± 0.01	0.087 ± 0.011	0.042 ± 0.01	0.048 ± 0.006	0.018 ± 0.003

n.d. = not determined.

nate yield was higher when no potential was applied. It cannot be ruled out though, that the addition of CO_2 led to increased yields due to the availability of an inorganic carbon source.[18] However, the difference between the addition of CO_2 and pure N_2 is noteworthy. For instance, without supplementary CO_2, lactate, pyruvate, and ethanol are accumulated while succinate is absent. Comparing our BES with supplemented CO_2 to the results from the anaerobic cultivation by Hoffart et al., our experiment led to higher succinate and acetate yields.[17] These results indicate, that *V. natriegens* is using the MET pathway to respire through the anode, but to a very small extent. The fermentative pathway is still the dominant way to dispose of excess electrons.

To confirm the assumption from Conley et al., that *V. natriegens* can perform a DET through MtrCAB/CymA homologous cytochromes, we performed BES cultivations with an applied potential of 500 mV vs. Ag/AgCl (satd. KCl) in M1 medium and without the addition of a redox mediator and supplementary CO_2.[5] Here, a current response after inoculation with a maximum of 6.6 $\mu A\,cm^{-2}$ (Figure 4) was measured. Even though the current density appears quite low, the fact that a clear current response occurred immediately after the inoculation is still outstanding, showing that a direct electron transfer between *V. natriegens* and a graphite electrode is possible. An abiotic electrochemical reaction or other parasitic currents can be ruled out since no significant current density evolved in the abiotic phase.

The current density might be limited by the metabolic capacity of the MtrCAB/CymA homologous cytochromes or the electrode surface. Here, the pH was not controlled, resulting in the fast drop and concurrent decline in growth after 24 h. The growth rate before reaching the critical pH was calculated as 0.455 h^{-1} (Figure S4d), which is comparable to purely anaerobic conditions in M1 medium without CO_2, achieving a growth rate of 0.549 h^{-1} (Figure S4b). This is probably due to the fact that

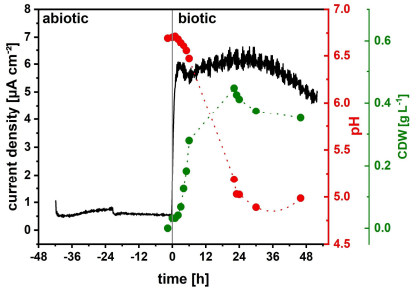

Figure 4. Anaerobic batch cultivation of *V. natriegens* at 30 °C in 300 mL stirred-tank bioreactors at 400 rpm and applied potential of 500 mV vs. Ag/AgCl (satd. KCl) in M1 medium. The headspace of each reactor was flushed with 45 mL min^{-1} N_2. Current density (black line), pH value (red dots), and cell density measured by OD_{600} (green dots). Dotted lines: interpolation of the data points. Data points represent the mean values of duplicates.

planktonic cells cannot interact with the electrode and therefore switch to anaerobic metabolism, thereby enabling a higher cell density than in a mediated system without supplementary CO_2. CV scans at a rate of 50 $mV\,s^{-1}$ before inoculation and after 48 h of cultivation did not show any distinct peaks (Figure S13a). Since biofilm formation is not visible to the eye and current densities during cultivation are very low, the number of adsorbed cells is therefore probably also low. A lower scan rate CV or differential pulse voltammetry may therefore be more applicable to look into the DET of *V. natriegens*. This can also be done electrochemically via CVs at different scan rates. In a diffusion-less system, the Laviron equation describes the relationship between the scan rate and the electron transfer rate of adsorbed redox species.[22] Scanning electron microscopy imaging of electrodes out of a BES reactor could further be used to demonstrate the presence of a thin (electroactive) biofilm. The electroactivity of this biofilm can then be demonstrated by transferring the overgrown electrodes into fresh medium without planktonic cells, to monitor the evolving current from the biofilm exclusively. Similarly, *V. natriegens* may be grown inside an electrochemical flow cell, to specifically support the growth of an electroactive biofilm.

Conclusions

In summary, we demonstrated that *V. natriegens* produces high current densities in a BES via a MET pathway. Further, our experiments showed that a DET to an anode is also possible with a drawback in current density most likely due to the low surface-to-volume ratio of the anode. These findings further support the suggested EET model published by Conley et al.[5] By adding HCO_3^- and further sparging CO_2 into the anode compartment, microbial growth was enhanced and the current density increased to a stable maximum of 196.27 ± 16.95 $\mu A\,cm^{-2}$. This current stayed constant, even when the substrate glucose was depleted.

Our findings set the basis for using *V. natriegens* as a novel broad-range electroactive strain in microbial electrosynthesis. Via genetic manipulation tools, which are becoming more and more available for this strain, the production of reduced products might be enhanced by supplying additional electrons to the organism by reversing the Mtr pathway or via appropriate redox mediators.

Experimental Section

Bacterial strains and chemicals

Vibrio natriegens wild-type DSM 759 purchased from the German Collection of Microorganisms and Cell Cultures GmbH was used for all experiments. All chemicals used in this work were supplied by Merck KGaA (Germany), VWR Chemicals (USA), Carl Roth GmbH & Co. KG (Germany), or Sigma–Aldrich (USA).

Media and culture conditions

V. natriegens was cultivated in BHIN medium consisting of brain heart infusion with an additional 10 g L^{-1} NaCl added. Cultures were incubated at 30 °C and 180 rpm in cultivation tubes filled with 2.5 mL BHIN. Cryo-stocks were prepared by adding 25 % (*v/v*) glycerol in total to an exponential culture and freezing it at −80 °C. Cultivation in BES reactors was performed in two different minimal media. The first one being a modified minimal medium from Schwarz and co-workers, herein referred to as M1 medium, containing 13.21 g L^{-1} Na_2HPO_4, 6.59 g L^{-1} K_2HPO_4, 25.71 g L^{-1} NaCl, 1.18 g L^{-1} NH_4Cl, 1.63 g L^{-1} $MgSO_4$ 7·H_2O, 73.5 mg L^{-1} $CaCl_2$·H_2O, 50 mg L^{-1} EDTA, 8.3 mg L^{-1} $FeCl_3$, 0.84 mg L^{-1} $ZnCl_2$, 0.13 mg L^{-1} $CuCl_2$, 0.1 mg L^{-1} $CoCl_2$·6 H_2O, 0.1 mg L^{-1} H_3BO_3, and 0.016 mg L^{-1} $MnCl_2$·2 H_2O.[2] For succinate production, the second medium (referred to as M2) was adapted from Hoffart and colleagues, which contained 5 g L^{-1} $(NH_4)_2SO_4$, 1 g L^{-1} KH_2PO_4, 1 g K_2HPO_4, 15 g L^{-1} NaCl, 0.01 g L^{-1} $CaCl_2$·H_2O, 0.25 g L^{-1} $MgSO_4$ 7·H_2O, 16.4 mg L^{-1} $FeSO_4$·H_2O, 10 mg L^{-1} $MnSO_4$·H_2O, 1 mg L^{-1} $ZnSO_4$ 7·H_2O, 0.3 mg L^{-1} $CuSO_4$ 5·H_2O, and 0.02 mg L^{-1} $NiCl_2$ 6·H_2O.[17] MOPS (3-(N-morpholino)propanesulfonic acid) buffer was not used since cultivations were performed in pH-controlled reactors. The medium was adjusted to pH 7.5 with 5 M KOH. $KHCO_3$ was added to the M2 medium just before cultivation to a final concentration of 10 g L^{-1}. Glucose was used as substrate with a concentration of 10 g L^{-1} in both media. For BES precultures, cryo-stocks were first streaked on BHIN agar plates and incubated overnight. One colony was used to inoculate a 250 mL flask with baffles filled with 50 mL of the respective culture medium and placed in an orbital shaker at 180 rpm (2.5 cm orbit, Infors, Switzerland). Aerobic cultivation in shake flasks was performed identically to BES precultures in shake flasks with baffles and M1 medium filled to 20 % of the flask volume. Anaerobic cultivations were performed in 250 mL serum flasks filled to 50 mL with M1 medium and flushed with nitrogen for 2 h prior to inoculation.

Bioelectrochemical system

Batch BES cultivations were performed in 4 parallel DASGIP stirred reactors with 300 mL working volume (Eppendorf DASGIP, Germany). Heating and stirring were controlled via the temperature control module (Eppendorf, Germany). The whole reactor volume was used as anodic compartment with the cathodic compartment separated in a 10 mL glass tube fitted with a GL14 thread on one end. The tube was immersed in the reactor and sealed with a circular cation exchange membrane (Nafion 117, QuinTech, Germany). The membrane is pressed against the tube by a sealing ring and a GL14 cap with a 9.5 mm diameter hole. This enables the flow of protons from the anodic to the cathodic chamber. Polished graphite rods with a diameter of 7 mm were used as working electrodes (Graphite24, Germany). The working electrode was further isolated to a length of 80 mm and submerged for 2 h in ethanol and then soaked in water overnight prior to installation. The graphite was contacted with titanium wire (Ø 0.5 mm, 99.6 %, GoodFellow Cambridge Ltd., England) and fixated with conductive carbon cement (Leit-C, Sigma–Aldrich, USA). The electrode was further strapped to a PTFE rod to hold it in place during stirring (Figure S1B). The pH control was performed via pH electrodes (Hamilton, Germany) fitted through the PTFE lid and the respective pH control and feed pump module (Eppendorf, Germany), dosing 5 M KOH into the medium. Furthermore, a sampling port consisting of a stainless-steel needle was installed. A potential of 500 mV was applied vs. a Ag/AgCl (satd. KCl) reference electrode (Xylem Analytics, Germany). In this work, all potentials will be stated against this reference. In the reactor, the reference electrode was immersed into a Luggin capillary filled with saturated KCl as an electrolyte and placed near the working electrode. As a counter electrode, a stainless-steel sheet (SS 1.4404, 4 cm^2 surface area, 0.5 mm thickness) was immersed into the cathodic chamber containing a 50 mM phosphate buffer solution with added 15 g L^{-1} NaCl. The potential was controlled and the current response measured via a multi-channel potentiostat (PalmSens BV, Netherlands). The potential was chosen at 500 mV vs. Ag/AgCl (satd. KCl) based on prior cyclic voltammetry (CV) analysis of the mediator $K_3[Fe(CN)_6]$ at a concentration of 1 mM. Anaerobic conditions in the reactor were maintained by flushing sterile nitrogen gas (99.999 % Nippon Gases GmbH, Germany) at a rate of 45 mL min^{-1} through the headspace. To keep the evaporation losses at a minimum, a condenser was mounted on the reactor and cooled with water at 4 °C. For CO_2 transfer into the medium, micro spargers (Eppendorf DASGIP, Germany) were used with a gas mixture of 20 % CO_2 and 80 % N_2 (Nippon Gases GmbH, Germany). To prevent excessive foaming, 100 μL of sterile 10 % (*v/v*) Antifoam 204 was added after inoculation.

Substrate and product quantification

Culture broth samples were collected from the reactor and centrifuged at 16900 g and 4 °C for 5 min. The supernatant was further filtered (0.2 μm, cellulose acetate) for HPLC analysis. Using an Agilent 1200 high-performance liquid chromatography system combined with an Aminex HPX-87H column (Bio-Rad Laboratories GmbH, Germany) concentrations of the substrate glucose and the product ethanol were detected with a refractive index detector. The additional products acetate, lactate, pyruvate, and formate were measured by absorption at 210 nm with a diode array detector. The column was heated to 50 °C while 5 mM H_2SO_4 at a flow rate of 0.6 mL min^{-1} was used to isocratically elute the analytes. The amino acid alanine was measured via a HPLC method according to Holzgrabe et al. using an evaporative light scattering detector (Sedere, France) added to a Knauer HPLC system (Germany).[23] A Phenomenex Kinetex 5 μ C18 column was used for separation at 30 °C (150×4.6 mm, Phenomenex, USA). The mobile phase contained 96 % (*v/v*) water, 4 % (v/v) methanol, and 1.5 mM perfluorheptanoic acid as an ionic coupler at a flow rate of 1 mL min^{-1}. The column was pre-treated overnight with 50 % (*v/v*) methanol in water at 0.2 mL min^{-1}. The ELSD was preheated to 50 °C and used 99.999 % nitrogen gas for evaporation of the mobile phase. After that, the column was flushed for 3 h with the mobile phase before 40 μL of each sample was loaded onto the column. A calibration with 6 alanine standards was performed to enable quantification (Figure S15).

Mediator redox state

Concentrations of the oxidized mediator were measured by absorption in a UV/Vis spectrophotometer (Thermo Scientific GmbH, Germany). The characteristic absorption wavelengths for the oxidized mediator are 320 and 420 nm. In contrast, the reduced species only absorbs at 320 nm. The absorption at 420 nm was therefore used to determine the concentration of the oxidized species. For calibration, 7 concentrations of $K_3[Fe(CN)_6]$ were used (Figure S16).

Cell dry weight and cell density

The optical density was determined via the absorption of the culture broth at 600 nm in a UV/Vis spectrophotometer (Evolution 201, Thermo Scientific GmbH, Germany). For high cell densities (OD_{600} > 0.6), the samples were diluted with 9 g L^{-1} NaCl solution. To determine dry biomass, samples of at least 10 to 20 mL culture

broth were taken and centrifuged for 15 min at 4 °C at 3214 g (Centrifuge 5810 R, Eppendorf, Germany). The supernatant was discarded and the pellet resuspended in pure water to remove inorganic media components from the measurement. The cell suspension was then dried and weighed at the same time on a scale fitted with a heating element (Kern, Germany) until no water loss remained measurable.

Electrochemical analysis and calculations

Cyclic voltammetry analysis was conducted to examine interactions between redox-active species and the electrode. The redox-active species in this case can be *V. natriegens*, ferricyanide, as well as fermentation products or compounds from the cultivation medium. For each CV, the gas was turned off to ensure static conditions in the liquid phase. The potential was then swept between −0.2 and 0.8 V vs. Ag/AgCl (satd. KCl) at a scan rate of 50 mV s^{-1} for 5 cycles to ensure reproducibility. The midpoint potential (E_m) of redox-active substances was then determined as the average of anodic- and cathodic peak potentials, according to the equation:

$$E_{m=}(E_{ox+}E_{red})/2. \quad (1)$$

The carbon recovery was calculated as the sum of carbon in the products and biomass in relation to the carbon provided by the substrate. Measurements for CO_2 in the off-gas were not available. Hence, for the carbon balance, a ratio of 1 mol CO_2 per mol of acetate synthesized was assumed. For succinate production via the oxidative TCA cycle, 2 mol of CO_2 are to be expected for each mol of succinate produced.[18] However, our results indicated that succinate was mainly produced via the reductive TCA cycle, where 1 mol of CO_2 is consumed to synthesize 1 mol of succinate. Therefore, CO_2 formation by *V. natriegens* was only calculated via the produced acetate. Electron recovery rates were determined in a similar way, by calculating the percentage of substrate-derived electrons located in the products and transferred to the anode. A detailed description of both equations is given in the supplementary file.

The coulombic efficiency was calculated as described in the literature.[24]

$$CE\ [\%] = Q_{anode}/(Q_{substrate} - Q_{products}) \times 100 \quad (2)$$

With Q being the charge transferred to the anode in [C]. The total turnover number of ferricyanide was calculated as follows:

$$TTN = (Q_{anode}/F)/(M_{mediator} \cdot z_{mediator}) \quad (3)$$

Were $M_{mediator}$ is the absolute amount of mediator in the system in [mol], $z_{mediator}$ the number of electrons that can be transferred by the mediator in one turnover, and F is Faraday's constant (96485.3365 C mol^{-1}). For ferricyanide, z is equal to 1.

Supporting Information

The authors have cited additional references within the Supporting Information.[25]

Acknowledgements

This work was created as part of the project "Bioelectrochemical and engineering fundamentals to establish electro-biotechnology for biosynthesis – Power to value-added products (eBiotech)", which is funded by the Deutsche Forschungsgemeinschaft (DFG, German Research Foundation) – Project number 422694804. Open Access funding enabled and organized by Projekt DEAL.

Conflict of Interests

The authors declare no conflict of interest.

Data Availability Statement

The data that support the findings of this study are available from the corresponding author upon reasonable request.

Keywords: anodic respiration · biocatalysis · electrochemistry · electron transfer · redox mediators

[1] R. G. Eagon, *J. Bacteriol.* **1962**, *83*, 736.
[2] S. Schwarz, D. Gerlach, R. Fan, P. Czermak, *Electron. J. Biotechnol.* **2022**.
[3] a) J. Xu, F. Dong, M. Wu, R. Tao, J. Yang, M. Wu, Y. Jiang, S. Yang, L. Yang, *Front. Microbiol.* **2021**, *12*, 627181; b) G. A. Ellis, T. Tschirhart, J. Spangler, S. A. Walper, I. L. Medintz, G. J. Vora, *Mar. Drugs* **2019**, *17*, 679.
[4] a) W. J. Payne, *J. Bacteriol.* **1960**, *80*, 696; b) B. Austin, A. Zachary, R. R. Colwell, *Int. J. Syst. Bacteriol.* **1978**, *28*, 315.
[5] B. E. Conley, M. T. Weinstock, D. R. Bond, J. A. Gralnick, *Appl. Environ. Microbiol.* **2020**, *86*.
[6] a) L. M. Proctor, R. P. Gunsalus, *Environ. Microbiol.* **2000**, *2*, 399; b) G. T. Macfarlane, R. A. Herbert, *J. Gen. Microbiol.* **1982**, *128*, 2463.
[7] C. P. Goldbeck, H. M. Jensen, M. A. TerAvest, N. Beedle, Y. Appling, M. Hepler, G. Cambray, V. Mutalik, L. T. Angenent, C. M. Ajo-Franklin, *ACS Synth. Biol.* **2013**, *2*, 150.
[8] a) L. Shi, D. J. Richardson, Z. Wang, S. N. Kerisit, K. M. Rosso, J. M. Zachara, J. K. Fredrickson, *Environ. Microbiol. Rep.* **2009**, *1*, 220; b) T. C. Santos, M. A. Silva, L. Morgado, J. M. Dantas, C. A. Salgueiro, *Dalton Trans.* **2015**, *44*, 9335; c) M. Firer-Sherwood, G. S. Pulcu, S. J. Elliott, *J. Biol. Inorg. Chem.* **2008**, *13*, 849.
[9] B. R. Lam, C. R. Barr, A. R. Rowe, K. H. Nealson, *Front. Microbiol.* **2019**, *10*, 1979.
[10] a) S. Hall, C. McDermott, S. Anoopkumar-Dukie, A. J. McFarland, A. Forbes, A. V. Perkins, A. K. Davey, R. Chess-Williams, M. J. Kiefel, D. Arora et al, *Toxin Rev.* **2016**, *8*; b) T. D. Harrington, V. N. Tran, A. Mohamed, R. Renslow, S. Biria, L. Orfe, D. R. Call, H. Beyenal, *Bioresour. Technol.* **2015**, *192*, 689; c) P. Ertl, B. Unterladstaetter, K. Bayer, S. R. Mikkelsen, *Anal. Chem.* **2000**, *72*, 4949.
[11] A. Gemünde, B. Lai, L. Pause, J. Krömer, D. Holtmann, *ChemElectroChem* **2022**, *9*.
[12] a) S. Hintermayer, S. Yu, J. O. Krömer, D. Weuster-Botz, *Biochem. Eng. J.* **2016**, *115*, 1; b) L. Gu, X. Xiao, G. Zhao, P. Kempen, S. Zhao, J. Liu, S. Y. Lee, C. Solem, *Microb. Biotechnol.* **2023**, *16*, 1277.
[13] R. A. Rozendal, H. V. M. Hamelers, R. J. Molenkamp, C. J. N. Buisman, *Water Res.* **2007**, *41*, 1984.
[14] a) D. Belanger, *Synth. Met.* **1989**, *29*, 563; b) G. I. Hanania, D. H. Irvine, W. A. Eaton, P. George, *J. Phys. Chem.* **1967**, *71*, 2022.
[15] J. Luo, A. Sam, B. Hu, C. DeBruler, X. Wei, W. Wang, T. L. Liu, *Nano Energy* **2017**, *42*, 215.
[16] C. P. Long, J. E. Gonzalez, R. M. Cipolla, M. R. Antoniewicz, *Metab. Eng.* **2017**, *44*, 191.
[17] E. Hoffart, S. Grenz, J. Lange, R. Nitschel, F. Müller, A. Schwentner, A. Feith, M. Lenfers-Lücker, R. Takors, B. Blombach, *Appl. Environ. Microbiol.* **2017**, *83*.

[18] F. Thoma, C. Schulze, C. Gutierrez-Coto, M. Hädrich, J. Huber, C. Gunkel, R. Thoma, B. Blombach, *Microb. Biotechnol.* **2021**, *15*, 1671.
[19] F. Thoma, B. Blombach, *Essays Biochem.* **2021**, *65*, 381.
[20] B. Lai, A. V. Nguyen, J. O. Krömer, *Methods Protoc.* **2019**, *2*.
[21] F. Li, Y.-X. Li, Y.-X. Cao, L. Wang, C.-G. Liu, L. Shi, H. Song, *Nat. Commun.* **2018**, *9*, 3637.
[22] E. Laviron, *J. Electroanal. Chem. Interfacial Electrochem.* **1979**, *101*, 19.
[23] U. Holzgrabe, C.-J. Nap, S. Almeling, *J. Chromatogr. A* **2010**, *1217*, 294.
[24] A. Chukwubuikem, C. Berger, A. Mady, M. A. Rosenbaum, *Microb. Biotechnol.* **2021**.
[25] a) A. M. Erian, P. Freitag, M. Gibisch, S. Pflügl, *Bioresour. Technol. Rep.* **2020**, *10*, 100408; b) D. Molenaar, R. van Berlo, D. de Ridder, B. Teusink, *Mol. Syst. Biol.* **2009**, *5*, 323.

Manuscript received: February 7, 2023
Revised manuscript received: April 18, 2023
Accepted manuscript online: April 23, 2023
Version of record online: June 26, 2023

A.3 Publication III

André Gemünde, Jonas Gail, Jürgen Janek, and Dirk Holtmann

e-Cuvettes parallelize electrochemical and photometric measurements in cuvettes and facilitate applications in bio-electrochemistry

In *Biosensors and Bioelectronics: X*, Volume 14, 2023
DOI: https://doi.org/10.1016/j.biosx.2023.100378

Contribution: My contribution to this work was the development and testing of the e-Cuvette apparatus, the development of all methods mentioned in the Publication, and the execution of the experiments. The original draft and all figures were also created by myself.

Biosensors and Bioelectronics: X 14 (2023) 100378

Contents lists available at ScienceDirect

Biosensors and Bioelectronics: X

journal homepage: www.journals.elsevier.com/biosensors-and-bioelectronics-x

e-Cuvettes parallelize electrochemical and photometric measurements in cuvettes and facilitate applications in bio-electrochemistry

André Gemünde [a,*], Jonas Gail [a], Jürgen Janek [b], Dirk Holtmann [a]

[a] Institute of Bioprocess Engineering and Pharmaceutical Technology and Competence Centre for Sustainable Engineering and Environmental Systems, University of Applied Sciences Mittelhessen, 35390, Giessen, Germany
[b] Institute of Physical Chemistry and Center for Materials Research, Justus-Liebig-University Giessen, 35392, Giessen, Germany

ARTICLE INFO

Keywords:
Redox mediators
Bioelectrochemical systems
Parallelization
Anodic respiration
Spectroelectrochemistry

ABSTRACT

Parallelized and automated screening systems are widely used in process development and optimization in bioelectrochemical applications. This includes the rapid testing and measuring of electrochemical potentials, electrical current densities, mediators, buffers, and biocatalysts. While different methods for screening electroactive organisms have been developed and evaluated in recent studies, there is no parallel device available so far, that can imitate a gas-fed and mediator-based bioelectrochemical system. Here we propose a device that is based on common 3.5 mL cuvettes as reaction vessels that implement commercially available screen-printed electrodes. In combination with a photometer fitted with an autosampler, the device measures the cell density as well as the mediator redox state online. The design enables cultivation times up to 120 h in 8 parallel e-Cuvettes and was validated by cultivating the well-characterized electroactive strain *Pseudomonas putida* KT2440 with 1 mM $K_3[Fe(CN)_6]$ as redox mediator. With this setup, high current densities up to 113.42 ± 22.09 μA cm^{-2} were obtained. Via e-Cuvettes, setup times can be shortened from days to hours in comparison to established bioelectrochemical reactor systems, while maintaining sufficient liquid volume to allow for sampling of the culture broth.

1. Introduction

Generally, systems combining enzyme or microbial reactions with an electrochemical cell are called bioelectrochemical systems (BES). Their applications range from the production of bulk and fine chemicals, wastewater treatment, and energy recovery to analytical uses. BESs enable new possibilities for standard bioprocesses like balancing the redox metabolism via an additional electron sink (Sturm-Richter et al., 2015; Bursac et al., 2017; Förster et al., 2017), making oxygen transfer into the medium obsolete by using redox mediators (Lai et al., 2016), recovering energy from waste streams (Aelterman et al., 2006; Rossi et al., 2022), regenerating cofactors for enzymatic catalysis (Kochius et al., 2014; Ruinatscha et al., 2014), or the electrosynthesis of reduced products with additional electrons provided by an electrode (Guerrero et al., 2021).

For a microbial BES to function properly, microorganisms need a path to transfer electrons between their intracellular electron carriers and the electrode. Current research proposes mainly three concepts for extracellular electron transfer (EET). The first one applies to organisms directly attached to the electrode and is therefore termed direct electron transfer (DET). By this, electrons are transferred via membrane-located cytochromes or conductive cell appendages (El-Naggar et al., 2010; Edwards et al., 2018). The second one, termed mediated electron transfer (MET), can be utilized by many organisms, even if they are not able to perform DET. It is based on redox-active mediators, endogenous or artificial, which can reversibly shuttle electrons between the electrode and the organism's molecular interaction site (Gemünde et al., 2022). EET is hereby not limited to the electrode surface, as it is for the DET mechanism, since solvated mediators are ubiquitously available in the cultivation medium (Lai et al., 2020). The third model, called indirect electron transfer (IET), differs from MET regarding the origin and reusability of the electron shuttle. "Indirect" means, that electron shuttles can be synthesized at the electrode and used up by the organism, or, in reverse, the organism releases a reduced product which is then oxidized at the electrode. In both cases, electrons are transferred in a one-way process (Sydow et al., 2014).

Nonetheless, BESs still suffer from the same issues as traditional bioprocesses. In order to bring down the time to market, many experiments have to be done and parallelization is laborious due to the setup of the reactors. In particular, when establishing a BES, the pre-screening of

* Corresponding author.
E-mail address: andre.gemuende@lse.thm.de (A. Gemünde).

https://doi.org/10.1016/j.biosx.2023.100378
Received 16 February 2023; Received in revised form 20 June 2023; Accepted 30 June 2023
Available online 13 July 2023

different electro-active organisms, culture conditions, electrochemical potentials, and different electron shuttles (if necessary) is mandatory. Most laboratory-scale BESs rely on H-cell-type reactors that have to be set up and maintained with effort. With these setups, the demand for fast screening of different mediators and cultivation conditions cannot be fulfilled. For traditional bioprocesses, this issue is often resolved by downscaling and parallelizing the established reactors while retaining the control capabilities of the system (Kostov et al., 2001). The same principle can be applied to a BES and has already been done to some extent.

One example of such a highly parallelized screening device was recently published by Tahernia and colleagues (Tahernia et al., 2020). In their study, they implemented a separated two-electrode setup into a 96-well microbial fuel cell platform achieving rapid polarization curves and output power measurements with *Pseudomonas aeruginosa* in a microliter volume of around 5 μL. The system is based on a DET mechanism or endogenous mediators for electron transfer but does not allow for photometric measurements or sampling of the culture broth due to the small volume. Szydlowski and co-workers employed a similar two-electrode system based on DET or endogenous mediators in a 1 mL volume without a separating membrane (Szydlowski et al., 2022). However, both these systems only allow for the measurement of electric current density and are not suitable for mediator characterization.

A more complex microfluidic device was developed by Hou and associates (Hou et al., 2012). It consists of 24 independent chambers where anolyte and catholyte can be replenished through microvalves at any given time. Additionally, the anode and cathode chambers are separated by a proton exchange membrane. Nonetheless, like the systems mentioned before, it only allows for the measurement of power and current density.

In 2013, Ley and colleagues provided a non-separated, three-electrode setup that could be integrated into a standard microplate reader, allowing for the parallel recording of electrochemical and optical data in 8 chambers (Ley et al., 2013b). Fitted with a Ag/AgCl micro-reference electrode, the electrochemical microtiter plate was used to characterize the discoloration of the dye indigo carmine via ABTS. In addition, the system was used for the investigation of an electro-enzymatic process. A P450 monooxygenase library was screened for its performance in a mediator-driven production (Ley et al., 2013a). Yet, the setup is disadvantageous for electrotrophic cultivation, since shaking can only be performed in between measurements and the gas atmosphere has to be controlled via the atmosphere surrounding the plate, which most plate readers are not capable of from the factory.

Another example of the implementation of electrodes into well plates was presented by Piermarini and associates (Piermarini et al., 2007). Here, they used a modified 96-well plate for the detection of aflatoxin B_1 in an immunoassay, where the bottom of each well was fitted with a single-use screen printed electrode (SPE). A pseudo Ag/AgCl reference electrode and graphite working and counter electrodes allowed for intermittent pulse amperometry, which could potentially be used for the cultivation of electrotrophs, but the design prohibits the measurement of cell density by absorption. The same applies to the design by Frank and co-workers, which is based on a custom-printed 96-well plate with indium tin oxide working electrodes on borosilicate plates at the bottom of each well (Frank et al., 2022). The design features a combination of potentiostatic and fluorometric measurements, which is of great use for bioelectrocatalysis. In theory, the total concentration of fluorescent mediators would also be measurable, but the mediator redox state is still not measurable with this setup, as it is the case for all of the above-mentioned systems. Despite its great use for parallelization, the small volumes of the mentioned systems prohibit sampling of the culture broth during cultivation, which is a major information loss for downscaling a BES.

Therefore, our study aimed to develop a novel cuvette-based screening system specifically for mediated microbial BESs. Herein, we extend the range of applications by engineering a miniature BES in cuvettes that enables the measurement of mediator redox state, current, and cell density online as well as providing enough volume to take samples during cultivation. As model electrotrophic microorganism, *Pseudomonas putida* KT2440 was used to evaluate the system, since its anodic respiration capability via the mediator $K_3[Fe(CN)_6]$ has already been demonstrated (Schmitz et al., 2015; Hintermayer et al., 2016).

2. Materials and methods

2.1. Bacterial strains and chemicals

Pseudomonas putida KT2440, kindly provided by Dr. Bin Lai from the Helmholtz Centre for Environmental Research – UFZ in Leipzig, was used throughout the experiments. All chemicals used for this work were supplied by Merck KGaA (Germany), VWR Chemicals (USA), Carl Roth GmbH & Co. KG (Germany), or Sigma Aldrich (USA).

2.2. Media and culture conditions

Cultures were incubated at 30 °C and 180 rpm in cultivation tubes with 2.5 mL LB medium (10 g L^{-1} tryptone, 5 g L^{-1} yeast extract, 10 g L^{-1} NaCl). Cryo stocks were prepared by adding 25% glycerol to an exponential culture and freezing it at −80 °C. For BES precultures, cryostocks were first streaked on LB agar plates (15 g L^{-1} agar) and incubated overnight at 30 °C. Liquid precultures were then prepared by transferring one colony into a 100 mL flask with baffles filled to 20 mL with defined mineral medium (DM9) as it has been described by Lai et al. (2019). The medium contained 1.5 g L^{-1} glucose as carbon source, 6 g L^{-1} Na_2HPO_4, 3 g L^{-1} KH_2PO_4, 1 g L^{-1} NH_4Cl, 0.1 g L^{-1} $MgSO_4{\cdot}7H_2O$, 1.5 mL of sterile-filtered 10 g L^{-1} $CaCl_2{\cdot}2H_2O$ stock solution, and 1 mL of trace element solution. The trace element solution consisted of 1.5 g L^{-1} $FeCl_3{\cdot}6H_2O$, 0.15 g L^{-1} H_3BO_3, 0.03 g L^{-1} $CuSO_4{\cdot}5H_2O$, 0.18 g L^{-1} KI, 0.12 g L^{-1} $MnCl_2{\cdot}4H_2O$, 0.06 g L^{-1} $Na_2MoO_4{\cdot}2H_2O$, 0.12 g L^{-1} $ZnSO_4{\cdot}7H_2O$, 0.15 g L^{-1} $CoCl_2{\cdot}6H_2O$, 0.023 g L^{-1} $NiCl_2{\cdot}6H_2O$, and 10 g L^{-1} EDTA. Cultures were then incubated in an orbital shaker at 180 rpm (2.5 cm orbit, Multitron, Infors, Bottmingen, Switzerland).

2.3. Preparation of the screening device based on e-Cuvettes

The eightfold e-Cuvette system (Fig. 1) consists of parallel 4 mL polystyrene macro cuvettes (Th. Geyer GmbH & Co. KG, Germany) covered by a 3D-printed lid made from Rigur RGD450 resin in an SLA printer (Stratasys, USA). Peripheral attachments for cable and gas line management were printed from polylactic acid (PLA, Prusa Research a. s., Czech Republic). The medium was filled to a maximum of 3.5 mL in each vessel to avoid overflowing. Sterile cannulas (Ø 0.6 mm, B. Braun, Germany) were fitted through holes in the lid for sparging and mixing of the medium with sterile filtered 99.99% nitrogen gas. Gas flow was controlled for all channels separately via needle valves (Wagner GmbH, Germany) and a wash bottle was installed to humidify the gas. The flow rates were set before each experiment between 1.2 and 5 ± 0.1 mL min^{-1}, measured via water displacement in triplicates.

The 3 electrodes were added into each cuvette by immersing screen-printed electrodes (C220 AT, Deutsche Metrohm GmbH & Co. KG, Germany) into the medium. Each SPE consisted of a working and counter electrode (working electrode area: 0.125 cm^2) made from gold with a silver pseudo reference electrode on a ceramic back plate. Silver contacts connect the electrodes at the top. The remaining area is covered with an insulating layer. The contacts fit into a circuit board plug mounted on the lid that is sealed with silicone against the surrounding atmosphere (Fig. 1E). In total, two designs were tested. The first one depicted in Fig. 1(A and B) uses the pseudo Ag reference electrode of the SPE in combination with the working and counter electrode on one chip. The second one was constructed to fit Ag/AgCl (3 M KCl) reference electrodes (Pine Research Instrumentation Inc., USA) through fittings in

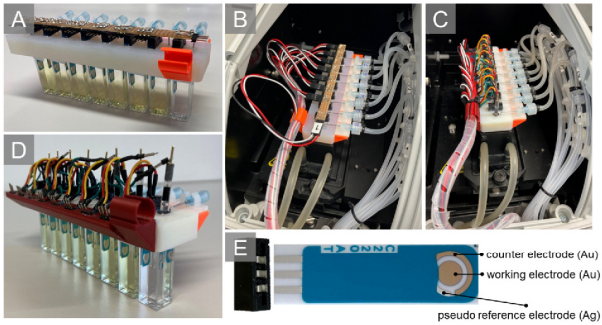

Fig. 1. e-Cuvette setups. Setup with pseudo Ag reference electrodes in use outside (A) and inside the photometer (B). Identical setup with the addition of Ag/AgCl reference electrodes (C, D). Screen printed electrode with the respective 3-pin circuit board plug (E).

the lid (Fig. 1C and D). SPEs, reference electrodes, and lid were sterilized by immersion in 80% isopropanol for 5 min before adding the pre-filled sterile cuvettes and transferring the setup into the automatic sampler of the photometer (Evolution 201, Thermo Scientific GmbH, Germany). The cultivation temperature was set via a thermostat (Julabo GmbH, Germany) cycling water at 30 °C through the autosampler. Monitoring of the mediator redox state was performed by constantly measuring the extinction at 420 nm in 15-min intervals. At the same time, the cell density was measured by extinction at 600 nm. Since the *P. putida* cells absorb at 420 nm as well, the Ext_{420} values were corrected by subtracting the Ext_{600} values.

2.4. Analytics

Culture broth samples were collected from the cuvettes and centrifuged at 16,900×*g* and 4 °C for 5 min. The supernatant was collected and further filtered through a 0.2 μm cellulose acetate or PTFE filter for HPLC analysis. Using an Agilent 1200 high-performance liquid chromatography system combined with an Aminex HPX-87H column (Bio-Rad Laboratories GmbH, Germany), concentrations of the substrate glucose were detected through a refractive index detector at 32 °C. The column was heated to 50 °C while 5 mM H_2SO_4 at a flow rate of 0.5 mL min^{-1} was used to isocratically elute the analytes. Standards were measured between 0.01 and 1.5 g L^{-1} in 7 concentration steps and the corresponding area fitted by linear regression (Fig. S1).

Oxygen saturation was measured via optical oxygen sensor spots (PyroScience GmbH, Germany) glued onto the inside of a single cuvette. These spots are small enough (Ø 5 mm, 0.15 mm thickness) to not disturb the flow inside the reaction vessel. Oxygen saturation is then measured via an optical fiber through the transparent cuvette wall. 2-point calibration was performed by gassing the medium with air for 100% saturation and afterward with 99.99% nitrogen and added sodium sulfite for 0% saturation.

2.5. Spectroelectrochemical mediator characterization

The extinction characteristics of the mediator $K_3[Fe(CN)_6]$ were determined by spectroelectrochemical analysis. Hereby, optical measurements can be taken simultaneously with cyclic voltammetry (CV) analysis. For this, a spectroelectrochemical cell kit in a quartz cuvette was used (Pine Research Instrumentation Inc., USA). The electrode consists of a gold working electrode with micro holes and a gold counter electrode on one ceramic substrate. A Ag/AgCl (3 M KCl) reference electrode is immersed into the solution separately. The analytes as well as light can penetrate the working electrode, while the electrochemical reaction occurs. This enables the measurement of absorption changes during a CV of the mediator. The cell was heated to 30 °C and kept oxygen-free by sparging the headspace with nitrogen gas. To eliminate any pH changes affecting the CV, the measurements were carried out in 100 mM phosphate buffer (8.23 g L^{-1} Na_2HPO_4, 5.04 g L^{-1} NaH_2PO_4) at pH 7.

2.6. Electrochemical analysis and calculations

Calibration of the silver pseudo reference electrode was done by performing a CV in each channel containing the mediator prior to each experiment. Therefore, the gas was turned off to ensure static conditions in the liquid phase. The potential was then swept between −0.4 and 0.8 V *vs.* Ag at a scan rate of 50 mV s^{-1} for 3 cycles to ensure reproducibility. The midpoint potential (E_m) was then determined as the average of anodic - and cathodic peak potentials, according to the equation $E_m = (E_{ox} + E_{red})/2$.

The resulting E_m value was then compared to a CV conducted with Ag/AgCl (3 M KCl) reference electrodes to determine the potential shift. In chronoamperometric BES experiments, the potential was chosen at 0.5 V *vs.* the respective reference. This potential is situated above the oxidation potential to ensure a thermodynamic driving force toward the oxidation of the mediator. Both electrochemical methods were applied via an 8-channel multi-potentiostat (Palmsens BV, Netherlands).

The total turnover number of the mediator (TTN) was calculated by dividing the total amount of electrons q in [mol] transferred to the anode by the total amount of mediator used (n_{RM}) in [mol]. The electron transfer capabilities of the mediator are indicated by the number of electrons that can be transferred per molecule of redox mediator in one turnover step (z_{RM}). For $K_3[Fe(CN)_6]$ z_{RM} is equal to 1.

$$TTN = \frac{q}{n_{RM} \cdot z_{RM}} \tag{1}$$

The amount of electrons q results from the measured current I in [A] over the reaction time t in [s] divided by Faraday's constant F in [A s mol^{-1}]:

$$q = \frac{\int |I|\, dt}{F} \tag{2}$$

3. Results and discussion

3.1. Spectroelectrochemical mediator characterization

The photometric behaviour of $K_3[Fe(CN)_6]$ under reducing and oxidizing conditions was measured via a spectroelectrochemical approach. Here, the mediator is electro-chemically reduced and oxidized via CV at the working electrode while light can pass through micro-holes of the electrode simultaneously. This allows for the measurement of the spectroscopic properties of the mediator, where the extinction changes due to the alteration of the redox state.

Fig. 2 depicts the data obtained for 1 mM $K_3[Fe(CN)_6]$ in phosphate buffer at pH 7 and 30 °C. A CV scan at 50 mV s^{-1} was performed while extinction spectra were taken simultaneously at every second of the scan. The black line shows the extinction spectrum of the oxidized state, where a clear peak at 420 nm is visible. This spectrum was taken at 315 mV, before the electrochemical reduction begins. In red, the spectrum of the reduced form (red dot in the CV at 86 mV) shows a shrinking peak at 420 nm. This behaviour can therefore be used to determine the redox state of the mediator online by measuring the extinction at 420 nm, as it has been done by Lai et al. (2016). By looking at the peak currents in the CV, the electrochemical reaction of the redox mediator shows a reversible behaviour with a cathodic to anodic peak current ratio ($I_{p,c}/I_{p,a}$) of 0.9. The reversibility is of great interest for the long-term usability of the mediator within the screening device. From the peak potentials, $E_m = 194.5$ mV *vs.* Ag/AgCl (3 M KCl) was determined. The potential of this reference can be converted to the SHE by adding 210 mV to the measured potential (Friis et al., 1998). This results in $E_m = 401.5$ mV *vs.* SHE at 30 °C and pH 7, which is slightly lower than the 416–430 mV reported in the literature (Fultz and Durst, 1982; Ley et al., 2013b; Lai et al., 2016). Since the potential of the $[Fe(CN)_6]^{3-}$ /$[Fe(CN)_6]^{4-}$ couple is strongly dependent on the ionic strength of the electrolyte, a slight shift is to be expected (Kolthoff and Tomsicek, 1935). To ensure comparability of the two different references, all potentials given in this work will be stated against the respective Ag or Ag/AgCl reference electrodes.

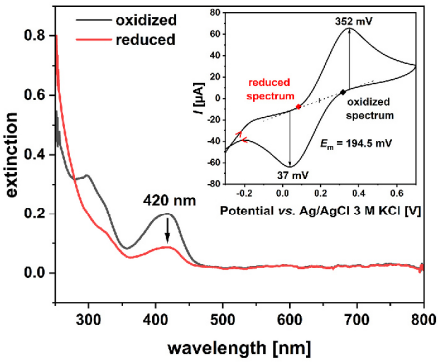

Fig. 2. Spectroelectrochemical mediator characterization. 1 mM $K_3[Fe(CN)_6]$ at 30 °C in 100 mM phosphate buffer at pH 7 in the spectroelectrochemical cell. Spectra were recorded shortly before re-reduction or re-oxidation of the mediator is about to happen, marked by the black and red dot in the CV scan. Red arrows in the CV indicate the direction of the potential sweep from the starting potential at 300 mV.

3.2. Calibration of pseudo reference electrodes

Pseudo reference electrodes are convenient to use since they can be scaled down with ease and often only require platinum or silver wires. With thin-layer technologies being available for several years, screen printing of such electrodes became an attractive method for disposable electrode systems. However, their stability is limited and a thermodynamic equilibrium between aqueous and solid phases cannot be achieved due to the lack of a common ion in both phases. Furthermore, they are susceptible to a potential shift during longer experiments (Inzelt, 2013). Therefore, it is necessary to calibrate these kinds of electrodes against a stable reference electrode like the Ag/AgCl electrode.

Therefore, CVs were performed in each e-Cuvette containing mediator prior to polarization and compared to a CV using an Ag/AgCl (3 M KCl) reference electrode. Fig. 3 exemplarily shows one of these scans with a pseudo silver reference (a) against a Ag/AgCl reference (b). As electrolyte, 1 mM $K_3[Fe(CN)_6]$ was dissolved in DM9 medium. Both scans were conducted with the screen printed working and counter electrodes at a scan rate of 50 mV s^{-1}. Using the Ag reference, $E_m = 55.5$ mV with a peak separation of 241 mV was calculated. Contrary to that, with the Ag/AgCl reference in use, $E_m = 204$ mV with a peak separation of 166 mV was determined. Having both midpoint potentials estimated, the shift of the pseudo reference *vs.* the Ag/AgCl reference can be determined as −148.5 mV.

For the reversible transfer of one electron at the electrode, a peak separation of 2.22 (*RT*/*F*) is to be expected (Savéant, 2006). At 30 °C this corresponds to 58 mV under ideal conditions. One cause for increased separation could be the ohmic drop due to the distance between reference and working electrode (Elgrishi et al., 2018). In case of the pseudo reference, the distance is 1 mm vertical and the electrodes do not face each other. For the Ag/AgCl electrode, the distance is slightly larger (~5–6 mm), but the frit is placed directly in front of the working electrode. At room temperature and in DM9 medium with 1 mM $K_3[Fe(CN)_6]$ as electrolyte, the uncompensated resistance between the pseudo Ag reference and gold WE amounts to 103.4 Ω. With the Ag/AgCl reference in place, the resistance rises to 152.9 Ω. Furthermore, both reference systems show nearly ideal reversibility of the redox reaction. The $I_{p,c}/I_{p,a}$ ratios can be approximated by 1.06 for the Ag reference, and 0.94 for the Ag/AgCl reference electrode.

3.3. Evaluation and optimization of the e-Cuvette

The e-Cuvette screening system is based on macro cuvettes as reaction vessels. In those, a gold working electrode positioned on a one-chip three-electrode setup is used for regenerating any reduced mediator originating from the organism's electron transfer pathway. A sterile cannula is used to bubble nitrogen gas from the bottom of the cuvette through the medium, acting as a mixer and simultaneously removing oxygen. Via this method, the light pathway of the photometer is not perturbed, and electrochemical as well as photometric data can be recorded continuously throughout the cultivation. The gas was humidified beforehand by bubbling through a column of water to reduce evaporation losses during cultivation. Further, finding the optimal gas flow rate was essential for two reasons. First, if the flow rate is set too high, the evaporation losses will lead to the electrode being exposed. Second, if the gas flow rate is set too low, oxygen is not fully removed from the cuvette and the mixing effectiveness is diminished. Therefore, the gas flow rate for the initial verification experiments over multiple days was set at a low flow rate (1.2 mL min^{-1}) to ensure evaporation losses were minimal and the electrodes stay in contact with the electrolyte.

3.3.1. Verification of e-Cuvettes with Ag reference electrodes

Verification was performed with *P. putida* KT2440 since its interaction with $K_3[Fe(CN)_6]$ is well known (Hintermayer et al., 2016). First, we consider the simple setup with the Ag pseudo reference in use. Each

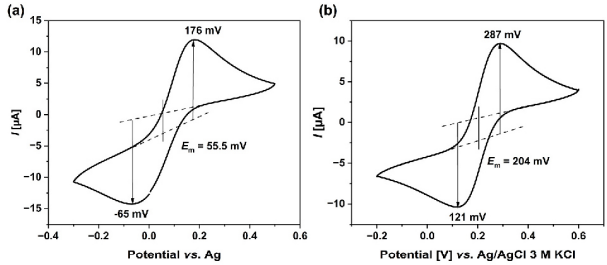

Fig. 3. CV calibration of the pseudo reference electrode. CV scans of 1 mM ferricyanide with pseudo Ag reference (a) and Ag/AgCl reference (b) in a single e-Cuvette with 3.5 mL DM9 medium including 1 mM $K_3[Fe(CN)_6]$ at 30 °C. The scan rate was set to 50 mV s^{-1} for both experiments. E_m stands for the midpoint potential.

of the 8 channels was filled with DM9 medium and $K_3[Fe(CN)_6]$ was added to a final concentration of 1 mM. The SPEs were connected to the lid and placed on the 8 cuvettes. Together with the sterile cannulas, the setup is transferred to the preheated autosampler where the gas ports connect to the cannulas. After the initial mixing and heating of the cuvettes, the gas was turned off to perform the CV calibration as described above. Fig. 4(a) shows the third CV scan of all 8 e-Cuvettes. As expected, the abiotic e-Cuvette without mediator present (Ch 1) showed no significant oxidation or reduction of the minimal medium. All remaining channels containing $K_3[Fe(CN)_6]$ displayed a clear oxidation peak between 177 and 275 mV. However, a definite reduction peak cannot be determined from the voltammogram and the variations between the channels are quite high. Here, the reduction peak might be covered up by a cathodic oxygen reduction. This reaction is visible in the CV of Ch1 containing only DM9 medium in Fig. 4(a). At a potential below −150 mV, a cathodic current can be observed, most likely linked to oxygen reduction.

The calibration of the reference electrodes was followed by a 2 h abiotic polarization phase at 500 mV *vs.* Ag. Therefore, the gas supply was again turned on to set up micro-aerobic conditions before 6 channels are inoculated from an aerobic preculture to an OD_{600} of 0.37 ± 0.07. With the inoculation, the current density from the 6 biotic channels starts to rise immediately until 22 h after inoculation. At this point, the slope increases even more. The maximum current density is reached after 47.8 h with 56.74 ± 11.73 µA cm^{-2} and stays nearly constant until around 60 h after the inoculation when the current response starts to drop off. The minor percentage deviation from the mean current values of 23.36% in the first 48 h of cultivation is particularly noteworthy. The current transferred in the biotic channels would theoretically result in 4.2 ± 0.68 total turnovers of the mediator over the entire cultivation period. By keeping the time frame of the experiment constant, the TTN can give insight into the interaction efficiency of different mediators by giving a rough approximation of the electron transfer rate.

In a perfectly mixed system, $[Fe(CN)_6]^{3-}$ would be reduced at the counter electrode preferably to the hydrogen evolution reaction, since $[Fe(CN)_6]^{3-}$ reduction appears at a higher potential. The reduction of $[Fe(CN)_6]^{3-}$ is also electrochemically more favourable than oxygen reduction due to a lower overpotential (Ucar et al., 2017). With the constant cycling of the mediator, the TTN has to be considered differently. The "real" TTN would describe all turnovers of the redox mediator within a cuvette. Those include reduction by the cathode or the organism and the re-oxidation at the anode. In reality, these reactions cannot be measured separately. However, as long as there is an increasing current originating from glucose metabolism, a "measurable" TTN can be deduced from the electron flow which is used here.

Mediator reduction is also visible in the decreasing extinction of the culture broth at 420 nm after the inoculation. As the current density reaches its peak, the oxidation state of the mediator does not change any further, indicating the oxidation rate of $[Fe(CN)_6]^{4-}$ seems to be in equilibrium with the reduction rate caused by *P. putida* and the reaction at the counter electrode. It has to be considered though, that with the low flow rate used the mass transfer inside each cuvette is most likely diffusion limited in turn, leading to hydrogen evolution when no $[Fe(CN)_6]^{3-}$ is present at the counter electrode. In the setup presented here, evolving hydrogen can leave the cuvettes through the venting hole or interact again with the organism or the anode and be re-oxidized.

During the whole cultivation period, the abiotic e-Cuvette (Ch 1) shows no current response to the polarization. In the abiotic e-Cuvette (Ch 2) with added $K_3[Fe(CN)_6]$ however, a constantly increasing current density was measured. One could argue that this may be the result of

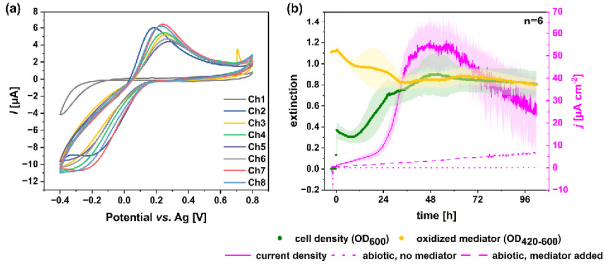

Fig. 4. BES cultivation of *P. putida* KT2440 in e-Cuvettes with pseudo Ag reference electrodes. Calibration of the pseudo Ag reference electrodes via CVs of the mediator (1 mM $K_3[Fe(CN)_6]$) in all 8 channels (a). Obtained current density (magenta), extinction of the oxidized mediator (yellow), and cell density at 600 nm (green) during 102 h BES cultivation at 500 mV *vs.* Ag in e-Cuvettes (b). The dotted and dashed lines resemble abiotic controls (dotted line: without mediator, dashed line: added mediator). Standard deviations were calculated from 6 equal channels. Cultivation Parameters: 1.2 mL min^{-1} N_2, 30 °C, 3.5 mL DM9 medium.

residual $[Fe(CN)_6]^{4-}$ present from the stock solution being oxidized to $[Fe(CN)_6]^{3-}$. However, by looking at the extinction of the oxidized mediator in the abiotic channel (Fig. S3 (b)), there is no significant change during the course of the experiment. It can be assumed though, that over short time periods, this reaction is locally limited to the interspace between the working and counter electrode, thereby not affecting the overall Ext_{420} value. The previously discussed constant redox cycling of $[Fe(CN)_6]^{3-/4-}$ cannot explain this phenomenon, since the redox reaction would result in a constant current based on the amount of initially available $[Fe(CN)_6]^{4-}$ (Ley et al., 2013b). Since the pure medium (Fig. S3 (a)) does not react electrochemically in any form, the current therefore most likely results from a mediator reaction which is yet unexplained and needs further research. One hypothesis might be the solubility of gold in the presence of CN^- ions as described by the "Elsner equation". This would lead to the oxidation of the gold electrodes and the formation of the very stable and soluble complex $[Au(CN)_2]^-$ in the presence of oxygen. Since oxygen is always present in trace amounts and the electrode itself acts as an additional oxidizer, this oxidation might result in a constantly increasing current.

The comparably large volume of the cuvettes allows for sampling of the culture broth in order to perform substrate analysis via HPLC. Analysis showed that all biotic channels were depleted of glucose at the end of the experiment. As expected, the glucose concentration of the abiotic e-Cuvettes did not change throughout the cultivation period (data not shown). The complete uptake of glucose in the biotic channels suggests that a total of 67,480 C of charge from 8.33 mM glucose were available to the organism. If we assume a CE of 4.1%, as determined by Chukwubuikem and colleagues (Chukwubuikem et al., 2021), and do not count the minor product peaks from HPLC analysis, which were not quantified, a theoretical charge transfer to the anode of around 2767 C occurs from glucose metabolization. In reality, only 1.42 ± 0.23 C were transferred to the anode. This is most probably due to the micro-aerobic conditions in the system. Oxygen hereby acts as an alternative electron acceptor, favoured by the organism.

The residual current, when the substrate is already depleted, might result from metabolite reserves of the cell. Therefore, the mediator is not recovered to its oxidized state at the end of the cultivation.

According to the cell density measured by extinction, the cells could grow after an initial lag phase of around 8.5 h with an approximated growth rate of 0.047 h^{-1} (Fig. S2 (a)). Under micro-aerobic conditions, growth was to be expected. Under strictly anaerobic conditions this strain was only reported to grow under BES conditions at a rate of 0.01 h^{-1} at high stir rates and high $[Fe(CN)_6]^{3-}$ concentrations (Hintermayer et al., 2016). However, for a BES reactor with lower mixing rates, growth on phenazine-1-carboxylic acid and pyocyanin as expressed mediators was demonstrated recently for *P. putida* KT2440 (Chukwubuikem et al., 2021). Current densities in this recent report stated between 8 and 18 $\mu A\ cm^{-2}$. In our system, even higher current densities could be reached, which possibly enables sufficient electron transfer to support growth under anaerobic conditions.

3.3.2. Integration of Ag/AgCl reference electrodes into the e-Cuvettes

From the data presented above, it can be concluded that pseudo reference electrodes are not able to produce ideal CVs during calibration. More importantly, deterioration of the Ag material and sometimes even detachment from the substrate was visible after the experiment (Fig. S4). Sawhney et al. (2019) studied the interactions of potassium ferrous cyanides with pseudo Ag reference electrodes in detail and concluded, that $[Fe(CN)_6]^{3-/4-}$ exposure results in the transformation of the Ag surface due to side reactions and deposition leading to a high risk of inaccuracies when performing impedance spectroscopy. Therefore, a Ag/AgCl (3 M KCl) reference electrode was implemented into each e-Cuvette to chemically isolate the reference electrode and eliminate the risk of inaccuracies. The verification experiment with *P. putida* KT2440 was then repeated with the same procedure as described before but with a reduced liquid volume of 3.2 mL due to the larger reference electrodes. For 7 e-Cuvettes containing $K_3[Fe(CN)_6]$ and one control with just DM9 medium, CV scans at 50 mV s^{-1} were conducted (Fig. 5(a)). The e-Cuvettes containing mediator delivered clear oxidation and reduction peaks with a mean $E_m = 144.07 \pm 22.73$ mV *vs.* Ag/AgCl (3 M KCl) and a peak separation of 351.29 ± 47.56 mV.

Cultivation data acquired during the experiment is reported in Fig. 5 (b). Each cuvette was inoculated to an $OD_{600} = 0.46 \pm 0.04$. This time, the current density increased faster than in the first verification with Ag reference electrodes. But as before, the slope of the current density started to increase further after 22 h. The maximum current density reached $59.24 \pm 17.31\ \mu A\ cm^{-2}$ after 27.5 h. The current started to drop off after only 38.3 h of cultivation. Over the whole experiment, the TTN of the mediator can be calculated with 3.42 ± 1.73 turnovers, which is slightly lower than before. As before, reduction of $[Fe(CN)_6]^{3-}$ occurs measurable when the extinction at 420 nm starts to decrease after 22 h simultaneous to the current slope increasing further. The maximum current density seems to keep the equilibrium between oxidation of the mediator at the anode and reduction due to the organism and the counter electrode until the current suddenly drops. With this change, the mediator is further reduced until at the end only 1/3 of the initially oxidized mediator remains in its oxidized state.

Again, the abiotic reference without added mediator seems to be electrochemically inert since no current flows in response to the polarization. With added mediator, a steadily increasing low current density occurs like in the previously discussed experiment. HPLC analysis revealed no glucose consumption in abiotic e-Cuvettes and total depletion of the substrate in all biotic cuvettes after 118 h, while 1.16 ± 0.59 C of charge were transferred to the anode. This again indicates that oxygen is the preferred electron acceptor for *P. putida* and has to be eliminated.

The cell density measurements showed that growth starts with a minor lag phase of 1.75 h and a rate of 0.038 h^{-1} (Fig. S2 (b)). Current density values reach a maximum and drop at the same time as the cell density. This indicates an interdependency, as it was already described for an electrochemical bioactivity sensor (Holtmann et al., 2006). The drop of both these values most probably indicates the point of total glucose consumption when the cells enter stationary and death phase. Mediator reduction still occurs after this point, visible by the declining extinction of the oxidized mediator in Fig. 5(b). This phenomenon could have two potential origins. First, the counter electrode reduction of $K_3[Fe(CN)_6]$, and second, the remaining vital cells may metabolize electron donors from lysed cells or from their maintenance metabolism, as it was discussed before for the Ag pseudo reference system.

Comparing both setups, the pseudo reference electrode setup showed only minor standard deviations for the current density of 6 biotic cuvettes. However, the CV calibration implies that further electrochemical analysis like impedance spectroscopy might not be feasible. In contrast, using Ag/AgCl reference electrodes led to clear oxidation and reduction peaks in the CV scans but attained high deviations between the current densities of the 6 biotic channels. Therefore, both setups can be used for screening mediators in BESs, with the pseudo reference offering a cheaper setup.

By comparing the performance data of the small-scale e-Cuvettes to larger-scale reference data provided by the literature (Schmitz et al., 2015; Hintermayer et al., 2016) it can be concluded, that our parallel system obtains similar, but overall lower current density curves. Minor deviations from the mean from 6 parallel channels further support the use of e-Cuvettes in favour of H-cells or large BES reactors for screening purposes.

3.4. Oxygen removal in the e-Cuvette

We recorded the oxygen saturation of one e-Cuvette outside the photometer via a sensor spot to determine the flow rate at which oxygen is completely removed from the system. The flow rate was set from initially 1.5 mL min^{-1} to finally 5 ml min^{-1} in 0.5 mL min^{-1} steps (Fig. 6

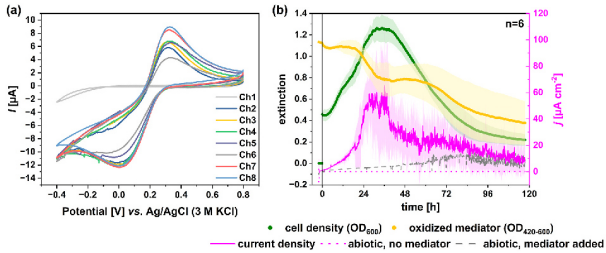

Fig. 5. BES cultivation of *P. putida* KT2440 in e-Cuvettes with Ag/AgCl reference electrodes. Cyclic voltammetry of mediator (1 mM $K_3[Fe(CN)_6]$) and medium for reference in all 8 channels (a). Obtained current density (magenta), extinction of the oxidized mediator (yellow), and cell density at 600 nm (green) during 118 h BES cultivation 500 mV *vs.* Ag/AgCl in e-Cuvettes (b). The dotted lines resemble abiotic controls (dotted line: without mediator, dashed line: added mediator). Standard deviations were calculated from 6 equal channels. Cultivation Parameters: 1.2 mL min^{-1} N_2, 30 °C, 3.2 mL DM9 medium.

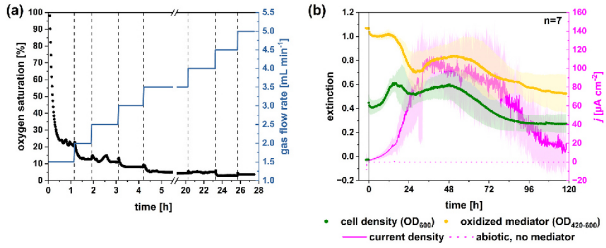

Fig. 6. Oxygen concentration in e-Cuvettes. Oxygen saturation (black dots) at different gas flow rates (blue) in a single e-Cuvette (a). BES cultivation with the adapted N_2 flow rate of 4.5 mL min^{-1} at 500 mV *vs.* Ag/AgCl in 8 e-Cuvettes (b) Obtained current density (magenta), extinction of the oxidized mediator (yellow) and cell density at 600 nm (green) during 118 h cultivation. Dotted line: abiotic control without mediator. Standard deviations were calculated from 7 equal channels. Cultivation Parameters: 30 °C, 3.5 mL DM9 medium.

(a)). With the lowest rate at 1.5 mL min ^{1}, a saturation of ~20% was reached after 1 h. By stepping up the rate to 5 mL min ^{1}, a minimum of 3% could be determined for a flow rate of 4.5 mL min ^{1}. Further increasing the flow rate to 5 mL min ^{1} did not decrease the oxygen saturation any further. This could be the result of oxygen permeating through the gas tubing before entering the cuvette or by ambient air passing through the venting hole of the lid.

The determined flow rate of 4.5 mL min ^{1} was then used for cultivation in 7 parallel e-Cuvettes (Fig. 6(b)). Right away, cell growth was minimal and a maximum current density of 113.42 ± 22.09 μA cm ^{2} was reached after 43.3 h. Nonetheless, glucose was again consumed completely after 118 h of cultivation leading to a low coulombic efficiency of 0.005%, indicating that oxygen is still favoured as an electron acceptor.

Even if oxygen cannot be removed entirely in the current setup, for screening purposes, this is still a promising result. All $K_3[Fe(CN)_6]$ mediated channels could achieve a mean TTN of 9.35 ± 2.35 and the reduction of the mediator was measured online together with the cell and current density. With this, a screening of different mediators can be achieved fast and easily for different organisms and mediators. However, to achieve complete oxygen removal, the system has to be further optimized.

4. Conclusions

To date, combining optical and electrochemical techniques for bioelectrochemistry in one compact system is still challenging and has not yet been shown in combination with photometric measurements. In this work, we combined online electrochemical measurements with photometric analysis in up to 8 parallel channels. A major benefit of this system is the compatibility with a standard photometer and commercially available cuvettes and electrodes. These screen-printed electrodes are affordable and enable easy exchange of electrode materials. To mitigate the uncertainty of the pseudo Ag reference printed on those SPEs, the incorporation of Ag/AgCl reference electrodes further facilitated detailed and durable electrochemical analysis. Via the "mixing through sparging" method, the system can be used to study mediated electron transfer under conditions closely resembling those of a BES reactor. This resemblance was shown with *P. putida* KT2440 in 7 parallel e-Cuvettes, delivering current densities up to 113 μA cm ^{2}. Furthermore, by keeping the setup simple and all structural parts 3D printable, the system can be adapted to fit nearly every commercially available photometer. One main advantage of the system, besides parallelization, is the working volume of 3.5 mL, which allows for sampling during the process time. This is usually not possible in the microliter systems described above. It is also possible to carry out long-term experiments since the evaporation rate at the optimal gas flow rate of 4.5 mL min ^{1} is low enough to not expose the electrodes. The described system thus complements existing systems for rapid process development with the limitation to lower cell densities, still measurable by the photometer. Finally, the wide applicability of the system must be mentioned. Besides the microbial electrosynthesis, the system can also be used for electroenzymatic process development. In addition, all electrochemical and bioelectrochemical processes can be measured in which photometric measurements indicate the time course of the reaction. By integrating transparent electrodes (e.g., ITO electrodes), even biofilm-based processes can be monitored online.

CRediT authorship contribution statement

André Gemünde: Investigation, Methodology, Data curation, Writing – original draft. **Jonas Gail:** Investigation. **Jürgen Janek:** Supervision, Writing – review & editing, Conceptualization. **Dirk Holtmann:** Supervision, Writing – review & editing, Conceptualization, Funding acquisition, Project administration.

Declaration of competing interest

The authors declare the following financial interests/personal relationships which may be considered as potential competing interests:

Dirk Holtmann reports financial support was provided by German Research Foundation.

Data availability

Data will be made available on request.

Acknowledgements and Funding

This work was created as part of the project "Bioelectrochemical and engineering fundamentals to establish electro-biotechnology for biosynthesis – Power to value-added products (eBiotech)", which is funded by the Deutsche Forschungsgemeinschaft (DFG, German Research Foundation) – Project number 422694804.

Appendix A. Supplementary data

Supplementary data to this article can be found online at https://doi.org/10.1016/j.biosx.2023.100378.

References

Aelterman, P., Rabaey, K., Clauwaert, P., Verstraete, W., 2006. Microbial fuel cells for wastewater treatment. Water Sci. Technol.: J. Int. Assoc. Water Pollut. Res. 54, 9–15.
Bursac, T., Gralnick, J.A., Gescher, J., 2017. Acetoin production via unbalanced fermentation in Shewanella oneidensis. Biotechnol. Bioeng. 114, 1283–1289.
Chukwubuikem, A., Berger, C., Mady, A., Rosenbaum, M.A., 2021. Role of phenazine-enzyme physiology for current generation in a bioelectrochemical system. Microb. Biotechnol.
Edwards, M.J., White, G.F., Lockwood, C.W., Lawes, M.C., Martel, A., Harris, G., Scott, D. J., Richardson, D.J., Butt, J.N., Clarke, T.A., 2018. Structural modeling of an outer membrane electron conduit from a metal-reducing bacterium suggests electron transfer via periplasmic redox partners. J. Biol. Chem. 293, 8103–8112.
Elgrishi, N., Rountree, K.J., McCarthy, B.D., Rountree, E.S., Eisenhart, T.T., Dempsey, J. L., 2018. A practical beginner's guide to cyclic voltammetry. J. Chem. Educ. 95, 197–206.
El-Naggar, M.Y., Wanger, G., Leung, K.M., Yuzvinsky, T.D., Southam, G., Yang, J., Lau, W.M., Nealson, K.H., Gorby, Y.A., 2010. Electrical transport along bacterial nanowires from Shewanella oneidensis MR-1. Proc. Natl. Acad. Sci. USA 107, 18127–18131.
Förster, A.H., Beblawy, S., Golitsch, F., Gescher, J., 2017. Electrode-assisted acetoin production in a metabolically engineered Escherichia coli strain. Biotechnol. Biofuels 10, 65.
Frank, R., Ramos, J.V., Azendorf, R., Prönnecke, C., Schmidt, S., Jahnke, H.-G., Robitzki, A.A., 2022. Real-time 96-well optoelectronic micro plate for kinetic and stability investigation of cytochrome P450 BM3. Sensor. Actuator. B Chem. 361, 131752.
Friis, E.P., Andersen, J.E., Madsen, L.L., Bonander, N., Møller, P., Ulstrup, J., 1998. Dynamics of Pseudomonas aeruginosa azurin and its Cys3Ser mutant at single-crystal gold surfaces investigated by cyclic voltammetry and atomic force microscopy. Electrochim. Acta 43, 1114–1122.
Fultz, M.L., Durst, R.A., 1982. Mediator compounds for the electrochemical study of biological redox systems: a compilation. Anal. Chim. Acta 140, 1–18.
Gemünde, A., Lai, B., Pause, L., Krömer, J., Holtmann, D., 2022. Redox mediators in microbial electrochemical systems. ChemElectroChem.
Guerrero, K., Gallardo, R., González, E., Veliz, F., Conejeros, R., Gentina, J.C., Aroca, G., 2021. Butanol production by Clostridium acetobutylicum ATCC 824 by electro-fermentation in culture medium supplemented with butyrate and neutral red. J. Chem. Technol. Biotechnol.
Hintermayer, S., Yu, S., Krömer, J.O., Weuster-Botz, D., 2016. Anodic respiration of Pseudomonas putida KT2440 in a stirred-tank bioreactor. Biochem. Eng. J. 115, 1–13.
Holtmann, D., Schrader, J., Sell, D., 2006. Quantitative comparison of the signals of an electrochemical bioactivity sensor during the cultivation of different microorganisms. Biotechnol. Lett. 28, 889–896.
Hou, H., Li, L., Ceylan, C.Ü., Haynes, A., Cope, J., Wilkinson, H.H., Erbay, C., Figueiredo, P. de, Han, A., 2012. A microfluidic microbial fuel cell array that supports long-term multiplexed analyses of electricigens. Lab Chip 12, 4151–4159.
Inzelt, G., 2013. Pseudo-reference electrodes. In: Handbook of Reference Electrodes. Springer, Berlin, Heidelberg, pp. 331–332.
Kochius, S., Park, J.B., Ley, C., Könst, P., Hollmann, F., Schrader, J., Holtmann, D., 2014. Electrochemical regeneration of oxidised nicotinamide cofactors in a scalable reactor. J. Mol. Catal. B Enzym. 103, 94–99.
Kolthoff, I.M., Tomsicek, W.J., 1935. The oxidation potential of the system potassium ferrocyanide–potassium ferricyanide at various ionic strengths. J. Phys. Chem. 39, 945–954.
Kostov, Y., Harms, P., Randers-Eichhorn, L., Rao, G., 2001. Low-cost microbioreactor for high-throughput bioprocessing. Biotechnol. Bioeng. 72, 346–352.
Lai, B., Bernhardt, P.V., Krömer, J.O., 2020. Cytochrome c reductase is a key enzyme involved in the extracellular electron transfer pathway towards transition metal complexes in Pseudomonas putida. ChemSusChem 13, 5308–5317.
Lai, B., Nguyen, A.V., Krömer, J.O., 2019. Characterizing the anoxic phenotype of Pseudomonas putida using a bioelectrochemical system. Methods protoc 2 2.
Lai, B., Yu, S., Bernhardt, P.V., Rabaey, K., Virdis, B., Krömer, J.O., 2016. Anoxic metabolism and biochemical production in Pseudomonas putida F1 driven by a bioelectrochemical system. Biotechnol. Biofuels 9, 39.
Ley, C., Schewe, H., Ströhle, F.W., Ruff, A.J., Schwaneberg, U., Schrader, J., Holtmann, D., 2013a. Coupling of electrochemical and optical measurements in a microtiter plate for the fast development of electro enzymatic processes with P450s. J. Mol. Catal. B Enzym. 92, 71–78.
Ley, C., Zengin Çekiç, S., Kochius, S., Mangold, K.-M., Schwaneberg, U., Schrader, J., Holtmann, D., 2013b. An electrochemical microtiter plate for parallel spectroelectrochemical measurements. Electrochim. Acta 89, 98–105.
Piermarini, S., Micheli, L., Ammida, N.H.S., Palleschi, G., Moscone, D., 2007. Electrochemical immunosensor array using a 96-well screen-printed microplate for aflatoxin B1 detection. Biosens. Bioelectron. 22, 1434–1440.
Rossi, R., Hur, A.Y., Page, M.A., Thomas, A.O., Butkiewicz, J.J., Jones, D.W., Baek, G., Saikaly, P.E., Cropek, D.M., Logan, B.E., 2022. Pilot scale microbial fuel cells using air cathodes for producing electricity while treating wastewater. Water Res. 215, 118208.
Ruinatscha, R., Buehler, K., Schmid, A., 2014. Development of a high performance electrochemical cofactor regeneration module and its application to the continuous reduction of FAD. J. Mol. Catal. B Enzym. 103, 100–105.
Savéant, J.M., 2006. Elements of Molecular and Biomolecular Electrochemistry: an Electrochemical Approach to Electron Transfer Chemistry. Wiley-Interscience, Hoboken, N.J., p. 485
Sawhney, M.A., Azzopardi, E.A., Rodrigues Teixeira, S., Francis, L.W., Conlan, R.S., Gazze, S.A., 2019. Measuring the impact on impedance spectroscopy of pseudo-reference electrode accumulations. Electrochem. Commun. 105, 106508.
Schmitz, S., Nies, S., Wierckx, N., Blank, L.M., Rosenbaum, M.A., 2015. Engineering mediator-based electroactivity in the obligate aerobic bacterium Pseudomonas putida KT2440. Front. Microbiol. 6, 284.
Sturm-Richter, K., Golitsch, F., Sturm, G., Kipf, E., Dittrich, A., Beblawy, S., Kerzenmacher, S., Gescher, J., 2015. Unbalanced fermentation of glycerol in Escherichia coli via heterologous production of an electron transport chain and electrode interaction in microbial electrochemical cells. Bioresour. Technol. 186, 89–96.
Sydow, A., Krieg, T., Mayer, F., Schrader, J., Holtmann, D., 2014. Electroactive bacteria - molecular mechanisms and genetic tools. Appl. Microbiol. Biotechnol. 98, 8481–8495.
Szydlowski, L., Ehlich, J., Goryanin, I., Pasternak, G., 2022. High-throughput 96-well bioelectrochemical platform for screening of electroactive microbial consortia. Chem. Eng. J. 427, 131692.
Tahernia, M., Mohammadifar, M., Gao, Y., Panmanee, W., Hassett, D.J., Choi, S., 2020. A 96-well high-throughput, rapid-screening platform of extracellular electron transfer in microbial fuel cells. Biosens. Bioelectron. 162, 112259.
Ucar, D., Zhang, Y., Angelidaki, I., 2017. An overview of electron acceptors in microbial fuel cells. Front. Microbiol. 8, 643.

A.4 Publication IV

André Gemünde, Jonas Gail, and Dirk Holtmann

Redox mediator interaction with *Cupriavidus necator* – spectroelectrochemical online analysis

In *Electrochemistry Communications*, Volume 162, 2024
DOI: https://doi.org/10.1016/j.elecom.2024.107705

Contribution: My contribution to this work was the spectroelectrochemical screening of the mediators, the development of all methods mentioned in the Publication, and the data analysis of the experiments. Furthermore, I supervised the experimental work performed by Jonas Gail. The original draft and all figures were also created by myself.

Electrochemistry Communications 162 (2024) 107705

Contents lists available at ScienceDirect

Electrochemistry Communications

journal homepage: www.elsevier.com/locate/elecom

Redox mediator interaction with *Cupriavidus necator* – spectroelectrochemical online analysis

André Gemünde [a], Jonas Gail [a], Dirk Holtmann [a,b,*]

[a] Institute of Bioprocess Engineering and Pharmaceutical Technology and Competence Centre for Sustainable Engineering and Environmental Systems, University of Applied Sciences Mittelhessen, 35390 Giessen, Germany
[b] Institute of Process Engineering in Life Sciences, Karlsruhe Institute of Technology, Kaiserstraße 12, 76131, Karlsruhe, Germany

ARTICLE INFO

Keywords:
Redox mediators
Anodic respiration
Cupriavidus necator
Parallelization
Bioelectrochemical system

ABSTRACT

Bioelectrochemical systems with *Cupriavidus necator* present a viable solution for harnessing H_2/CO_2 mixtures as substrates, employing mediated electron transfer to an infinite electron acceptor in the form of an anode instead of O_2. Fourteen redox mediators were spectroelectrochemically characterized, and their efficiency was evaluated through screening with *C. necator* in common cuvettes with screen printed electrodes (e-Cuvettes). Key performance indicators, including total turnover number, reduction rate, and growth, were analyzed. Ferricyanide emerged as highly effective for anodic respiration, reaching a total turnover number of 8.38 over 120 h of cultivation. On the other hand, phenazine methosulfate exhibited the highest reduction rate at 2.49 mM h^{-1} with a total of 5.16 turnovers. Contrary, growth impairment is reported for menadione, possibly leading to deficient anodic electron transfer. The utilization of a broad spectrum of these shuttle molecules highlights the potential for optimizing bioelectrochemical applications involving *C. necator*.

1. Introduction

A robust CO_2-utilizing strain capable of thriving on H_2 as an electron donor would be an ideal candidate for industrial fermentation of value-added products in the future. A promising microorganism to fulfil this task was found to be *Cupriavidus necator*. The conversion of H_2 as electron, and CO_2 as carbon source to products like the polymer alternative polyhydroxybutyrate [1] or terpenes for fragrance applications [2] is the key feature of *C. necator*. As genetic tools become more accessible, metabolic engineering facilitates the production of a broader array of products and applications [3,4].

However, challenges surface when O_2 is needed as the electron acceptor, particularly in large-scale reactors where the use of H_2/O_2 mixtures poses a significant explosion risk, which call for special precautions [5]. Bioelectrochemical systems offer a potential solution by replacing O_2 with an anode, circumventing safety concerns while at the same time overcoming oxygen transfer limitations and cost implications of transferring O_2 into the medium. Moreover, an anode serves as an inexhaustible electron acceptor, unlike gaseous or solid acceptors that necessitate replacement or regeneration [6,7].

Electron transfer mechanisms in this context involve direct contact with the electrode via redox-active proteins in the membranes, as well as via redox-active electron shuttles in the medium in a mediated electron transfer. Notably, *C. necator* lacks expression of redox-active proteins for maintaining a conductive "electron bridge" across the periplasmic space, necessitating the use of redox mediators (RMs) for efficient electron transfer to the anode.

The choice of RMs is critical and multifaceted, considering characteristics like membrane permeation (including hydrophobicity and charge), stability, toxicity, redox potential, solubility in aqueous media, and fast electron transfer [8,9]. Despite this, limited information exists regarding the interaction of *C. necator* with various redox mediators in so called "anodic respiration". Given that the process does not align with respiration in terms of generating a proton gradient through an electron transport chain, it should be emphasized that anodic respiration denotes the substitution of the terminal electron acceptor with the anode. Despite sporadic research efforts in this domain, a critical gap exists in the form of a mediator database specific to anodic respiration with

Abbreviations: BES, bioelectrochemical system; CV, cyclic voltammetry; DCIP, 2,6-dichloroindophenole; DHB, 3,4-dihydroxybenzaldehyde; FEC, ferricyanide; HNQ, 2-hydroxy-1,4-naphtaquinone; MB, methylene blue; MV, methyl viologen; PES, phenazine ethosulfate; PMS, phenazine methosulfate; RES, resorufin; RF, riboflavin; RM, redox mediator; RZ, resazurin; MEN, menadione; NR, neutral red; TTN, total turnover number.

* Corresponding author at: Institute of Process Engineering in Life Sciences, Karlsruhe Institute of Technology, Kaiserstraße 12, 76131 Karlsruhe, Germany.
E-mail address: dirk.holtmann@kit.edu (D. Holtmann).

https://doi.org/10.1016/j.elecom.2024.107705
Received 17 January 2024; Received in revised form 14 February 2024; Accepted 17 March 2024
Available online 18 March 2024

C. necator (and other organisms), underscoring the need for comprehensive exploration.

This study aims to address this gap by firstly, establishing a comprehensive dataset comprising crucial spectroelectrochemical data for diverse redox mediators, extending the scope of already existing data. Secondly, these RMs will be screened with *C. necator* for specific key performance indicators to determine their suitability for anodic respiration. By delving into the interaction dynamics between *C. necator* and various RMs, this research aims to pave the way for leveraging anodic respiration as a sustainable and efficient means of electron transfer, offering valuable insights for bioprocessing applications.

2. Materials and methods

2.1. Bacterial strains and chemicals

The strain *Cupriavidus necator* PHB$^-$4 [10] was employed in all biotic trials. Chemicals were sourced from Merck KGaA (Germany), VWR Chemicals (USA), Carl Roth GmbH & Co. KG (Germany), or Sigma Aldrich (USA).

2.2. Media and culture conditions

Cultures were incubated at 30 °C and 180 rpm in tubes containing 2.5 mL of LB medium (10 g L^{-1} tryptone, 5 g L^{-1} yeast extract, 10 g L^{-1} NaCl). For BES precultures, cryostocks were initially streaked on LB agar plates (15 g L^{-1} agar) and incubated overnight at 30 °C. Liquid precultures were subsequently generated by transferring a single colony into a 100 mL flask with baffles containing 20 mL of MMasy minimal medium [11] with 4 g L^{-1} fructose as carbon and electron source. The medium further contained 2.895 g L^{-1} Na_2HPO_4, 2.707 g L^{-1} $NaH_2PO_4{\cdot}H_2O$, 0.94 g L^{-1} $(NH_4)_2SO_4$, 0.8 g L^{-1} $MgSO_4{\cdot}7H_2O$, 0.097 g L^{-1} $CaSO_4{\cdot}2H_2O$, 0.17 g L^{-1} K_2SO_4, and 0.1 % (v/v) of trace element solution. The trace element stock solution consisted of 15 g L^{-1} $FeSO_4{\cdot}7H_2O$, 2.4 g L^{-1} $MnSO_4{\cdot}H_2O$, 2.4 g L^{-1} $ZnSO_4{\cdot}7H_2O$, 0.48 g L^{-1} $CuSO_4{\cdot}5H_2O$, 1.8 g L^{-1} $Na_2MoO_4{\cdot}2H_2O$, 1.5 g L^{-1} $Ni_2SO_4{\cdot}6H_2O$, and 0.04 g L^{-1} $CoSO_4{\cdot}7H_2O$ dissolved in 0.1 M HCl. Cultures were then incubated in an orbital shaker at 180 rpm (2.5 cm orbit, Multitron, Infors, Bottmingen, Switzerland).

2.3. Spectroelectrochemical mediator characterisation

Extinction characteristics of different mediators were determined by spectroelectrochemical analysis. Hereby, optical measurements are combined with cyclic voltammetry (CV) analysis. A spectroelectrochemical cell kit in a quartz cuvette was used (AKSTCKIT3, Pine Research Instrumentation Inc., USA). The electrode consisted of a gold working electrode with micro holes and a gold counter electrode on a ceramic substrate. A micro Ag/AgCl (3 M KCl) reference electrode (RRPEAGCL2, Pine Research Instrumentation Inc., USA) was immersed into the solution separately. The cell was heated to 30 °C and kept oxygen-free by sparging the headspace with N_2 (99.99 %). To eliminate any pH changes affecting the CV, measurements were carried out in 100 mM phosphate buffer (8.23 g L^{-1} Na_2HPO_4, 5.04 g L^{-1} NaH_2PO_4) at pH 7. Data was recorded on a Gamry Interface 1010B potentiostat (Gamry Instruments Inc., USA) at 50 and 10 mV s^{-1}. Each RM was used within a concentration range of 100 μM to 1 mM, if the solubility in aqueous buffer allowed. Poorly soluble mediators (such as menadione) were used at their maximum solubility.

2.4. BES screening

The screening device holds 8 independent 4 mL polystyrene cuvettes (Th. Geyer GmbH & Co. KG, Germany) in an automatic cuvette sampler within a spectrophotometer (Evolution 201, Thermo Scientific GmbH, Germany). Implementing screen-printed gold electrodes (C220 AT, Deutsche Metrohm GmbH & Co. KG, Germany) into each channel turns the cuvettes into an unseparated BES. For long term stability, the micro Ag/AgCl (3 M KCl) reference electrode was used again instead of the printed Ag pseudo electrode on the chip. Additionally, N_2 is sparged through the channels at a flow rate of 3.5 mL min^{-1} to keep the channels anaerobic and mixed. A detailed description of the device can be found in [12].

2.5. Electrochemical analysis and calculations

Cyclic voltammetry within the BES was carried out in using the screen-printed gold electrodes and Ag/AgCl (3 M KCl) reference electrodes. CVs were recorded at scan rates between 10 and 1000 mV s^{-1} at 30 °C without mixing the medium.

The midpoint potential (E_m) was derived as the mean of anodic and cathodic peak potentials obtained from CV analysis via the equation $E_m = (E_{ox} + E_{red})/2$. The total turnover number of the mediators (TTN) within the BES was calculated following a previously established method [13]. Reduction rates of redox mediators were determined by linear regression of the extinction values during the initial reduction of the respective mediator during BES cultivation. With calibration standards in the relevant concentrations of the mediator, the depleting or increasing linear extinction could be transformed into reduction rates in μM h^{-1}.

3. Results and discussion

3.1. Spectroelectrochemical redox mediator characterisation

A selection of fourteen RMs, each exhibiting different midpoint potentials (E_m) and featuring redox indicator properties (colour change upon reduction/oxidation), was chosen for assessment regarding their interaction with *C. necator* in a BES designed for anodic respiration (see Table 1). Via an online screening device based on cuvettes in an automatic sampler of a photometer, the redox state of each indicator RM can be monitored via a colour change upon reduction by *C. necator* at a characteristic wavelength (λ_c). This wavelength was determined by combining cyclic voltammetry with spectrophotometric analysis.

In total, during the experiment 3 oxidations and 3 reductions take

Table 1
E_m, ΔE, $I_{p,c}/I_{p,a}$, and λ_c of each RM measured by the described spectroelectrochemical approach. Conditions. 30 °C, anaerobic, pH 7, CV scan rate. 10 mV s^{-1}.

Redox mediator	E_m vs. Ag/AgCl (3 M KCl) [mV]	ΔE [mV]	$I_{p,c}/I_{p,a}$	λ_c [nm]
2,2′-azino-bis(3-ethylbenzothiazoline-6-sulfonic acid) (ABTS)	492	82	0.881	338/415
Methyl red (MR)	205.5	177	–	430
Ferricyanide (FEC)	194.6	315.1	0.925	320/420
3,4-dihydroxybenzaldehyde (DHB)	156.5	81	0.664	317
2,6-dichloroindophenole (DCIP)	16.3	66.5	0.889	607
Phenazine methosulfate (PMS)	−134.5	62	0.748	383
Phenazine ethosulfate (PES)	−144	68	0.682	383
Menadione (MEN)	−226.3	192.5	0.999	262/325
Resorufin (RES)	−242.3	51.5	1.037	568
Methylene blue (MB)	−261.5	63	1.024	642
2-hydroxy-1,4-naphtaquinone (HNQ)	−364.5	261	1.010	452
Riboflavin (RF)	−411	64	1.095	373/445
Neutral red (NR)	−553.5	73	1.575	445
Methyl viologen (MV)	−666.8	156.5	0.822	390/602

place (3 CV scans). Fig. 1 shows an example of how the λ_c of resazurin (RES) was determined via the aforementioned method. In Fig. 1 (a), the extinction spectra recorded over time create a 3-dimensional image of the redox reaction taking place at the working electrode during reduction and oxidation. For better visibility, Fig. 1 (b) depicts these spectra as a 2D topographic map. The repetitive redox reaction now enables to read off the λ_c and monitor side reactions. At the start of the CV scan at 400 mV (Fig. 1 (c)), meaning also 0 s in the extinction time-frame, distinct peaks at 270, 375 and 600 nm are visible. Now, as the potential is lowered (direction of the scan is shown with a red arrow) and the first reduction at −390 mV takes place, the extinction spectrum shifts to a single peak at 568 nm which rises and declines according to the reduction or oxidation occurring at the working electrode. Furthermore, the first reduction current appears to be much higher than in the second or third scan, indicating an irreversible reduction.

The observed phenomenon conforms to resazurin's characteristics, undergoing irreversible reduction to resorufin and resulting in a pink colour change. (Fig. 1 (d)) [14]. Resorufin can undergo a reversible redox reaction to dihydroresorufin in a two-electron transfer step. The colourless dihydroresorufin formation is evident through the extinction spectrum peak at 568 nm disappearing during reduction and the subsequent reappearance during resorufin formation at the working electrode (indicated with the black dashed line in Fig. 1 (b)). Therefore, λ_c can be determined with 568 nm, as this wavelength determines the redox state of the reversible electron transfer.

The same method was also applied to all 13 remaining RM to determine the λ_c. E_m for each RM for a single, reversible electron transfer reaction can also be obtained from the CVs. With this, both the reduction- and oxidation-potential can be determined and any following chemical reactions of the reactants are visible in peak current ratios ($I_{p,c}/I_{p,a}$) divergent from 1, since some of the reactant is now missing for the reverse reaction leading to a smaller peak current [15]. Furthermore, peak separation values (ΔE) can hint towards reversible or irreversible redox reactions of the RM, with a typical ΔE value close to 58 mV for a perfectly reversible one electron transfer process (at 25 °C). Fig. 2 shows all CVs obtained for 13 of the 14 RMs (except methyl red). For better visualisation, the obtained current values were normalized to equal values.

The determined E_m values as well as the $I_{p,c}/I_{p,a}$ ratios are listed in Table 1. Since a reaction can appear reversible at slower scan rates, these values are not universally valid [15]. In this case, a scan rate of 10 mV s^{-1} was applied. High ΔE values, especially higher than 58 mV under standard conditions, are a further indicator for quasi-reversible or irreversible reactions. For 2 electron transfer reactions, higher peak separations are to be expected, if one of the electron transfer steps is thermodynamically less favourable. However, above 140 mV both electron transfer steps should separate into single waves in the CV scan separation [16,17].

The CV of MR, depicted separately in Fig. 3, shows a typical irreversible behaviour within the wide potential range applied. For the first reversible electron transfer step, a potential of 140 to 165 mV is to be expected [18,19]. In this range, a smaller oxidation and reduction peak

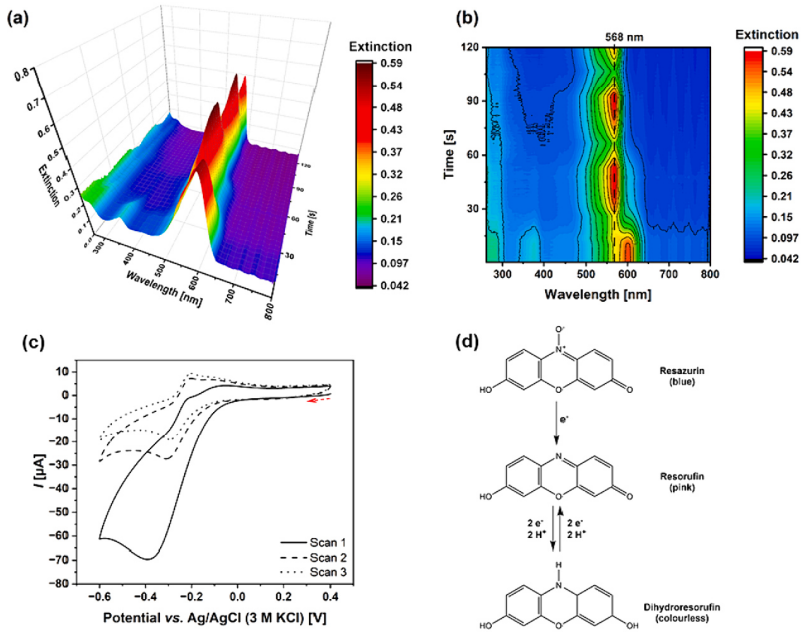

Fig. 1. Spectroelectrochemical characterisation of resazurin. (a) Extinction spectra over the course of 3 CV scans. (b) Topographical visualisation of the extinction spectra. (c) CV scans of 100 µM resazurin. Red arrow indicates the start of CV scan 1. Scan rate: 50 mV s^{-1}, 30 °C, anaerobic, pH 7. (d) Resazurin reaction scheme. Created with ChemDraw®.

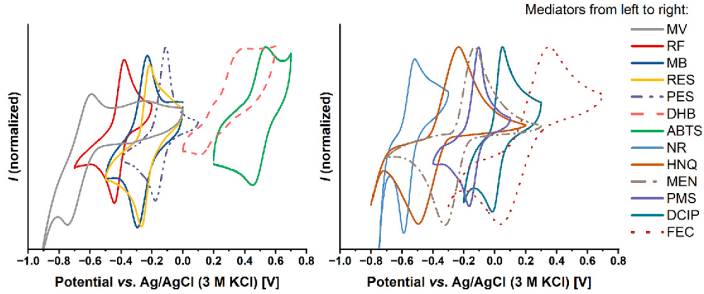

Fig. 2. CV scans of 13 redox mediators recorded with the spectroelectrochemical cell. Current values were normalized from 0 to 1 for better comparability of the mediators. Abbreviations: **MV:** methyl viologen, **RF:** riboflavin, **MB:** methylene blue, **RES:** resazurin, **PES:** phenazine ethosulfate, **DHB:** 3,4-dihydroxybenzaldehyde, **ABTS:** 2,2′-azino-bis(3-ethylbenzothiazoline-6-sulfonic acid, **NR:** neutral red, **HNQ:** 2-hydroxy-1,4-naphtaquinone, **MEN:** menadione, **PMS:** phenazine methosulfate, **DCIP:** 2,6-dichloroindophenole, **FEC.** ferricyanide. Conditions: 10 mV s^{-1}, 30 °C, anaerobic, pH 7.

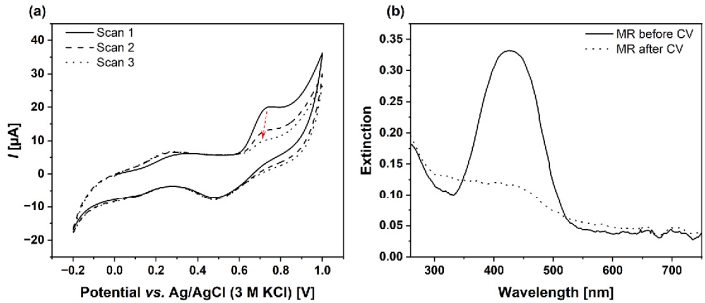

Fig. 3. (a) 3 CV scans of methyl red. The red arrow indicates the decrease in peak intensity over the course of the 3 scans. (b) Extinction spectrum taken before and after the CV scans. The vanished extinction maximum indicates an irreversible reaction took place. Scan rate. 50 mV s^{-1}, 30 °C, anaerobic, pH 7.

is visible in the CV scan. The oxidation potential of 294 mV and reduction potential of 117 mV result in E_m = 205.5 mV. However, a redox state characterisation by extinction measurement becomes impossible after MR is degraded above 700 mV [20]. The compound is therefore only applicable as a redox mediator below 700 mV. Side reactions like this could potentially degrade other mediators as well. However, within the potential ranges stated in Fig. 2, no such reaction was observed.

For all other RMs, Fig. 4 depicts the topographic view to determine each λ_e. The extinction spectrum of DHB did not exhibit a λ_e shift, possibly attributed to either a high scan rate, an inadequate concentration, or a slow electrochemical reaction. This phenomenon is also discernible in the minor peaks within the CV of DHB (Fig. 2). In the spectrum of MB, only one growing and decreasing peak is visible at 642 nm. The reasons for this might also be found within the electrochemical parameters. For MR and DHB, the maximum extinction from a separate spectrum was chosen as the λ_e for further biotic screening.

Table 1 summarizes the formal potentials and electrochemical peak separations calculated from CV scans and the λ_e determined from Fig. 4 for all examined RMs. In the case of MR, the reversible peaks were too small to determine the $I_{p,c}/I_{p,a}$ ratio accurately.

3.2. *In vivo* mediator interaction screening

Screening of the RMs was carried out in the e-Cuvette screening device, as already described elsewhere [12]. With this setup, the current density and the redox state of a RM can be determined online via the λ_e while simultaneously measuring OD_{600} for changes in cell density. Exemplarily, Fig. 5 illustrates a typical BES cultivation of *C. necator* in 6 parallel cuvettes and 2 abiotic controls with and without FEC. Prior to t_0 (abiotic phase), there is no evolution of current in the system. As soon as *C. necator* is introduced into the system at t_0, an anodic current starts to rise (magenta), while the FEC extinction at 420 nm (yellow dots) drops as it is reduced. Throughout cultivation, the anode partially re-oxidizes FEC, leading to an anodic current and an increase in extinction. After 118 h (t_1) the polarisation is stopped. The decline in extinction at 420 nm reaffirms that oxidized FEC remains present and is being reduced by viable cells.

The abiotic control including FEC polarized at 500 mV returns a steadily increasing current over time (Fig. 5 (a), dashed line), while FEC is also reduced as indicated by the declining extinction at 420 nm (Fig. 5 (b), yellow dots). It is most likely, that FEC is reduced at the cathode and simultaneously oxidized at the anode within this unseparated chamber (Fig. 5 (c)), while the cathodic reaction seems to be dominant and therefore shifts the ratio towards the reduced form. Other reactions, like

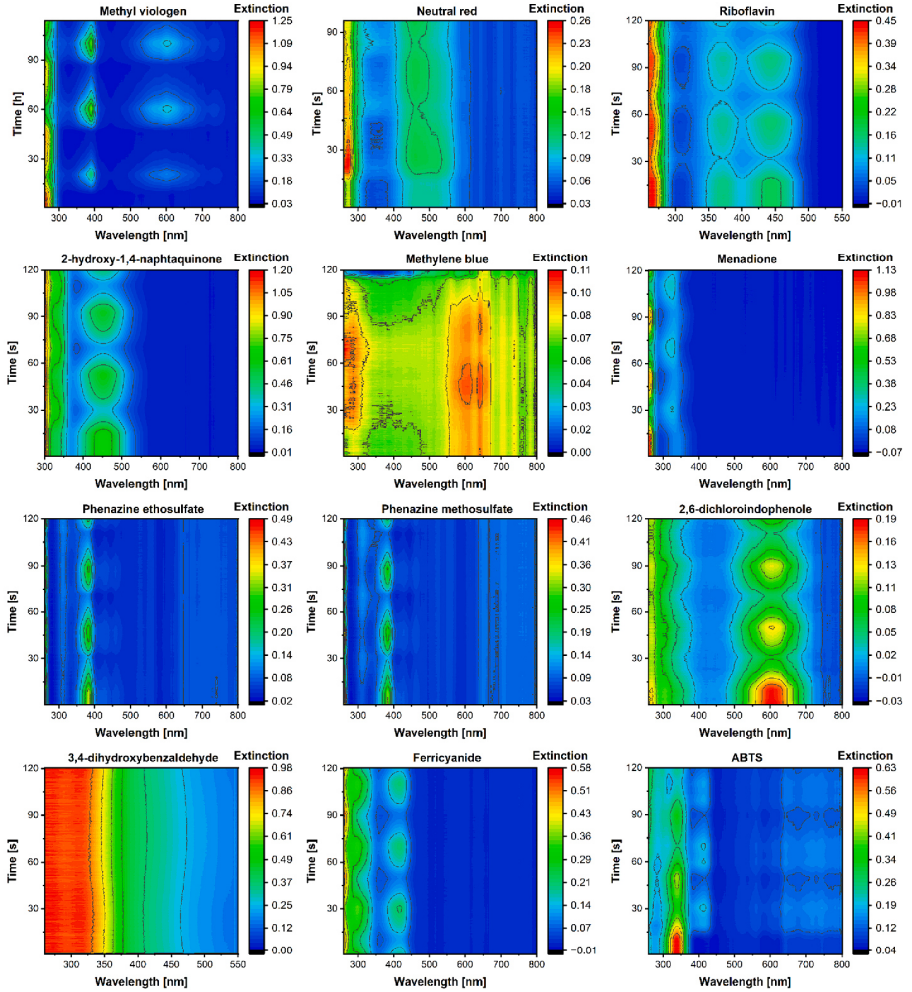

Fig. 4. Topographic visualization of the extinction spectra during 3 CV scans over the vertical time scale for each mediator used in this study (except MR and RES). The λ_c h of each mediator can be deduced from the recurring peaks over time. Conditions. 30 °C, anaerobic, pH 7, CV scan rate. 10 mV s^{-1}.

O_2 development (1.033 V *vs.* Ag/AgCl according to ΔG value) are not feasible at 500 mV and don't occur in CV analysis (Fig. 5 (d), dashed lines). Unknown side reactions from the medium can be observed within the CV. From the control cuvette without FEC, the direct involvement of these side reactions can be ruled out though, since the polarization of the pure medium doesn't result in a current evolving over time (Fig. 5 (a), dotted line).

The real-time analysis of current and extinction provides insights into three performance indicators, defining the efficiency of the mediator for anodic respiration. First, the slope of the extinction value during reduction of the RM enables reduction rate analysis. The reduction rate may indicate highly efficient mediators, regardless of the electrochemical regeneration system's efficiency. Second, with the charge transferred to the anode, the TTN can be calculated, giving further insight into the efficiency of the RM, independent of the concentration used. Moreover, the interaction between *C. necator* and a RM with a

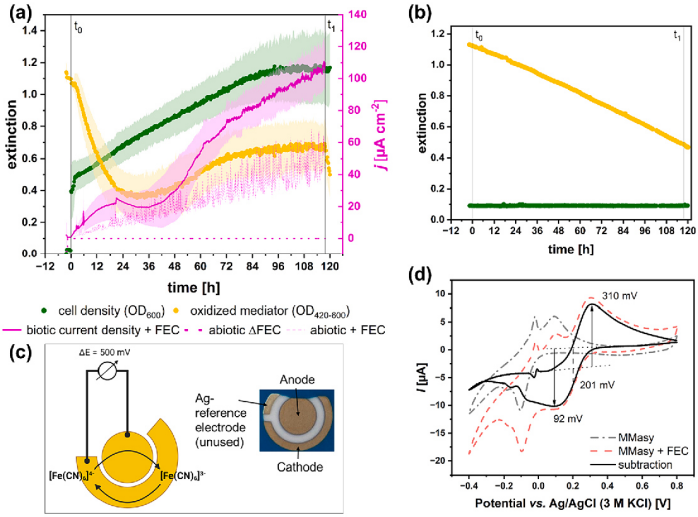

Fig. 5. (a) *C. necator* cultivation in e-Cuvettes with 1 mM FEC as redox mediator. t_0 marks the inoculation, while t_1 designates the point at which the polarisation is stopped. Current density (magenta) during polarisation at 500 mV for biotic cuvettes (solid line), abiotic control with FEC (dashed line), and without FEC (dotted line). Extinction values at 420 nm are plotted in yellow and cell density at 600 nm in green. (b) Abiotic control cuvette with FEC displays reduction of FEC, as indicated by the decline in OD_{420}. (c) Screen-printed electrode setup and abiotic redox cycle of FEC in the unseparated system. (d) CV scans of pure medium in comparison to medium with FEC in e-Cuvettes. Conditions. 3.5 mL MMasy medium, 30 °C, anaerobic, n = 6.

known redox potential provides insights into the minimum potential required for the oxidation of the yet unidentified interaction site(s) of *C. necator*. And third, growth rate analysis can hint towards impairments stemming from the redox mediator.

The described method was employed to screen all previously characterized RMs and evaluate their suitability for anodic respiration. Potentials for re-oxidation of the mediator were chosen above the oxidation potential of the RM, as determined by CV analysis. The first performance indicator, the reduction rate, is summarized in Table 2 including the applied concentrations and the observed growth rate. From the results, both phenazines, PMS and PES stand out with reduction rates of 2.49 and 0.25 mM h^{-1}, respectively.

Phenazine compounds are known for their high affinity towards the intracellular electron transfer chain. However, their stability within a BES varies between one and more than 10 days [21]. PMS decomposition to pyocyanine [22] also plays a role during the experiment. Abiotic controls of PMS at 300 mV exhibit a consistent decline in extinction at 383 nm with minimal current response, indicating both degradation and cathodic reduction. Moreover, the current density within the biotic cuvettes containing PMS never reaches a steady state, instead, it rapidly decreases after 2 h (Fig. 6 (a)).

The second performance indicator, the TTN, was determined over a 118 h cultivation period (Fig. 7). Interaction of the RM with *C. necator* is linked to the E_m of the respective RM and can reveal a minimum redox potential that is necessary for an electron shuttle compound to enable electron transfer from the still unknown interaction site(s) to the RM. By listing the TTN in a descending order according to their determined E_m, a major cut-off potential below –261 mV can be determined. However, HNQ is still interacting with *C. necator* in the first 10 h (data not shown), but the resulting current is extremely low resulting in a TTN of only 0.01. In conclusion, any mediator between 206 and −365 mV is able to interact with *C. necator*, indicating the interaction site(s) offer a broad potential range.

Table 2
RM reduction rates, concentrations, and observed growth rates of *C. necator* in BES cultivations.

RM	Concentration [µM]	Applied potential [mV *vs.* Ag/AgCl 3 M KCl]	Reduction rate [µM*h $^{-1}$]	Growth rate μ [h $^{-1}$]
ABTS	100	700	–	0.017
PEC	1000	500	49.43	0.015
DHB	120	700	3.73	0.013
MR	50	300	1.98	0.012
DCIP	80	300	35.3	0.009
PMS	50	300	2492.83	0.009
RES	100	0	99.85[a]	0.013
PES	50	300	245.15	0.011
MEN	50 % saturated solution	230	1.16[b]	0.003
MB	20	100	0.63	0.007
HNQ	400	100	–	0.007
RF	100	300	–	0.016
NR	100	−200	–	0.008
MV	625	−400	–	0.014
No RM				**0.011**

[a] only the initial reduction of RZ→RES was quantified in µM*h^{-1}
[b] measured in % h^{-1}

Upon comparing the TTN with the determined reduction rates, it becomes evident that slowly reduced redox mediators can still contribute to anodic respiration through consistent and stable cycling. E. g., MR is able to perform 4.2 cycles per molecule while only being reduced by *C. necator* at 1.98 µM h^{-1}. RES, on the other hand, is reduced

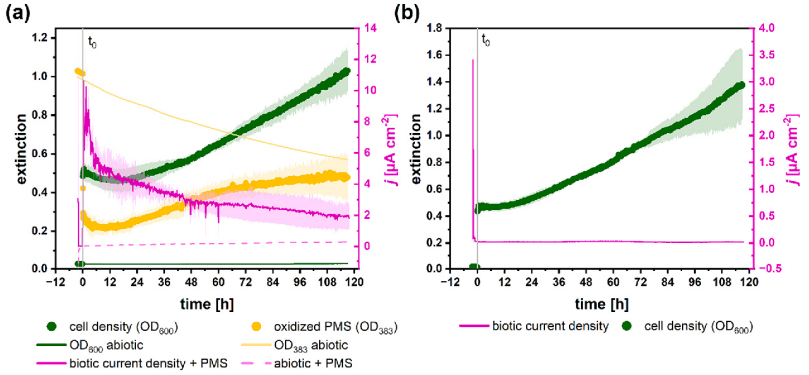

Fig. 6. (a) Current density of *C. necator* with 50 µM PMS in e-Cuvettes at 300 mV (magenta, n 3) with extinction data (λ 383 nm, yellow). Abiotic control with PMS at 300 mV (yellow line and magenta dashed line). (b) Control experiment with *C. necator* at 500 mV lacking a RM. Current density (magenta) and OD_{600} (green).

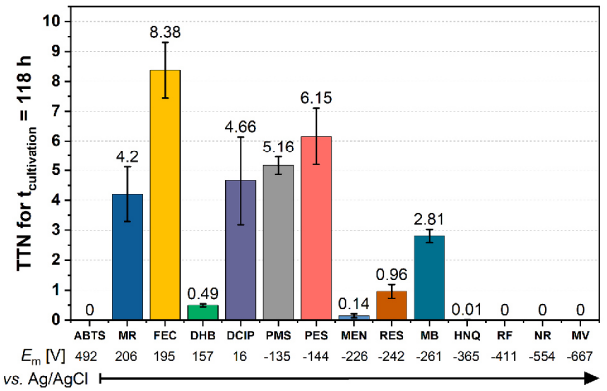

Fig. 7. TTN for all 14 RM in biotic electrochemical cultivations over 118 h with their respective redox potential *vs.* Ag/AgCl (3 M KCl). Conditions. 3.5 mL MMasy medium, 30 °C, anaerobic, n 3. Error bars depict the standard deviation.

at 99.85 µM h^{-1} and only achieves 0.96 turnovers. As a lipophilic molecule, RES can most likely penetrate the cell membrane even though it is negatively charged [23]. This enables the direct oxidation of intracellular NADH, FADH or intracellular cytochromes. Transport within the bulk medium may limit the TTN and could hence benefit from a secondary, more hydrophilic redox mediator like FEC to facilitate electron transport to the anode. Furthermore, MR proves to be an effective RM with intact indicator properties in our BES when used at 300 mV *vs.* Ag/AgCl, were the molecule is not electrochemically degraded. MR, DCIP, PMS, PES, and FEC all resulted in a TTN above 4.2 promising future applications for anodic respiration. Both phenazines, MR, and DCIP share the hydrophobic characteristics with logP values of 3.06/2.9 for PES/PMS, 1.67 for MR, and 3.12 for DCIP [18,24]. FEC on the other hand, is more hydrophilic according to the logP value of −0.26 [18] and is most likely not membrane permeable due to the high negative charge. Hence, outer membrane porins likely play an important role in FEC transport. The affinity towards non-polar solvents is therefore not the key parameter for RM selection.

In a control experiment without a RM (Fig. 6 (b)), growth still occurs without the development of a current. Therefore, the growth is most likely caused by traces of O_2 entering the system as described before [12]. Comparing the growth rates with RMs from Table 2 to the reference rate without a RM, only MEN stands out with a significant inhibitory effect. This could also explain the exceptionally low TTN attributed to potential toxic effects on the metabolism. MB, HNQ, and NR have a slight inhibitory effect. Among them, only MB is deemed feasible for anodic respiration, with a TTN of 2.81.

4. Conclusions

In this study, λ_c and E_m values for 14 RMs were determined These values enable the online determination of redox states during BES

cultivation within a standard spectrophotometer. The determined ΔE and $I_{p,c}/I_{p,a}$ values CVs provided insights into which RM is capable of achieving reversible electron transfer with a gold electrode.

In BES screening experiments, phenazines proved to be highly efficient with maximum reduction rates of 2.49 mM h^{-1} and 0.25 mM h^{-1} for PMS/PES and a TTN of 5.16 and 6.15 respectively. Nevertheless, their stability constrains their applicability for long-term experiments. The screening further revealed that high reduction rates can occur independent of a high TTN. Especially FEC, delivering 8.38 turnovers while only being reduced at a rate of 49.43 μM h^{-1}, stands out in this context. The affinity towards organic solvents for each RM was termed secondary for selecting a RM, since both hydrophobic and hydrophilic RMs resulted in a similar TTN. However, to achieve an efficient process, the combination of both may lead to an optimal mediated electron transfer.

CRediT authorship contribution statement

André Gemünde: Writing – original draft, Visualization, Methodology, Investigation, Data curation. **Jonas Gail:** Investigation. **Dirk Holtmann:** Writing – review & editing, Supervision, Project administration, Funding acquisition, Conceptualization.

Declaration of competing interest

The authors declare that they have no known competing financial interests or personal relationships that could have appeared to influence the work reported in this paper.

Data availability

Data will be made available on request.

Acknowledgements and Funding

This work was created as part of the project "Bioelectrochemical and engineering fundamentals to establish electro-biotechnology for biosynthesis – Power to value-added products (eBiotech)", which is funded by the Deutsche Forschungsgemeinschaft (DFG, German Research Foundation) – Project number 422694804.

References

[1] R.R. Dalsasso, F.A. Pavan, S.E. Bordignon, G.M.F. de Aragão, P. Poletto, Polyhydroxybutyrate (PHB) production by cupriavidus necator from sugarcane vinasse and molasses as mixed substrate, Process Biochem. 85 (2019) 12–18, https://doi.org/10.1016/j.procbio.2019.07.007.

[2] T. Krieg, A. Sydow, S. Faust, I. Huth, D. Holtmann, CO_2 to terpenes: autotrophic and electroautotrophic α-humulene production with cupriavidus necator, Angew. Chem. Int. Ed. Engl. 57 (2018) 1879–1882, https://doi.org/10.1002/anie.201711302.

[3] M. Ehsaan, J. Baker, K. Kovács, N. Malys, N.P. Minton, The pMTL70000 modular, plasmid vector series for strain engineering in cupriavidus necator H16, J. Microbiol. Meth. 189 (2021) 106323, https://doi.org/10.1016/j.mimet.2021.106323.

[4] J. Panich, B. Fong, S.W. Singer, Metabolic engineering of cupriavidus necator H16 for sustainable biofuels from CO_2, Trends Biotechnol. 39 (2021) 412–424, https://doi.org/10.1016/j.tibtech.2021.01.001.

[5] K. Tanaka, A. Ishizaki, T. Kanamaru, T. Kawano, Production of poly(D-3-hydroxybutyrate) from $CO_{(2)}$, $H_{(2)}$, and $O_{(2)}$ by high cell density autotrophic cultivation of alcaligenes eutrophus, Biotechnol. Bioeng. 45 (1995) 268–275, https://doi.org/10.1002/bit.260450312.

[6] I. Vassilev, G. Gießelmann, S.K. Schwechheimer, C. Wittmann, B. Virdis, J. O. Krömer, Anodic electro-fermentation: anaerobic production of L-lysine by recombinant corynebacterium glutamicum, Biotechnol. Bioeng. 115 (2018) 1499–1508, https://doi.org/10.1002/bit.26562.

[7] L. Gu, X. Xiao, S. Yup Lee, B. Lai, C. Solem, Superior anodic electro-fermentation by enhancing capacity for extracellular electron transfer, Biocesour. Technol. 389 (2023) 129813, https://doi.org/10.1016/j.biortech.2023.129813.

[8] M.L. Fultz, R.A. Durst, Mediator compounds for the electrochemical study of biological redox systems: a compilation, Anal. Chim. Acta 140 (1982) 1–18, https://doi.org/10.1016/S0003-2670(01)95447-9.

[9] Y. Yang, M. Xu, J. Guo, G. Sun, Bacterial extracellular electron transfer in bioelectrochemical systems, Process Biochem. 47 (2012) 1707–1714, https://doi.org/10.1016/j.procbio.2012.07.032.

[10] H.G. Schlegel, R. Lafferty, I. Krauss, The isolation of mutants not accumulating poly-beta-hydroxybutyric acid, Arch. Mikrobiol. 71 (1970) 283–294, https://doi.org/10.1007/BF00410161.

[11] A. Sydow, T. Krieg, R. Ulber, D. Holtmann, Growth medium and electrolyte-how to combine the different requirements on the reaction solution in bioelectrochemical systems using cupriavidus necator, Eng. Life Sci. 17 (2017) 781–791, https://doi.org/10.1002/elsc.201600252.

[12] A. Gemünde, J. Gail, J. Janek, D., Holtmann, e-Cuvettes parallelize electrochemical and photometric measurements in cuvettes and facilitate applications in bio-electrochemistry, Biosens. Bioelectron. X (2023) 100378, https://doi.org/10.1016/j.biosx.2023.100378.

[13] A. Gemünde, J. Gail, D. Holtmann, Anodic respiration of Vibrio natriegens in a bioelectrochemical system, ChemSusChem (2023) e202300181.

[14] R.S. Twigg, Oxidation-reduction aspects of resazurin, Nature 155 (1945) 401–402, https://doi.org/10.1038/155401a0.

[15] G.A. Mabbott, An introduction to cyclic voltammetry, J. Chem. Educ. 60 (1983) 697, https://doi.org/10.1021/ed060p697.

[16] E.S. Da Barreto, B.E.L. Baêta, M.C. Pereira, D. Pasquini, V.M. Guimarães, L.V. A. Gurgel, 2-Hydroxy-1,4-naphthoquinone (lawsone) as a redox catalyst for the improvement of the alkaline pretreatment of Sugarcane bagasse, Energy Fuels 34 (2020) 16228–16239, https://doi.org/10.1021/acs.energyfuels.0c02990.

[17] N. Elgrishi, K.J. Rountree, B.D. McCarthy, E.S. Rountree, T.T. Eisenhart, J. L. Dempsey, A Practical beginner's guide to cyclic voltammetry, J. Chem. Educ. 95 (2018) 197–206, https://doi.org/10.1021/acs.jchemed.7b00361.

[18] F.J. Rawson, A.J. Downard, K.H. Baronian, Electrochemical detection of intracellular and cell membrane redox systems in Saccharomyces cerevisiae, Sci. Rep. 4 (2014) 5216, https://doi.org/10.1038/srep05216.

[19] D. Kul, G. Öztürk, Poly(Methyl red) modified glassy carbon electrodes: electrosynthesis, characterization, and sensor behavior, Electroanalysis 29 (2017) 1721–1730, https://doi.org/10.1002/elan.201700043.

[20] C.C.d.O. Morais, A.J.C. Da Silva, M.B. Ferreira, D.M. de Araújo, C.L.P.S. Zanta, S.S. L. Castro, Electrochemical degradation of methyl red using $Ti/Ru_{0.3}Ti_{0.7}O_2$: fragmentation of azo group, Electrocatalysis 4 (2013) 312–319, https://doi.org/10.1007/s12678-013-0166-x.

[21] A. Chukwubuikem, C. Berger, A. Mady, M.A. Rosenbaum, Role of phenazine-enzyme physiology for current generation in a bioelectrochemical system, Microb. Biotechnol. (2021).

[22] B. Jahn, N.S.W. Jonasson, H. Hu, H. Singer, A. Pol, N.M. Good, H.J.M.O. den Camp, N.C. Martinez-Gomez, L.J. Daumann, Understanding the chemistry of the artificial electron acceptors PES, PMS, DCPIP and Wurster's blue in methanol dehydrogenase assays, J. Biol. Inorg. Chem. 25 (2020) 199–212, https://doi.org/10.1007/s00775-020-01752-9.

[23] J.L. Chen, T.W.J. Steele, D.C. Stuckey, Metabolic reduction of resazurin; location within the cell for cytotoxicity assays, Biotechnol. Bioeng. 115 (2018) 351–358, https://doi.org/10.1002/bit.26475.

[24] M. Surmeian, A. Hibara, M. Slyadnev, K. Uchiyama, H. Hisamoto, T. Kitamori, Distribution of methyl red on the water-organic liquid Interface in a microchannel, Anal. Lett. 34 (2001) 1421–1429, https://doi.org/10.1081/AL-100104916.

A.5 Publication V

*André Gemünde, *Elena Rossini, Oliver Lenz, Stefan Frielingsdorf, and Dirk Holtmann

Chemoorganotrophic electrofermentation by *Cupriavidus necator* using redox mediators

In *Bioelectrochemistry*, Volume 158, 2024
DOI: https://doi.org/ 10.1016/j.bioelechem.2024.108694

*Both authors contributed equally to this work

Contribution: My involvement in this study included the application of mediators in BES reactors and the electrochemical analysis detailed in Chapters 3.2 and 3.3 of the Publication. I also undertook conceptualization and initial drafting. This concept extends from Elena Rossini's mediator pre-screening for biocompatibility (Chapter 3.1), thereby, both of us are credited equally as authors of this Publication.

Bioelectrochemistry 158 (2024) 108694

Contents lists available at ScienceDirect

Bioelectrochemistry

journal homepage: www.journals.elsevier.com/bioelectrochemistry

Chemoorganotrophic electrofermentation by *Cupriavidus necator* using redox mediators

André Gemünde [a,1], Elena Rossini [b,1], Oliver Lenz [b], Stefan Frielingsdorf [b,*], Dirk Holtmann [a,c,*]

[a] Institute of Bioprocess Engineering and Pharmaceutical Technology and Competence Centre for Sustainable Engineering and Environmental Systems, University of Applied Sciences Mittelhessen, 35390 Giessen, Germany
[b] Institute of Chemistry, Biophysical Chemistry, Technische Universität Berlin, Straße des 17. Juni 135, 10623 Berlin, Germany
[c] Institute of Process Engineering in Life Sciences, Karlsruhe Institute of Technology, Kaiserstraße 12, 76131 Karlsruhe, Germany

ARTICLE INFO

Keywords:
Cupriavidus necator
Bioelectrochemical systems
Redox mediators
Biocompatibility
Anodic respiration

ABSTRACT

The non-pathogenic β-proteobacterium *Cupriavidus necator* has the ability to switch between chemo-organotrophic, chemolithoautotrophic and electrotrophic growth modes, making this microorganism a widely used host for cellular bioprocesses. Oxygen usually acts as the terminal electron acceptor in all growth modes. However, several challenges are associated with aeration, such as foam formation, oxygen supply costs, and the formation of an explosive gas mixture in chemolithoautotrophic cultivation with H_2, CO_2 and O_2. Bio-electrochemical systems in which O_2 is replaced by an electrode as a terminal electron acceptor offer a promising solution to these problems. The aim of this study was to establish a mediated electron transfer between the anode and the metabolism of living cells, i.e. anodic respiration, using fructose as electron and carbon source. Since *C. necator* is not able to transfer electrons directly to an electrode, redox mediators are required for this process. Based on previous observations on the extracellular electron transfer enabled by a polymeric mediator, we tested 11 common biological and non-biological redox mediators for their functionality and inhibitory effect for anodic electron transfer in a *C. necator*-based bioelectrochemical system. The use of ferricyanide at a concentration of 15 mM resulted in the highest current density of 260.75 μA cm^{-2} and a coulombic efficiency of 64.1 %.

1. Introduction

Biotechnological processes are becoming increasingly efficient and used in various industries, e.g. pharmaceuticals, wastewater treatment, synthesis of fine and base chemicals, and energy production [1–3]. For these processes, highly efficient microorganisms are a key element to be economically viable. Among those organisms, *Cupriavidus necator* (formerly *Ralstonia eutropha*) is demonstrating promise as a production strain for several reasons. This Gram-negative, strictly respiratory β-proteobacterium possesses the ability to utilize a wide range of carbon sources such as fructose, organic acids, and glycerol in chemo-organotrophic cultivation [4]. Furthermore, chemolithoautotrophic cultivation of *C. necator* with "Knallgas" (H_2/O_2) and CO_2 as feedstock can be exploited to produce valuable compounds such as α-humulene [5] and biopolymers such as polyhydroxybutyrate (PHB) [6]. In addition, *C. necator* is genetically amenable and appropriate genetic tools are available [7,8].

A "Knallgas" mixture in conjunction with CO_2 represents a simple and inexpensive feedstock, but can pose a significant explosion risk in (large-scale) fermenters. Bioelectrochemical systems in which O_2 is replaced by an electrode as terminal electron acceptor offer a promising solution to this problem [9–11]. Such systems could overcome the limitations associated with O_2 solubility and transfer while preventing excessive foaming due to aeration. Moreover, using an electrode as the terminal electron acceptor provides an inexhaustible electron sink, which distinguishes it from molecular electron acceptors in general

Abbreviations: DCIP, 2,6-dichloroindophenole; DHB, 3,4-dihydroxybenzaldehyde; DPV, differential pulse voltammetry; FEC, ferricyanide; HNQ, 2-hydroxy-1, 4-naphtaquinone; MB, methylene blue; MV, methyl viologen; PES, phenazine ethosulfate; PMS, phenazine methosulfate; RES, resazurin; RF, riboflavin; RM, redox mediator.

* Corresponding authors at: Institute of Process Engineering in Life Sciences, Karlsruhe Institute of Technology, Kaiserstraße 12, 76131 Karlsruhe, Germany (D. Holtmann); Institute of Chemistry, Biophysical Chemistry, Technische Universität Berlin, Straße des 17. Juni 135, 10623 Berlin, Germany (S. Frielingsdorf).
E-mail addresses: stefan.frielingsdorf@tu-berlin.de (S. Frielingsdorf), dirk.holtmann@kit.edu (D. Holtmann).

[1] These two authors contributed equally to this work.

https://doi.org/10.1016/j.bioelechem.2024.108694
Received 3 November 2023; Received in revised form 13 March 2024; Accepted 16 March 2024
Available online 18 March 2024

[10]. Microorganisms require an efficient electron transfer mechanism that overcomes the non-conductive cell membranes. This so-called extracellular electron transfer (EET) to and from an electrode can occur via three principal routes. First, certain microorganisms are able to attach directly to the electrode surface and can reversibly transfer electrons between the electrode and the cell via a chain of redox-active proteins that electronically connect the outer membrane and the cytoplasmic membrane. This mechanism is referred to as direct electron transfer (DET) and only happens when cells are in the immediate vicinity of the electrode surface and synthesize special redox-active proteins. *Geobacter sulfurreducens* and *Shewanella oneidensis*, for example, employ this mechanism for the dissimilatory reduction of solid Fe(III) [12,13]. The other two possibilities involve soluble molecular redox shuttles that do not necessarily require outer membrane cytochromes. These can be molecules that are produced by the electrode or the organism and are oxidized/reduced only once (indirect electron transfer, IET). This includes, for example, the electrochemical production of H_2 or O_2, which *C. necator* can then use as electron donor/acceptor [5]. On the other hand, shuttle molecules can be used that can undergo multiple redox cycles and mediate the electron exchange between electrode and organism (mediated electron transfer, MET). Here, shuttle-based electron transfer is not limited to the confined electrode surface, but can occur throughout the entire volume of the bioreactor. Some of these mediators can be produced endogenously by the microorganisms enabling a constant supply of the shuttle molecule [14]. The addition of artificial redox mediators to the culture medium can either support these natural shuttles or enable EET in a non-electrogenic microorganism such as *Pseudomonas putida* [15].

A variety of redox mediators (RM) offer the possibility of facilitating EET between living organisms and an electrode. However, their selection must be carefully made based on factors such as redox potential, molecular interaction site, inhibitory effects, and membrane permeability [16]. Monitoring chromatic properties of the RMs using UV–vis in the bioreactor allows a rapid assessment of the redox properties of the different RMs *in situ* and provides insight on their suitability for efficient microorganism-mediator interaction [15].

Proficient electronic extracellular interaction of *C. necator* with RMs has already been demonstrated. For example, *C. necator* cultures grown on 10 mM fructose showed enhanced aerobic PHB production in the presence the RM poly(2-methacryloyloxyethyl phosphorylcholine-co-vinylferrocene) recycled from an anode [17]. Nevertheless, the achieved current density of ca. 6.5 μA cm^{-2} was very low, since O_2 was introduced as additional electron acceptor into the working electrode chamber. In another approach using neutral red as RM and an applied current of 10 mA, the PHB yield in a bioelectrochemical system (BES) has been increased by cathodic supplementation of electrons [18]. Furthermore, chemolithoautotrophic photo-electro-cultivation has recently been demonstrated by the addition of riboflavin, in which a cathode acts as the sole electron donor [19]. This was even further enhanced in a recent publication by Tu and co-workers [20]. Here, the authors implemented the Mtr electron transfer pathway from *S. oneidensis* together with a *Gloebacter* rhodopsin. The rhodopsin hereby ensures a proton motive force while the Mtr pathway supplies electrons for NAD reduction to drive CO_2 fixation to biomass. Additionally, flavins have been artificially added to further facilitate the electron transfer. However, "anodic respiration", describing the anode acting as a terminal electron acceptor, in the absence of O_2 to mitigate explosion risks of "Knallgas"-fermentation has not yet been demonstrated.

Recent advances suggest that artificial DET may be possible for *C. necator* by introducing conductive pili or flagella-like structures whose conductive properties have been enhanced by increasing their aromaticity [21]. Although this might be a promising strategy, it has been described that *C. necator* is unable to grow stable biofilms necessary for DET [22]. RMs can circumvent this problem since MET does not require biofilm formation.

Anodic respiration in *C. necator* has not been reported so far, and many RMs, including ferricyanide, phenazine methosulfate, or pyocyanin, cannot be added to the cell culture in large quantities because of their inhibitory effect on microorganisms [23,24]. To investigate the applicability of available RMs to *C. necator*, 11 RMs with different redox potentials were characterized in this study for their inhibitory effects on growing *C. necator* cultures. Since the anodic electron transfer should not depend on the type of electron donor and limitations of mass transfer by poorly soluble gases are undesirable, fructose was used as substrate instead of H_2/CO_2 in this study. Four of the most promising RMs were then tested for their ability to support fructose-driven anodic respiration of *C. necator* in a BES.

2. Materials and methods

2.1. Bacterial strains and chemicals

Cupriavidus necator PHB$^-$4 [25] was used in all biotic experiments. All chemicals used for this work were supplied by Merck KGaA (Germany), VWR Chemicals (USA), Carl Roth GmbH & Co. KG (Germany), Alfa Aesar (USA), or Sigma Aldrich (USA). The redox mediators (abbreviation, redox potential *vs.* SHE, purity) used in this study were methyl viologen dichloride·hydrate (MV, −440 mV, 98 %), riboflavin (RF, −208 mV, 98 %), 2-hydroxy-1,4-naphtaquinone (HNQ, −140 mV, 97 %), 1,9-Dimethyl-methylene blue (MB, 11 mV, 80 %), phenazine ethosulfate (PES, 55 mV, >95 %), resazurin sodium salt (RES, 65 mV, 74 %), phenazine methosulfate (PMS, 80 mV, >90 %), 2,6-dichloroindophenole sodium salt hydrate (DCIP, 217 mV, 99 %), 3,4-dihydroxybenzaldehyde (DHB, 402 mV, 97 %), potassium ferricyanide (FEC, 416 V, >98 %), 2,2'-azino-bis(3-ethylbenzothiazoline-6-sulfonic acid) diammonium salt (ABTS, 668 mV, 98 %), neutral red sodium salt (NR, −325 mV, >90 %), methyl red sodium salt (MR, 370 mV, 99 %), and menadione (MEN, 30 mV, >98 %) [26–29].

2.2. Media and culture conditions

C. necator precultures grew in 2.5 mL LB medium (10 g L^{-1} tryptone, 5 g L^{-1} yeast extract, 10 g L^{-1} NaCl) in cultivation tubes at 30 °C and 180 rpm. Cryo stocks were prepared by adding 25 % glycerol to an exponential culture and subsequent freezing at −80 °C. For BES precultures, cryo stocks were first cultivated on LB agar plates (15 g L^{-1} agar) and incubated overnight at 30 °C. Liquid precultures were then prepared by transferring one colony into a baffled 100 mL flask containing 20 mL LB medium. After 24 h, baffled 1 L shake flasks filled with 200 mL MMasy medium were inoculated with the exponential preculture to an OD_{600} of 0.1. MMasy medium contained 4 g L^{-1} fructose as carbon and electron source, 2.895 g L^{-1} Na_2HPO_4, 2.707 g L^{-1} $NaH_2PO_4{\cdot}H_2O$, 0.94 g L^{-1} $(NH_4)_2SO_4$, 0.8 g L^{-1} $MgSO_4{\cdot}7H_2O$, 0.097 g L^{-1} $CaSO_4{\cdot}2H_2O$, 0.17 g L^{-1} K_2SO_4, and 0.1 % (v/v) of trace element solution. The trace element stock solution consisted of 15 g L^{-1} $FeSO_4{\cdot}7H_2O$, 2.4 g L^{-1} $MnSO_4{\cdot}H_2O$, 2.4 g L^{-1} $ZnSO_4{\cdot}7H_2O$, 0.48 g L^{-1} $CuSO_4{\cdot}5H_2O$, 1.8 g L^{-1} $Na_2MoO_4{\cdot}2H_2O$, 1.5 g L^{-1} $Ni_2SO_4{\cdot}6H_2O$, and 0.04 g L^{-1} $CoSO_4{\cdot}7H_2O$ dissolved in 0.1 M HCl [30]. The BES precultures were then incubated in an orbital shaker at 180 rpm (2.5 cm orbit, Multitron, Infors, Bottmingen, Switzerland) for 48 h to ensure the stationary phase was reached before inoculating the reactor.

To test the impact of RM on cell growth, cells were pre-cultured in MMasy medium containing fructose for ~ 24 h until they reached optical density (OD) values of 3.5–4.5 at 600 nm. The cells were washed once with carbon-free MMasy medium and inoculated to an initial OD_{600} of 0.5 in MMasy medium (4 g L^{-1} fructose) for the growth experiment. Cell growth was monitored in 96-well plates (Microtitration plates ROTILABO® F-profile, Carl Roth). Each well contained 150 μL of MMasy medium and serial dilutions of RM. For each experiment, a control culture without RM was included. Breath-Easy® sealing membrane (Sigma-Aldrich) was used to prevent evaporation. The OD was monitored in a SPECTRAmax® 340PC microplate spectrophotometer with

constant shaking and the OD was measured every twelve minutes. To ensure the reliability of obtained OD values, the linearity of the SPECTRAmax® plate reader was confirmed in the range from 0.1 to 1.5.

Interference of the RM absorbance with the OD measurements was avoided by monitoring the OD at a wavelength where the RM absorbance is minimal or absent. The wavelengths used were 470, 600, and 800 nm. In addition, solutions of each RM concentration were included in the measurements to subtract the respective blank values. Since the pathlengths of a standard cuvette (1 cm) and the plate well are different, the plate reader OD values were converted to a pathlength of 1 cm using the factors 2.93 for OD_{600}, 2.45 for OD_{800}, and 3.13 for OD_{470} for the standardized representation of the growth curves. Growth curves shown represent the average of three independent experiments (n = 3). To relate RM concentration to growth rate, the ratio between growth rate in the presence and absence of mediator (μ_i/μ_0) was plotted against the RM concentration.

In the dose–response graph, the IC50 indicates half the maximum inhibitory concentration of inhibitor *I* by fitting the data with an equation based on previous work [31]. Since the data was normalised to relative growth rates in the range from 0 to 1, the equation was simplified as follows (Eq. (1). [*I*] is the concentration of the inhibitor (here the RM), and b is the factor describing the steepness of the linear part of the curve between 0 and 1.

$$\frac{\mu_i}{\mu_0} = \frac{1}{1 + \left(\frac{[I]}{IC50}\right)^b} \quad (1)$$

The reduction of ferricyanide (FEC) was monitored in an independent experiment by measuring absorbance at 420 nm in minimal medium containing 3.75 mM FEC inoculated with cells to an OD_{600} of 0.5. Cell-free minimal medium containing FEC was used for the blank. The resulting absorbance values were converted to 1 cm pathlength by multiplying by a factor of 2.23.

2.3. Bioelectrochemical system

The BES reactor (300 mL working volume, SR0400SS, Eppendorf DASGIP, Germany) was set up as described in detail before [9] but without the sparger. Instead, 99.999 % nitrogen was purged through the reactor headspace at 45 mL min^{-1} throughout the experiment to maintain anoxic conditions. In short, a polished graphite rod, held in place by a PTFE rod, with a length isolated to 80 mm and a diameter of 7 mm (Graphite 24, Germany) was used as working electrode in combination with a stainless-steel mesh electrode (1.4404, mesh size 0.1 mm, wire diameter 0.065 mm, Jaera GmbH + Co.KG, Germany) with a geometrical surface area of 20 cm^2 as a counter electrode. The anodic and cathodic compartment were separated from each other with a cation exchange membrane (Nafion117, QuinTech, Germany), while the cathodic compartment is made out of a glass tube with a thread on one side and open on the other side holding 10 mL of cathode buffer (28.95 g L^{-1} Na_2HPO_4, 27.07 g L^{-1} $NaH_2PO_4{\cdot}H_2O$). As anodic buffer, MMasy medium was used with 4 g L^{-1} fructose as substrate. The applied potential was controlled via a multi-channel potentiostat (MultiEmStat3+, PalmSens, Netherlands) and Ag/AgCl (satd. KCl) reference electrodes (Xylem Analytics, Germany). Additionally, the reactors were covered in aluminium foil to exclude light-induced decomposition of the RMs. Phenazine methosulfate (PMS) and ferricyanide (FEC) were added to the reactor medium as concentrated stock solutions. 2-hydroxynapthaquinone (HNQ) and 2,6-dichloroindophenole (DCIP) are less soluble in aqueous media and were therefore dissolved directly in the minimal medium. An anodic overpotential of approximately 200 mV above the oxidation potential of the respective RM was applied to ensure sufficient driving force for mediator oxidation, resulting in the following applied voltages: 697 mV for FEC, 497 mV for DCIP, 297 mV for PMS, and 197 mV for HNQ. The potentiostat used could not compensate for the ohmic drop due to the resistance between the working and reference electrode. Nevertheless, the estimated resistance values of 8 to 24 Ω in each reactor, determined by double potential step amperometry, were negligibly small compared to the applied overpotential. The pH was controlled by pH sensors (Hamilton, Germany) together with Eppendorf DASGIP pH and pump modules, feeding 2.5 M NaOH through the headspace of each reactor. With this, a pH of 6.8 was kept in the anodic compartment, while the cathodic chamber is uncontrolled.

2.4. Analytics

Culture samples were withdrawn from the reactors and centrifuged at 16,900 x g and 4 °C for 5 min. The resulting supernatant was further filtered through a 0.2 μm PTFE filter for HPLC analysis. Fructose concentrations were determined using an Agilent 1200 high-performance liquid chromatography system in combination with an Aminex HPX-87H column (Bio-Rad Laboratories GmbH, Germany) and a refractive index detector at 32 °C. The column was heated to 50 °C, and 5 mM H_2SO_4 at a flow rate of 0.5 mL min^{-1} was used to isocratically elute the analytes. Fructose standards were measured at seven concentrations between 0.1 and 4 g L^{-1}, and the corresponding peak area fitted by linear regression (Figure S1).

The cell dry weight was determined by first centrifuging the entire culture volume of the reactor at 4 °C and 3214 x g (Centrifuge 5810 R, Eppendorf, Germany). The cell pellet was washed twice in pure water to remove media components. Finally, the washed cells were weighed on a scale equipped with a heating element (KP-7291, Kern, Germany) until no water loss was measurable.

2.5. Mediator concentration and redox state

RM concentrations in the BES were determined by absorbance measurements as previously described [9] at wavelengths 420 and 320 nm for FEC, 383 nm for PMS, 452 nm for HNQ, and 607 nm for DCIP. Calibration was performed with 7 different concentrations at the characteristic wavelength of the respective mediator (Figure S2).

2.6. Electrochemical analysis and calculations

The midpoint potential (E_m) was determined as the average of anodic and cathodic peak potentials using the equation $E_m = (E_{ox} + E_{red})/2$. Total mediator turnover number (TTN) and coulombic efficiency (CE) in the BES were calculated as previously described [9] with the formula $TTN = Q_{anode}/(F{*}M_{mediator}{*}z_{mediator})$. With Q as the total charge transferred to the anode from the inoculation until the end of the experiment in coulomb, F being Faraday's constant (96485.3365C mol^{-1}), $M_{mediator}$ the absolute amount of mediator molecules in mol, and $z_{mediator}$ the number of electrons that can be transferred by the mediator in one cycle.

The uncompensated resistance (R_u) between the working and reference electrodes of the BES reactors was determined via a double potential step chronoamperometry. Here, a potential step of 100 mV was applied after a 10 s offset polarisation. The initial current of the potential step was used to calculate the R_u via Ohm's law. Differential pulse voltammetry (DPV) was carried out in the BES reactors with 50 mV pulses for 300 ms between −800 and 600 mV *vs.* Ag/AgCl (saturated KCl).

3. Results and discussion

3.1. Redox mediator impact on growth

To determine the appropriate RM concentrations for the application in a BES, the impact of redox mediators on cell growth was first evaluated. The mediators were chosen based on their redox potential in the physiological range of −440 to + 668 mV, which allows both cathodic electrosynthesis and anodic respiration within a BES. In this study, all

redox potentials are given against the standard hydrogen electrode (SHE). Neutral red, methylene red, and menadione could not be analysed, because of their poor solubility in aqueous solutions and, for the same reason, not more than 90 μM of RF could be tested.

In the case of methylene blue, it was not possible to reliably determine the inhibitory concentration for growth as growth curves lack completely the lag phase typically observed, and the cultures reached an optical density (OD) of 1 in less than forty minutes, much faster than the control culture without MB (Figure S3). Interestingly, this behaviour was more pronounced with increasing MB concentrations. This could imply a benefit for the cells, e.g. through additional respiratory capacity due to MB reduction. However, since MB has been shown to be toxic for certain bacteria [32], the OD increase might even be caused by cell lysis and would thus not be based on cell number.

Initial experiments to determine if the initial OD of the culture after inoculation affects the tolerance of the cells to the RM were performed. *C. necator* cell cultures inoculated at an OD 0.5 were found to tolerate higher RM concentrations than cultures inoculated at OD 0.1. This behaviour was confirmed for FEC and DCIP but was not studied for all mediators. Cells inoculated at an initial OD of 0.5 grow vigorously in the presence of 15 mM FEC (Figure S4), whereas no growth was observed for cells inoculated at an OD of 0.1. In the case of DCIP, growth was observed for cells inoculated at an OD 0.5 in the presence of 2 mM RM, whereas significant growth was noted for cells inoculated at OD 0.1 only at 500 μM RM (Figure S4). Based on these results, it can be assumed that for the same mediator concentration, lower cell concentrations are more affected as each cell is exposed to a larger number of mediator molecules compared to higher ODs. Hence, we decided to analyze the growth inhibition by RM at an initial OD of 0.5, since even higher cell densities should be used in BES, but cannot be tested photometrically *in situ* due to the limited linearity of the light scattering measurements.

To ensure that no substrate limitation occurred during the growth experiment, it was first examined in the plate reader which substrate concentration was sufficient by testing the fructose concentrations in minimal medium of 2 g L^{-1}, 4 g L^{-1}, and 8 g L^{-1} (Figure S5). A concentration of 4 g L^{-1} turned out to be not limiting and although 2 g L^{-1} fructose were already sufficient to achieve an OD (at 600 nm) of 1.2, the growth experiments were carried out at a concentration of 4 g L^{-1} fructose to comply with the medium composition developed by Sydow et al. for *C. necator* in BES [30].

In another control experiment, we checked if the redox mediators were quantitatively reduced under aerobic growth conditions. Since most reduced RMs are immediately re-oxidized by O_2 [33–37], ferricyanide was used for this assay, since its reduced form ferrocyanide is only slowly re-oxidized under aerobic conditions [35,38]. Therefore, the characteristic absorbance of FEC at 420 nm was used to monitor its reduction while tracking the cell density [9]. Right at the start of the experiment, a significant decrease in absorbance at 420 nm was observed (Figure S6), showing that ferricyanide was reduced by the cells even in presence of O_2. Thus, the cells reduce the redox mediator in parallel with O_2 respiration.

The experiments on the inhibition of cell growth revealed that the presence of a RM usually affects the lag phase, growth rate, and/or the rate of reaching the stationary phase (Figure S3). Of the mediators tested, ABTS had the least impact, as the cell culture in the presence of 5 mM ABTS exhibited a lag phase and growth rate similar to that of the control. FEC, ABTS and RES were the RMs that could be used at the highest concentrations at 15 mM, 10 mM, and 10 mM, respectively. In the case of ABTS and RES, the limiting factor was their solubility in the minimal medium rather than their inhibitory effect to cells.

To better compare the relationship between mediator concentration and growth rate, relative growth rates μ_i/μ_0 were plotted against the inhibitor (RM) concentration in Figure 1, where μ_i is the "inhibited" growth rate in the presence of RM and μ_0 is the growth rate of the control culture without RM.

In cases where the increase of RM concentration clearly affected the growth rate (Figure 1 a, b, c, d, e, f, g, h, and i), the half-maximal inhibitor concentration (IC50) could be determined (Figure S7). The found IC50 values, the RM concentrations that had no or minimal effect on cell growth and the highest tested concentration that still allowed decent growth are summarised in Table 1.

3.2. Mediated anodic respiration in a BES reactor

The RMs FEC, DCIP, HNQ, and PMS, were selected for anodic respiration of *C. necator* in the following BES experiments, covering a wide range of redox potentials from E_m = -137 mV (HNQ) to 416 mV (FEC). An interaction of *C. necator* with HNQ would provide valuable insight into the lower limit of redox potentials that a mediator can possess to still accept electrons from the organism. FEC, on the other hand, is a promising artificial RM that is frequently used with gram-negative bacteria [15,39]. Phenazines are often used as natural RMs [14,40] and can be produced by the cells within the BES. DCIP has a very high affinity for organic phases [29], which should promote membrane permeability. Here, 15 mM FEC was used to maximize availability of shuttle molecules without inhibiting *C. necator* too much (Table 1). A similar principle was used with PMS (390 μM), and HNQ (1.25 mM). DCIP was used at a concentration of 80 μM, at which biocompatibility should be ensured.

Fig. 2 (a) shows the current densities recorded with the 4 different mediators over the entire BES experiment. After inoculation with the *C. necator* preculture at t = 0 h, the current density showed an immediate increase. The maximum current density achieved with FEC surpassed that of the other RMs by 10-fold, reaching 260.75 μA cm^{-2} after 15.8 h. In comparison, DCIP resulted in a maximum current density of 21.67 μA cm^{-2}, while PMS delivered 12.14 μA cm^{-2}, and HNQ 28.85 μA cm^{-2}. With FEC, DCIP, and PMS, the current density peaked at about 24 h, which subsequently decreased significantly. In the case of PMS, the current density eventually returned to the abiotic baseline level after approximately 124 h. In contrast, a stable current density was achieved with HNQ throughout the cultivation period.

Anodic current from HNQ was not expected due to the low E_m of −137 mV of the mediator. Comparison with the redox potentials of potential molecular interaction sites for the RM suggests that HNQ can accept electrons directly from NADH (E_m = −320 mV), FMN/FAD (E_m = -219 mV), or periplasmic hydrogenases (E_m = −414 mV for the reaction $H_2 \rightarrow 2H^+ + 2e^-$), whereas menaquinone and ubiquinone have higher E_m of −74 and 90 mV, respectively [41,42]. However, it is not yet clear whether HNQ can penetrate the outer and even the cytoplasmic membrane to reach NADH as a reaction partner. For the Gram-positive *Staphylococcus aureus*, unmodified HNQ was shown not to alter the membrane integrity. Furthermore, the calculated log*P* values between 1.2 and −1.7 indicate that HNQ is not very lipophilic, implying that membrane transfer is less likely to occur [43]. Consequently, periplasmic interaction sites accessible through outer membrane porins are most likely the target of HNQ. Among these, membrane bound [NiFe]-hydrogenase (MBH) and respiratory chain complexes (ranging from −320 to 820 mV) are possible interaction partners in terms of their redox potentials. The nitrate respiration pathway can be ruled out due to the high redox potential of 420 mV for the nitrate/nitrite couple [44]. At this potential, however, FEC (E_m = 416 mV) could interact with nitrate reductase. This could also explain why the highest current density is obtained with FEC, as this mediator may also interact with other components of the respiratory chain(s) in addition to nitrate reductase. It should also be noted that *C. necator* may not synthesize the nitrate respiration machinery until later in the experiment since the preculture for inoculation was grown aerobically. Nevertheless, the possibility of multiple interaction sites could be crucial for FEC to achieve high current densities due to its relatively high redox potential in combination with its high solubility.

DCIP and PMS are likely to be membrane permeable due to their lipophilic properties [29,45]. The corresponding interaction could be

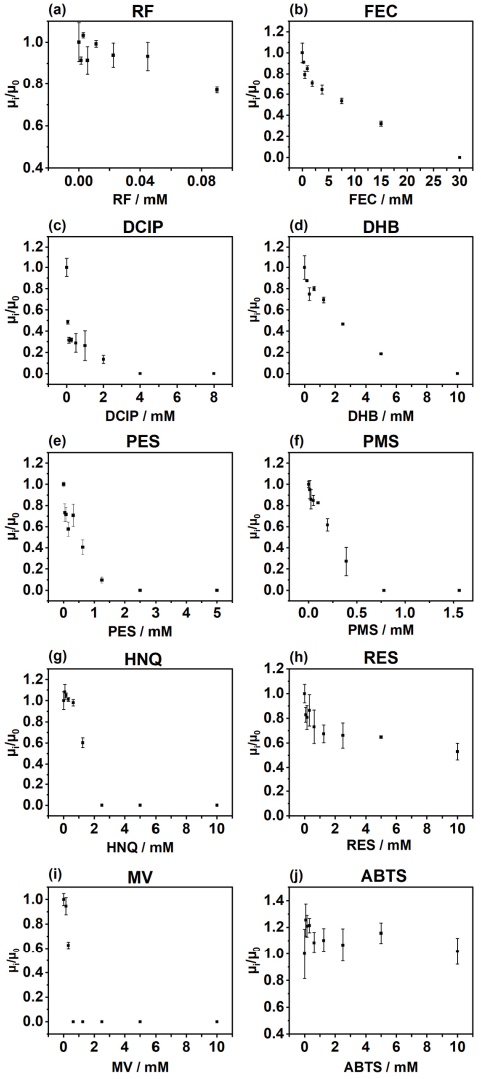

Fig. 1. Analysis of different RMs for their inhibitory effects on *C. necator* growth rates. The relative growth rate μ_i/μ_0 is plotted *vs.* RM concentration. *C. necator* was cultivated in minimal medium in the presence or absence of each RM. The corresponding growth curves are depicted in Figure S3. The redox mediators employed were (a) riboflavin (RF), (b) ferricyanide (FEC), (c) 2,6-dichloroindophenole (DCIP), (d) 3,4-dihydroxybenzaldehyde (DHB), (e) phenazine ethosulfate (PES), (f) phenazine methosulfate (PMS), (g) 2-hydroxynapthaquinone (HNQ), (h) resazurin (RES), (i) methyl viologen (MV), and (j) 2,2'-azino-bis(3-ethylbenzothiazoline-6-sulfonic acid) (ABTS).

Table 1
Mediator concentrations with (A) minimal impact on cell growth, (B) the highest tolerated mediator concentrations, and (C) values of IC50.

Redox mediator	A		B		C
	RM[a] [mM]	Growth rate[c,d] [h^{-1}]	RM[b] [mM]	Growth rate[c,d] [h^{-1}]	IC50 [mM]
Methyl viologen (MV)	0.156	0.247	0.313	0.163	0.33
Riboflavin (RF)	0.045	0.281	0.090	0.232	184.30
2-hydroxy-1,4-naphtaquinone (HNQ)	0.313	0.257	1.25	0.153	1.32
Methylene blue (MB)[e,f]	ND	ND	ND	ND	ND
Resazurin (RES)	0.313	0.237	10	0.144	54.21
Phenazine ethosulfate (PES)	0.040	0.235	1.25	0.032	0.28
Phenazine methosulfate (PMS)	0.025	0.200	0.390	0.063	0.22
2,6-dichloroindophenole (DCIP)	0.063	0.119	2	0.033	0.05
3,4-dihydroxybenzaldehyde (DHB)	0.625	0.225	5	0.052	1.83
Ferricyanide (FEC)	0.470	0.239	15	0.096	5.70
2,2′-azino-bis(3-ethylbenzothiazoline-6-sulfonic acid) (ABTS)[f]	5	0.214	10	0.189	ND

[a] RM concentrations at which the impact on cell growth was minimal. The qualitative evaluation is based on the similarity between mediator-containing cultures and control cultures for growth rate, lag phase, and the rate of reaching the stationary phase.
[b] RM concentrations relevant for the BES experiments where *C. necator* cells are used that are in the stationary phase, cell growth is not to be expected, and high RM concentrations allow efficient electron transfer between the cells and the anode.
[c] The average growth rate of the control cultures without RM was $0.252 \pm 0.046\ h^{-1}$.
[d] The mean of three individual measurements is given (n 3).
[e] The growth rates in the presence of MB could not be determined (ND – not determined, see text for details).
[f] The IC50 could not be determined (ND – not determined, see text for details).

anything below the E_m of DCIP/PMS. Studies with *Dehalococcoides ethenogenes* have suggested a possible interaction of PMS with the periplasmic hydrogenase [46], whereas in the case of *Saccharomyces cerevisiae* and *S. aureus* an interaction of DCIP with complex III and I of the respiratory chain has been proposed [45,47]. The obtained current density curves indicate that the overall electron transfer to the anode lags well behind that of FEC (Fig. 2 (a)). Nevertheless, the reduction of DCIP within the reactor could even be observed visually. When the cells were added to the reactor, the colour of DCIP changed from an intense blue to colourless, indicating its reduction by the cells (Figure S8). This observation hints to a possible limitation in the re-oxidation of DCIP by the anode. The use of different anode materials in future experiments could improve the interaction of mediator and anode.

The coulombic efficiency (CE) was calculated to determine the percentage of electrons transferred from the electron donor fructose to the anode (electron acceptor). A CE of 64.1 % for FEC (Table S1) indicates that 64.1 % of the available electrons from fructose were transferred to the anode. In contrast, only 11.9 % of the available electrons were transferred with HNQ. For DCIP and PMS, the fructose consumption was too low to reliably determine CEs. The remaining percentage of released electrons in the FEC and HNQ reactors that were not transferred to the anode can be attributed to undetermined metabolites on the one hand, and possible biomass accumulation in the first hours after inoculation on the other (Fig. 2 (b)). The reduced mediator molecules present in the medium, which have not yet been reoxidized at the end of cultivation, represent a further electron sink. A periplasmic sugar oxidation pathway, as reported for *P. putida* [15], is not known for *C. necator* and can therefore not be used as the cause of the high CE.

Our results show, that of the 4 RMs compared, anodic respiration of *C. necator* was most efficient with FEC, as it diverts the highest percentage of electrons to the anode. Thus, if the objective is to produce an oxidized product through unbalanced fermentation, similar to what was done previously for acetoin by *S. oneidensis* [48], FEC might be a preferable choice rather than HNQ. In contrast, the latter might offer a better option for production of reduced compounds as more electrons are available for metabolism.

Fructose consumption (Fig. 2 (c)) clearly indicates that *C. necator* showed detectable metabolic activity within the anaerobic BES only with FEC and HNQ. In contrast, *C. necator* did not show significant fructose consumption with either PMS or DCIP. Instead, the fructose concentration slightly increased, possibly as a result of evaporation with a determined rate of 0.15 mL h^{-1}. However, even with FEC and HNQ, the fructose uptake rate was low over 195 h of cultivation. Within the first 24 h, the highest uptake rate was 4.42 and 3.72 mg L^{-1} h^{-1} for FEC and HNQ, respectively. Between 24 and 96 h, the rates decreased to 2.81 and 1.53 mg L^{-1} h^{-1}, respectively, until the rates for both RMs were less than 0.67 mg L^{-1} h^{-1} after 120 h (Figure S9).

Simultaneously with the increase in current density, the cathodic pH in the reactor with FEC shifted to more basic values. This shift is a consequence of the intense proton consumption caused by the cathodic hydrogen evolution reaction (Fig. 2 (d)). Theoretically, oxygen reduction would be thermodynamically more favourable at the cathode, but due to the lack of stirring in the cathode compartment, oxygen transfer to the cathode was diffusion-limited. It is therefore conceivable that the cathodic pH limits the electrochemical reaction, since a large pH difference between anodic- and cathodic electrolyte lowers the cell voltage according to the Nernst equation [49]. However, a limited re-oxidation of FEC due to an increased cell potential was not observed in our experiment. The opposite was the case, since the mediator was constantly oxidized at the anode (Fig. 3 (a)). Therefore, the cathode reaction probably did not limit the process of anodic respiration with FEC as mediator. However, the reason why the anodic current was restricted to 260.75 μA cm^{-2} after 12 h of cultivation remains unclear. The most plausible explanation might be found on the genomic level, since no obvious limitation in the electrochemical setup was observed. This indicates that the observed anodic electron discharge is not able to replace oxygen as electron acceptor to enable growth.

The cell density was recorded during the cultivation by OD_{600} measurements. As DCIP has an absorption maximum at 607 nm, OD_{700} was used in this particular case. From Fig. 2 (b) it can be recognized that the cell density of the FEC culture slightly increases in the phase of increase of the current density and showed a downward trend after 48 h. This downward trend was also observed for the PMS and HNQ cultures, while the DCIP culture showed a stable cell density. It should be noted that these results are based on single reactor runs, which does not allow statistical conclusions to be drawn. After cultivation, planktonic cells were harvested, dried, and the resulting dry weight confirmed the optical density data, indicating that the FEC reactor ended up with significantly less biomass compared to the other reactors (Table S1). One reason for this might be that the cells aggregated and attached between the cathode compartment lid and the reactor wall (Figure S10).

Since RMs were introduced into the medium at different

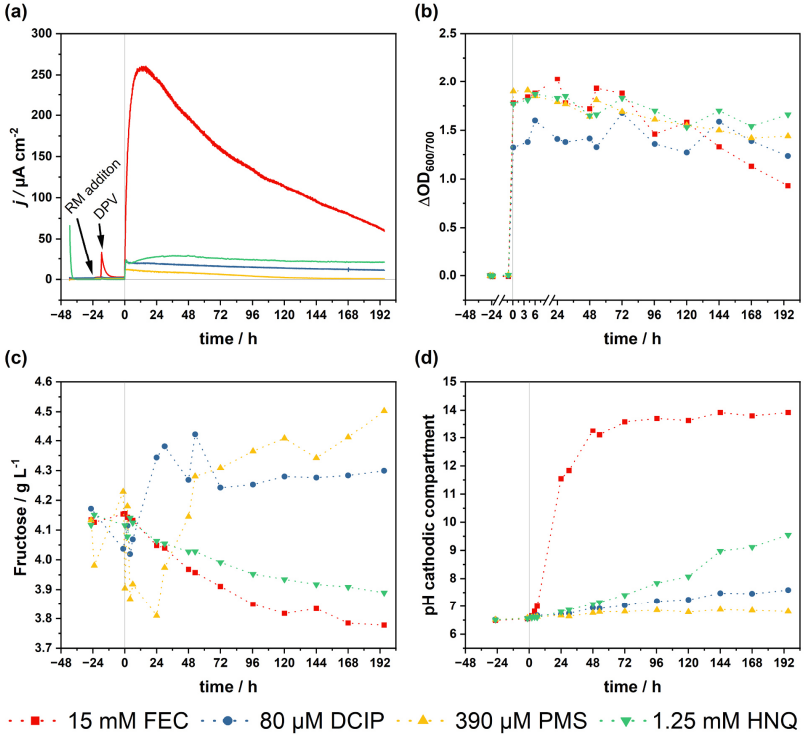

Fig. 2. Anodic respiration of *C. necator* with FEC (red), DCIP (blue), PMS (yellow), and HNQ (green) as mediators. (a) Current density during fermentation. The addition of FEC and PMS as well as the DPV measurement, which resulted in a current peak in the chronoamperometric measurement, are marked by arrows. (b) Cell density determined by OD measurement. (c) Fructose concentration determined by HPLC. (d) pH values in the cathodic compartment. Conditions: Applied anodic potential: FEC, 697 mV; DCIP, 497 mV; PMS, 297 mV; HNQ, 197 mV. 300 mL minimal medium made anaerobic through flushing the headspace with 45 mL min^{-1} N_2, 400 rpm, 30 °C, n = 1. The inoculate was added at t = 0 h time.

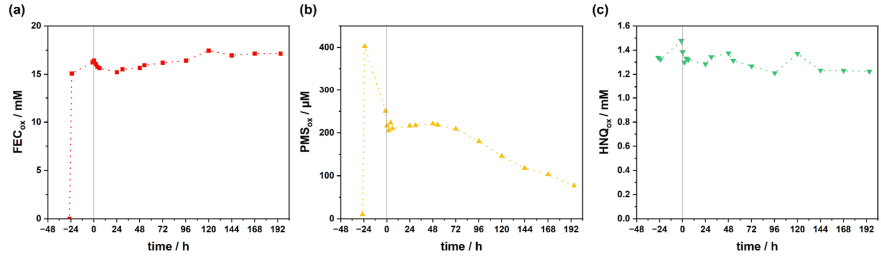

Fig. 3. Concentrations of oxidized RMs during BES cultivation. Culture samples were withdrawn at different time points, centrifuged, and the concentrations of oxidized (a) FEC, (b) PMS, and (c) HNQ in the supernatant were determined spectrophotometrical. FEC and PMS were added 24 h prior to inoculation. Wavelengths: 320/420 nm (FEC), 383 nm (PMS), 452 nm (HNQ). The inoculate was added at t = 0 h time.

concentrations, the calculation of the total turnover number (TTN) provides an opportunity to compare their performance independent of their concentration. After 195 h of cultivation, the TTN was 4.18 for FEC, 41.04 for DCIP, 2.62 for PMS, and 4.13 for HNQ. The total concentration of the individual RMs is taken into account when calculating the TTN. DCIP therefore shows a very high TTN, although the resulting current is comparably low. Interestingly, HNQ achieved the same number of turnovers as FEC even though it was added in a 12-fold lower concentration. However, it is important to consider that not every mediator molecule is constantly shuttling electrons back and forth between the microbe and the electrode. Accordingly, in the case of FEC, it might be possible to use a lower mediator concentration if only a fraction of the RM molecules is reduced by the cells. Optimization of electron transfer efficiency by lowering the mediator concentration should be considered in future experiments.

By utilising the characteristic wavelengths of the oxidized RMs, quantitative offline measurements of the RM pool were conducted during the BES experiments. Cell-free samples were prepared from the reactors and measured spectrophotometrically. Fig. 3 depicts the resulting concentration curves for FEC, PMS, and HNQ. The redox state of the DCIP pool could not be measured with the available equipment, as it re-oxidizes immediately upon contact with air. Reduced PMS is also known to re-oxidize in contact with O_2 at a rate constant of about 180 M $^{1}s^{-1}$ to form the semiquinone, which increases the absorbance at 387 and 440 nm [50]. The subsequent oxidation to fully oxidized PMS proceeds more slowly and shifts the absorbance maximum to 387 nm [51]. The photometric measurement is therefore prone to error and can only show a trend of the oxidation state present in the reactor. Furthermore, PMS is known to decompose upon illumination under anaerobic conditions in equal amounts to reduced PMS and pyocyanine. Pyocyanine can be detected photometrically due to its absorption maximum of about 310 nm [50]. The experimental data show that the absorption at 311 nm indeed increased slightly after the cells were added to the system (Figure S11), suggesting that some degradation occurred even though the reactors were protected from light. The initial RM concentrations determined by absorption measurements, showed slight deviations from the calculated initial concentrations (Fig. 3). One partial reason for this might be the inaccuracy that comes with adding the RMs to the reactors with syringes.

In the case of FEC, after an initial decrease shortly after inoculation, the amount of oxidized FEC steadily increased, even beyond the amount initially added. Reasons for this can only be speculated. Again, a possible factor includes a concentration effect due to evaporation in the reactor. Another possibility might be the accumulation of metabolites in the medium with similar absorption as FEC, which were not detectable with the applied HPLC method. Further investigations are required to understand the reasons for this observation. Nevertheless, the results clearly show that FEC is efficiently re-oxidized at the electrode and thus the availability of oxidized mediator molecules does not limit the overall process. The amount of oxidized HNQ appeared to increase in the first abiotic polarisation phase. This might be due to residual reduced HNQ being oxidized at the anode. After inoculation, the concentration of oxidized HNQ first decreased slightly and then increased again to approximately 1.35 mM after 30 h. Consequently, the concentration of oxidized HNQ remained relatively stable, hovering around 1.25 mM, taking into account the variations of the method. This might imply that only a fraction of the FEC and HNQ pools was reduced by the cells and most of the available mediator molecules remained in the oxidized state. However, it is more likely that the anode re-oxidized the RMs at a relatively high rate, which contributes to the observed concentration patterns. In contrast, PMS appeared to be reduced or degraded in the abiotic phase, the latter being more plausible because of the oxidizing potential applied to the medium and because of the known degradation reaction discussed above. However, pyocyanine was most likely not formed in this reaction, since the absorption at 311 nm remained almost constant in the abiotic phase (Figure S11). After inoculation, the concentration of oxidized PMS appeared to stabilize until it dropped again after 72 h. At the end of the experiment, only 77 μM of oxidized PMS remained.

3.3. *Electrochemical mediator analysis by DPV*

For electrochemical characterization of the RMs during the BES cultivation, DPV (differential pulse voltammetry) measurements were conducted instead of conventional cyclic voltammetry because the former is less susceptible to capacitive currents. Comparison of DPV scans of HNQ and FEC (Fig. 4 (a,d)) in the abiotic and post-biotic phases revealed no significant changes in potential and peak current. Together with the concentrations measured via absorption and the constant current density, it can be concluded that HNQ and FEC are very stable RMs under the applied conditions.

From the current density curve and the spectrophotometric concentration measurement it can be deduced that PMS is not stable over longer time periods, as has already been described for aqueous PMS solutions [52]. The DPV measurements indicate a side reaction of PMS in the BES reactor, as illustrated by a prominent secondary peak at –127 mV in the voltammogram after 195 h of cultivation (Fig. 4 (c)). In contrast, only a single peak at 90 mV was visible for PMS in the abiotic phase. Remarkably, the total peak current did not decrease significantly, although PMS was already degraded/reduced in the first abiotic 24 h according to the absorption measurements. According to DPV, no secondary peak formed during this time period. As discussed before, the anaerobic photodegradation of PMS to pyocyanine is expected to some extent. However, the redox potential of pyocyanine is reported to be –60 mV [26]. Therefore, another degradation product might be present in the solution. Heterologous production of a biological phenazine mediator might therefore be a preferable option for continuous supply of the RM, as previously shown for *P. putida* KT2440 [14].

The DCIP-added culture showed a significantly decreased peak current after 195 h compared to the abiotic phase, indicating a decrease in the amount of electrochemically active molecules in the system, as peak currents correlate with the concentration of the RM (Fig. 4 (b)) [53,54]. This could be due to either RM accumulation within the cells or degradation. Therefore, DCIP may not be suitable for use as the sole mediator over long time periods, but its high TTN could still be useful when combined with a secondary mediator to support electron transfer to the cytoplasmic membrane.

4. Conclusions

Analysis of the inhibitory effect of redox mediators on *C. necator* cell cultures revealed that the higher the initial cell density, the higher the permissible concentration of redox mediators. In case of *C. necator*, FEC, ABTS, and RES are the redox mediators that can be used in larger amounts. However, in some instances, the limited solubility of the RM does not allow for higher concentrations, preventing an adequate analysis of their inhibitory effect.

According to our BES data, FEC appears to be the most promising redox mediator for anodic respiration by *C. necator*. It is stable during the fermentation process, can be used at concentrations up to 15 mM without having a significant inhibitory effect, when stationary cells are used. Furthermore, it does not appear to limit the electrochemical reaction. A stable but low anodic current was achieved with HNQ, which was not to be expected due to its low E_m. As already hypothesized for *P. putida*, the high charge and hydrophilic character of the $[Fe(CN)_6]^{3-}$ molecule most likely prohibits FEC to penetrate the hydrophobic cytoplasmic membrane. Therefore, a possible interaction with periplasmic electron transferring proteins is most likely. The same applies to HNQ until its ability to penetrate the cytoplasmic membrane is demonstrated. PMS and DCIP provided only low current densities, although they have been shown to pass bacterial membranes. However, the lack of fructose consumption of the *C. necator* cultures with PMS and DCIP indicates that

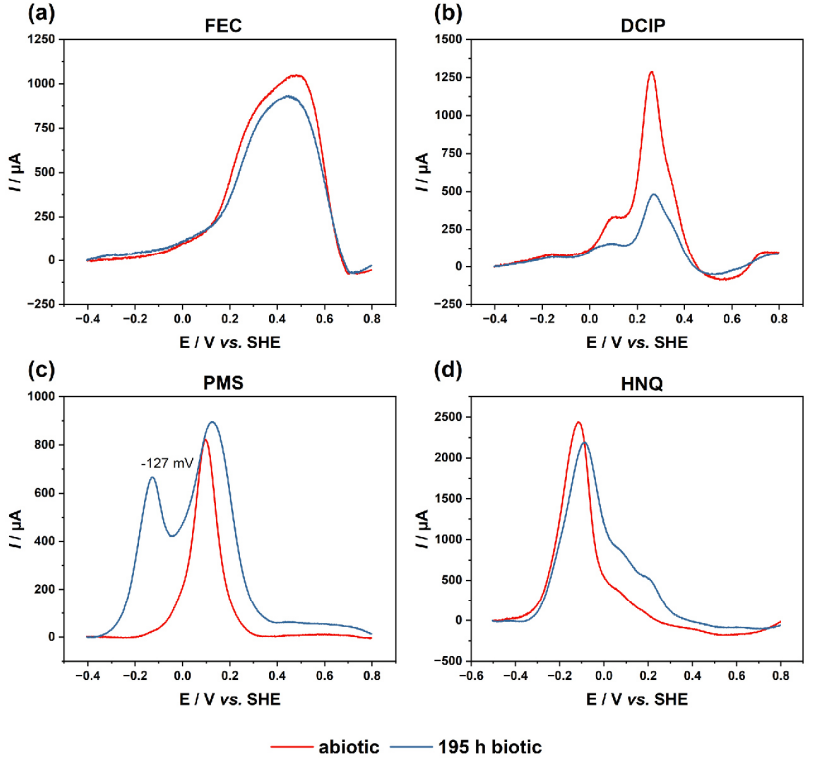

Fig. 4. DPV analysis of the four RMs used in the BES. Measurements were conducted for (a) FEC, (b) DCIP, (c) PMS, and (d) HNQ in the abiotic polarisation phase (red traces) and after 195 h of cultivation (blue traces). The baseline is normalised to an initial current of 0 mA.

neither RM is suitable for BES, and in case of PMS, additional problems arise from constant degradation. Future experiments combining FEC with a redox-compatible RM that can cross the cytoplasmic membrane may even increase the EET capabilities of *C. necator* to achieve 100 % substitution of O_2.

CRediT authorship contribution statement

André Gemünde: Writing – original draft, Visualization, Methodology, Investigation, Data curation. **Elena Rossini:** Writing – original draft, Visualization, Methodology, Investigation, Data curation. **Oliver Lenz:** Writing – review & editing, Project administration, Funding acquisition. **Stefan Frielingsdorf:** Writing – review & editing, Supervision, Project administration, Funding acquisition, Conceptualization. **Dirk Holtmann:** Writing – review & editing, Supervision, Project administration, Funding acquisition, Conceptualization.

Declaration of competing interest

The authors declare that they have no known competing financial interests or personal relationships that could have appeared to influence the work reported in this paper.

Data availability

Data will be made available on request.

Acknowledgements

This work was created as part of the project "Bioelectrochemical and engineering fundamentals to establish electro-biotechnology for biosynthesis – Power to value-added products (eBiotech)", which is funded by the Deutsche Forschungsgemeinschaft (DFG, German Research Foundation) – Project number 422694804. Furthermore, this work was funded by the DFG under Germany's Excellence Strategy – EXC 2008 – 390540038 – UniSysCat.

Appendix A. Supplementary data

Supplementary data to this article can be found online at https://doi.org/10.1016/j.bioelechem.2024.108694.

References

[1] P. Aelterman, K. Rabaey, P. Clauwaert, W. Verstraete, Microbial fuel cells for wastewater treatment, water sci. technol.: j, Int. Assoc. Water Pollut. Res. 54 (2006) 9–15.

[2] R.M. Alonso, M.I. San-Martín, R. Mateos, A. Morán, A. Escapa, Scale-up of bioelectrochemical Systems for Energy Valorization of waste streams, in: Microbial Electrochemical Technologies, CRC Press, 2020, pp. 447–459.

[3] R. Rossi, A.Y. Hur, M.A. Page, A.O. Thomas, J.J. Butkiewicz, D.W. Jones, G. Baek, P.E. Saikaly, D.M. Cropek, B.E. Logan, Pilot scale microbial fuel cells using air cathodes for producing electricity while treating wastewater, Water Res. 215 (2022) 118208.

[4] H. Wohlers, L. Assil-Companioni, D. Holtmann, Chapter 11 cupriavidus necator – a broadly applicable aerobic hydrogen-oxidizing bacterium, in: R. Kourist, S. Schmidt (Eds.), The Autotrophic Biorefinery: Raw Materials from Biotechnology, De Gruyter, 2021, pp. 297–318.

[5] T. Krieg, A. Sydow, S. Faust, I. Huth, D. Holtmann, CO_2 to terpenes: autotrophic and electrosynthetic α-humulene production with cupriavidus necator, Angew. Chem. Int. Ed. Engl. 57 (2018) 1879–1882.

[6] R.R. Dalsasso, F.A. Pavan, S.E. Bordignon, G.M.F. de Aragão, P. Poletto, Polyhydroxybutyrate (PHB) production by cupriavidus necator from sugarcane vinasse and molasses as mixed substrate, Process Biochem. 85 (2019) 12–18.

[7] J. Panich, B. Fong, S.W. Singer, Metabolic engineering of cupriavidus necator H16 for sustainable biofuels from CO2, Trends Biotechnol. 39 (2021) 412–424.

[8] O. Lenz, L. Lauterbach, S. Frielingsdorf, Chapter five - O2-tolerant [NiFe]-hydrogenases of ralstonia eutropha H16: physiology, molecular biology, purification, and biochemical analysis, in: F. Armstrong (Ed.), Methods in Enzymology Enzymes of Energy Technology, Academic Press, 2018, pp. 117–151.

[9] A. Gemünde, J. Gail, D. Holtmann, Anodic respiration of Vibrio natriegens in a bioelectrochemical system, ChemSusChem (2023) e202300181.

[10] I. Vassilev, N.J.H. Averesch, P. Ledezma, M. Kokko, Anodic electro-fermentation: empowering anaerobic production processes via anodic respiration, Biotechnol. Adv. 107728 (2021).

[11] L. Gu, X. Xiao, S. Yup Lee, B. Lai, C. Solem, Superior anodic electro-fermentation by enhancing capacity for extracellular electron transfer, Bioresour. Technol. 389 (2023) 129813.

[12] L. Shi, D.J. Richardson, Z. Wang, S.N. Kerisit, K.M. Rosso, J.M. Zachara, J. K. Fredrickson, The roles of outer membrane cytochromes of shewanella and geobacter in extracellular electron transfer, Environ. Microbiol. Rep. 1 (2009) 220–227.

[13] G. Reguera, K.D. McCarthy, T. Mehta, J.S. Nicoll, M.T. Tuominen, D.R. Lovley, Extracellular electron transfer via microbial nanowires, Nature 435 (2005) 1098–1101.

[14] S. Schmitz, S. Nies, N. Wierckx, L.M. Blank, M.A. Rosenbaum, Engineering mediator-based electroactivity in the obligate aerobic bacterium Pseudomonas putida KT2440, Front. Microbiol. 6 (2015) 284.

[15] B. Lai, S. Yu, P.V. Bernhardt, K. Rabaey, B. Virdis, J.O. Krömer, Anoxic metabolism and biochemical production in Pseudomonas putida F1 driven by a bioelectrochemical system, Biotechnol. Biofuels 9 (2016) 39.

[16] A. Gemünde, B. Lai, L. Pause, J. Krömer, D. Holtmann, Redox mediators in microbial electrochemical systems, ChemElectroChem (2022).

[17] K. Nishio, Y. Kimoto, J. Song, T. Konno, K. Ishihara, S. Kato, K. Hashimoto, S. Nakanishi, Extracellular electron transfer enhances polyhydroxybutyrate productivity in ralstonia eutropha, Environ. Sci. Technol. Lett. 1 (2014) 40–43.

[18] Y.H. Lai, J.-C.-W. Lan, Enhanced polyhydroxybutyrate production through incorporation of a hydrogen fuel cell and electro-fermentation system, Int. J. Hydrogen Energy 46 (2021) 16787–16800.

[19] P.A. Davison, W. Tu, J. Xu, S. Della Valle, I.P. Thompson, C.N. Hunter, W.E. Huang, Engineering a rhodopsin-based photo-Electrosynthetic system in bacteria for CO2 fixation, ACS synth, Biol. 11 (2022) 3805–3816.

[20] W. Tu, J. Xu, I.P. Thompson, W.E. Huang, Engineering artificial photosynthesis based on rhodopsin for CO2 fixation, Nat Commun 14 (2023) 8012.

[21] B. Myers, F. Catrambone, S. Allen, P.J. Hill, K. Kovacs, F.J. Rawson, Engineering nanowires in bacteria to elucidate electron transport structural-functional relationships, Sci. Rep. 13 (2023) 8843.

[22] M.A.D. de Rienzo, I.M. Banat, B. Dolman, J. Winterburn, P.J. Martin, Sophorolipid biosurfactants: possible uses as antibacterial and antibiofilm agent, N, Biotechnol. 32 (2015) 720–726.

[23] C. Liu, T. Sun, Y. Zhai, S. Dong, Evaluation of ferricyanide effects on microorganisms with multi-methods, Talanta 78 (2009) 613–617.

[24] O. Simoska, E.M. Gaffney, K. Lim, K. Beaver, S.D. Minteer, Understanding the properties of phenazine mediators that promote Extracellular electron transfer in Escherichia coli, J. Electrochem. Soc. 168 (2021) 25503.

[25] H.G. Schlegel, R. Lafferty, I. Krauss, The isolation of mutants not accumulating poly-beta-hydroxybutyric acid, Arch. Mikrobiol. 71 (1970) 283–294.

[26] M.L. Fultz, R.A. Durst, Mediator compounds for the electrochemical study of biological redox systems: a compilation, Anal. Chim. Acta 140 (1982) 1–18.

[27] D.H. Park, J.G. Zeikus, Utilization of electrically reduced neutral red by actinobacillus succinogenes: physiological function of neutral red in membrane-driven fumarate reduction and energy conservation, J. Bacteriol. 181 (1999) 2403–2410.

[28] A.H. Förster, S. Beblawy, F. Golitsch, J. Gescher, Electrode-assisted acetoin production in a metabolically engineered Escherichia coli strain, Biotechnol. Biofuels 10 (2017) 65.

[29] F.J. Rawson, A.J. Downard, K.H. Baronian, Electrochemical detection of intracellular and cell membrane redox systems in Saccharomyces cerevisiae, Sci. Rep. 4 (2014) 5216.

[30] A. Sydow, T. Krieg, R. Ulber, D. Holtmann, Growth medium and electrolyte-how to combine the different requirements on the reaction solution in bioelectrochemical systems using cupriavidus necator, Eng. Life Sci. 17 (2017) 781–791.

[31] J.L. Sebaugh, Guidelines for accurate EC50/IC50 estimation, Pharm. Stat. 10 (2011) 128–134.

[32] K. Liu, Y. Luo, L. Hao, J. Chen, Antimicrobial effect of methylene blue in microbiologic culture to diagnose periprosthetic joint infection: an in vitro study, J Orthop Surg Res 17 (2022) 571.

[33] M.A. Thirumurthy, A.K. Jones, Geobacter cytochrome OmcZs binds riboflavin: implications for extracellular electron transfer, Nanotechnology 31 (2020) 124001.

[34] V. Ponti, M.U. Dianzani, K. Cheeseman, T.F. Slater, Studies on the reduction of nitroblue tetrazolium chloride mediated through the action of NADH and phenazine methosulphate, Chem. Biol. Interact. 23 (1978) 281–291.

[35] R. Naumann, D. Mayer, P. Bannasch, Voltammetric measurements of the kinetics of enzymatic reduction of 2, 6-dichlorophenolindophenol in normal and neoplastic hepatocytes using glucose as substrate, Biochim. Biophys. Acta. Mol. Cell. Res. 847 (1985) 96–100.

[36] M. Bahari, M.A. Malmberg, D.M. Brown, S. Hadi Nazari, R.S. Lewis, G.D. Watt, J. N. Harb, Oxidation efficiency of glucose using viologen mediators for glucose fuel cell applications with non-precious anodes, Appl. Energy. 261 (2020) 114382.

[37] S.-A. Ong, E. Toorisaka, M. Hirata, T. Hano, Biodegradation of redox dye methylene blue by up-flow anaerobic sludge blanket reactor, J. Hazard. Mater. 124 (2005) 88–94.

[38] U. Schröder, FUEL CELLS – EXPLORATORY FUEL CELLS | microbial fuel cells, in: J. Garche (Ed.), Encyclopedia of Electrochemical Power Sources, Elsevier, Amsterdam, 2009, pp. 206–216.

[39] P. Ertl, B. Unterladstaetter, K. Bayer, S.R. Mikkelsen, Ferricyanide reduction by Escherichia coli: kinetics, mechanism, and application to the optimization of recombinant fermentations, Anal. Chem. 72 (2000) 4949–4956.

[40] A. Chukwubuikem, C. Berger, A. Mady, M.A. Rosenbaum, Role of phenazine-enzyme physiology for current generation in a bioelectrochemical system, Microb. Biotechnol. (2021).

[41] K.I. Takamiya, P.L. Dutton, Ubiquinone in Rhodopseudomonas sphaeroides. some thermodynamic properties, Biochim. Biophys. Acta 546 (1979) 1–16.

[42] T.D. Harrington, V.N. Tran, A. Mohamed, R. Renslow, S. Biria, L. Orfe, D.R. Call, H. Beyenal, The mechanism of neutral red-mediated microbial electrosynthesis in Escherichia coli: menaquinone reduction, Bioresour. Technol. 192 (2015) 689–695.

[43] R. Song, B. Yu, D. Friedrich, J. Li, H. Shen, H. Krautscheid, S.D. Huang, M.-H. Kim, Naphthoquinone-derivative as a synthetic compound to overcome the antibiotic resistance of methicillin-resistant S. aureus, Commun. Biol. 3 (2020) 529.

[44] B.C. Berks, S.J. Ferguson, J.W. Moir, D.J. Richardson, Enzymes and associated electron transport systems that catalyse the respiratory reduction of nitrogen oxides and oxyanions, Biochim. Biophys. Acta 1232 (1995) 97–173.

[45] R.Y.A. Hassan, U. Wollenberger, Mediated bioelectrochemical system for biosensing the cell viability of Staphylococcus aureus, Anal. Bioanal. Chem. 408 (2016) 579–587.

[46] I. Nijenhuis, S.H. Zinder, Characterization of hydrogenase and reductive dehalogenase activities of dehalococcoides ethenogenes strain 195, Appl. Environ. Microbiol. 71 (2005) 1664–1667.

[47] J. Zhao, Z. Wang, C. Fu, M. Wang, Q. He, The mediated electrochemical method for rapid fermentation ability assessment, Electroanalysis 20 (2008) 1587–1592.

[48] T. Bursac, J.A. Gralnick, J. Gescher, Acetoin production via unbalanced fermentation in shewanella oneidensis, Biotechnol. Bioeng. 114 (2017) 1283–1289.

[49] R.A. Rozendal, H.V.M. Hamelers, R.J. Molenkamp, C.J.N. Buisman, Performance of single chamber biocatalyzed electrolysis with different types of ion exchange membranes, Water Res. 41 (2007) 1984–1994.

[50] F.G. Halaka, G.T. Babcock, J.L. Dye, Properties of 5-methylphenazinium methyl sulfate. reaction of the oxidized form with NADH and of the reduced form with oxygen, J. Biol. Chem. 257 (1982) 1458–1461.

[51] W.S. Zaugg, Spectroscopic Characteristics and some chemical properties of N-methylphenazinium methyl sulfate (phenazine methosulfate) and pyocyanine at the semiquinoid oxidation level, J. Biol. Chem. 239 (1964) 3964–3970.

[52] R. Ghosh, J.R. Quayle, Phenazine ethosulfate as a preferred electron acceptor to phenazine methosulfate in dye-linked enzyme assays, Anal. Biochem. 99 (1979) 112–117.

[53] L.E. Leon, D.T. Sawyer, Simultaneous determination of iron(II) and iron(III) at micromolar concentrations by differential pulse polarography, Anal. Chem. 53 (1981) 706–709.

[54] K.J. Stutts, M.A. Dayton, R.M. Wightman, Integration of differential pulse voltammograms for concentration measurements, Anal. Chem. 54 (1982) 995–998.

A.6 Publication VI

André Gemünde, Nils-Lennart Ruppert, and Dirk Holtmann

Unraveling the Electron Transfer in *Cupriavidus necator* - Insights into Mediator Reduction Mechanics

In *ChemElectroChem*, Volume 11, 2024
DOI: 10.1002/celc.202400273

Contribution: My contribution to the work was the experiment design and setup, the conceptualization, and the supervision of the experimental work performed by Nils-Lennart Ruppert, who carried out the NPN assays. Furthermore, I wrote the original manuscript.

Check for updates

ChemElectroChem

Research Article
doi.org/10.1002/celc.202400273

Chemistry Europe
European Chemical Societies Publishing

www.chemelectrochem.org

Unraveling the Electron Transfer in *Cupriavidus necator* – Insights Into Mediator Reduction Mechanics

André Gemünde,[a] Nils-Lennart Ruppert,[a] and Dirk Holtmann*[a, b]

Cupriavidus necator, despite lacking direct electron transfer capabilities, demonstrates efficient reduction of various redox mediators in oxygen-free cultivation within bioelectrochemical systems. This study investigates the reduction site of ferricyanide through inhibition and expression rate analysis of oxygen and nitrate respiration chain complexes, comparing aerobic cultivation conditions with fructose as carbon and electron donor to autotrophic (CO_2/H_2/O_2) and anodic cultivation conditions (fructose/anode). Azide inhibition identified cytochrome c oxidase as the primary complex facilitating electron transfer to ferricyanide, with a secondary role proposed for nitrite reductase NirS, demonstrating a 3.9±1.1-fold higher expression when exposed to anodic conditions. The 2.9±0.6-fold increase in the expression of the natural porin OmpA under anodic conditions implies its potential involvement in ferricyanide uptake. Additionally, chemically permeabilizing cell membranes with cetyltrimethylammonium bromide doubles ferricyanide reduction rates without an anode present, offering insights for optimizing redox mediation in *C. necator* based bioelectrochemical systems. This study opens up new possibilities for the targeted optimization of mediated electron transfer in *C. necator* and other organisms.

Introduction

To develop sustainable biotechnological applications, the utilization of microorganisms capable of efficient CO_2 conversion has raised immense interest. Among these, *Cupriavidus necator* emerged as a promising strain for chemolithoautotrophic and chemoorganotrophic cultivation, demonstrating its potential as a capable producer of polyhydroxyalkanoates as biological polymer alternative,[1] terpenes as a basis for fragrances and advanced biofuels,[2–4] precursors for aroma components like ferulic acid,[5] and branched-chain alcohols (isobutanol and 3-methyl-1-butanol) as alternative biofuels.[6] The genetic accessibility further allows for even more products to be integrated for industrial-scale production.[7] When fed with CO_2 and H_2, *C. necator* is able to fix the carbon through the Calvin-Benson-Bassham cycle and acquires electrons through the oxidation of H_2 via its soluble hydrogenase. On the electron acceptor side, *C. necator* proves to be respiratory flexible, as it can naturally rely on two different terminal electron acceptors, NO_3^- and O_2. However, with NO_3^- as the terminal electron acceptor, the growth rate is greatly reduced.[8] Most of the nitrate respiration as well as the hydrogen oxidation genes are located on the pHG1 megaplasmid. The pHG1 plasmid further contains 429 potential genes including the CO_2 fixation enzymes and cytochrome c maturation genes.[9] While the prospects of utilizing this strain in chemolithoautotrophic cultivation systems for CO_2 fixation and industrial-scale production are encouraging, challenges persist, particularly concerning explosion risks of H_2/O_2 gas mixtures and operation costs from O_2 transfer into the cultivation medium. With the use of microbial electrochemical technologies, these challenges might be addressed through anodic electron discharge. Hereby, an anode offers the possibility to act as terminal and inexhaustible electron acceptor for *C. necator* instead of O_2.

However, one major obstacle when using bioelectrochemical systems often lies in the lack of a detailed understanding of the electron transfer mechanisms. This also applies to *C. necator*. The proteome of *C. necator* provides no known genes enabling a direct extracellular electron transfer (DET). Nevertheless, using a mediated extracellular electron transfer (MET), electron transfer between planktonic cells and an electrode can still be established. It has already been recognized, that *C. necator* can interact with ferricyanide and various other mediators.[10–13] The specific interaction site that engages with ferricyanide or any other mediator in *C. necator* still remains unclear. The MET process has further been demonstrated with the polymeric redox mediator poly(2-methacryloyloxyethyl phosphorylcholine-co-vinylferrocene) in the presence of oxygen as the main electron acceptor.[10] Here, an upregulation of three nitrate reductases was detected, indicating their potential role in MET. Another study used neutral red to supply electrons in the opposite direction from a cathode to *C. necator*,[11] but the study lacks a clear definition of the mediator interaction site.

The determination of the interaction sites for various redox mediators in other organisms has yet been challenging. So far,

[a] A. Gemünde, N.-L. Ruppert, Prof. D. Holtmann
Institute of Bioprocess Engineering and Pharmaceutical Technology and Competence Centre for Sustainable Engineering and Environmental Systems
University of Applied Sciences Mittelhessen
35390 Giessen, Germany

[b] Prof. D. Holtmann
Institute of Process Engineering in Life Sciences
Karlsruhe Institute of Technology
76131 Karlsruhe, Germany
E-mail: dirk.holtmann@kit.edu

Supporting information for this article is available on the WWW under https://doi.org/10.1002/celc.202400273

inhibition results with antimycin A and azide hint towards cytochrome c reductase as the interaction site of the mediators ferricyanide and tris(2,2′-bipyridyl)cobalt(III) in *Pseudomonas putida* KT2440.[14] In *Lactococcus lactis*, the endogenous mediator 2-amino-3-carboxy-1,4-naphthoquinone accepts electrons from the type II NADH dehydrogenase (NoxAB) which then reduces ferricyanide in the periplasm or extracellular.[15] Adding to the complexity, various mediators may interact with different interaction sites. As an example, the lipophilic compound 2,6-dichlorphenolindophenol (DCIP) can accept electrons directly from complex I of the respiration chain in *Staphylococcus aureus*,[16] while neutral red can penetrate both membranes and most likely reduces NAD^+ directly in the cytosol.[17]

In *C. necator*, the so far reached current densities via MET are insufficient to replace O_2 entirely.[12] Therefore, methods to enhance mediator reduction rates are needed. A significant bottleneck for MET is the cell membrane itself. Theoretically, its lipophilic characteristics pose a disadvantage for numerous hydrophilic or charged mediators, preventing their passage. However, it has been demonstrated, that some hydrophilic redox mediators, like ferricyanide,[14,18] can penetrate the outer membrane of Gram-negative bacteria while lipophilic mediators can most likely pass both membranes.[19] The uptake mechanisms are still barely known and further research is needed. It is conceivable though, that outer membrane porins, like OmpF in *P. putida*, play an important role in the uptake of hydrophilic, charged mediators.[18]

In this context, our study aims to elucidate the interaction sites of ferricyanide within *C. necator* using fructose as electron and carbon donor and an anode as the only available terminal electron acceptor. Hypothesized interaction sites are narrowed down through inhibition studies, qPCR analysis, and the use of a pHG1 megaplasmid deficient strain (Illustrated in Scheme 1). Additionally, our objective is to optimize MET by increasing mediator membrane transfer as a potential bottleneck. In this preliminary investigation, our research is focused on understanding the involvement of key cellular components in MET, particularly in the context of ferricyanide reduction. Additionally, our study explored the permeabilization of cellular membranes to gain insights into potential strategies for enhancing electron transfer efficiency

Results and Discussion

Reduction of Ferricyanide in a BES

In this study, a BES reactor system with ferricyanide as a redox mediator was used to elucidate the mediated electron transfer mechanisms within *C. necator*. A PHB deficient strain (*C. necator* PHB^-) was used primarily to eliminate side effects from stored metabolic reserves. As a benchmark with 5 mM ferricyanide and an anode poised at 500 mV *vs.* Ag/AgCl (satd. KCl), *C. necator* PHB^- reached a maximum current density of $183 \pm 5\ \mu A\ cm^{-2}$ and a total charge of 1686 ± 101 C was transferred within 192 h

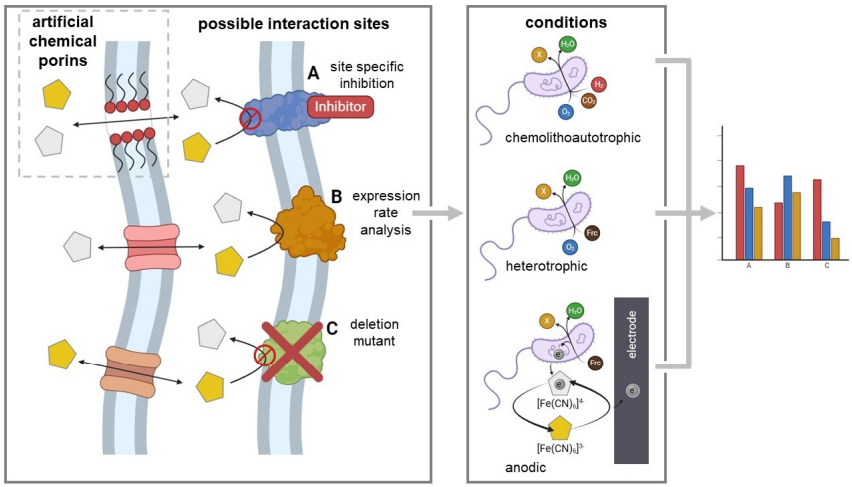

Scheme 1. Illustration of the aims of the study. Possible interaction sites of ferricyanide (pentagons, yellow: oxidized, grey: reduced) within *C. necator* are narrowed down via specific inhibition, applying deletion mutants, and expression rate analysis comparing chemolithoautotrophic, heterotrophic, and anodic cultivation conditions. Furthermore, the influence of creating artificial porins with chemical permeabilizers on anodic electron transfer is studied. Created with BioRender.

(Figure 1a). While the current density increases, the ΔOD_{600} rises slightly from 1.2 (0 h) to 1.7 after 6 h. The cell density remains almost constant for the rest of the cultivation period. The total fructose consumption is only $0.3 \pm 0.02\ g\,L^{-1}$ (Figure 1b). The electrons originating from fructose are transferred through ferricyanide to the anode at a coulombic efficiency of $63.1 \pm 5.7\%$, with no side products detectable by HPLC analysis. The remaining fraction of electrons could, in theory, be disposed of through the bidirectional soluble hydrogenase, generating gaseous H_2.[20] A further option would be the conversion into biomass, hence the observed growth within the first 6 h. Most of the oxidized ferricyanide is also reduced within the first 6 h, while the current rises. The maximum mediator reduction rate in this phase reached $0.22\ mM\,h^{-1}$. As the current drops over time, the ratio of oxidized to reduced ferricyanide tends towards the oxidized state. It seems likely, that *C. necator* is not able to support the high initial current and reduction rate over extended time periods. Limitations can be assumed within the metabolism and the mediator transfer-rate, since the anode provides enough oxidized ferricyanide in the bulk medium to keep up the electron transfer from *C. necator* to the anode (Figure 1a, red squares).

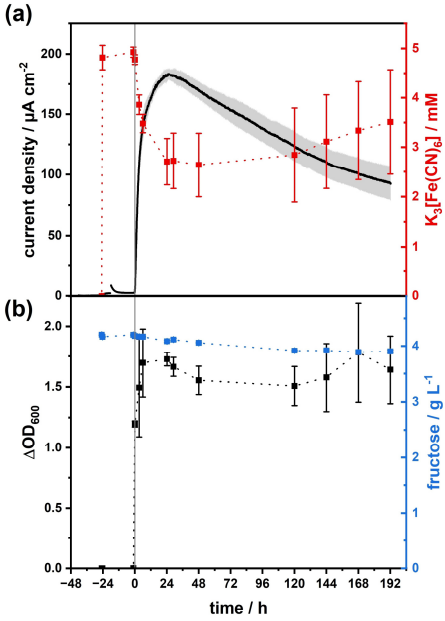

Figure 1. *C. necator* reference BES cultivation with 5 mM ferricyanide as mediator. (a) Current density (black line) and concentration of oxidized ferricyanide (red) from a biological triplicate. (b) cell density determined via ΔOD_{600} (black squares) measurement and fructose concentration (blue) during cultivation. Conditions: MMasy minimal medium, 30 °C, 400 rpm, pH = 6.8, n = 3, 500 mV *vs.* Ag/AgCl (satd. KCl). Error bars depict the standard deviation.

Expression Rate Analysis within BES Cultures

To get a deeper understanding of the MET mechanism, the first step is to shed some light on the interaction site of ferricyanide with *C. necator*. So far, it can be assumed that *C. necator* is unable to transfer electrons directly to an anode, as control experiments without ferricyanide as a mediator in the BES show no current evolution (Figure S1). It is therefore most likely, that no electron-transferring cytochromes are located on the outer membrane, as it is known for *Geobacter sulfurreducens, Shewanella oneidensis*, or *Vibrio natriegens*.[21–23] The interaction site is therefore expected to be located on the cytoplasmic membrane, or in the cytosol. Cytosolic sites are excluded in this study since ferricyanide is most likely not able to reach the cytosol.[24]

Therefore, several hypothesized interaction sites that are located on the cytoplasmic membrane or in the periplasmic space (Table S1) were chosen for expression rate analysis by qPCR. Of these interaction sites, one group comprises the respiration chain complexes (Figure 2a), another group includes both the soluble and membrane-bound hydrogenases together with three channel proteins (OmpA, ImpK, czcC2), which might be involved in the outer-membrane transfer of ferricyanide (Figure 2b). Additionally, the nitrate respiration proteins were chosen for analysis (Figure 2c), since the interaction of nitrate reductase with ferricyanide has already been suggested in *E. coli*.[24] Expression rates for all identified interaction sites were compared to stationary aerobic cultures (48 h after inoculation) without ferricyanide in a shake flask. Cultivation conditions to compare were stationary (54 h) autotrophic cultures on $CO_2/H_2/O_2$ and BES cultures with ferricyanide and the anode as a terminal electron acceptor. Samples from BES cultures were taken 24 h after inoculation, where current densities peaked. Within the BES cultivation, a specific mutant lacking the pHG1 megaplasmid (*C. necator* ΔpHG1) was chosen as negative control for qPCR analysis. Via this control, the missing interaction sites from the pHG1 megaplasmid and their relevance for MET can be elucidated. The relative gene expression rates for autotrophic cultivation, BES cultivation and the ΔpHG1 strain *vs.* aerobic conditions as reference were determined via the $2^{-\Delta\Delta Ct}$ method.

From the relative expression rates gathered, it can be concluded that the respiration chain proteins are not over-expressed significantly under BES conditions. One exception is the cytochrome c oxidase (cbb3) with a relative expression *vs.* aerobic conditions of 1.9 ± 0.3 in a BES. Slightly higher expression rates were determined for autotrophically grown cells with values ranging from 1.2 ± 0.1-fold for cytochrome c reductase to 1.9 ± 0.1-fold for the ATPase (Figure 2a). The pHG1 deficient strain expresses the respiration chain complexes within the same range (minding the error) as the pHG1 containing strain.

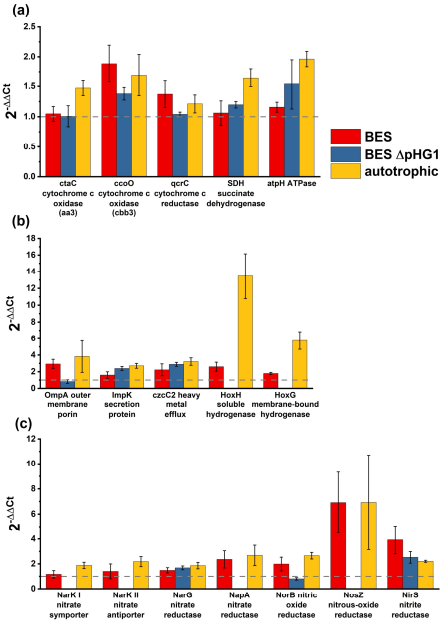

Figure 2. Relative gene expression levels in BES and autotrophic cultures of hypothesized proteins involved in the MET process *vs.* stationary aerobic culture as calibrator. BES samples were taken from the reactor 24 h after inoculation. Autotrophic samples were cultivated until stationary (54 h). (GyrB (pos. control, housekeeping; CtaC (aa3-type cytochrome oxidase, subunit II), CcoO (cbb3-type cytochrome oxidase, monohaem subunit II), GcrC (ubiquinol-cytochrome c reductase, cytochrome c1), SDH (succinate dehydrogenase iron-sulfur subunit), NuoD (NADH-quinone oxidoreductase subunit D), AtpH (F-type H+-transporting ATPase subunit delta, NarK I (nitrate/proton symporter), NarK II (nitrate/nitrite antiporter), NarG (respiratory nitrate reductase catalytic subunit), NapA (periplasmic nitrate reductase large subunit), NorB (nitric oxide reductase subunit B), NosZ (nitrous-oxide reductase), NirS (cytochrome cd1 nitrite reductase), OmpA (outer membrane protein or related peptidoglycan-associated (lipo)protein), ImpK (type VI secretion system protein), CzcC2 (outer membrane protein, heavy metal efflux system). Error bars depict the standard deviation.

From the three porins chosen for qPCR analysis, OmpA is expressed 2.9±0.6 and 3.8±1.9-fold higher under both anaerobic conditions (BES and autotrophic) compared to aerobic cultivation. This seems to be independent of the anodic conditions. Contrary to that, the expression in the ΔpHG1 strain under BES conditions is comparable to aerobic conditions, even though OmpA is encoded on chromosome 1, rather than the pHG1 plasmid. In a broader context, OmpA proteins are characterized by an N-terminal domain that configures an eight-stranded, antiparallel β barrel embedded within the outer membrane.[25] The globular C-terminal domain of OmpA is situated within the periplasmic space. Outer membrane proteins in Gram-negative bacteria serve diverse functions, e.g., signal transduction, adhesion to host cells, catalysis of crucial reactions, and facilitation of active and passive transport of solutes and nutrients across the cell membrane.[26] This may enable the MET in the first place, by importing and exporting ferricyanide.

The two other efflux proteins are expressed by a factor of 1.6±0.4 (ImpK) and 2.2±0.7 (czcC2) in a BES with pHG1. Since the expression is even higher within the ΔpHG1 strain in BES and autotrophic cultures, the effect is most probably triggered by the lack of O_2. ImpK is a primarily inner membrane protein with a C-terminal OmpA-like domain facing the periplasm. However, a small fraction of the total ImpK amount was also located in the outer membrane of Gram-negative *Agrobacterium tumefaciens*.[27] The protein is associated with the bacterial type VI secretion system providing a membrane channel with a pore size of 40 Å,[28] large enough for small molecules like ferricyanide to pass. CzcC is equally an efflux protein complex, transporting divalent cations through the outer membrane as a proton antiporter.[29] A passive or active import of ferricyanide via one of the two complexes cannot be proven by qPCR and might be unlikely when looking into the mechanisms, but cannot be ruled out. Further research in mediator membrane transport will be needed to shed light on the exact mechanism(s).

As expected, both the soluble (SH) and membrane-bound hydrogenases (MBH) are not expressed when the pHG1 plasmid is absent and significantly over-expressed under autotrophic cultivation conditions with hydrogen present (5.8±1.1 times for MBH and 13.5±2.7 times for SH). Within the BES, these hydrogenases can be found at expression rates of 2.6±0.5-fold higher for SH and 1.8±0.1-fold higher for MBH in comparison to aerobic conditions. These hydrogenases are reportedly only expressed under autotrophic conditions feeding on $H_2/CO_2/O_2$ gas mixtures as well as under heterotrophic conditions with a switch from fructose to the less favourable substrate glycerol.[30,31] Based on our results, it can be concluded that these hydrogenases are expressed under BES conditions, but to a very limited extent.

The obtained data from the denitrification pathway proteins supports the conclusion that both the membrane-bound nitrate reductase (NarG) and periplasmic nitrate reductase (NapA) are expressed under BES conditions (1.5±0.2 and 2.4±0.7 respectively), similar to autotrophic cultivation conditions (1.9±0.3 and 2.7±0.8). These enzymes catalyse the first step in denitrification ($NO_3^- \rightarrow NO_2^-$, E^0 = 420 mV),[32] when nitrate is available as an electron acceptor. It has to be noted, that the present minimal medium only contains ammonium sulphate as a nitrogen source. It is known, that NarG only forms in the absence of O_2, while NapA forms in the stationary phase of growth under aerobic conditions.[32] Therefore, NapA is already present from the stationary pre-culture when *C. necator* is added to the BES. Furthermore, the NapA genes are located on the pHG1 megaplasmid, hence it is not expressed in the ΔpHG1 BES cultivation. The proven expression in a BES together with the accessibility from the periplasm and standard redox potential of 420 mV of these reductases makes the reduction of

ferricyanide theoretically feasible (E^0 = 416 mV *vs.* SHE for ferricyanide).[33] It has to be considered though, that ferricyanide might mimic oxygen in a way, that the oxidizing conditions within the culture broth may inhibit the nitrate reduction pathway during the cultivation.[34]

Periplasmic nitrite reductase (NirS) converts NO_2 into the toxic intermediate NO. Regarding the redox potential, the reaction with ferricyanide is feasible, since the NO_2/NO reaction couple exhibits an E^0 of 375 mV *vs.* SHE.[32] In Figure 2c, NirS is expressed 3.9 ± 1.1-fold in a BES *vs.* 2.2 ± 0.1-fold with H_2/CO_2/O_2. This reductase is encoded on the chromosome, hence the expression is also measurable 2.5 ± 0.5-fold with the pHG1 deficient strain. The nitric oxide reductase (Nor) catalyses the reaction of NO→N_2O (E^0 = 1175 mV).[32] The necessary genes are located in two copies, one on the pHG1 megaplasmid and one on the chromosome.[35] From our data, this is visible in the expression rate of NorB. The difference between autotrophic and BES cultivation is marginal (2.0 ± 0.6 *vs.* 2.7 ± 0.3) with respect to the error. The ΔpHG1 strain expresses NorB 0.8 ± 0.1-times the amount that an aerobically grown strain with the pHG1 plasmid achieves. The NorB subunit contains two *b*-type hemes, but no heme *c*. The enzyme was also able to accept electrons from reduced phenazine methosulfate (E^0 = 80 mV *vs.* SHE) .[36,37] If the enzyme is also able to reduce ferricyanide is speculative, since the redox potential of the catalysed reaction might be too high compared to the E^0 of ferricyanide.

The nitrous-oxide reductase (NosZ) catalyses the last step from N_2O→N_2 (E^0 = 1335 mV).[32] For this specific site, the expression rate was equal for autotrophic and BES conditions with a 6.9-fold higher rate. It has to be noted though, that standard deviations were uncommonly high. Both NarK nitrate transport proteins were not significantly over-expressed with ferricyanide in a BES. Their involvement in ferricyanide import is not yet determined. The fact that these transporters are naturally importing anions might benefit the ferricyanide uptake. However, there is evidence for a reversible inactivation of NarK under oxidizing conditions, which in turn, stops the transport.[38] The nitrate assimilatory enzyme (Nas) is inhibited by ammonium, which is always present in the medium.[39] Therefore, it was not part of the analysis. To summarize, both nitrate reductases (NapA and NarG) expose reachable interaction sites for ferricyanide in the periplasm and the reduction is thermodynamically feasible. The same applies for the nitrite reductase (NirS).

Eliminating Megaplasmid Encoded Interaction Sites

The role of the nitrite/nitrate reductases and both hydrogenases in MET cannot be concluded via qPCR alone. Therefore, BES data comparing the ΔpHG1 *vs.* the PHB^- strain can shed light on their role in MET. The pHG1 megaplasmid contains all hydrogenases, including the regulatory and actinobacterial hydrogenases,[7] as well as most of the nitrate respiration genes (Table S1). With those possible interaction sites missing, as it was confirmed via qPCR, no current response should be possible with this strain if one of the missing genes plays a crucial role in ferricyanide reduction.

Figure 3a shows the result for a BES cultivation of the ΔpHG1 strain with ferricyanide in a biological triplicate. The black line indicates the current density increasing right after inoculation at t = 0 h. As for the control with the PHB^- strain (Figure 1), the current density for the ΔpHG1 strain reaches a slightly lower maximum of 161 ± 14 μA cm^{-2} and a similar coulombic efficiency of 68.1 ± 9 %. Even without the soluble and membrane-bound hydrogenase, a part of the electrons is not transferred to the anode, ruling out the theory of H_2 production through the hydrogenases. Ferricyanide (red squares) is reduced at the highest rate (0.19 mM h^{-1}) during the initial phase when the current rises after inoculation, as observed before with *C. necator* PHB^-. With the current density reaching a plateau, the reduction rate of *C. necator* seems to be equal to the re-oxidation rate by the anode. Hence, the concentration of oxidized ferricyanide stays nearly constant. When the current starts to decline, the equilibrium shifts

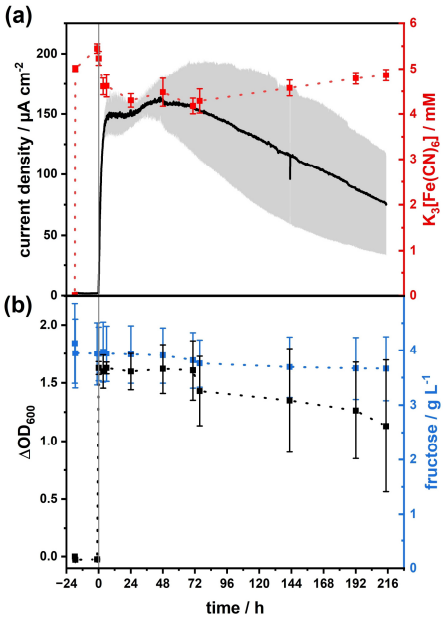

Figure 3. BES cultivation of *C. necator* HF210 strain, lacking the pHG1 megaplasmid. (a) Current density (black) and concentration of oxidized ferricyanide (red) from a biological triplicate. (b) cell density determined via ΔOD_{600} (black squares) measurement and fructose concentration (blue) during cultivation. Conditions: MMasy minimal medium, 30 °C, 400 rpm, pH 6.8, n = 3, 500 mV *vs.* Ag/AgCl (satd. KCl). Error bars depict the standard deviation.

towards the anode re-oxidizing ferricyanide, so the concentration starts to rise to the originally added value.

Figure 3b depicts the cell density as ΔOD_{600} values. In contrast to the PHB^- strain, the ΔOD_{600} doesn't increase within the first 6 h of cultivation. However, both strains share the low fructose uptake in a BES cultivation, with the ΔpHG1 strain consuming $0.27 \pm 0.02\ g\,L^{-1}$ of fructose during 216 h of cultivation. The overall standard deviations were significantly higher with the ΔpHG1 strain. This originates from reactor cultures varying in ΔOD_{600}, current density, and total fructose concentration, although stemming from parallel pre-cultures and using one identical medium stock.

In summary, the current density in the ΔpHG1 strain follows the same pattern as observed in the strain containing the pHG1 plasmid. This observation rules out all hydrogenases and the nitrate respiration pathway, except membrane-bound nitrate (NarG) and nitrite (NirS) reductases which are also located on the chromosome, as the main interaction site for ferricyanide.

Inhibition of Suspected Interaction Sites

A common method for identifying interaction sites is specific inhibition. By applying inhibitors of the respiration chain complexes and the nitrate reductases during BES cultivation of *C. necator*, the effects of site-specific inhibition on the current generation and redox state of ferricyanide can be studied. The specific inhibition site, the postulated inhibition mechanism, and the applied concentration of each substance used in this study are listed in Table 1. The resilience of *C. necator* against the inhibitors was determined via growth analysis in aerobic cultivation. In the end, the concentration where growth is inhibited but no rapid cell death occurs was chosen for BES experiments (data not shown). Myxothiazol and rotenone are poorly soluble in aqueous buffers leading to increased turbidity, hence the OD values become more uncertain.

The applied inhibitors listed in Table 1 were added within the stable/declining current phase, so the effect of each inhibitor is visible. The current density plots and the respective concentrations of ferricyanide are plotted in Figure 4. The associated ΔOD_{600} values are plotted in the supplementary information (Figure S2).

The inhibition of cytochrome c reductase with antimycin A affects the current response from *C. necator* in the BES immediately (Figure 4a). As antimycin A is introduced into the reactor, the current density drops fast. The reduced ferricyanide is not re-oxidized by the anode as the current declines, indicating an interaction of antimycin A with the electrode or ferricyanide itself, preventing the oxidation. It cannot be ruled out, that this side reaction causes the observed drop in current density, rather than the inhibition itself. The same effect was observed for *C. necator* ΔpHG1 (Figure S3) and was also demonstrated by Lai and co-workers in their BES with *P. putida*.[14] Antimycin A blocks the quinone reduction from Q to QH_2 at the Q_i site of cytochrome c reductase (Table 1). Nevertheless, if ferricyanide is reduced at the Q_o site, where QH_2 is oxidized back to Q, antimycin A would not directly interfere with this reaction. Ferricyanide reduction could therefore continue until the QH_2-pool is deprived and the insufficient proton gradient starves ATP synthesis. The inhibition of the antimycin A insensitive Q_o site with myxothiazol, however, had no effect on the current density with 6.8 µM of the inhibitor added into the culture (Figure 4b). It is conceivable though, that the inhibitor concentration might be too low, due to the poor solubility, to effectively inhibit cytochrome c reductase. With the substantial number of cells in the reactor, the inhibition of only a few cytochrome c reductase enzymes would therefore not affect the current density curve. Because of the unclear way antimycin A interacts with ferricyanide or the electrode and the fact that myxothiazol doesn't dissolve well, we can't say for sure if cytochrome c reductase is an important site for ferricyanide interaction.

Table 1. Inhibitors used in this study with their respective interaction sites and known inhibition mechanism.

Inhibitor	Inhibition site	Inhibition mechanism	Concentration used
Antimycin A	Cytochrome c reductase Q_i site	Blocks quinone reduction site (Q_i) of the bc_1 complex near heme b_H, preventing generation of the semiquinone in the second half of the Q-cycle.[40]	20 µg mL^{-1}
Myxothiazol	Cytochrome c reductase Q_o site	Blocks Fe–S oxidation of ubiquinol at Q_o site.[41]	6.8 µM
Rotenone	NADH dehydrogenase	Inhibition of last electron transfer step from Fe–S cluster to ubiquinone.[42] Side effect: generation of reactive oxygen species leading to apoptosis.[43]	200 µM
	Nitrate reduction	Unknown[44]	
Sodium azide	Cytochrome c oxidase	Binding between heme a_3 and Cu_B in O_2 reduction site.[45] Side effect: ATP hydrolase activity of the ATPase is inhibited.[46]	5 mM
	Nitrate reductases (Nar, Nap)	Unknown. Nar is sensitive to azide in the µM, Nap in the mM range.[47,48]	
$ZnSO_4$	Periplasmic nitrate reductase (NapA)	Uncompetitive, Zn^{2+} binding site (sulphur or methionyl residue of methionine 153) is revealed when nitrate is bound.[49]	400 µM
Malonate	Succinate dehydrogenase	Unknown.[50]	20 mM

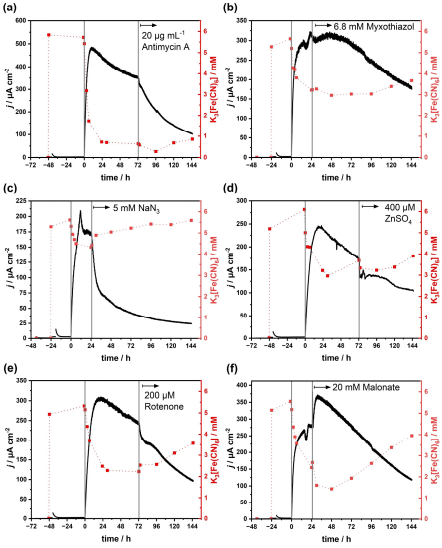

Figure 4. Inhibition studies with *C. necator* BES cultures containing 5 mM ferricyanide as mediator. Inhibition: (a) cytochrome c reductase Q_i site with 20 µg mL^{-1} antimycin A, (b) cytochrome c reductase Q_o site with 6.8 µM myxothiazol, (c) cytochrome c oxidase with 5 mM sodium azide, (d) periplasmic nitrate reductase with 400 µM zinc sulphate, (e) NADH dehydrogenase with 200 µM rotenone, (f) succinate dehydrogenase with 20 mM malonate. Current density (black) and concentration of oxidized ferricyanide (red). Conditions: MMasy minimal medium, 30 °C, 600 rpm, pH 6.8, 500 mV *vs.* Ag/AgCl (satd. KCl). Cell densities measured via ΔOD_{600} can be found in Figure S2.

The addition of 5 mM sodium azide (Figure 4c) led to an immediate drop in current density with simultaneous re-oxidation of ferricyanide. Contrary, in experiments conducted with *P. putida* F1, no current changes were observed when cytochrome c oxidase was inhibited with 3 mM sodium azide.[14] It's important to note that the reduction of the mediator follows a similar pattern to the control experiment: as the current density decreases, the concentration of oxidized mediator increases. In contrast to the inhibition with antimycin A, this demonstrates that ferricyanide and the electrode are not affected by azide. Furthermore, the cell density measured by ΔOD_{600} doesn't decrease significantly in the first 24 h following the addition of azide (Figure S2b), indicating the current decline is not a result of cell lysis. Studies in *E. coli* could demonstrate, that 6 mM of potassium cyanide added to mid-exponential cells limits the ferricyanide reductase activity of cytochrome c oxidase to 14%.[51] In our experiment with stationary cells, the current response, which indicates reductase activity, decreased from 170 µA cm^{-2} to 24 µA cm^{-2} (and continued to decline slightly) within 120 h after adding azide, representing approximately 14% of the initial current remaining.

Mechanistically, cytochrome c oxidase catalyses oxygen reduction between cytochrome a_3 and the Cu_B site, accessible for oxygen located in the cytoplasmic membrane.[52] Interrupting the electron transfer chain at cytochrome c oxidase would lead to the over-reduction of chain components upstream. However, since molecular oxygen is excluded from the medium, no reactive oxygen species should result from this effect. Most importantly, inhibiting the oxygen reduction site with azide would have no effect on ferricyanide reduction, if the mediator cannot access the a_3/Cu_B binuclear site. This is likely the case, since the charged molecule will not penetrate the cytoplasmic membrane. This indicates, that $[Fe(CN)_6]^{3-}$ can't replace oxygen within the normal catalytic cycle of cytochrome c oxidase. Nevertheless, reduced $[Fe(CN)_6]^{4-}$ can likely donate electrons to cytochrome c oxidase through the Cu_A site, accessible from the periplasm.[53] Studies with isolated cytochrome c oxidase placed in liposomes further suggested that the oxidized $[Fe(CN)_6]^{3-}$ can be reduced at the cytochrome c reduction site via Cu_A and heme a.[54] If this mechanism results in a proton translocation, e.g., via the release of redox Bohr protons, remains speculative.[55]

It has to be considered though, that azide concentrations in the mM range will also inhibit both nitrate reductases Nar and Nap (Table 1). The pHG1 deficient strain, which lacks NapA and still effectively reduces ferricyanide, rules out NapA as a possible interaction site for ferricyanide. This suggests that NarG could be an alternative active site for ferricyanide reduction, distinct from cytochrome c oxidase. The 14% leftover current after inhibition suggests that the nitrite reductase NirS might be responsible for maintaining the remaining anodic electron transfer.

As a control, the periplasmic nitrate reductase (Nap) was inhibited with 400 µM of $ZnSO_4$, which resulted in an instant decline in current by 40 µA cm^{-2} before reaching a plateau and proceeding with the initial decline, 36 h after inhibition (Figure 4d). Ferricyanide seems to be recovered as expected while the ΔOD_{600} increases rapidly from 1.16 to 1.69 and stabilizes over the next 72 h at about 1.5. This sudden increase can only be explained by adsorbed cells being resuspended again since $ZnSO_4$ doesn't absorb at 600 nm. Hence, the inhibition of the periplasmic nitrate reductase (NapA) doesn't seem to affect the MET in great effect, validating the previously discussed results.

The inhibition of NADH dehydrogenase with rotenone (Figure 4e) led to a similar observation as the inhibition with $ZnSO_4$. After adding the inhibitor, the current density drops by 50 µA cm^{-2}, then reaches a plateau before continuing to decline as observed before the inhibition. Additionally, ferricyanide undergoes rapid oxidation during the decline in current. Afterwards, the ferricyanide concentration mirrors the current density curve, as observed in the control experiment (Figure 1). Similar results were observed with 250 µM of rotenone in *P. putida* F1,[14] leading to the assumption that NADH dehydrogenase is not a reduction site for ferricyanide.

Finally, 20 mM malonate was used to inhibit succinate dehydrogenase. The briefly occurring pH drop caused by the addition of malonic acid resulted in a short current spike, which was quickly recovered by the pH control unit (Figure 4f).

Interestingly, after inhibition, there was an initial increase in the current response along with a further reduction of ferricyanide. However, this effect is not stable, and the current density quickly decreases again. A reducing effect of malonate on ferricyanide was ruled out in abiotic tests over 24 h (data not shown). Moreover, a metabolic pathway utilizing malonic acid as a substrate is unknown for *C. necator*. A comprehensive justification explaining this effect cannot be provided in this context. Continued investigation into this observation may provide a pathway for optimizing MET.

While it is not possible to create a mutant strain lacking parts of the respiration chain, total RNA sequencing to compare expression levels for all available mRNA during BES cultivation might be a further option to identify the interaction sites of different mediators accurately. However, the azide inhibition performed in this study suggests that cytochrome c oxidase is the primary site of reduction for ferricyanide under BES conditions. This observation leads to similar conclusions as those stated by Ertl and Unterladstaetter[51] for *E. coli* and likely applies to other Gram-negative organisms as well: The rate of ferricyanide reduction ultimately depends on the expression rate of transport proteins and respiratory cytochrome c oxidase.

Overcoming the Membrane Obstacle

Since an artificial over-expression of the respiratory enzymes is not feasible, the first step in optimizing MET is to increase the membrane transfer rate of ferricyanide to circumvent a possible limitation.[56,57] This was initially addressed by expressing various porins in *C. necator* PHB$^-$. The heterologous expression of the FhuA porin from *E. coli* and its derivative missing the "cork" domain FhuA Δ1-160, along with the channel protein OprF from *Pseudomonas aeruginosa*, did not exhibit a positive impact on mediated electron transfer in *C. necator*. Contrarily, the metabolic burden associated with expressing these porins led to a reduction in current densities (Figure S4). However, our qPCR investigations suggest that the outer membrane protein OmpA may be involved in the artificial electron transfer process and should be further investigated.

Alternatively, we investigated cetyltrimethylammonium bromide (CTAB), benzalkonium chloride, EDTA, Triton X 100, polyethylenimine (PEI), Tween 20, and succimer (dimercaptosuccinic acid), as possible chemical permeabilizing agents. These substances are expected to create artificial pores in the outer (and potentially inner) membrane, to facilitate the membrane transfer of ferricyanide.[57–59] Toxic concentrations for the respective substances were determined via growth curves at increasing concentrations (Figure S5). Via an uptake assay of the fluorescent probe N-Phenyl-1-naphthylamine (NPN) *vs.* non-treated cells, increased membrane permeation could be demonstrated for succimer, PEI, benzalkonium chloride, and CTAB (Figure S6, Figure 5a). In contrast, EDTA, Triton-X-100, and Tween 20 could not increase the uptake of NPN (Figure S6). In a further step, the concentrations for effective membrane permeabilization and minimal cell toxicity were determined and prepared for reduction assays with ferricyanide. However, side reactions with the mediator like clumping, precipitation, increased turbidity, and reduction of ferricyanide prohibited the use of succimer, PEI, and benzalkonium chloride for BES cultivation (Figure S7). This issue might be resolved when other mediators are used. At last, only CTAB was compatible with ferricyanide, with a minimal turbidity increase with 20 μM CTAB.

Figure 5a depicts the NPN uptake with ascending CTAB concentrations. Increased emission rates *vs.* background therefore hint towards increased cell membrane permeation. Stepping up the CTAB concentration in the range of 20 to 300 μM doesn't result in higher fluorescence signals of NPN, indicating a concentration-independent mechanism for the number of cells applied within the well. However, a limiting amount of NPN cannot be ruled out.

In growth analysis experiments conducted in 96-well plates, *C. necator* could not replicate in CTAB containing growth medium (Figure 5b). For minimal medium with a starting ΔOD_{600} of 0.5 supplemented with 300 μM CTAB, a decrease in ΔOD_{600} suggests the maximum concentration for vital resting cells is 220 μM. As previously described, membrane permeability is not concentration-dependent. Therefore, a concentration of 20 μM CTAB was selected for BES experiments to minimize toxic stress on the cells. Preliminary experiments in anaerobic serum flasks with fructose as electron and carbon source and ferricyanide as the sole electron acceptor were performed to determine ferricyanide reduction rates. In comparison to non-permeabilized cells, CTAB treated cells with identical ΔOD_{600} values reduce ferricyanide 2-fold faster with 53 $\mu M\,h^{-1}$ *vs.* 27 $\mu M\,h^{-1}$ (Figure 5c, d).

A recent study by Wu and co-workers[58] applied CTAB to anaerobic sludge biofilms in a MFC with an optimum of 200 μM CTAB to facilitate riboflavin-mediated electron transfer. However, there are no studies yet about the actual application of CTAB using pure cultures within a BES. Hence, our objective was to enhance the MET process with *C. necator* by introducing 20 μM CTAB into the BES reactor. Additionally, the impact of artificial pores on fructose uptake is a subject of further investigation. Figure 6 depicts the recorded current densities with (red) and without (black) CTAB (Figure 6a) and the respective concentrations of oxidized ferricyanide (Figure 6b). Current densities were normalized to the CDW, to eliminate current variations caused by minor deviations in cell number between both conditions.

The current densities vary only slightly between CTAB treated cells and the control. In the first 24 h, CTAB treated cells reach minimal higher maximal current densities (1095.7 *vs.* 973.5 $\mu A\,g_{CDW}^{-1}\,cm^{-2}$), which cancels out during further cultivation, as the same charge is transferred after 120 h for treated and untreated cells. A similar effect is visible for oxidized ferricyanide concentration. With CTAB, slightly more ferricyanide is reduced, but at an identical rate. To rule out a concentration limitation for CTAB, another 20 μM of CTAB was added after 120 h for a final concentration of 40 μM CTAB. This, however, had a detrimental effect on the metabolism of the cells, resulting in an instant current decline. Moreover, an increased substrate uptake was not observed (data not shown).

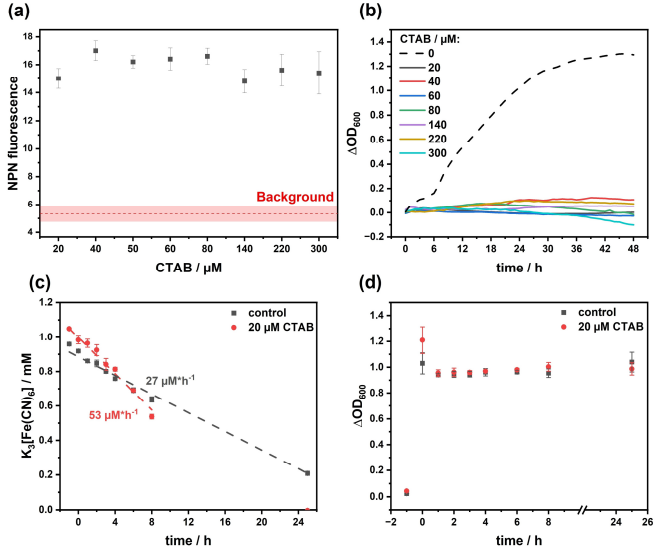

Figure 5. (a) NPN uptake assay with increasing CTAB concentrations with the background of NPN, buffer solution, and CTAB. (b) Growth analysis with increasing CTAB concentrations from a starting ΔOD_{600} of 0.5. (c) Reduction rates of ferricyanide with (red) and without (black) 20 µM of CTAB. (d) ΔOD_{600} of cultures reducing ferricyanide with and without CTAB. Conditions: MMasy minimal medium, 30 °C, anaerobic, n = 3. Error bars depict the standard deviation.

In conclusion, CTAB has a beneficial effect in low concentrations on the reduction rate of ferricyanide, but BES experiments suggest the effect is only minor. This opens up two hypotheses. Firstly, the natural membrane transfer of ferricyanide was not limiting the overall MET and secondly, the limitation must be in the metabolism or the interaction site, as enough oxidized mediator is provided during cultivation, excluding the anodic oxidation reaction as the limiting factor. Nevertheless, the first hypothesis stands against the obtained result of a faster reduction rate with CTAB in anaerobic serum flasks. The second hypothesis has to be further investigated e.g., via metabolic flux analysis.

Conclusions

Mediated extracellular electron transfer in *C. necator* via ferricyanide was characterized regarding the reduction site within the cell. Previous work by Nishio and co-workers[10] revealed higher expression levels of three nitrate reductases (NapD, NarK, NasD) when a polymeric ferrocene mediator transferred surplus electrons to an anode during aerobic cultivation. In this study, for the first time, expression rate analysis of hypothesized interaction sites, namely the nitrate and oxygen respiration chains, as well as the hydrogenases and three porins (OmpA, ImpK, czcC2) was performed in anaerobic BES reactors *vs.* aerobic cultivation conditions to elucidate on the ferricyanide reduction site(s). Furthermore, individual sites were specifically inhibited during BES cultivation with 5 mM ferricyanide mediating electrons to an anode as the sole terminal electron acceptor.

Inhibition with 5 mM azide hints towards cytochrome c oxidase as a reduction site due to an imminent decrease to 14% leftover current density after inhibition, consistent with the work of Ertl and Unterladstaetter[51] in *E. coli*. However, the specific inhibition with azide targeting the oxygen reduction site, which is not accessible for ferricyanide, results in an unclear mechanism for ferricyanide reduction. As demonstrated in the publication by Lai and co-workers,[14] cytochrome c reductase was found to be affected by antimycin A. However, an unclear side reaction of antimycin A prohibits ferricyanide oxidation by the anode. Therefore, the role of cytochrome c reductase in ferricyanide reduction remains questionable. The nitrate reductase NarG, also inhibited by azide, was proven to be present in BES cultures via qPCR and could also serve as reduction site for ferricyanide.

Comparing the megaplasmid deficient *C. necator* ΔpHG1 to the PHB^- strain in BES cultivations revealed that both strains can transfer electrons to ferricyanide, resulting in equal current densities. This excluded all hydrogenases present in *C. necator* from the list of potential interaction sites and further narrowed down the possible sites to respiration chain and nitrate

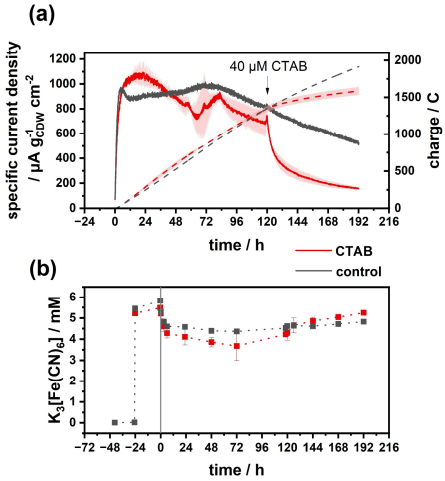

Figure 6. (a) specific current density normalized to CDW for BES cultures with 20 µM of CTAB (red, n = 3) and a control cultivation without CTAB (black, n = 1). Dashed lines indicate the charge transferred to the anode via ferricyanide. (b) concentrations of oxidized ferricyanide during BES cultivation with (red squares) and without (black squares) the addition of CTAB. Conditions: MMasy minimal medium, 30 °C, 400 rpm, pH 6.8, 500 mV *vs.* Ag/AgCl (satd. KCl). Error bars depict the standard deviation.

reduction proteins encoded on the chromosome. Of these, nitrite reductase (NirS) stood out as a possible candidate, catalysing a reaction with a redox potential close to that of ferricyanide alongside an observed 3.9 ± 1.1-fold expression under BES conditions. Furthermore, a 2.9 ± 0.6-fold overexpression *vs.* aerobic conditions of the porin OmpA was observed when cultivating *C. necator* under BES conditions. This might imply a ferricyanide transport property of this porin and opens up the possibility of enhancing ferricyanide membrane transfer. Alternatively, CTAB was applied as chemical permeabilizer to facilitate membrane transfer via artificial pores in the outer membrane. The reduction rate of ferricyanide was doubled with 20 µM CTAB added to the medium in anaerobic serum flasks. In contrast, the effect of CTAB was minor when applied in BES reactors and could not yield a higher charge transfer compared to untreated cells. Therefore, the hypothetical membrane transport limitation could not be eliminated via CTAB. Nevertheless, it cannot be ruled out that other mediators might benefit from chemical permeabilizers.

In a broader context, this study is a first step to elucidate MET for *C. necator* with one exemplary mediator. In future studies, whole transcriptome analysis comparing aerobic conditions to BES and autotrophic cultivations could reveal additional interaction sites, which have not yet been looked into.

Experimental Section

Bacterial Strains and Chemicals

Cupriavidus necator PHB$^-$4,[60] as well as *C. necator* HF210[61] (missing the pHG1 megaplasmid) were used in this study. All chemicals utilized in the study were procured from reputable suppliers, including Merck KGaA (Germany), VWR Chemicals (USA), Carl Roth GmbH & Co. KG (Germany), and Sigma Aldrich (USA).

Media and Culture Conditions

Cultures were incubated at 30 °C and 180 rpm in cultivation tubes containing 2.5 mL LB medium (10 g L^{-1} tryptone, 5 g L^{-1} yeast extract, 10 g L^{-1} NaCl). Cryo stocks were prepared by adding 25% glycerol to an exponential culture, which was subsequently frozen at −80 °C. For BES precultures, cryostocks were cultivated on LB agar plates (15 g L^{-1} agar) and incubated overnight at 30 °C. Liquid precultures were prepared by transferring a single colony into a 100 mL flask with baffles filled to 20 mL with LB. After 24 h, 1 L shake flasks with baffles filled to 200 mL with MMasy medium were inoculated with the exponential pre-culture to achieve an ΔOD_{600} of 0.1. The MMasy medium, as described by Sydow and co-workers,[62] consisted of 4 g L^{-1} fructose as the carbon and electron source, 2.895 g L^{-1} Na_2HPO_4, 2.707 g L^{-1} $NaH_2PO_4 \cdot H_2O$, 0.94 g L^{-1} $(NH_4)_2SO_4$, 0.8 g L^{-1} $MgSO_4 \cdot 7H_2O$, 0.097 g L^{-1} $CaSO_4 \cdot 2H_2O$, 0.17 g L^{-1} K_2SO_4, and 0.1% (v/v) of a trace element solution. The trace element stock solution was composed of 15 g L^{-1} $FeSO_4 \cdot 7H_2O$, 2.4 g L^{-1} $MnSO_4 \cdot H_2O$, 2.4 g L^{-1} $ZnSO_4 \cdot 7H_2O$, 0.48 g L^{-1} $CuSO_4 \cdot 5H_2O$, 1.8 g L^{-1} $Na_2MoO_4 \cdot 2H_2O$, 1.5 g L^{-1} $Ni_2SO_4 \cdot 6H_2O$, and 0.04 g L^{-1} $CoSO_4 \cdot 7H_2O$ dissolved in 0.1 M HCl. Cultures were then incubated in an orbital shaker at 180 rpm (2.5 cm orbit, Multitron, Infors, Bottmingen, Switzerland). The BES precultures were incubated for 48 h to ensure the stationary phase was reached before inoculating the reactor.

Autotrophic or anaerobic cultures were inoculated from liquid precultures in LB in gas-tight serum flasks (1000 mL). Each flask was filled to 200 mL with MMasy minimal medium without fructose. The headspace was then pressurized with the respective gas. For autotrophic conditions, a $H_2/CO_2/O_2$ gas mixture with a composition of 64 : 16 : 20 as described by Sydow and colleagues[62] was used. In the case of anaerobic cultivations with ferricyanide, 99.999% N_2 was applied. The gas phase was renewed after taking a sample.

Bioelectrochemical System

The BES reactor was used in the configuration already described before.[12] In brief, a polished graphite rod (Graphite 24, Germany) with a length of 80 mm and a diameter of 7 mm (geometrical surface area of 18 cm^2), held in place by a PTFE rod, served as the working electrode inside the 300 mL DASGIP stirred tank reactor. It was paired with a stainless-steel mesh electrode (1.4404, mesh size 0.1 mm, wire diameter 0.065 mm, Jaera GmbH + Co.KG, Germany) with a geometrical surface area of 20 cm^2, functioning as the counter electrode. The anodic and cathodic compartments were separated by a cation exchange membrane (Nafion117, QuinTech, Germany). The cathodic compartment, enclosed in a glass tube with one threaded side and an open side, held 10 mL of cathode buffer (28.95 g L^{-1} Na2HPO4, 27.07 g L^{-1} $NaH_2PO_4 \cdot H2O$). The anodic buffer consisted of MMasy medium with 4 g L^{-1} fructose as the substrate. The applied potential of 500 mV was controlled using a multi-channel potentiostat (MultiEmStat3 +, PalmSens, Netherlands) and Ag/AgCl (satd. KCl) reference electrodes (Xylem Analytics, Germany). 2 mL of ferricyanide was added as a concentrated stock solution (750 mM) for a final concentration of 5 mM. The anodic overpotential of 500 mV was applied to ensure

sufficient driving force for ferricyanide oxidation. pH control was achieved using pH sensors (Hamilton, Germany) along with Eppendorf DASGIP pH and pump modules, with 2.5 M NaOH being fed through the headspace of each reactor. This maintained a pH of 6.8 in the anodic compartment, while the cathodic chamber remained uncontrolled.

Analytics and Calculations

Culture broth samples were obtained from the reactors and subjected to centrifugation at 16,900 x g and 4 °C for 5 minutes. The resulting supernatant was filtered through a 0.2 µm PTFE filter. HPLC analysis was performed using an Agilent 1200 high-performance liquid chromatography system equipped with an Aminex HPX-87H column (Bio-Rad Laboratories GmbH, Germany). Concentrations of the substrate fructose were determined using a refractive index detector at 32 °C. The column temperature was maintained at 50 °C, and 5 mM H_2SO_4 at a flow rate of 0.5 mL min^{-1} was employed for isocratic elution of the analytes. Fructose standards ranging from 0.1 to 4 g L^{-1} in seven concentration steps were measured, and the corresponding areas were fitted using linear regression.

Determination of the redox state of the RM in the BES was performed as described before.[12,63] In short, the extinction of the characteristic wavelengths of ferricyanide (320/420 nm) were monitored offline with a spectrophotometer. Reduced ferricyanide does not absorb at 420 nm and can therefore be distinguished from the oxidized form. The concentrations were then determined via 7 standards of oxidized ferricyanide.

The coulombic efficiency (CE) was calculated via the following equation: CE [%] = $Q_{anode}/(Q_{substrate}-Q_{products})$*100. Q indicates the charge transferred to the anode in [C]. Fructose was used as the only substrate, contributing 24 equivalents of electrons per mol of fructose. Since no products were detected in culture supernatants, $Q_{products}$ was assumed to be 0.

RT-qPCR

Expression rates of the genes of interest encoding for possible mediator interaction sites were determined via qPCR. Analogous to qPCR reactions performed with *C. necator* mRNA in the literature, the housekeeping gene *gyrB* was used as positive control.[64] Cells were prepared immediately after taking samples from the cultures. Since all experiments were at least performed as triplicates, mRNA extraction was performed for each of those triplicates using the Monarch Total RNA miniprep Kit (T2010, NEB, USA), according to the manual for tough-to-lyse samples (available online). Here, an enzymatic lysis with 1 g L^{-1} lysozyme in 10 mM TRIS buffer (pH = 8.4) at 25 °C for 5 min was performed prior to adding monarch RNA lysis buffer. During the extraction, an on-column DNAse I treatment was performed to remove any residues of DNA. The transcription into cDNA was performed with a Luna® Universal One-Step RT-qPCR Kit (E3005, NEB, USA) with a total RNA concentration of < 0.05 g L^{-1}. The reaction setup was performed as described in the associated manual. Primers for the specific genes of interest are listed in (Table S1) The transcription as well as the qPCR reaction was done in an Agilent AriaMX qPCR system with the SYBR® scan mode. Relative gene expression rates were determined *vs.* aerobic control cultivations as calibrator using the $2^{-\Delta\Delta Ct}$ method.[65]

Supporting Information

The authors have cited additional references within the Supporting Information (Ref. [66,67]).

Acknowledgements

This work was created as part of the project "Bioelectrochemical and engineering fundamentals to establish electro-biotechnology for biosynthesis – Power to value-added products (eBiotech)", which is funded by the Deutsche Forschungsgemeinschaft (DFG, German Research Foundation) – Project number 422694804. Open Access funding enabled and organized by Projekt DEAL.

Conflict of Interests

The authors declare no conflict of interest.

Data Availability Statement

The data that support the findings of this study are available from the corresponding author upon reasonable request.

Keywords: Bioelectrochemical system · Cytochromes · Electron transfer · Mediator interaction · Respiratory inhibition

[1] R. R. Dalsasso, F. A. Pavan, S. E. Bordignon, G. M. F. de Aragão, P. Poletto, *Process Biochem.* **2019**, *85*, 12.
[2] T. Krieg, A. Sydow, S. Faust, I. Huth, D. Holtmann, *Angew. Chem. Int. Ed. Engl.* **2018**, *57*, 1879.
[3] S. Milker, A. Sydow, I. Torres-Monroy, G. Jach, F. Faust, L. Kranz, L. Tkatschuk, D. Holtmann, *Biotechnol. Bioeng.* **2021**, *118*, 2694.
[4] S. Milker, D. Holtmann, *Microb. Cell Fact.* **2021**, *20*, 89.
[5] J. Overhage, A. Steinbüchel, H. Priefert, *Appl. Environ. Microbiol.* **2002**, *68*, 4315.
[6] J. Lu, C. J. Brigham, C. S. Gai, A. J. Sinskey, *Appl. Microbiol. Biotechnol.* **2012**, *96*, 283.
[7] J. Panich, B. Fong, S. W. Singer, *Trends Biotechnol.* **2021**, *39*, 412.
[8] A. Tiemeyer, H. Link, D. Weuster-Botz, *Appl. Microbiol. Biotechnol.* **2007**, *76*, 75.
[9] E. Schwartz, A. Henne, R. Cramm, T. Eitinger, B. Friedrich, G. Gottschalk, *J. Mol. Biol.* **2003**, *332*, 369.
[10] K. Nishio, Y. Kimoto, J. Song, T. Konno, K. Ishihara, S. Kato, K. Hashimoto, S. Nakanishi, *Environ. Sci. Technol. Lett.* **2014**, *1*, 40.
[11] Y. H. Lai, J. C.-W. Lan, *Int. J. Hydrogen Energy* **2021**, *46*, 16787.
[12] A. Gemünde, E. Rossini, O. Lenz, S. Frielingsdorf, D. Holtmann, *Bioelectrochemistry* **2024**, *158*, 108694.
[13] A. Gemünde, J. Gail, D. Holtmann, *Electrochem. Commun.* **2024**, *162*, 107705.
[14] B. Lai, P. V. Bernhardt, J. O. Krömer, *ChemSusChem* **2020**, *13*, 5308.
[15] L. Gu, X. Xiao, G. Zhao, P. Kempen, S. Zhao, J. Liu, S. Y. Lee, C. Solem, *Microb. biotechnol.* **2023**, *16*, 1277-1292.
[16] R. Y. A. Hassan, U. Wollenberger, *Anal. Bioanal. Chem.* **2016**, *408*, 579.
[17] D. H. Park, J. G. Zeikus, *J. Bacteriol.* **1999**, *181*, 2403.
[18] S. Hintermayer, S. Yu, J. O. Krömer, D. Weuster-Botz, *Biochem. Eng. J.* **2016**, *115*, 1.
[19] C. Cai, B. Liu, M. V. Mirkin, H. A. Frank, J. F. Rusling, *Anal. Chem.* **2002**, *74*, 114.
[20] H. Teramoto, T. Shimizu, M. Suda, M. Inui, *Int. J. Hydrogen Energy* **2022**, *47*, 22010.

[21] B. E. Conley, M. T. Weinstock, D. R. Bond, J. A. Gralnick, *Appl. Environ. Microbiol.* **2020**, *86*, e01253–20.
[22] B. R. Ringeisen, E. Henderson, P. K. Wu, J. Pietron, R. Ray, B. Little, J. C. Biffinger, J. M. Jones-Meehan, *Environ. Sci. Technol.* **2006**, *40*, 2629.
[23] S. Ishii, K. Watanabe, S. Yabuki, B. E. Logan, Y. Sekiguchi, *Appl. Environ. Microbiol.* **2008**, *74*, 7348.
[24] J. Boonstra, H. J. Sips, W. N. Konings, *Eur. J. Biochem.* **1976**, *69*, 35.
[25] A. W. Confer, S. Ayalew, *Vet. Microbiol.* **2013**, *163*, 207.
[26] J. Shearer, D. Jefferies, S. Khalid, *J. Chem. Theory Output* **2019**, *15*, 2608.
[27] L.-S. Ma, J.-S. Lin, E.-M. Lai, *J. Bacteriol.* **2009**, *191*, 4316.
[28] J. D. Mougous, M. E. Cuff, S. Raunser, A. Shen, M. Zhou, C. A. Gifford, A. L. Goodman, G. Joachimiak, C. L. Ordoñez, S. Lory et al., *Science* **2006**, *312*, 1526.
[29] C. Rensing, T. Pribyl, D. H. Nies, *J. Bacteriol.* **1997**, *179*, 6871.
[30] C. G. Friedrich, B. Friedrich, B. Bowien, *J. Gen. Microbiol.* **1981**, *122*, 69.
[31] B. Friedrich, E. Heine, A. Finck, C. G. Friedrich, *J. Bacteriol.* **1981**, *145*, 1144.
[32] B. C. Berks, S. J. Ferguson, J. W. Moir, D. J. Richardson, *Biochim. Biophys. Acta* **1995**, *1232*, 97.
[33] B. Lai, S. Yu, P. V. Bernhardt, K. Rabaey, B. Virdis, J. O. Krömer, *Biotechnol. Biofuels* **2016**, *9*, 39.
[34] P. R. Alefounder, J. E. McCarthy, S. J. Ferguson, *FEMS Microbiol. Lett.* **1981**, *12*, 321.
[35] A. Pohlmann, R. Cramm, K. Schmelz, B. Friedrich, *Mol. Microbiol.* **2000**, *38*, 626.
[36] R. Cramm, A. Pohlmann, B. Friedrich, *FEBS Lett.* **1999**, *460*, 6.
[37] M. L. Fultz, R. A. Durst, *Anal. Chim. Acta* **1982**, *140*, 1.
[38] J. W. Moir, N. J. Wood, *Cell. Mol. Life Sci.* **2001**, *58*, 215.
[39] U. Warnecke-Eberz, B. Friedrich, *Arch. Microbiol.* **1993**, *159*, 405.
[40] L.-S. Huang, D. Cobessi, E. Y. Tung, E. A. Berry, *J. Mol. Biol.* **2005**, *351*, 573.
[41] G. von Jagow, P. O. Ljungdahl, P. Graf, T. Ohnishi, B. L. Trumpower, *J. Biol. Chem.* **1984**, *259*, 6318.
[42] T. Friedrich, P. van Heek, H. Leif, T. Ohnishi, E. Forche, B. Kunze, R. Jansen, W. Trowitzsch-Kienast, G. Höfle, H. Reichenbach, *Eur. J. Biochem.* **1994**, *219*, 691.
[43] N. Li, K. Ragheb, G. Lawler, J. Sturgis, B. Rajwa, J. A. Melendez, J. P. Robinson, *J. Biol. Chem.* **2003**, *278*, 8516.
[44] Z. Xi, J. Guo, J. Lian, H. Li, L. Zhao, X. Liu, C. Zhang, J. Yang, *Bioresour. Technol.* **2013**, *140*, 22.
[45] M. J. Fei, E. Yamashita, N. Inoue, M. Yao, H. Yamaguchi, T. Tsukihara, K. Shinzawa-Itoh, R. Nakashima, S. Yoshikawa, *Acta Crystallogr. Sect. D* **2000**, *56*, 529.
[46] D. J. Hyndman, Y. M. Milgrom, E. A. Bramhall, R. L. Cross, *J. Biol. Chem.* **1994**, *269*, 28871.
[47] A. Craske, S. J. Ferguson, *Eur. J. Biochem.* **1986**, *158*, 429.
[48] J. Simon, M. Sänger, S. C. Schuster, R. Gross, *Mol. Microbiol.* **2003**, *49*, 69.
[49] S. Dementin, P. Arnoux, B. Frangioni, S. Grosse, C. Léger, B. Burlat, B. Guigliarelli, M. Sabaty, D. Pignol, *Biochemistry* **2007**, *46*, 9713.
[50] E. Maklashina, G. Cecchini, *Arch. Biochem. Biophys.* **1999**, *369*, 223.
[51] P. Ertl, B. Unterladstaetter, K. Bayer, S. R. Mikkelsen, *Anal. Chem.* **2000**, *72*, 4949.
[52] M. S. Al-Abdul-Wahid, F. Evanics, R. S. Prosser, *Biochem.* **2011**, *50*, 3975.
[53] A. A. Konstantinov, T. Vygodina, N. Capitanio, S. Papa, *Biochim. Biophys. Acta* **1998**, *1363*, 11.
[54] N. Capitanio, G. Capitanio, D. Boffoli, S. Papa, *Biochem.* **2000**, *39*, 15454.
[55] M. Wikström, K. Krab, V. Sharma, *Chem. Rev.* **2018**, *118*, 2469.
[56] J. Liu, Y. Qiao, Z. S. Lu, H. Song, C. M. Li, *Electrochem. Commun.* **2012**, *15*, 50.
[57] Q. Wen, F. Kong, F. Ma, Y. Ren, Z. Pan, *J. Power Sources* **2011**, *196*, 899.
[58] J. Wu, Y. Li, X. Chen, N. Li, W. He, Y. Feng, J. Liu, *Sci. Total Environ.* **2022**, 822, 153443.
[59] I. M. Helander, H.-L. Alakomi, K. Latva-Kala, P. Koski, *Microbiol.* **1997**, *143*, 3193.
[60] H. G. Schlegel, R. Lafferty, I. Krauss, *Arch. Mikrobiol.* **1970**, *71*, 283.
[61] C. Kortlüke, B. Friedrich, *J. Bacteriol.* **1992**, *174*, 6290.
[62] A. Sydow, T. Krieg, R. Ulber, D. Holtmann, *Eng. Life Sci.* **2017**, *17*, 781.
[63] A. Gemünde, J. Gail, D. Holtmann, *Chemsuschem* **2023**, 16, e202300181.
[64] C. Windhorst, J. Gescher, *Biotechnol. Biofuels* **2019**, *12*, 163.
[65] K. J. Livak, T. D. Schmittgen, *Methods* **2001**, *25*, 402.
[66] A. J. Ruff, M. Arlt, M. van Ohlen, T. Kardashliev, M. Konarzycka-Bessler, M. Bocola, A. Dennig, V. B. Urlacher, U. Schwaneberg, *J. Mol. Catal. B* **2016**, *134*, 285.
[67] I. M. Helander, T. Mattila-Sandholm, *Int. J. Food Microbiol.* **2000**, *60*, 153.

Manuscript received: March 28, 2024
Revised manuscript received: April 30, 2024
Version of record online: ■■, ■■

Appendix B

B.1 Declaration of Authorship

I declare that I have completed this dissertation single-handedly without the unauthorized help of a second party and only with the assistance acknowledged therein. I have appropriately acknowledged and cited all text passages that are derived verbatim from or are based on the content of published work of others, and all information relating to verbal communications. I consent to the use of an anti-plagiarism software to check my thesis. I have abided by the principles of good scientific conduct laid down in the regulations of the leading University which were delivered to me in carrying out the investigations described in the dissertation.

_____ _____

Place, Date Original Signature

B.2 List of Figures

Der Lebenslauf wurde aus der elektronischen Version der Arbeit entfernt.

The curriculum vitae was removed from the electronic version of the paper.

Publications as first author
(* shared authorship)

Gemünde, André; Lai, Bin; Pause, Laura; Krömer, Jens; Holtmann, Dirk (2022): Redox mediators in microbial electrochemical systems. In: *ChemElectroChem* **9**, DOI: 10.1002/celc.202200216.

Gemünde, André; Gail, Jonas; Holtmann, Dirk (2023): Anodic Respiration of Vibrio natriegens in a Bioelectrochemical System. In: *Chemsuschem* **16**, DOI: 10.1002/cssc.202300181.

Gemünde, André; Gail, Jonas; Janek, Jürgen; Holtmann, Dirk (2023): e-Cuvettes parallelize electrochemical and photometric measurements in cuvettes and facilitate applications in bio-electrochemistry. In: *Biosens. Bioelectron. X* **14**, DOI: 10.1016/j.biosx.2023.100378.

Gemünde, André; Gail, Jonas; Holtmann, Dirk (2024): Redox mediator interaction with Cupriavidus necator – spectroelectrochemical online analysis. In: *Electrochem. commun*. **162**, DOI: 10.1016/j.elecom.2024.107705.

*Gemünde, André; *Rossini, Elena; Lenz, Oliver; Frielingsdorf, Stefan; Holtmann, Dirk (2024): Chemoorganotrophic electrofermentation by Cupriavidus necator using redox mediators. In: *Bioelectrochemistry* **158**, DOI: 10.1016/j.bioelechem.2024.108694.

Gemünde, André; Ruppert, Nils-Lennart; Holtmann, Dirk (2024): Unraveling the Electron Transfer in Cupriavidus necator – Insights Into Mediator Reduction Mechanics. In: *ChemElectroChem* **11,** DOI: 10.1002/celc.202400273

Publications as co-author

Stöckl, Markus; Gemünde, André; Holtmann, Dirk (2022): Microbial electrotechnology – Intensification of bioprocesses through the combination of electrochemistry and biotechnology. In: *Phys. Sci. Rev.* DOI: 10.1515/psr-2022-0108.

Conference contributions

07/2024	André Gemünde, Dirk Holtmann 4th International Meeting Biochemical Foundation of Microbial Extracellular Electron Transfer, Hamburg, Germany Oral presentation: "Mediated extracellular electron transfer with *Cupriavidus necator*"
05/2023	André Gemünde, Jonas Gail, Dirk Holtmann Himmelfahrtstagung on Bioprocess engineering, Weimar, Germany Oral presentation: „*Vibrio natriegens* – a novel bioelectrochemical workhorse?"
09/2022	André Gemünde, Jonas Gail, Dirk Holtmann ISMET8 - International Society for Microbial Electrochemistry and Technology, Chania, Greece Oral presentation: „Online monitored bioelectrochemical system for screening purposes in a commercial photometer"
05/2022	André Gemünde, Dirk Holtmann Himmelfahrtstagung on Bioprocess engineering, Mainz, Germany Poster presentation: „Anodic respiration of *Pseudomonas putida* in parallel bioelectrochemical systems"
09/2021	André Gemünde, Hendrik Schewe, Roland Ulber, Dirk Holtmann EU-ISMET - International Society for Microbial Electrochemistry and Technology, Girona, Spain Poster presentation: „Anaerobic cultivation of genetically engineered *Pseudomonas putida* in a bioelectrochemical system"

Supervised student theses

2022	Jonas Gail, Bachelor thesis „Optimization of the cultivation conditions of *Vibrio natriegens* in a bioelectrochemical system for potential use in industrial biotechnology“
2022	Leonie Marie Fratini, Master thesis „Characterization of alternative media for the cultivation of *Vibrio natriegens* and investigation of electron transfer“
2023	Nils-Lennart Ruppert, Bachelor thesis „Optimization of mediator uptake by *Cupriavidus necator* in a bioelectrochemical system“